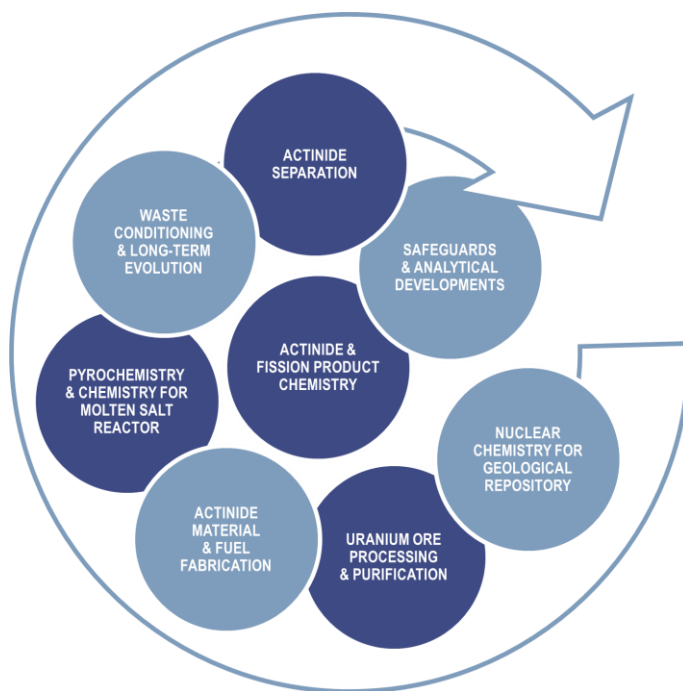


BOOK OF ABSTRACTS



September 1-6, 2024 – Avignon, France



PLENARY TALKS 12

Global Overview on the Nuclear Fuel Cycle Backend and IAEA Related Activities.....	13
<i>Clément Hill, Amparo Gonzalez-Espartero.....</i>	13
Status of the French Nuclear Fuel Cycle Program	15
<i>François Sudreau.....</i>	15
Nuclear Fuel Recycle Activities in the Office of Nuclear Energy	17
<i>Stephen Kung.....</i>	17
Future Fuel Cycles – a UK Perspective	19
<i>Paul Nevitt.....</i>	19

ACTINIDE AND FISSION PRODUCTS SEPARATION22

Overview of the Material Recovery and Waste Form Development Program	23
<i>Kenneth C Marsden.....</i>	23
Lab-Scale Pulsed Columns Trials for a New Nuclear Fuel Recycling Process	25
<i>Garzon Losik German, Lamadie Fabrice, Roussel Hervé.....</i>	25
Potential of Aggregation Control for Solvent Extraction Separation	27
<i>Cyril Micheau,^a Yuki Ueda,^a Ryuhei Motokawa,^a Kazuhiro Akutsu-Suyama,^{b,c} Norifumi L. Yamada,^d Masako Yamada,^d Sayed Ali Moussaoui,^e Elizabeth Makombe,^e Daniel Meyer,^e Laurence Berthon,^f Damien Bourgeois^g.....</i>	27
Evolution of Uranium Recovery: Past, Present, and Future Perspectives.....	29
<i>Santa Jansone Popova¹, Jopaul Mathew¹, Jeffrey Einkauf¹, Alexander Ivanov¹, Ilja Popovs¹, Connor Parker¹, Peter Zalupski², Travis Grimes², Corey Pilgrim².....</i>	29
Experimental and Modeling Study of Uranium(VI) and Nitric Acid Extraction With a N,N-Dialkylamide Solvent	31
<i>Thibau Blanc¹, Donatien Gomes Rodrigues¹, Pauline Moeyaert^{1*}, Thomas Dumas¹, Philippe Guilbaud^{1*}.....</i>	31
Feasibility Study on PUREX–NUMAP Hybrid Reprocessing: Precipitation–Based Recovery of U(VI) from Organic Phases with 30% TBP	33
<i>Ririka Tashiro¹, Satoru Tsushima¹⁽²⁾, Koichiro Takao¹.....</i>	33
Demonstration of U(VI)/Pu(IV) Separation by Solvent Extraction in Modified Lab-Scale Annular Centrifugal Contactors Using D2EHiBA Extractant.....	35
<i>Dominic Maertens^{a,b*}, Koen Binnemans^b, Thomas Cardinaels^{a,b}.....</i>	35
Current TRL Status and Strategy for the Development of the Next Generation of Reprocessing Plant	37
<i>B. Arab-Chapelet¹, C. Sorel¹, I. Hablot², A. Gil Martin², M. Phelip³, A. Salvatores³, L. Diaz⁴, G. Vaast⁴.....</i>	37
Towards a Single-Solvent Process for U/TRU Recovery and Minor Actinide/Lanthanide Separations: Speciation and Partitioning of Tetravalent (Th, Pu) and Hexavalent (U) Actinides with HEH[EHP] and T2EHDGA.....	39
<i>Artem Gelis[*], Joel Castillo, Logan Smith, Quinn Summerfield, Frederic Poineau.....</i>	39

Horizon 2020 PuMMA: Studies Considering Reprocessing of 40–45 %Pu Fast Reactor MOx	41
<i>Chris Maher</i> [*] , Nathalie Chauvin ² , Francisco Álvarez ³ , Martin Giraud ² , Jessica Gunning ¹ , Victoria Hayter ¹ , Rebecca Sanderson ¹ , Nathalie Reynier-Tronche ² , Eva de Visser Týnová ⁴	
First-Principles Study of a New TODGA Degradation Compound	43
<i>Lucas Zubillaga-Maharg</i> ^{1,2,3} , Iván Sánchez-García ⁴ , Hitos Galán ⁴ , J. Manuel Perlado ^{1,2} , Emma del Río ^{1,2}	
Demonstration of the Single Cycle Am(III) Separation AmSEL Process in Laboratory-scale Annular Centrifugal Contactors	45
<i>Andreas Wilden</i> ^{1,*} , Fynn S. Sauerwein ¹ , Vincent Vanel ² , Andreas Geist ³ , Giuseppe Modolo ¹	
Flowsheets for the Validation of the Reference AmSEL System	47
<i>Vincent Vanel</i> ^{1,*} , Andreas Wilden ² , Giuseppe Modolo ² , Andreas Geist ³ , Marc Montuir ¹	
Novel Water-soluble and CHON-compliant Ligands for Selective Americium Separation from PUREX Raffinate	49
<i>Elena Macerata</i> ¹ , Alberto Arici ¹ , Giulia Firenze ¹ , Letizia Di Matteo ¹ , Fabrizio Piromalli ² , Andrea Salomone ¹ , Gabriele Magugliani ¹ , Eros Mossini ¹ , Mario Mariani ¹ , Alessandro Sacchetti ²	
Extraction and Speciation Studies of New Diglycolamides with Varying Alkyl Chains for Selective Americium Partitioning	51
<i>Filip Kolesar</i> [1,2], Karen Van Hecke [2], Ken Verguts [2], Cécile Marie [3], Laurence Berthon [3], Koen Binnemans [1], Thomas Cardinaels [1,2]	
Selective Americium Separation: New insights into the Complexation of SO ₃ -Ph-BTBP with Trivalent f-Elements	53
<i>Fynn S. Sauerwein</i> ^{1,*} , Thomas Sittel ² , Andreas Geist ² , Andreas Wilden ¹ , Giuseppe Modolo ¹	
Purification of Neptunium and Plutonium by Ion Exchange for Plutonium-238 Production at Oak Ridge National Laboratory	55
<i>Lætitia H. Delmau</i> , David W. DePaoli, Brad N. Tinker, Dennis E. Benker, and Robert M. Wham	
Experimental Studies and Molecular Modeling of the Physico-chemical Properties of Pure Monoamides Extractants	57
<i>Abderrazak Masmoudi</i> , Dominique Guillaumont, Philippe Guilbaud	
Development of Integrated Actinide Chemistry Application, AACE, for Acceleration of Actinide Chemistry Experiments	59
<i>Masahiko Nakase</i> ^{1,2} , Takahiro Nishihara ^{1,2} , Fauzia Hanum Ikhwan ¹ , Tomohiro Okamura ^{1,2} , Kota Matsui ³	
Actinide Oxide Dissolution in Tributyl Phosphate	61
<i>Jarrod M. Gogolski</i> , Chelsea M. Goetzman, Robert J. Lascola, Tracy S. Rudisill	
Direct Extraction of Uranium from Used Nuclear Fuel with DEHiBA	63
<i>Gabriel B. Hall</i> , Nathan P. Bessen, Daria Boglaienko, Gregg J. Lumetta	
New Monoamide Based Extractants for U(VI) and Pu(IV) Efficient Separation	65
<i>Cécile Marie</i> ¹ , Pape Diabate ¹ , Audrey Beillard ¹	
Efficient Manufacture of DEHiBA through Industry 4.0	67
<i>Tom Shaw</i> , Prof. Bruce Hanson, Prof. Richard Bourne	
Interinstitutional Study of the New EURO-GANEX Process Resistance by Gamma Irradiation Test Loops	69

Ivan Sanchez-Garcia¹, Xavier Heres², Dean. R. Peterman³, Hitos Galan¹, Sylvain Costenoble², Sylvain Broussard², Johann Sinot², Travis S. Grimes³, Kash Reid Anderson³, Santa Jansone-Popova⁴, Maria Chiara Gullo⁵, Alessandro Casnati⁵, Andreas Wilden⁶, and Andreas Geist⁷69

Americium Separation Processes Developed within the European PATRICIA Project71

Christian Sorel¹, **Andreas Geist**², Giuseppe Modolo³, Laure Ramond¹, Christian Ekberg⁴, Hitos Galán⁵, Bruce Hanson⁶, Gregory Leinders⁷, Elena Macerata⁸, Cécile Marie¹, Petra J. Panak^{2,9}, Mark Sarsfield¹⁰, Dan Whittaker¹⁰, Andreas Wilden³71

Radiolytic Stability of Metal (IV) Phosphonate Sorbents Designed for Minor Actinide-Lanthanide Separations73

Taren Cataldo¹, Jessica Velisek-Carolan², Nicholas Bedford¹, Sophie Le Caër³73

Optimization of Minor Actinides Recovery Conditions by Combining Mathematical Analysis and Process Simulation75

Yuichi Sano¹, Akane Kojima², Tomoyuki Yajima², Yoshiaki Kawajiri²75

Recent Results from Lab Scale Testing of Advanced Aqueous Separation Processes for the Future Recycling of Spent Nuclear Fuels77

Robin Taylor¹, Dan Whittaker¹, Mark Sarsfield¹, Michael Carrott¹, Billy Keywood¹, Rebecca Sanderson¹, David Woodhead¹, Kate Wallace¹, Hongyan Chen², Clint Sharrad³77

Research on Sustainable Nuclear Energy Use with Actinide Management: Scenario Study on High-Level Waste Generation with MA Separation and Intermediate Storage Technology Implementation79

Tomohiro Okamura¹, Ryo Takahashi², Takashi Shimada², Nakase Masahiko¹, Tomoo Yamamura³ and Kenji Takeshita¹79

Recovery of Strategic High-Value Fission Products from Spent Nuclear Fuel during Reprocessing81

Alastair F. Holdsworth^[1], Harry Eccles^[2], Kathryn George^[1], and Clint A. Sharrad^[1]81

Demonstration of Advanced Voloxidation and Direct Extraction Using Irradiated UO₂83

Peter Tkac¹, Michael Kalensky¹, Sergey Chemerisov²83

Zirconium Molybdate Rinsing With Carbonate: From R&D to Industrialization in the La Hague Plants85

Nicolas Golles¹, Céline Quenault², Pierre Sarrat³, Sandrine Jakab-Costenoble³, Bénédicte Arab-Chapelet³, Nicolas Vigier⁴, Jean-Luc Emin⁴85

ACTINIDE MATERIALS AND NUCLEAR FUELS 88

The Potentials of Nano-Scaled Actinide Dioxides89

Olaf Walter, Karin Popa89

Influence of Uranium Oxide Nature on MOX Fuel Fabrication Process91

F. Sauvaire¹, J-B. Parise¹, A. Delevaque¹, A. Selmil¹, R.Delville², **T. Genevès**¹, V.Garat¹91

New Insights in the Structural-Redox Chemistry of Cr, Mn, Fe and V doped-UO₂ Nuclear Fuel Materials93

G. L. Murphy [1], Philip Kegler [1], Robert Gericke [2], S. Gilson [2], Martina Klinkgenberg [1], Daniil Sirochii [1], Andrey Bukaemskiy [1], Kristina Kvashnina [2], Volodymyr Svitlyk [2], Christop Henig [2], Peter Kaden [2] and Nina Huittinen [2]93

ESEM-Monitored Dissolution of (U,Th)O ₂ Heterogeneous Mixed Oxides for Spent Fuel Modeling	95
<i>L. Claparede</i> [2], <i>C. Hours</i> [1], <i>I. Viallard</i> [3], <i>N. Reynier-Tronche</i> [1], <i>N. Dacheux</i> [2]	
Defect Chemistry, Thermal Oxidation, and Thermodynamics of metal-doped UO ₂	97
<i>Xiaofeng Guo</i> ¹ , <i>Juejing Liu</i> ¹ , <i>Shinhyo Bang</i> ¹ , <i>Lorenzo Callejon</i> ^{1,2} , <i>Romain Sicard</i> ^{1,2} , <i>Sam Karcher</i> ¹ , <i>John McCloy</i> ¹ , <i>Hongwu Xu</i> ³ , <i>Arjen van Veelen</i> ³ , <i>Nicolas Clavier</i> ² , <i>Nicolas Dacheux</i> ²	
Heat Capacity Measurements of Self-Damaged Mixed Actinide Oxides: a Method to Assess Defects in Spent Fuels	99
<i>Thierry Wiss</i> ¹ , <i>Rudy Konings</i> ¹ , <i>Dragos Staicu</i> ¹ , <i>Alessandro Benedetti</i> ¹ , <i>Jean-Yves Colle</i> ¹ , <i>Emilio Mauger</i> ^{1,2} , <i>Zeynep Talip</i> ² , <i>Emanuele De Bona</i> ³ , <i>Oliver Dieste</i> ⁴ , <i>Gianguido Baldinozzi</i> ⁵ , <i>Christine Guéneau</i> ⁶	
Conversion of U(VI) and Pu(IV) by Peroxide Precipitation and Hydrothermal Treatment	101
<i>L. Muller</i> ^{a,b} , <i>P. Estevenon</i> ^a , <i>C. Tamain</i> ^a , <i>N. Dacheux</i> ^b , <i>N. Clavier</i> ^b	
Densification Study of Cr-doped UO ₂ Fuel Pellets with Addition of Fission Products Surrogates	103
<i>Antonin De Azevedo</i> ¹ , <i>Fabienne Audubert</i> ¹ , <i>Nathalie Moncoffre</i> ² , <i>Jacques Lechelle</i> ¹	
Hydrothermal Reducing Conversion of Uranium(VI) Oxalate into Oxides	105
<i>S. Benarib</i> ¹ , <i>I. Munoz</i> ¹ , <i>I. Kieffer</i> ² , <i>J. L. Hazemann</i> ³ , <i>N. Dacheux</i> ¹ , N. Clavier ¹	
Actinide Thioamidates as Precursors For Actinide Sulfide Nanomaterials	107
Sheridon N. Kelly ^{a,b} , <i>Dominic R. Russo</i> ^{a,b} , <i>Appie A. Peterson</i> ^b , <i>Erik T. Ouellette</i> ^a , <i>Michael A. Boreen</i> ^a , <i>Jacob A. Branson</i> ^{a,b} , <i>S. Olivia Gunther</i> ^b , <i>Patrick W. Smith</i> ^b , <i>John Arnold</i> ^a , <i>Stefan G. Minasian</i> ^b	
Synthesis of PuO ₂ and (U,Pu)O ₂ Solid Solution by Citric Acid Assisted Combustion Synthesis	109
<i>A. Hauteau</i> ^{1,2} , P. Estevenon [1], <i>C. Rey</i> [2], <i>X. Deschanel</i> [2]	
Phase Separation in Fluorite-Related U _{1-y} Ce _y O _{2-x} : New Insights via Variable Temperature Neutron Diffraction	111
<i>David Simeone</i> ¹ , <i>Xavier Deschanel</i> ² , <i>Philippe Garcia</i> ³ , <i>Maxim Avdeev</i> ⁴ , <i>Timothy Ablott</i> ⁵ , Gordon J Thorogood ⁶	
Fabrication and Dissolution of Americium Plutonium Oxide Fuels	113
Eva de Visser-Týnová , <i>Jessica Bruin</i> , <i>Frank Oud</i>	
Fission Products Speciation in Irradiated MOx Fuel During Interim Storage Accidental Scenarios	115
R. Caprani ¹ , <i>Ph. Martin</i> ¹ , <i>J. Martinez</i> ¹ , <i>D. Prieur</i> ² , <i>F. Lebreton</i> ¹ , <i>K. Kvashnina</i> ² , <i>E. Bazarkina</i> ² , <i>D. Menu</i> ³ , <i>N. Clavier</i> ⁴	
Synthesis and Characterisation of CeO ₂ and PuO ₂ Pellets with Representative Microstructure for General Purpose Heat Sources	117
Jérémie Manaud , <i>Walter Bonani</i> , <i>Jacobus Boshoven</i> , <i>Marco Cologna</i> , <i>Michael Holzhäuser</i> , <i>Karin Popa</i> , <i>Sorin-Octavian Vălu</i> , <i>Daniel Freis</i>	
Incorporation of Fission Products into Oxide Nuclear Fuel: Towards a New Paradigm?	119
L. Desgranges	
Quantification of the Morphology and Roughness of Oxide Powder Particles In Relation to their Manufacturing History and Flow Properties	121
Christophe D'Angelo ¹ , <i>Solène Bertolotto</i> ¹ , <i>Anne-Charlotte Robisson</i> ¹ and <i>Christelle Duguay</i> ¹	
Field Assisted Sintering of UO ₂ Based Nuclear Fuels	123
R.W. Harrison ¹ , <i>J. Morgan</i> ¹ , <i>J. Buckley</i> ¹ , <i>T. Abram</i> ¹ , <i>D. Pearmain</i> ² , <i>S. Bostanchi</i> ² , <i>C. Green</i> ² , <i>R. White</i> ² , <i>D. Goddard</i> ³ , <i>N. Barron</i> ⁴	

Characterization of the Phases Formed During the High Temperature Oxidation of (U,Pu)O ₂ Mixed Oxides.....	125
<i>Priscilla Berenguer-Besnard^{a,b}, Philippe Martin^a, Loïc Marchetti^a, Loïc Favergeon^b</i>	125
Fundamental Insights into Defect Generation and Transport Phenomena at Grain Boundaries in Nuclear Fuel.....	127
<i>S. Finkeldei¹, J. Proctor¹, O. Lori¹, S. Dillon¹, J. White², Y. Wang², M. Cooper², D. Andersson²</i>	127
Impact of Ru, Rh, Pd and Mo Metallic Particles on the Dissolution Kinetics of UO ₂	129
<i>Kaczmarek T.¹, Szenknect S.¹, Le Goff X.¹, Podor R.¹, Dacheux N.¹</i>	129
Thermal Oxidation and High Temperature Structures of Uranium Carbide: in situ X-Ray Diffraction Studies	131
<i>Emma C. Kindall¹, Natalie S. Yaw¹, Juejing Liu¹, Malin C. Wilkins¹, Sam Karcher¹, Hongwu Xu¹, Arjen van Veelen¹, Josh T. White¹, John McCloy¹, Xiaofeng Guo¹</i>	131

WASTE CONDITIONING AND GEOLOGICAL REPOSITORY.....134

REGAIN project – Recycling of Zirconium from Nuclear Hulls.....	135
<i>Mathilde Guilpain¹, Isabelle Hablot¹, Bertrand Morel¹</i>	135
Successful Lasergrammetry Operation in an ATALANTE Hot Cell: First Step for Deploying Digital Technologies on Hot Cells In Operation.....	137
<i>Caroline Chabal^{(1)*}, Michaël Gauthier⁽¹⁾, Julien Delrieu⁽¹⁾, Thibaud Durand⁽¹⁾, Christian Père^{(2)**}</i>	137
Effects of Radiolysis Products and Acidic Media on the Aggregation Behaviour of Nuclear Fuel Debris Nanoparticle Simulants via Stochastic Simulations	139
<i>Miguel Pineda¹, Cong Chao¹, Yiwei Zhang^{1,2}, Takehiko Tsukahara², Panagiota Angelī¹, Eric S. Fraga¹</i>	139
Insights into Glass Alteration Mechanisms from the Study of Long Term Burial Experiments ..	141
<i>Clare L. Thorpe¹, Garry Manifold¹, Rachel Crawford¹ and Russell J. Hand¹</i>	141
Impact of Lanthanide and PGM Elements on the Chemical Durability and Surface Modifications during the Leaching Tests of FP Doped Pellets Mimicking Interim Repository	143
<i>P.H. Imbert¹, L. Claparede¹, S. Szenknect¹, N. Dacheux¹</i>	143
The Impact of Hot Isostatic Pressing on U Speciation and Local Coordination in Simulant Pu Ceramic Wasteforms	145
<i>Aidan Friskney¹, Ewan R. Maddrell², Claire L. Corkhill³ and Lewis R. Blackburn¹</i>	145
Impact of Gamma Dose Rate on the Alteration of Nuclear Glass in Geological Disposal Conditions.....	147
<i>M. Taron¹ [1, 2], H. Aréna¹ [1], F. Chupin¹ [1], K. Ressayre¹ [1], R. Podor² [2], M. Tribet¹ [1], S. Peugeot¹ [1]</i>	147
Low-Temperature Condensation and Solidification of Radioactive Liquid Waste by Freeze Drying	149
<i>Akihiko Kajinami¹, Sou Watanabe²</i>	149
Investigation of Cement-Based Materials with Dihydrogen Sequestration Properties	151
<i>H. Danis¹, C. Cau Dit Coumes¹, P. Antonucci¹, I. Pointeau², T. Cordara², N. Macé³, S. Savoye³</i>	151
Microwave Plasma-Assisted Combustion of Waste Organic Solvents	153

<i>Shimpei Ohno</i> ¹ , <i>Atsushi Sakamoto</i> ¹ , <i>Sou Watanabe</i> ¹ , <i>Masahiro Nakamura</i> ¹ , <i>Tsuyoshi Yamamoto</i> ² and <i>Ryou Tanaka</i> ³ .	153
Search for a Cement Matrix for ITER Beryllium Radwaste Conditioning.....	155
<i>Laflotte R.</i> ¹⁾ , <i>Cau Dit Coumes C.</i> ¹⁾ , <i>Cannes C.</i> ²⁾ , <i>Delpech S.</i> ²⁾ , <i>Haas J.</i> ¹⁾ , <i>Rivenet M.</i> ³⁾	155
Repercussions of Solubility for the Conditioning of Fission Products and Minor Actinides in Borosilicate Glasses	157
<i>L. Campayo</i> , <i>I. Giboire</i> , <i>S. Schuller</i> , <i>E. Régnier</i> , <i>D. Perret</i>	157
Progress towards the Immobilisation of the UK Plutonium Inventory in Titanate Ceramics....	159
<i>Lewis R. Blackburn</i> ¹ , <i>Amber R. Mason</i> ¹ , <i>Laura J. Gardner</i> ¹ , <i>Claire L. Corkhill</i> ²	159
Elaboration and Characterization of Iodate and/or Carbonate-Doped Apatites for Long-Lived Radionuclides Conditioning	161
<i>Olivier Dautain</i> ^{a,b} , <i>Céline Cau dit Coumes</i> ^b , <i>Christophe Drouet</i> ^a , <i>David Grossin</i> ^a , <i>Lionel Campayo</i> ^b , <i>Christèle Combes</i> ^a	161
The Effect of Cation Substitution and Valency on Formation Energetics of Brannerite Ceramics for Nuclear Waste Applications.....	163
<i>Natalie S. Yaw</i> , <i>Chris Dixon Wilkins</i> , <i>Nicolas Dacheux</i> , <i>John McCloy</i> , <i>Xiaofeng Guo</i>	163
Densification of Mesoporous Silicas Induced by Radiation Damage – New Perspectives for the Treatment of Radioactive Effluents.....	165
<i>Jun Lin</i> [*] , <i>Clara Grygiel</i> ^{**} , <i>Sandrine Dourdain</i> [*] , <i>Yannick Guari</i> ^{***} , <i>Cyrielle Rey</i> [*] , <i>Jérémy Causse</i> [*] , <i>Olaf Walter</i> ^{****} , <i>Xavier Deschanel</i> [*]	165
A Historical Overview of Corroded Microstructures and Present-day Best Practices.	167
<i>Mir Anamul Haq</i>	167
Compared Radiation Stability of Mesoporous Silica and Nuclear Glass Alteration Gels	169
<i>Pierre De Laharpe</i> ^{*1} , <i>Xavier Deschanel</i> ¹ , <i>Sylvain Peugot</i> ² , <i>Helene Arena</i> ² , <i>Melanie Taron</i> ^{1,2} , <i>Jun Lin</i> ¹ , <i>Bertrand Siboulet</i> ¹ , <i>Jean-Marc Delaye</i> ²	169
Insights into the Structural and Redox Chemistry of Cr-doped (Ln,U)O₂ Materials	171
<i>Daniil Shirokiy</i> ¹ , <i>Maximilian Henkes</i> ¹ , <i>Andrey Bukaemskiy</i> ¹ , <i>Kristina O. Kvashnina</i> ² , <i>Martina Klinkenberg</i> ¹ , <i>Philip Kegler</i> ¹ , <i>Dirk Bosbach</i> ¹ and <i>Gabriel L. Murphy</i> ¹	171
Simulating Auto-Irradiation of Glass Using External Irradiation Beams: Impact on Glasses Structure and Properties	173
<i>M. Taron</i> ^{1,2} , <i>H. Aréna</i> ¹ , <i>C. Gillet</i> ¹ , <i>F. Perrudin</i> ¹ , <i>R. Podor</i> ² , <i>M. Tribet</i> ¹ , <i>S. Miro</i> ¹ , <i>S. Peugot</i> ¹	173
The Influence of pH, Ionic Strength and Temperature on Cs, Ba, Co, and Eu Sorption on Biotite – Experiments and Modelling	175
<i>Pawan Kumar</i> , <i>Stellan Holgersson</i> , <i>Christian Ekberg</i>	175
Colloids Pose an Enhanced Transport Risk of Uranium in Saturated Porous Media: A Challenge for Immobilization Remediation of Uranium Contaminated Site	177
<i>Duoqiang Pan</i> , <i>Xiaoyan Wei</i> , <i>Xinyi Shi</i> , <i>Weixiang Xiao</i> , <i>Zhen Xu</i> , <i>Wangsuo Wu</i>	177
Processes Driven by Iron Reducing Bacteria on Technetium Immobilization	179
<i>Cardaio I.</i> , <i>Müller K.</i> , <i>Cherkouk A.</i> , <i>Stumpf T.</i> , <i>Mayordomo N.</i>	179

SAFEGUARDS AND ANALYTICAL CHEMISTRY 182

Real-Time and Automated Process Control via On-Line Monitoring	183
---	------------

Amanda M. Lines,^{1*} Poki Tse,¹ Nathan Bessen,¹ Thomas Serrano,¹ Alyssa Espley,¹ Gilbert Nelson,² Gabriel B. Hall,¹ Jarrod R. Allred,¹ Gregg J. Lumetta,¹ and Samuel A. Bryan¹	183
Photonic Lab-On-A-Chip, a Versatile and Powerful Tool for R&D Studies on Spent Fuel Reprocessing	185
Fabrice Lamadie^{1*}, Elodie Mattio¹, Manuel Miguiditchian¹, Amanda M. Lines², Samuel A. Bryan², Hope E. Lackey², Fabrice Onofri³, Isaac Rodriguez-Ruiz⁴	185
Real-Time Solution Analysis in Microfluidic Devices using Optical Spectroscopy	187
Samuel A. Bryan,^{1*} Hope E. Lackey,¹ Gilbert L. Nelson,² Job M. Bello,³ Fabrice Lamadie,⁴ and Amanda M. Lines¹	187
The Joint Research Centre's Expertise in Nuclear Safeguards Sample Analysis	189
A.M. Sánchez Hernández, R. Buda, K. Casteleyn, L. Commin, F. D'Amati, J. Horta, A. Le Terrier, A. Muehleisen, S. Stohr, H. Schorlé, M. Toma, M. Vargas Zuñiga, D. Wojnowski, J. Zsigrai, K. Mayer	189
A New Plutonium Metal Certified Reference Material at CETAMA: the MP4 Standard	191
S. Picard¹, M. Crozet¹, Y. Davrain¹, C. Bertorello¹, G. Canciani¹, C. Rivier¹, D. Cardona², G. Legay², G. Bailly², N. Caussignac², C. Zeleny², A. Quemet¹, S. Baghdadli¹, C. Maillard¹, V. Dalier¹, L. Montreuil¹, S. Jan¹, S. Mialle³, C. Cruchet³, H. Isnard³, W. Pacquentin³, F. Doreau¹, P. Estevenon¹, J. Lorino¹, L. Picard¹, S. Richter⁴, Y. Aregbe⁴, A. M. Sanchez Hernandez⁵, H. Schorle⁵, R. Buda⁵, U. Repinc⁶, M. Kohl⁶, J. Hiess⁶, G. Duhamel⁶, M. Sumi⁶	191
Development of Uranium Oxide-based Reference Microparticles for Particle Analysis in Nuclear Safeguards	193
Stefan Neumeier¹, Shannon Potts¹, Philip Kegler¹, Giuseppe Modolo¹, Martina Klinkenberg¹, Simon Hammerich², Dirk Bosbach¹, Irmgard Niemeyer¹	193
Laser Ablation- ICP-MS Method Development for a Self-Consistent Calibration in Post Irradiation Examination of Spent Fuels	195
Peter Zsabka¹, Kyle Johnson²	195
Burnup Determination of Irradiated U-Mo Alloy Fuel by ¹⁴⁸Nd Monitor Method	197
Hyejin Cho, Namuk Kim, Yang-Soon Park, Minjae Ha, Tae-Hong Park, Hye-Ryun Cho, Jai Il Park	197
On L-edges X-ray Emission Spectroscopy as a Tool to Study Actinide's Electronic Structure: The Case of Uranium in U_xO_y Compounds	199
P. Silvenoinnen, I. Prozhnev, R. Bes	199

PYROCHEMISTRY AND CHEMISTRY FOR MOLTEN SALTS 202

Overview of Plutonium Pyroprocessing By-Products Management	203
G. Bourgès, S. Faure, O. Lemoine, D. Cardona - Barrau	203
Spent Fuel Reprocessing for Molten Salts Fast Neutron Reactors	205
A. Handschuh¹, P. Ryckewaert¹, P. Baron¹, S. Delpech², C. Cannes², D. Lambertin¹, T. Kooyman¹	205
Pyrochemical Treatment for Molten Salt Nuclear Reactor	207
Joelle Costantine¹, Davide Rodrigues¹, Céline Cannes¹, Elisa Capelli², Bertrand Morel², Sylvie Delpech¹	207
Feasibility of Lanthanide Extraction Assisted by Electrolysis on Li-Bi Liquid Cathode in Molten Fluorides	209
Pierre Chamelot, Mathieu Gibilaro and Laurent Massot	209

Molten Salts and Pyrochemical Processing Progress at the UK's National Nuclear Laboratory	211
Ruth Carvajal-Ortiz, Mike J Edmondson , Moya Hay	211
Synthesis of Actinide Chlorides as Fuel for Fast Molten Salt Reactor	213
P. Chevreux ¹ , M. Duchateau ¹ , G. Serve ¹ , M. Pons ¹	213
Molten Salt Spectroelectrochemistry in Chloride Based Eutectic Systems with Uranium	215
Jessica A. Jackson , Nicole Hege, Jacob Tellez, Jenifer Shafer	215
Influence of Nitrogen on Uranium Metal Stability in Molten LiCl-KCl	217
Théo Caretero ¹ , Laurent Massot ¹ , Mathieu Gibilaro ¹ , Jérémie De Marco ² , Mehdi Arab ² , Pierre Chamelot ¹	217

ACTINIDE AND FISSION PRODUCTS CHEMISTRY 220

Elucidating the Radiation-Induced Redox Chemistry of Plutonium Under Used Nuclear Fuel Reprocessing Conditions	221
G. P. Holmbeck , Amy E. Kynman, Jacy K. Conrad, and Travis S. Grimes	221
How Plutonium "Brown" Peroxo Complex emerges from Aerated Electrolysis Experiments	223
Quentin Hervy ¹ , Richard Husar ¹ , Thomas Dumas ¹ , Philippe Guilbaud ¹ , Matthieu Viot ² , Philippe Moisy ¹	223
The Redox Chemistry of $[M^{VI/III}(3,4,3-LI(1,2-HOPO))]^{0/-}$ Complexes in Acidic Aqueous Media	225
Jeffrey R. McLachlan ^{ab*} , Andrae A. Tabbs ^a , Alex C. Rigby ^a , Joshua J. Woods ^a , Rebecca J. Abergel ^{ab*}	225
Chronicles of Peroxide Plutonium Species: Structural Characterization of New Pu(IV) Green Peroxide	227
J. Margate [1], M. Viot [1], S. Bayle [1], D. Menut [3] T. Dumas [2], E. Dalodière [1], C. Tamain [2], P. Estevenon [2], P. Moisy [2], S. I. Nikitenko [1]	227
Development of Water-Compatible N ₃ O ₂ -Pentadentate Planar Ligands for Uranium Harvesting from Seawater	229
Koichiro Takao ¹ , Takumi Mizumachi ¹ , Minami Sato ¹ , Koma, Ito ¹ , Ryuto Nabata ¹ , Masashi Kaneko ² , Tomoyuki Takeyama ^{1,3} , Satoru Tsushima ^{4,5}	229
Complexation and Solvent Extraction Properties of the N, N, N', N'-tetraethyl-1,10-phenanthroline-2,9-Diamide Extractant with Ln(III) and An(III)	231
Emma M. Archer ¹ , Jocelyn M. Riley ¹ , Felipe A. Pereiro [†] , Elizabeth B. Flynn [†] , Jacob P. Brannon [†] , Stosh A. Kozimor [†] , Jessica A. Jackson [†] , Jenifer C. Shafer [†] , and Shane S. Galley [†]	231
Speciation of Uranium(VI) with Amido-Phosphonate Ligands in Organic Phase and at the Solid/Liquid Interface Studied by Molecular Dynamics	233
Diego Moreno Martinez , Dominique Guillaumont, and Philippe Guilbaud	233
Probing the Metal Ion-Ligand Interaction in An(III) and Ln(III) Complexes: An Overview about Recent Advancements	235
Thomas Sittel ¹ , Patrik Weßling ^{1,2} , Andreas Geist ¹ , Petra J. Panak ^{1,2}	235
Reactivity of Actinides Mono-Cations with NH ₃ in Gas Phase: A Study Using ICP-MS and Quantum Chemistry	237
M. Goujet [1], A. Quémet [1] and D. Guillaumont [1]	237

Crystal Growth of New Uranium and Transuranic Phases via High Temperature Solution and Mild Hydrothermal Methods: Exploration of New Materials as Potential Nuclear Waste Forms	239
<i>H.-C. zur Loye</i> ^{1,2,3,*} , T. K. Deason ^{1,2,3} , A. T. Hines ^{1,2} , H. Tisdale ^{1,2} , T. M. Besmann ^{1,2} , J. Amoroso ^{1,3} , D. P. DiPrete ^{1,3}	239
Molecular and Crystal Structures of Pu(IV)-Nitrate Complexes with Double-Headed 2-Pyrrolidone Derivatives in HNO ₃ (aq).....	241
<i>Ryoma Ono</i> ¹ , Tomoyuki Takeyama ¹ , Robert Gericke ² , Juliana März ² , Tamara Duckworth ² , Satoru Tsushima ^{2,3} , Koichiro Takao ¹	241
The Adsorption of Pu(IV) in the Presence of Cesium Phosphomolybdate, Barium-Strontium Nitrate, Zirconium Molybdate and Zirconium Hydrogen Phosphate	243
<i>Joshua Turner</i> ^a , Christian White ^a , Jessica Blenkinsop ^a , Barbara Dunnett ^a , Adam Bragg ^a , Dan Whittaker ^a , Richard Lynn ^b	243
Performance and Design of HotXAS: the Future In-House XAS Apparatus at Atalante	245
S. Orlat ^{1,2} , R. Bes ² , F. Tuomisto ² , P. Martin ¹ , P. Moisy ¹	245
Investigation of the Microcosmic Dynamics Behaviors of Hydrogen and Oxygen in Plutonium Oxide via Ab Initio Molecular Dynamics Simulations	247
<i>Jun Tang</i>	247

PLENARY TALKS

Global Overview on the Nuclear Fuel Cycle Backend and IAEA Related Activities

Clément Hill, Amparo Gonzalez-Espartero

International Atomic Energy Agency, Vienna International Centre, PO Box 100, Vienna, Austria, 1400 (c.hill@iaea.org)

One of the main concerns of the population regarding nuclear power is the safe management of the Spent Nuclear Fuel (SNF) after discharged from the reactors. There are however technical solutions, implemented since the inception of nuclear power in the 50's, and SNF has been safely managed for more than 60 years, worldwide.

Currently, 417 nuclear power reactors operate in 31 countries. SNF is discharged at a rate of about 10,000 tHM/year. As of the end of 2022, the accumulated SNF inventory that has been globally discharged since the deployment of nuclear power amounts to approximately 430,000 tHM, of which around 70% are currently stored (under wet and dry conditions), waiting for further steps or final disposition, and the rest has been reprocessed (mostly for recycling valuable fissile materials). The lifetime extension of some nuclear reactors is contributing to an increase in the amount of stored SNF.

Understanding the behaviour of SNF in various storage systems, as well as the ageing and degradation mechanisms of storage structures, systems and components, remains vital to ensure that SNF can continue to be stored safely and subsequently transported to disposal or reprocessing facilities, even after long term storage. As spent fuel disposal programmes are progressing and approaching the final stages of construction in some Member States, there has been an increase in the number of preparation activities, such as the development of characterization programmes. Continuation of such efforts is particularly important when considering that greater reactor efficiencies have been achieved through the production of SNF with higher initial enrichments and higher burnups, leading to increases in thermal outputs and potentially higher risks of cladding embrittlement that may impact subsequent SNF management steps.

Despite an overall reduction in global spent fuel reprocessing capacity (after the closure of reprocessing plants in the United Kingdom), there is an increasing interest in the development of advanced recycling technologies. As new fuel designs are envisaged for both existing fleets of nuclear reactors and those of future advanced reactor designs (including SMRs), which may lead to potentially different behaviours in SNF management, innovative SNF management solutions will need to be sought to allow for their timely deployment. International collaboration and partnership will therefore be paramount for their success. The main goal of nuclear scientists, engineers, operators, and regulators, today, is thus to continue improving, developing and licensing new technologies to address current and future challenges of the nuclear fuel cycle backend, so as to ensure the nuclear fuel cycle sustainability, through advanced nuclear energy systems that can preserve natural resources and reduce the burden of the nuclear waste generated.

Integration of new and innovative fuel cycles with existing fuel cycles is an important undertaking to address current energy supply challenges and ensure the sustainable, safe and secure development of nuclear power. While already implemented in some countries, initiatives to address advanced reactors' spent fuel and radioactive waste management, in an integrated manner, are starting to be discussed and developed in several countries.

The International Atomic Energy Agency (IAEA) supports sustainable, safe, secure, reliable and economic nuclear fuel cycles associated with current and future generations of nuclear power reactors, by providing its 178 Member States with relevant technical information (guidance) based on operational experience and best industrial practices, through:

- The coordination of international research activities, via Coordinated Research Projects [1-3] (CRPs), the final reports of which compile research findings, and policy and strategy approaches in Member States;
- The organization of technical events, workshops and international conferences to provide Member States with fora for sharing technical information, such as:
 - o The Technical Meeting on "Challenges, Gaps and Opportunities for the Management of SNF from SMR Technologies", that gathered more than 100 participants from 32 countries in September 2022, the Proceedings of which were published last December [4],
 - o The International Conference on Spent Fuel Management from Nuclear Power Reactors, to be held in Vienna, on 10-14 June 2024;

- The publication of technical reports [5,6] or guides (including interactive publications [7]), compiling relevant information and best practices;
- The management of specific databases; and
- The development of e-learning materials [8] and infographics (Fig.1) for capacity building in Member States.

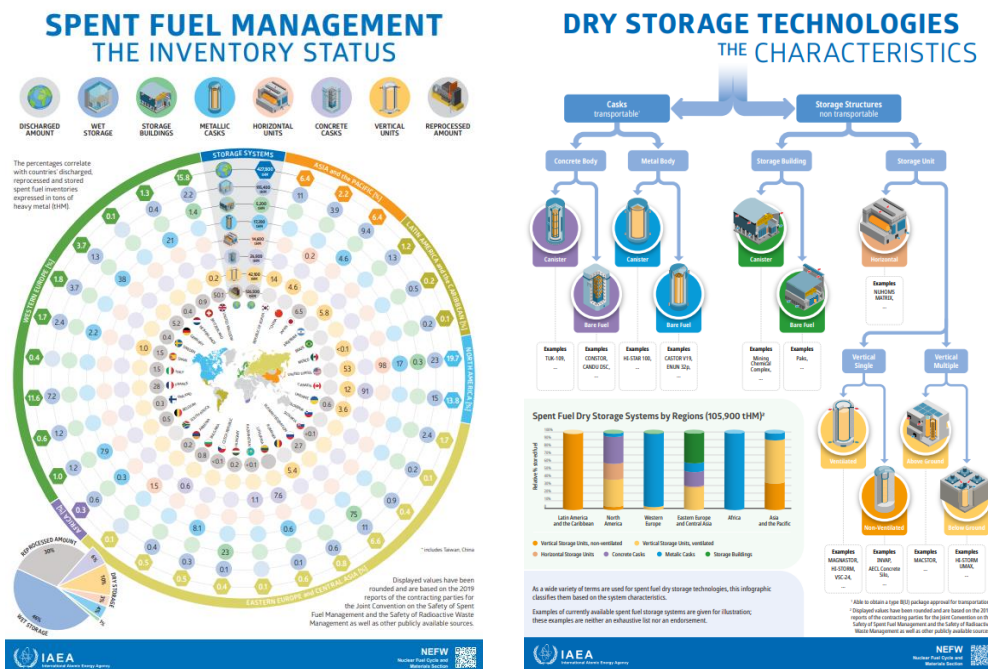


Fig.1. Inventory of SNF around the world (amount of SNF discharged, reprocessed and stored by country and by storage system) and Dry Storage technologies.

The presentation will provide an overview on the issues of the backend of the nuclear fuel cycle, worldwide, and on the IAEA programmatic activities in support of its Member States under the sub-Programme on the Management of Spent Fuel from Nuclear Power Reactor and Radioactive Material Transportation.

References:

- [1] CRP T13020 on "Spent Fuel Research and Assessment (SFERA)": <https://www.iaea.org/projects/crp/t13020>.
- [2] CRP T13019 on "Performance Assessment of Storage Systems for Extended Durations (PASSED)": <https://www.iaea.org/projects/crp/t13019>.
- [3] CRP T13021 on "Challenges, Gaps and Opportunities for Managing Spent Fuel from Small Modular Reactors": <https://www.iaea.org/projects/crp/t13021>.
- [4] INTERNATIONAL ATOMIC ENERGY AGENCY, IAEA-TECDOC-2040, Considerations for the Back End of the Fuel Cycle of Small Modular Reactors. Proceedings of a Technical Meeting, IAEA, Vienna (2023).
- [5] INTERNATIONAL ATOMIC ENERGY AGENCY, IAEA-TECDOC-1967, Status and Trends in Pyroprocessing of Spent Nuclear Fuels, IAEA, Vienna (2021).
- [6] INTERNATIONAL ATOMIC ENERGY AGENCY, IAEA Nuclear Energy Series No. NF-T-4.11, Technical Approaches for the Management of Separated Civilian Plutonium, Vienna (2023).
- [7] INTERNATIONAL ATOMIC ENERGY AGENCY, Guidebook on Spent Fuel Storage Options and Systems: [Guidebook on Spent Fuel Storage Options and Systems \(iaea.org\)](https://www.iaea.org/publications/guidebook-on-spent-fuel-storage-options-and-systems).
- [8] Course on Spent Fuel Management: [Course on Spent Fuel Management | IAEA](https://www.iaea.org/courses-and-training/spent-fuel-management).

Status of the French Nuclear Fuel Cycle Program

François Sudreau

Energy Division, CEA, Centre de Paris-Saclay, 91191 Gif-sur-Yvette, France

Context

This presentation gives an update concerning the French nuclear fuel cycle R&D program.

Currently, the French nuclear fuel cycle is based on plutonium monorecycling, that is to say that plutonium is recovered from UOx spent fuel and reused in MOX fuel. After irradiation, these MOX fuels are stored. They are not considered in France as nuclear waste as they contain valuable fissile materials, including around 6 % of plutonium, and as the feasibility of their reprocessing has been demonstrated since 70 tonnes of spent MOX fuels have already been reprocessed in France, at Marcoule and La Hague facilities.

This strategy allows to save 10 % of natural uranium compared to an open cycle, avoids to have plutonium in the final waste to be stored in deep geological repository, decreases the net production of plutonium of the nuclear reactor fleet and allows to stabilize the UOx spent fuel inventory.

On February 2022, President Macron expressed his wish that, in addition to pursuing the massive development of renewable energy sources, the lifespan of current reactors be extended, subject to the agreement of the ASN, whenever possible. In addition, a program for six EPR2 type reactors is launched as a first step to guarantee France's energy independence and achieve carbon neutrality by 2050. Moreover, French Government has launched a major Investment Plan for the Future called "France 2030". One objective of this plan is to promote the emergence, in France, of innovative nuclear reactors. In that plan, approximately €500 million are allocated to innovative reactor projects, based on a call for projects that has been published in March 2022. Research and innovation around breakthrough nuclear reactor concepts should thus provide new answers to the challenges specific to the nuclear industry, for example in terms of competitiveness, safety, security, closing the nuclear fuel cycle or reducing the volume and activity of radioactive waste. Thus, 11 projects (9 for fission reactors and 2 for fusion ones) were selected to be awarded, leading to a cumulative state support of 130 million euros.

All these decisions have an important impact on the future French nuclear fleet and consequently on possible nuclear fuel cycles. In this field, in February 2024, the Nuclear Policy Council, chaired by President Macron, confirmed the main thrusts of French policy on the fuel cycle back end, combining reprocessing and reuse of spent fuel, with an objective of a closed fuel cycle. Following this decision, Bruno Le Maire, French Minister of the Economy, Finance and Industrial Sovereignty, announces in March 2024 (i) a program to extend the lifetime of the La Hague and Melox plants beyond 2040, (ii) the launch of studies for a new MOX fuel fabrication plant and (iii) the launch of studies for a new spent fuel processing plant by 2045/2050.

Plutonium Multirecycling in LWR

For the medium term, CEA, Orano, EDF and Framatome have launched a major R&D program and associated industrial feasibility studies for plutonium multirecycling in Light Water Reactor. Three strategic objectives have been defined. First, characterize the interest of multirecycling compared to monorecycling in terms of materials and waste management. Second, assess the industrial feasibility of the multirecycling in Light Water Reactors considering, on one hand, the impacts on the reactors in terms of safety and performances and, on the other hand, on the current and future backend facilities and logistics (particularly transportations). Third, evaluate the technical and economic impact of multirecycling compared to monorecycling.

After several assessments and optimizations of fuels made with multi-recycled plutonium and core management strategies, a standard MOX fuel assembly, using a low fissile plutonium quality, called MOX-MR for "MOX-Multi-Recycling" has been defined. Industrial deployment scenarios have been simulated, considering a future French EPR fleet with a combined installed capacity of 40 or 50 GWe, and plutonium multirecycling from 2046. These simulations show that, until the end of the century (i) plutonium and uranium multirecycling in LWR could allow saving 40 % of natural uranium compared to an open cycle, (ii) spent MOX fuel inventory could be stabilized and total spent fuel inventory reduced and (iii) plutonium inventory can thus be stabilized.

Closing the nuclear fuel cycle

Beyond plutonium multirecycling in PWR, France maintains the objective of the full closure of the nuclear fuel cycle using Fast Reactors. The goals of this next step are (i) the full independence from natural uranium input using the depleted uranium stockpiles resulting from enrichment activities and (ii) the long-term stabilization of zero net production of plutonium and spent fuel. The reference path is to pursue the development of high-power Sodium-cooled Fast Reactor technology and deploy them, if necessary, by the end of the century. In the same time, in the frame of France 2030 plan, other concepts, particularly Advanced Modular Fast Reactors, such as SRF (sodium cooled), LFR (lead cooled) and MSR (molten salt) reactors, are considered by new comers to be part of the solution for the reduction of the MOX fuel inventory and even of the waste that today are destined to be stored in deep geological repositories.

In this context, studies have been launched to explore the potential of fast neutron molten salt reactors for actinide transmutation. These reactors could be fed only with plutonium (in particular plutonium with a low isotopic vector) or with plutonium and minor actinides. An R&D on the priority items, with lower technological maturity, is thus in progress in the frame of the Fourth Investment Program for the Future started in 2022.

Impacts on treatment and fabrication processes

Today, with plutonium monorecycling, there is no industrial MOX fuel treatment and MOX fuel is manufactured with a 9 % plutonium content. With plutonium multirecycling in PWR, it would be necessary to treat MOX and MOX2 fuels and MOX fuel production would be multiplied by around three. Moreover, plutonium multirecycling in Fast Reactors would need to treat and manufacture MOX fuels that could have a plutonium content up to, at least, 25 % and probably 30 %, or even more.

Thus, some challenges have to be overcome to implement plutonium multirecycling. Concerning MOX reprocessing, two main steps are considered in French R&D programs: dissolution and separation. For the dissolution step, voloxidation, which allows to turn irradiated fuel pellets into powders, and thus to increase surface contact and dissolution kinetics, is investigated theoretically and experimentally on fresh and irradiated MOX fuels. For the separation step, a program is performed to develop and industrialize a single cycle process without oxydoreduction reactions. Indeed, using monoamide solvents seems to be an interesting alternative to TBP due to their good stability, high selectivity and high recovery factor for uranium and plutonium. This high selectivity allows considering a simpler flowsheet with a single cycle for extraction and purification of plutonium and uranium. Moreover, in this process, partitioning is made by changing the acidity of the solution, avoiding using oxydoreduction and stabilisation agents. This will lead to a process well adapted to high plutonium contents, more compact, less expansive and easier to control than the current separation process.

Conclusion

To conclude, the use of nuclear energy will increase and diversify in the world in the next decades. Thus, it is necessary to preserve the natural resources recycling reusable fissile materials. France is evaluating a step-by-step approach starting with plutonium multirecycling in PWR, before reaching the full nuclear fuel cycle closure using Fast Reactors. In that way, France is performing a large R&D program, particularly on innovative reprocessing and fuel fabrication processes.

At the same time, through collaborations between CEA, Orano, EDF, Framatome and CNRS, as well as with new emerging players, the value of advanced technologies is being assessed with a view to improving the management of plutonium and minor actinides.

Nuclear Fuel Recycle Activities in the Office of Nuclear Energy

Stephen Kung

*Office of Nuclear Fuel Cycle, U.S. Department of Energy
19901 Germantown Road, Germantown, MD 20874-1207*

This presentation will cover the nuclear fuel recycle research and development (R&D) activities supported by the U. S. Department of Energy, Office of Nuclear Energy (DOE-NE). DOE-NE conducts applied R&D on advanced fuel recycle technologies that have the potential to improve resource utilization and energy generation, reduce waste generation, and limit proliferation risk. DOE-NE focuses on developing advanced fuel recycling technologies and addressing fundamental materials separations and recovery challenges that present significant degrees of technical risks and financial uncertainties. DOE-NE stewards the capabilities and knowledge relied upon by policy makers to make informed decisions regarding nuclear fuel cycle options. Such decisions in turn rely on the development of efficient and economical separation methods that can accept the used nuclear fuel containing actinides and fission products to recycle selected actinides, recover valuable by-products, and deliver waste streams that are suitable for disposal. DOE-NE supports the development and demonstration of various recycling technologies to make available small quantities of high-assay low enriched uranium materials for advanced reactor fuel-fabrication R&D needs.

Future Fuel Cycles – a UK Perspective

Paul Nevitt

National Nuclear Laboratory, Chadwick House, Birchwood Park, Warrington, WA3 6AE, UK

UK Civil Nuclear Roadmap and Current Perspective

UK Government has set out a vision and plan for fuel cycle in the UK. The UK Civil Nuclear Roadmap^a published earlier in 2024 by UK Government set out how the fuel cycle underpins both government's net zero and national security objectives. The roadmap set out key aspects of future fuel cycles in the UK. As the UK embarks on a nuclear renaissance, the ability to deliver this in a way that continues to enable national security outcomes depends on the UK regenerating its domestic fuel cycle capabilities. This focuses on three key areas: front end fuel production, research and innovation in advanced uranium-based fuels, and maintenance and development of a skilled workforce.

In addition, while the current inventory of spent nuclear fuel and radioactive waste is either stored on nuclear power station sites or at Nuclear Decommissioning Authority (NDA) sites such as Sellafield, the UK long-term strategy for finally disposing of the most highly active radioactive waste inventory is to develop an engineered Geological Disposal Facility (GDF). A process is well underway to identify a suitable site in which to develop a GDF that has suitable geology and the support of a local community. However, the first spent fuel is not expected to be placed into a GDF until the 2050s. Until then, there is sufficient interim storage for the inventory from UK legacy, existing nuclear fleet and currently planned future plants.

Finally, the UK reprocessed spent fuel on an industrial scale from the 1950s to 2022. Commercial industrial scale reprocessing came to an end in the UK with the closure of the Thermal Oxide Reprocessing Plant (THORP) in 2018. There is currently no industrial scale reprocessing in the UK and no plans to restart reprocessing.

Managing the UK Legacy

It is clear that the journey from nuclear fuel cycle to waste management and environmental restoration is evolving in the UK. The NDA has responsibility for managing inventories of legacy nuclear materials including spent fuels and plutonium on behalf of the nation^b. The NDA mission will span decades and takes billions in investment, it will require new plants, new processes, new stores, new disposal facilities. It is replete with technical challenges and opportunities. All needing highly multi-disciplinary teams with diverse skill sets. The strategic approach in the UK is focused around: consolidate, storage, disposition (right solution), safeguards assurance, counter-proliferation.

In relation to spent fuels disposition, in 2012 the NDA and UK government took the decision to complete the reprocessing contracts and commit the remaining (predominantly) Advanced Gas Reactor (AGR) fuel, and future arisings, to long-term pond storage. This is considered the most cost-effective and viable strategy but means that the UK had to underpin this approach including the storage and disposal of around 5,000 tonnes of AGR fuel. Research and development to underpin and support this includes: corrosion trials of fuels, condition monitoring of fuels, disposability studies.

The UK has also set out its approach to plutonium management through the NDA Strategy^b. Plutonium has been produced at Sellafield since the early 1950s from the reprocessing of spent fuel from UK power stations and overseas utilities. There is around 141 tonnes owned by NDA and its customers. Most of it is stored as a powdered oxide form in storage cans but some of the material is in the form of residues and various powders, pellets and assemblies. Government's objective is to put the plutonium beyond reach. This could be by reuse as Mixed Oxide Fuel (MOX) in nuclear reactors or as an immobilised product. This would put the material in a form which reduces the long-term security risks and burden during storage and is aligned with its ultimate disposal in a GDF. In addition, the plutonium science and support to can surveillance programme is critically important to reducing the risks with the long-term storage of plutonium. The NDA are continuing to progress the development of the reuse as MOX and immobilisation options.

^a <https://www.gov.uk/government/publications/civil-nuclear-roadmap-to-2050>

^b https://assets.publishing.service.gov.uk/media/605cb82fd3bf7f2f112f0f84/NDA_Strategy_2021_A.pdf

Key strategic decisions have been made by NDA and UK government over the last decade to bring about the benefits of consolidation of fuels and materials and the completion of reprocessing. There will be considerable demand for R&D to support future strategy development and underpinning. For spent fuels much of this technical work is around approaches to storage, transport and ultimately disposal. The plutonium programme will last decades, and the supporting R&D programme is a major UK endeavour.

Looking to the Future

Finally, looking over the longer term towards future sustainable fuel cycles, the UK invested significantly in the 'Nuclear Innovation Programme'. This included, the Advanced Fuel Cycle Programme (AFCP)^c, led by the National Nuclear Laboratory, to develop the next generation of nuclear fuels and fuel cycles. AFCP marked the biggest public investment in future nuclear fission fuel cycle R&D in a generation in the UK – AFCP looked at the role of advanced nuclear fuels and fuel cycles for a Net Zero future (Figure 1). With UK Government committed to achieve carbon neutrality by 2050, AFCP aimed to lay the foundation from which the UK could maximise its current capability, meet Net Zero and deploy sustainable fuel and recycling concepts through the future. AFCP pioneered a uniquely collaborative approach to innovation. Uniting NNl's unique nuclear infrastructure with the innovative skills and capabilities of more than 100 organisations across over 10 countries, AFCP delivered a suite of fuel cycle science themes with measurable impact across Britain's evolving low-carbon landscape. Including delivering future roadmaps across advanced fuels and fuel cycles^d.

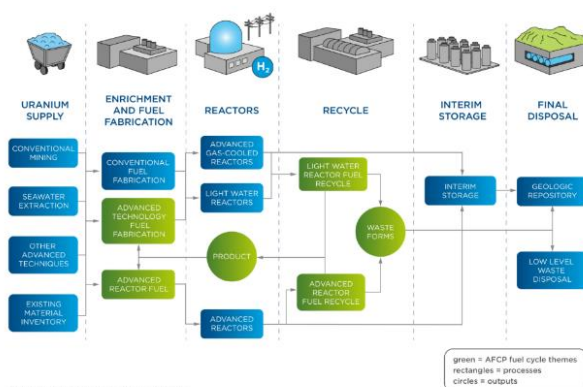


Figure 1. Schematic representation of the UK fuel cycle with the focus areas of the Advanced Fuel Cycle Programme (AFCP) highlighted in green.

Working collaboratively for a sustainable future

Through bilateral and multi-lateral international relationships the UK continues to drive forward the importance of sustainable fuel cycles and the R&D needed to underpin these, such that options are available to decision and policy makers in a timely fashion. The fuel cycle underpins and will continue to be an essential part and enabler to the UK government's net zero and national security objectives.

^c AFCP – Advanced Fuel Cycle Programme – Advancing fuel cycle innovation to secure a Net Zero future (nnl.co.uk)

^d <https://afcp.nnl.co.uk/wp-content/uploads/sites/3/2021/06/AFCP-Advanced-Nuclear-Roadmaps.pdf>

ACTINIDE AND FISSION PRODUCTS SEPARATION

Overview of the Material Recovery and Waste Form Development Program

Kenneth C Marsden

12525 N Fremont Ave, Idaho Falls, ID 83402

The Material Recovery and Waste Form Development program is led by and funded through the Office of Materials and Chemical Technologies inside the U.S. Department of Energy, Office of Nuclear Energy. It is a research program with a mission to develop advanced fuel recycling technologies to improve resource utilization, reduce repository burden, limit proliferation risk and improve economics. Program activities include (1) use of recycling technologies to produce HALEU materials for advanced reactor fuel-fabrication R&D needs; (2) resolution of nuclear materials separation and recovery challenges for various advanced reactor fuel designs; (3) development of efficient and economical technologies for commercially viable future industrial deployment; and (4) expansion of capabilities and knowledge in nuclear chemistry for a broad range of nuclear applications. Technical areas inside the research program include simplified aqueous separations, vapor phase processes, pyrochemical processes, molten salt fuels, recycling off-gas management, and advanced waste form development.

Lab-Scale Pulsed Columns Trials for a New Nuclear Fuel Recycling Process

Garzon Losik German, Lamadie Fabrice, Roussel Hervé

CEA, DES, ISEC, DMRC, Univ. Montpellier, Marcoule, France

Context and goals

CEA is currently developing a new spent nuclear fuel reprocessing process, which is especially effective for fuels with high plutonium content. The process uses an N,N-dialkylamide extracting molecule.

To validate the process chemistry, complete extraction cycles are performed using surrogate feed solutions (uranium and plutonium) or actual spent fuel solutions. These tests are performed in laboratory-scale mixer-settlers, which have the advantage of being miniaturisable and easy to operate in a nuclear confinement enclosure [1].

However, the pulsed column will be the device selected for a future facility, as in the current Orano plant at La Hague. This apparatus offers several advantages over the mixer-settler, such as cruds management, criticality control, and the absence of moving parts. It is mandatory to ensure that this type of apparatus performs correctly with the new solvent, both in terms of hydrodynamics and mass transfer efficiency.

The knowledge and experience of CEA and Orano in the operation of pulsed columns with the current TBP-based solvent cannot be directly applied to the new solvent due to its higher viscosity when loaded with uranium. Therefore, a new study on the operation of pulsed columns is necessary. The latter involves both experimental work and a modeling and simulation approach to support scaling up to an industrial size. This communication presents the results of the experimental part of this approach.

The objective of this experimental work is twofold: first, to demonstrate the suitability of the new solvent to be used in pulsed columns under the conditions specified for the new industrial process (including specific flow rates, flow rate ratios, and uranium load); and second, to collect data to validate the modelling of the pulsed column hydrodynamics.

Initial tests were conducted using the smallest columns available at the CEA (15 mm in diameter), in order to minimize the required quantities of uranium and solvent. These tests allowed us not only to optimize the column packing, taking into account the solvent viscosity, but also to demonstrate the efficiency of these columns for uranium extraction and back-extraction.

When scaling up from 15 mm columns, the first larger diameter chosen is 25 mm. This diameter allows for a significant increase in flow rates (by a factor of 2.8, corresponding to the cross-section ratio). Furthermore, it is the smallest diameter suitable for disc and doughnut packing, which is the type of packing used in industrial columns.

Material

The columns, of a height of 2 meters, used in the experiments are made of glass and have stainless steel packing with settlers located at both ends of them.

A pneumatic type pulser, similar to those used at industrial scale at La Hague plant, is used to ensure mixing inside the column. Fluids are circulated using pumps combined with Coriolis flowmeters.

Different types of characterisation are possible.

- For single-phase tests: measuring residence time distribution by injecting an optical tracer on the inlet side of the column and monitor its concentration on the outlet side using an online refractometer.
- For two-phase tests: measuring the dispersed phase hold-up by sampling the emulsion; additionally, capturing images using an endoscope (SOPAT GmbH) to obtain the droplet size distribution [2].

Single-phase tests

The tests begin with a single phase, either aqueous (simple distilled water) or organic (a mixture of alkanes with the same viscosity as the N,N-dialkylamide based solvent loaded with uranium).

The first objective of these tests is to verify the possibility of obtaining a pulsating movement in the column, despite the solvent's viscosity.

The main purpose is to determine the axial mixing by measuring the residence time distribution. Axial mixing is a critical parameter for column efficiency and is also a validation criterion for CFD simulations.

It was found that axial mixing is not dependent on the flow rate or phase nature, but solely on the pulsation amplitude. A correlation derived from previous studies on other fluids correctly estimates this axial mixing [3].

Two-phase tests

Various parameters have been tested including flow rates (ratio of organic to aqueous phase and total flow rate of both phases) and the pulsation amplitude. Both types of emulsions, oil-in-water and water-in-oil, were tested to cover the majority of operating conditions of the columns in the future process. Several hundred sets of operating parameters were tested.

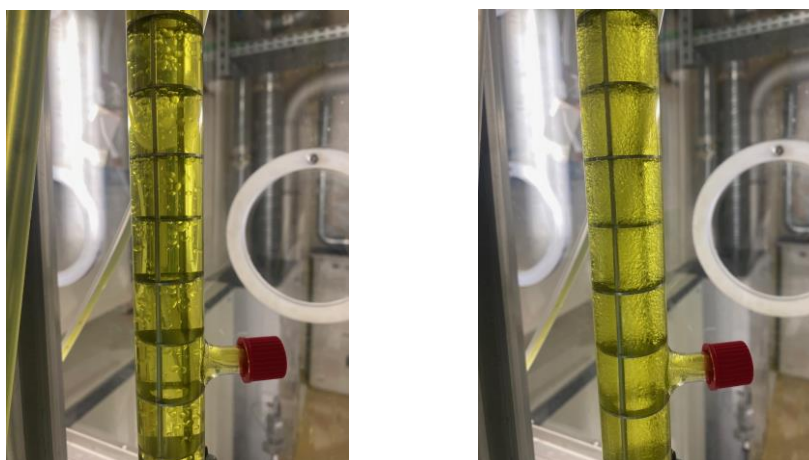
Among other results, the measurements allow:

- To plot the range of correct column operation on a Sege and Woodfield diagram,
- To monitor the evolution of the dispersed phase hold-up as a function of flow rates and pulsation amplitude,
- To quantify the trends of the droplet size distribution as a function of these parameters. It appears that this distribution is particularly sensitive to pulsation, with size decreasing as amplitude increases.

Conclusion and outlook

It has been experimentally demonstrated that the N,N-dialkylamide based solvent enables proper hydrodynamic operation of pulsed columns with disc and doughnut packing.

The study will continue by gradually approaching the operating conditions of industrial columns. The next steps will be to test extraction cycles with nitric acid and then with uranium in 25 mm diameter columns, and conducting hydrodynamic tests with uranium-loaded solvent in 100 mm diameter columns.



Various aspects of the emulsion in a 25 mm diameter pulsed column with disc and doughnut packing

References

- [1] Design, development and testing of miniature Liquid-Liquid Extraction contactors for R&D studies in nuclear environment, H. Roussel & S. Charton, *Procedia Chemistry* 21 (2016) 487-494
- [2] Automated drop detection using image analysis for online particle size monitoring in multiphase systems, S. Maaß et al., *Computers & Chemical Engineering* 45 (2012) 27-37
- [3] Axial dispersion in pulsed disk and doughnut columns: A unified law, S. Charton et al., *Chemical Engineering Science* 75 (2012) 468-477

Potential of Aggregation Control for Solvent Extraction Separation

Cyril Micheau,^a Yuki Ueda,^a Ryuhei Motokawa,^a Kazuhiro Akutsu-Suyama,^{b, c} Norifumi L. Yamada,^d Masako Yamada,^d Sayed Ali Moussaoui,^e Elizabeth Makombe,^e Daniel Meyer,^e Laurence Berthon,^f Damien Bourgeois^e

^a Materials Sciences Research Center, Japan Atomic Energy Agency, Tokai, Ibaraki 319-1195, Japan – ^b Comprehensive Research Organization for Science and Society, Tokai, Ibaraki 319-1106, Japan – ^c J-PARC Center, Japan Atomic Energy Agency, Tokai, Ibaraki 319-1195, Japan – ^d Institute of Materials Structure Science, High Energy Accelerator Research Organization (KEK), Tsukuba, Ibaraki 305-0801, Japan – ^e Institut de Chimie Séparative de Marcoule, ICSM, CEA, CNRS, ENSCM, Univ Montpellier, BP 17171, Marcoule, 30207 Bagnols-sur-Cèze, France – ^f CEA, DES, ISEC, DMRC, University of Montpellier, Marcoule, 30207 Bagnols-sur-Cèze, France

Among the several processes developed for the advanced reprocessing of spent nuclear fuel, the DIAMEX (DIAMide Extraction) process uses malonamide molecules for the separation and co-extraction of actinides and lanthanides from the raffinate of the PUREX (Plutonium Uranium Reduction Extraction) process. Several studies were dedicated to the so called third-phase formation that occurs at high metal loading or in specific acid conditions in aliphatic solvents.[1] It was usually concluded that this deleterious phase arises from the formation of supramolecular aggregates mainly composed of the extractant molecules.[2] On the other hand, recent study on the use of malonamide molecules for the extraction and separation of Pd(II) and Nd(III) by solvent extraction has pointed out two main driving forces that could explain the selectivity: coordination and extractant aggregation.[3] It has thus been demonstrated that, Pd(II) only needs coordination to be extracted whereas Nd(III) needs, in addition, the aggregation of the extractant. From these observations it has been highlighted that extractant aggregation can be beneficial for solvent extraction process if it can be controlled to enhance separation whilst avoiding third-phase formation.

In order to confirm a potential correlation between the separation efficiency and the extractant aggregation, and to determine the physicochemical parameters that triggers the supramolecular organization, a model malonamide molecule used in the DIAMEX process, *i.e.* DBMA (N,N'-Dimethyl-N,N'-dibutyl-2-tetradecylmalonamide), was investigated. This extractant was dissolved, at room temperature, in pure *n*-heptane, pure toluene, and mixtures of both solvents at different ratios, and contacted with different nitric acid solutions (0 M, 1 M, 3 M and 5 M HNO₃) with and without the presence of two metal ions, *i.e.* Pd(II) and Nd(III). These two solvents possess different relative permittivity at room temperature (*i.e.*, $\epsilon_{\text{heptane}} = 1.924$, $\epsilon_{\text{toluene}} = 2.392$), and topology with an aromatic ring for toluene that could lead to additional π -interaction with the extractant [4, 5].

For each experimental condition, distribution ratios of Pd(II) (D_{Pd}) and Nd(III) (D_{Nd}), as well as separation factors ($S_{\text{Pd/Nd}} = D_{\text{Pd}}/D_{\text{Nd}}$) were determined (see Figure 1a and b). In parallel, small-angle neutron scattering (SANS) technique was used to determine the size and shape of the aggregates formed (see Figure 1c and d). From these results, it can be said that *n*-heptane promotes the formation of large assemblies (high initial scattering intensity, I_0 , and large gyration radius, R_g), whereas the presence of toluene tends to reduce the size of the assemblies (low I_0 , small R_g) which was directly correlated to extraction separation efficiency. In addition, these results confirmed that water and nitric acid molecules contributes to the extractant aggregate's structure leading to larger aggregates, as the scattering intensity increases, when the nitric acid concentration increases.

Finally, it can be concluded that the selectivity of the process can be control by the size of the aggregates which is triggered by the organic solvent properties. In the present study, solvent nature was modified using different mixtures to control the process efficiency. In addition, the potential of aggregation control for solvent extraction separation can be directly applied for the extraction of Pd from automotive catalysts or shredded electronic scraps. This strategy can also be extended to most of the extractant molecules involved in the spent nuclear fuel recycling strategy as they all possess an amphiphilic nature and, for some of them, their aggregation properties have already been characterized in the literature.

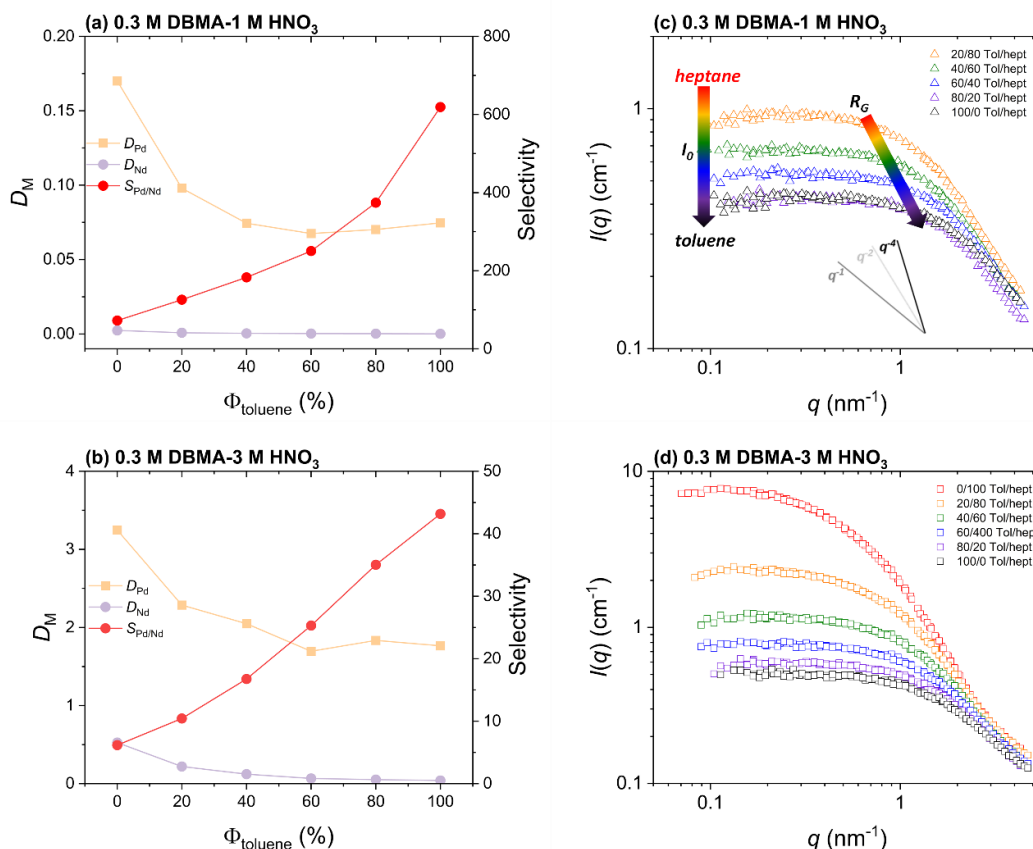


Figure 1: Distribution ratio (D_M) and selectivity factor ($S_{Pd/Nd}$) of Pd(II) and Nd(III) (a, b), and SANS data of DBMA (c, d) as function of toluene/n-heptane volume ratio, pre-contacted with 1 M nitric acid solution (a, c) and 3 M nitric acid solution (b, d) (initial metal concentration: $[\text{Pd(II)}]_{\text{aq}}=100\text{mg/L}$, $[\text{Nd(III)}]_{\text{aq}}=200\text{mg/L}$). I_0 represent the scattering intensity at low scattering wave vector q , and R_g is the gyration radius of the scatterers.

References:

- [1] B. F. Smith, K. V. Wilson, R. R. Gibson, M. M. Jones, G. D. Jarvinen, Sep. Sci. Technol., 32:1-4, 1997, 149-173, (DOI: 10.1080/01496399708003192)
- [2] F. Testard, T. Zemb, P. Bauduin, L. Berthon, Liquid/Liquid Extraction: A Colloidal Approach, Vol. 19 (Ed. B. A. Moyer), CRC Press, Boca Raton, 2010, pp. 381-428
- [3] R. Poirot, X. Le Goff, O. Diat, D. Bourgeois, D. Meyer, ChemPhysChem Commun., 17, 2016, 2112-2117 (DOI: 10.1002/cphc.201600305)
- [4] A. A. Maryott, E. R. Smith, Table of Dielectric Constants of Pure Liquids, National Bureau of Standards Circular 514, USA, 10, 1951
- [5] G. Ritzoulis, N. Papadopoulos, D. Jannakoudakis, J. Chem. Eng. Data, 31, 1986, 146-148 (DOI: 10.1021/jc00044a004)

Evolution of Uranium Recovery: Past, Present, and Future Perspectives

Santa Jansone Popova¹, Jopaul Mathew¹, Jeffrey Einkauf¹, Alexander Ivanov¹, Ilja Popovs¹,
Connor Parker¹, Peter Zalupski², Travis Grimes², Corey Pilgrim²

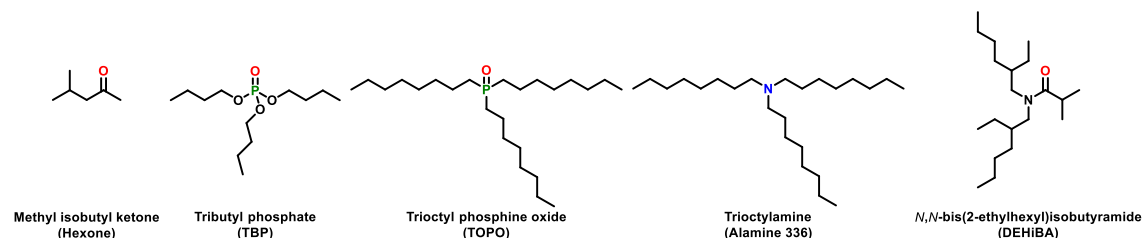
¹Oak Ridge National Laboratory, Oak Ridge, TN 37932

²Idaho National Laboratory, Idaho Falls, ID 83415

Over the past eight decades, extensive research has been dedicated to the domains of uranium recovery, purification, reprocessing, and recycling, propelled by its critical applications in nuclear technology. Nowadays, the nuclear power stands as an important source of electricity, contributing approximately 10% to global electricity generation.¹ The hydrometallurgical process for uranium extraction has undergone notable evolution throughout this period.

The REDOX plant, commissioned in 1951, was the very first reprocessing facility based on countercurrent, continuous flow separation of plutonium and uranium utilizing aliphatic ketone as an extractant.² A few years later, in 1955, the initiation of operations at the PUREX plant employed tributyl phosphate as an extractant.^{2,3}

The exploration of organic, lipophilic extractants, including trialkyl phosphine oxides⁴ and monoamides (GANEX 1st cycle process)⁵, as well as lipophilic ion exchangers like protonated trialkylamines (AMEX process)⁶, has been integral to the ongoing pursuit of efficient U(VI) separation in solvent extraction methods⁷. These developments underscore the dynamic nature of uranium processing methodologies, emphasizing the continuous quest for enhanced technologies in the realm of nuclear fuel cycle management.



This presentation will provide a concise overview of challenges encountered in established uranium recovery processes, encompassing issues like the stability of organic extractants under process-relevant conditions, solvent hydrodynamic properties, and variations in selectivity. A central focus will be on novel solvating extractants designed for U(VI) recovery. Particular attention will be given to exploring the impact of varying alkyl group size within extractants on both selectivity and stability.

The evolution of uranium processing spanning more than 80 years, bridging historical achievements with the latest cutting-edge developments, providing valuable insights into the continual refinement of uranium recovery methodologies will be presented.

References:

- [1] World Nuclear Association, World Nuclear Performance Report 2023. World Nuclear Association (2022).
- [2] M. S. Gerber, The Plutonium Production Story at the Hanford Site: Processes and Facilities History. Report WHC-MR-0532, Westinghouse Hanford Company (1996).
- [3] W. B. Lanham, T. C. Runion, PUREX Process for Plutonium and Uranium Recovery. Report ORNL-479, Oak Ridge National Laboratory (1949).
- [4] C. A. Horton, J. C. White, Separation of Uranium by Solvent Extraction with Tri-n-octylphosphine Oxide. *Analytical Chemistry* **1958**, 1779-1784.

- [5]** T. H. Siddall, III, Effects of structure of N,N-disubstituted amides on their extraction of actinide and zirconium nitrates and of nitric acid. *Journal of Physical Chemistry* **1960**, 1863–1866. C. Musikas, Potentiality of Nonorganophosphorus Extractant in Chemical Separations of Actinides. *Separation Science and Technology* **1988**, 1211–1226. S. Suzuki, Y. Sasaki, T. Yaita, T. Kimura, Study on Selective Separation of Uranium by N,N-dialkylamide in ARTIST Process. *ATALANTE* **2004**. M. Miguiditchian, L. Chareyre, C. Sorel, I. Bisel, P. Baron, M. Masson, development of the GANEX process for the reprocessing of Gen IV spent nuclear fuels. *ATALANTE* **2008**.
- [6]** D. J. Crouse, K. B. Brown, The Amex Process for Extracting Thorium Ores with Alkyl Amines. *Journal of Industrial & Engineering Chemistry* **1959**, 1461–1464.
- [7]** J. D. Law, Aqueous Reprocessing of Used Nuclear Fuel. Report INL/MIS-17-40915, Idaho National Laboratory (**2018**). C. R. Edwards, A. J. Oliver, Uranium Processing: A Review of Current Methods and Technology. *JOM* **2000**, 12–20.

Experimental and Modeling Study of Uranium(VI) and Nitric Acid Extraction With a N,N-Dialkylamide Solvent

Thibau Blanc¹, Donatien Gomes Rodrigues¹, Pauline Moeyaert^{1*}, Thomas Dumas¹, Philippe Guilbaud^{1*}

¹CEA, DES, ISEC, DMRC, Univ Montpellier, Marcoule, France

*Corresponding Author, E-mail: pauline.moeyaert@cea.fr

Innovative solvent extraction processes are currently under development at CEA for the reprocessing of MOX spent nuclear fuels. N,N-dialkylamides demonstrated their potentiality in the recovery and recycling of plutonium and uranium, as an alternative to TBP. First, they exhibit a good stability towards radiolysis and hydrolysis. Secondly, distribution ratios of plutonium(IV) and uranium(VI) with N,N-dialkylamide are such that their extraction and separation is possible, without using any reducing agent for the uranium – plutonium partitioning.

The extraction process is modeled using thermodynamic equilibrium calculations. Those calculations are based on activity coefficient determination for both aqueous and organic phases and on solving mass action law. For these models, assumptions have to be made related to the speciation of the complexes (N,N-dialkylamides- metallic cation for instance). Therefore, the knowledge of this speciation is essential to ensure a good predictivity of the model.

A bibliographical state of the art was established, and allowed to highlight the most promising methods described in the literature in order to obtain speciation diagrams of the complexes formed during the extraction of nitric acid and uranium(VI) with a N,N-dialkylamide solvent. Those methods include various spectroscopy studies, such as UV-Vis and IR as well as numeric processes to deconvolve the resulting spectra (including Principal Component Analysis).

Batch experiments were performed to study the behavior of water, nitric acid and U(VI) towards their extraction by a N,N-dialkylamide and to determine extraction isotherms. All extraction experiments were performed at 25°C by contacting the N,N-dialkylamide diluted in IP185 isane with aqueous solutions at various nitric acid and uranium concentrations. All organic phases were also characterized thanks to spectroscopic technics to obtain information about the speciation of the complexes in the organic phases.

Experimental distribution data were described with a physicochemical model based on the application of the mass action law on each extraction equilibrium and assumptions about the stoichiometry of the complexes formed in the organic phase. Deviations from ideality in aqueous phase were estimated by calculating the activity coefficient of each component according to the "simple solutions" model. Deviations from ideality were also determined in organic phase thanks to Sergievskii-Dannus approach. During the modeling work, assumptions have to be made regarding the speciation of the formed complexes. Agreement between simulated and experimental speciation allows refine the species hypothesis. That is why the experimental speciation data has been included as an input to the previously described model that was only fed with distribution data. The best group of complexes is the one that give the best agreement between experimental and calculated data for both distribution and speciation data. It is expected that this additional data will provide to the model a better robustness for various conditions (such as nitric acid, solvent and U(VI) concentrations).

Acknowledgments

The authors want to acknowledge Orano and EDF for financial support.

Feasibility Study on PUREX–NUMAP Hybrid Reprocessing: Precipitation–Based Recovery of U(VI) from Organic Phases with 30% TBP

Ririka Tashiro¹⁾, Satoru Tsushima¹⁾²⁾, Koichiro Takao¹⁾

¹⁾Laboratory for Zero–Carbon Energy, Tokyo institute of technology 2–12–1–NI–32, O-okayama, Meguro-ku, 152–8550 Tokyo, Japan. ²⁾institute of Resource Ecology, Helmholtz–Zentrum Dresden–Rossendorf, Bautzner Landstrasse 400, 01328 Dresden, Germany

Email: tashiro.r.ab@m.titech.ac.jp

For nuclear fuel recycling, the reprocessing process is the most essential. Currently, the PUREX method is exclusively employed in the spent fuel reprocessing, where U and Pu to be recycled are separated from fission products and minor actinides through selective solvent extraction using tributyl phosphate (TBP). This method is beneficial to gain high decontamination factor and technological reliability through its long history over 80 years. However, unavoidable concerns are still present in terms of potential isolation of Pu, safety risks arising from large excess amounts of organic solvents, and operation complexity through repeated extraction cycles. To improve the nuclear security aspect, Pu is once separated from UO_2^{2+} through reduction of extractable Pu^{4+} to unextractable Pu^{3+} , followed by remixing with U.

To address these issues, we have proposed an advanced reprocessing technology based on selective crystallization of nuclear fuel materials (NFM), *NUclear fuel Materials selective Precipitation (NUMAP)* [1], where double-headed *N*-alkylated 2-pyrrolidone derivatives (DHNRP, Fig.1) are employed for selective recovery of NFM, U, Pu and even Th. In our NUMAP method, separation of each NFM completes in a respective single step precipitation, where any organic solvents are no longer required to be used. Its another striking advantage is impossibility of Pu isolation, while Pu is always present with U even after separation.

Herein, we propose installation of the NUMAP principle to the U/Pu separation step after their primary decontamination in the PUREX process. If successful, there will be no chance for Pu isolation throughout the reprocessing process, making the security aspect of nuclear fuel cycle much improved. As a first step to know feasibility of this PUREX–NUMAP hybrid reprocessing, we studied behavior of U(VI) in 30% TBP/hydrocarbons after addition of DHNRP shown in Fig. 1 in terms of molecular and crystal structures of deposits as well as recovery yield of U(VI) from the organic phase.

To simulate the primary decontamination in PUREX, aliquots of 3.0 M HNO_3 aqueous solution containing 0.2 M U(VI) and 30% TBP/hydrocarbons (hexane, *n*-dodecane) were added to glass vials in 1:1 v/v, and shaken for 5 min. To the separated organic phase, DHNRP equivalent to U(VI) initially loaded was added as being done in NUMAP, followed by sonication. After centrifugation, the separated supernatant was mixed with 0.1 M HNO_3 (aq) in 1:1 v/v, and shaken for 5 min. The U concentrations in all aqueous phases were measured by ICP–AES to calculate efficiencies of respective steps in the PUREX–NUMAP hybrid reprocessing. The obtained precipitation was also characterized by pXRD and FT–IR. For crystal structure analysis, the organic phase (100 μL) after the primary decontamination was layered in a glass vial with 3 M HNO_3 (aq) (100 μL) dissolving DHNRP. The obtained crystals were analyzed by SCXRD.

When DHNRP was added directly to the organic phases of both hexane and *n*-dodecane, yellow precipitation was immediately obtained after sonication, except for L2 in the hexane system. A sticky chunk material was formed adding L4 in the hexane system, while fine crystalline powder of the U(VI) precipitate was yielded in *n*-dodecane in a similar manner to those of other DHNRP.

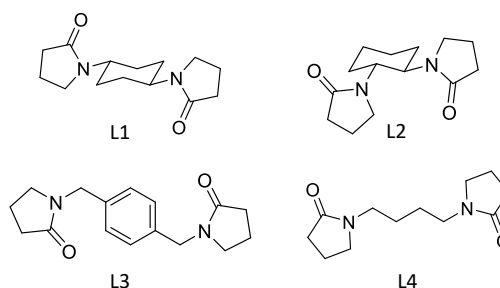


Fig.1 Double-headed 2-pyrrolidone derivatives (DHNRP) used in this work.

Figure 2 shows a typical result of a 1D coordination polymer of $[\text{UO}_2(\text{NO}_3)_2(\text{L4})]_n$. In our previous work, DHNRP reacted with UO_2^{2+} in $\text{HNO}_3(\text{aq})$ to form isomorphous and isostructural coordination polymer having the same composition in principle [2]. The obtained pXRD pattern of the yellow precipitation well agree with the calculated pXRD pattern from the SCXRD results, indicating that the yellow precipitation yielded in each system is a crystalline $[\text{UO}_2(\text{NO}_3)_2(\text{DHNRP})]_n$.

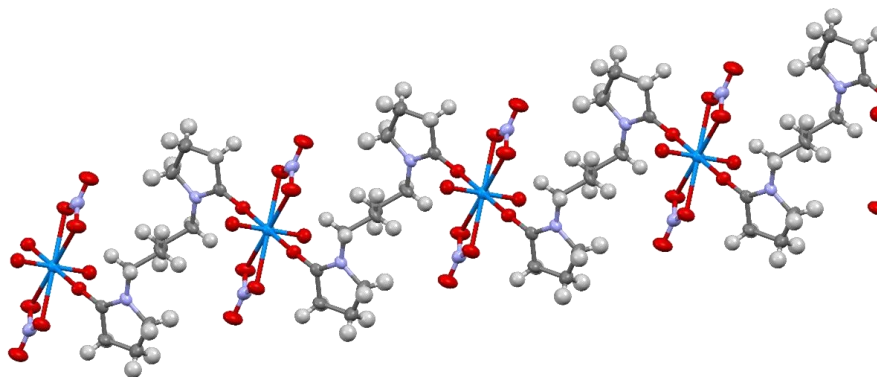


Fig.2 Crystal structure of $[\text{UO}_2(\text{NO}_3)_2(\text{L4})]_n$

A set of above results clearly demonstrates that DHNRP facilitates recovery of U(VI) from the organic phase after primary decontamination in the PUREX process. In addition to these data, the recovery efficiency of U(VI) was assessed to know suitability of this hybrid method for spent fuel reprocessing. Table 1 summarizes recovery efficiency of U(VI) at each step of the PUREX-NUMAP hybrid method in use of different diluents (hexane, *n*-dodecane) and different DHNRP (L1-L4). The total recovery of U(VI) after the PUREX primary decontamination and the NUMAP precipitation was 67%–86% in both diluent systems. In the primary decontamination using 30% TBP/hydrocarbons, U(VI) extractability (*E*%) was higher than 90%, while not always perfect. In general, such a solvent extraction step can be repeated to gain the U(VI) recovery as demanded. The most important finding in this study is that our NUMAP approach is applicable for recovery of U(VI) from non-aqueous phase even under the presence of 30% TBP, the strong and selective extractant for U(VI). The actual precipitation ratio (ppt%) was 73% (L1, *n*-dodecane) at the lowest, and 97% (L4, *n*-dodecane) at the highest. To improve ppt%, we can further optimize reaction conditions such as DHNRP loading and reaction time under sonication. As observed in use of L4, selection of diluent also gives large impact to the U(VI) recovery.

In conclusion, we have successfully demonstrated feasibility of the PUREX-NUMAP hybrid reprocessing in terms of the recovery of U(VI) from organic phase despite presence of 30% TBP. DHNRP best suitable for U(VI) recovery from *n*-dodecane is L4. The applicability of the PUREX-NUMAP hybrid method for the recovery of Pu, which is important in reprocessing, also needs to be further investigated using Pu simulants.

Table 1. U(VI) Recovery rate in PUREX-NUMAP Hybrid

diluent & DHNRP	PUREX <i>E</i> %	NUMAP ppt%	total recovery %
<i>n</i> -hexane			
L1	95	80	76
L3	95	83	80
L4	95	75	72
<i>n</i> -dodecane			
L1	92	73	67
L2	92	79	72
L3	91	85	77
L4	89	97	86

Reference

[1] K.Takao *et al*, *Eur. J. Inorg. Chem.* **2020**, 3443–3459

[2] H.Kazama *et al*, *Chem. Lett.* **2020**, 49, 1201–1205

Demonstration of U(VI)/Pu(IV) Separation by Solvent Extraction in Modified Lab-Scale Annular Centrifugal Contactors Using D2EHiBA Extractant

Dominic Maertens^{a,b*}, Koen Binnemans^b, Thomas Cardinaels^{a,b}

^a Belgian Nuclear Research Center (SCK CEN), Institute for Nuclear Energy Technology, Mol, Belgium

^b KU Leuven, Department of Chemistry, Leuven, Belgium

Background

The N,N-dialkylamide di(2-ethylhexyl)isobutyramide (D2EHiBA) shows great promise for selective uranium extraction from spent nuclear fuel solutions. Several successful hot experiments have been performed in the framework of past EU projects (e.g. ACSEPT) at the CEA and JRC ITU that demonstrated the U(VI)/Pu(IV) separation and decontamination of fission products from UOX and MOX fuel.^[1,2] For this purpose, D2EHiBA was proposed as CHON compliant extractant in the GANEX 1st cycle in a homogenous recycling strategy. The typical feed specifications are similar to a PUREX High Active Feed, and in the range of 5–6 M HNO₃. The co-extraction of Tc-99 and Pu/Np(VI) is suppressed by addition of hydrazine in the scrubbing solution.

For recycling of spent high assay low enriched uranium (HALEU), e.g. from future small modular reactors, the selective recovery and valorization of the enriched uranium fraction could also be envisioned by a D2EHiBA-based solvent extraction process.^[3] Similarly, HALEU can be recycled from residues of medical isotope production, where typically only ppm quantities of transuranic elements and Tc-99 are present. A single-cycle D2EHiBA-based process could be imagined without the need for an organic complexant or reductant in the scrubbing step, as the amounts of Np are not of major concern, and Tc-99 can still be efficiently removed further downstream, for example in an ammonium diuranate (ADU) precipitation step.

The objective of this work is to demonstrate the U(VI)/Pu(IV) separation without the use of complexant or reductant, obtaining a high decontamination factor (DF) for Pu(IV) and Ru(III), using TBP as a benchmark. For this purpose, the use of lab-scale short residence time annular centrifugal contactors (ACCs) have several advantages as they have a small footprint, low liquid hold-up, and hence steady-state is faster reached compared to mixer-settlers or pulsed columns, hereby minimizing the required volumes of process solutions and liquid waste.^[4]

Method

Rousselet BXP012 ACCs with inner rotor diameter of 12 mm were substantially modified for this work. The rotor length was increased with 2 cm to obtain a more consistent volume in the annular mixing zone, and increased phase separation performance. To obtain visual process feedback, translucent PMMA rotor surroundings were made, with an increased 4 mm annular gap. In-house designed and 3D-printed stainless steel stators were fitted with angled collector rings and optimized liquid flow paths. These modifications were essential for working with D2EHiBA at high flow rates and high uranium loading conditions.

The simulated feed solution for this experiment consisted of U, Pu, Tc, Ru and Am. Natural uranyl nitrate was used to prepare a 240 g U L⁻¹ feed solution in 3 M HNO₃. Natural ruthenium nitrosyl nitrate was irradiated in the BRI reactor (Mol, BE) to produce ~1 MBq Ru-103 (T_{1/2}: 39.26 d) tracer. 2 GBq Tc-99m (T_{1/2}: 6.01 h) was obtained from elution of a Mo-99/Tc-99m generator from a hospital (Geel, BE). A 10 MBq Pu-239 TMS spike solution was added to the simulated feed (A_{Pu-239}/A_{Pu-238} > 100; A_{Pu-239}/A_{Pu-241} ~ 5), also containing a small amount of Am-241. Finally, the equivalent of 0.1 M NaNO₂ was slowly added to the feed solution to set the oxidation state of Pu prior to the start of the experiment.

Gamma spectroscopy was used to quantify Tc-99m (140.5 keV, 89.1%) shortly after obtaining the inter-stage process samples at steady-state using a Canberra BEGe 3830 detector. The samples were then remeasured for quantification (or low MDAs) of Ru-103 (497 keV, 91%), U-235 (185 keV, 57.1%), and Am-241 (59.5 keV, 35.9%). Pu-239 was quantified with alpha spectroscopy using a Canberra Alpha Analyst.

The flow sheet shown in Figure 1 was used for the experiment, focused on high loading of the organic phase and maximum throughput. Nitric acid concentration of the feed was relatively low at 3 M HNO₃, to avoid build-up of Pu(IV) in the extraction

section, and minimize Np co-extraction. Online density measurement of the scrubbing solution flowing back to extraction was used to fine tune the process parameters.

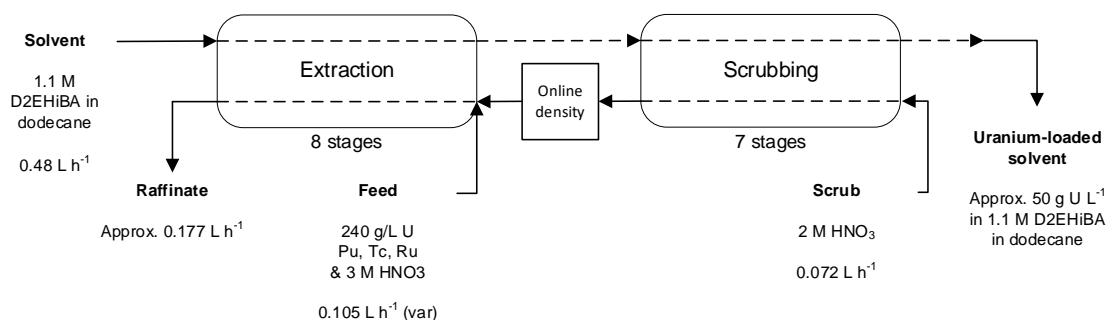


Figure 1: Flow sheet for experimental U(VI)/Pu(IV) separation using D2EHiBA extractant

Results

Steady-state conditions were obtained after approximately 100 minutes. Average residence times in the mixing zones varied between 30 and 40 seconds. More than 99.9% of U was recovered, and U(VI)/Pu(IV) separation was highly successful with a DF of higher than 10^4 . Build-up of Pu(IV) in the extraction section was effectively avoided under these process conditions. The scrubbing process was performant, even at a high O/A ratio of 6.66. Am-241 and Ru-103 were not extracted, and aqueous phase carry-over between extraction and scrubbing was calculated to be less than 0.1%, further demonstrating the performance of the modified BXP012 annular centrifugal contactors. D_{Ru} was determined to be less than 0.001 in the extraction section, demonstrating that D2EHiBA is superior in Ru decontamination compared to TBP. It was observed that 75% of Tc-99m was co-extracted by uranium in the form of $UO_2(NO_3)(TcO_4)$, and 25% eventually remained in the raffinate.

Conclusions

The U(VI)/Pu(IV) separation in modified lab-scale annular centrifugal contactors using D2EHiBA extractant without the need of using complexants or reductants was successful, and it was demonstrated that this solvent extraction process can be envisioned for selective recovery of uranium from spent enriched uranium solutions.

References

- [1] Miguiditchian, M.; Sorel, C.; Cames, B.; Bisel, I.; Baron, P.; Espinoux, D.; Calor, J. N.; Viallesoubrette, C.; Lorrain, B.; Masson, M. HA demonstration in the Atalante facility of the Ganex 1st cycle for the selective extraction uranium from HLW. *Global* **2009**, 1032-1035.
- [2] Malmbeck, R.; Magnusson, D.; Bourg, S.; Carrott, M.; Geist, A.; Hérès, X.; Miguiditchian, M.; Modolo, G.; Müllich, U.; Sorel, C.; et al. Homogeneous recycling of transuranium elements from irradiated fast reactor fuel by the EURO-GANEX solvent extraction process. *Radiochimica Acta* **2019**, 107 (9-11), 917-929. DOI: <https://doi.org/10.1515/ract-2018-3089>.
- [3] Hall, G. B.; Bessen, N. P.; Zalupski, P. R.; Campbell, E. L.; Grimes, T. S.; Peterman, D. R.; Lumetta, G. J. Extraction of Neptunium, Plutonium, Americium, Zirconium, and Technetium by Di-(2-Ethylhexyl)-Iso-Butyramide (DEHiBA) at High Metal Loadings. *Solvent Extraction and Ion Exchange* **2023**, 41 (5), 545-563. DOI: <https://doi.org/10.1080/07366299.2023.2215833>.
- [4] Maertens, D.; Binnemans, K.; Cardinaels, T. Design of a Modular Annular Centrifugal Contactor for Lab-Scale Counter-Current Multistage Solvent Extraction. *Solvent Extraction and Ion Exchange* **2023**, 41 (6), 741-766. DOI: <https://doi.org/10.1080/07366299.2023.2239882>.

Current TRL Status and Strategy for the Development of the Next Generation of Reprocessing Plant

B. Arab-Chapelet¹, C. Sorel¹, I. Hablot², A. Gil Martin², M. Phelip³, A. Salvatores³, L. Diaz⁴, G. Vaast⁴

¹ CEA, DES, ISEC, DMRC, Université de Montpellier, Marcoule, France

² Orano, 92320 Châtillon, France

³ Energy Division, CEA, Centre de Paris-Saclay, 91191 Gif-sur-Yvette, France

⁴ EDF, 93200 Saint-Denis, France

As part of the reflections on the next generation of spent nuclear fuel (SNF) reprocessing plant, the R&D carried out on innovative processes aims to respond to the challenges of multi-recycling of plutonium in PWR. The considered processes should therefore allow the treatment of all fuels (MOX1, MOX2, ENU and URE), which could include fuels with large grain microstructure. The current TRL status and the strategy adopted for the development of innovative processes involved for the SNF reprocessing are detailed in this paper.

The approach followed is based on a selection of innovative process bricks appropriate to integrate the next generation of reprocessing plant. The following processes have been considered: shearing by hyperbaric fluid jet, oxide/cladding separation by voloxidation, powder dissolution as well as innovative separation by solvent extraction without redox agents. The functional analysis carried out on these processes made it possible to identify the R&D programs to be carried out and to define the criteria to be achieved in order to increase their TRL level. At the current stage of R&D, only the innovative separation process has exceeded TRL 3 and the ongoing studies on the other process bricks aim to reach, a level of technological maturity sufficient to access the interest to pursue the research carried out with a view to industrial qualification.

During the last years, key results for the increase in TRL of innovative process bricks have been obtained. Thus, a voloxidation test of non-irradiated Cr-doped UOX fuel pellets showed that voloxidation is the only continuous technology tested yet which makes it possible to overcome the impact on the dissolution behavior of the microstructure of the large grains UOX fuels and therefore maintain the processing rate of this type of fuel. In addition, significant improvements of the solvent involved in the separation process have been obtained and its efficiency have been demonstrated during experimental trials performed with surrogate solutions and genuine MOX spent fuel dissolution solutions.

This work was carried out in the framework of a collaborative program involving CEA, Orano and EDF.

This program is financially supported by the French Government through the "France 2030" initiative.

Towards a Single-Solvent Process for U/TRU Recovery and Minor Actinide/Lanthanide Separations: Speciation and Partitioning of Tetravalent (Th, Pu) and Hexavalent (U) Actinides with HEH[EHP] and T2EHDGA

Artem Gelis*, Joel Castillo, Logan Smith, Quinn Summerfield, Frederic Poineau

Radiochemistry Program, Department of Chemistry, University of Nevada, Las Vegas, NV, USA

*artem.gelis@unlv.edu

Understanding actinide speciation in lipophilic organic systems is a critical factor for developing novel liquid-liquid extraction processes for advanced nuclear fuel reprocessing and lanthanide and actinide recovery from ore containing naturally occurring radioactive materials (NORM). A simplified process is desirable to reduce costs, secondary waste generation, and increase safety. Several advanced solvent extraction processes for the recovery of uranium, transuranics, and minor actinides (U/TRU/MA) have been developed worldwide: Euro-GANEX, ExAm, CHALMEX, NEXT, etc. A US-based process for separating minor actinides (MA) from lanthanides (Ln) in spent nuclear fuel has been previously developed, called the Actinide Lanthanide Separation Process (ALSEP). This process has proven effective in separating Am and Cm from Ln in spent fuel mixtures feasible by the combination of the organophosphorus acidic extractant 2-ethylhexylphosphonic acid mono-2-ethylhexyl ester (HEH[EHP], P507) and a neutral diglycolamide (DGA) extractant, N,N,N,N-tetra(2-ethylhexyl)diglycolamide (T2EHDGA) in n-dodecane. If processes such as ALSEP could be applied to also separate the other actinides (An) this could result in a more sustainable fuel cycle that would be an indispensable aid in combating the issues of pollution and greener energy.

We report here proof-of-principle experimental results and the speciation studies of An in organic media. In contrast to the EU approach, the proposed process does not separate Pu from U, thus creating a suitable stream for advanced fuel fabrication, while keeping the proliferation risks at minimum. Experimental data on Pu and Th partitioning with HEH[EHP] and EXAFS analysis of uranyl in the T2EHDGA organic phase are shown in Fig 1 and 2.

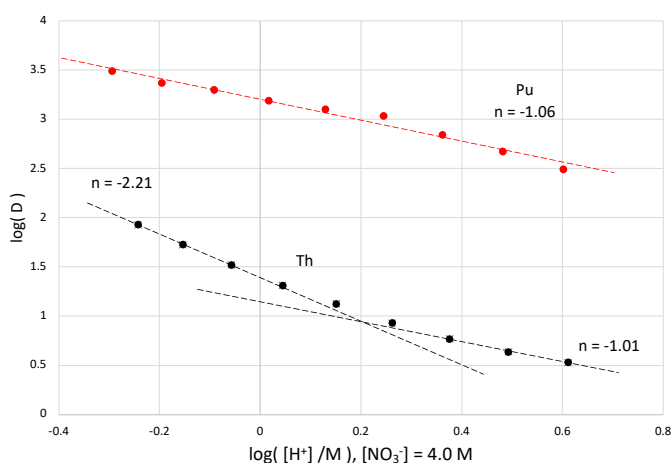


Figure 1. Extraction of Pu⁴⁺ and Th⁴⁺ by 0.01M HEH[EHP]/ddn, acid dependence.

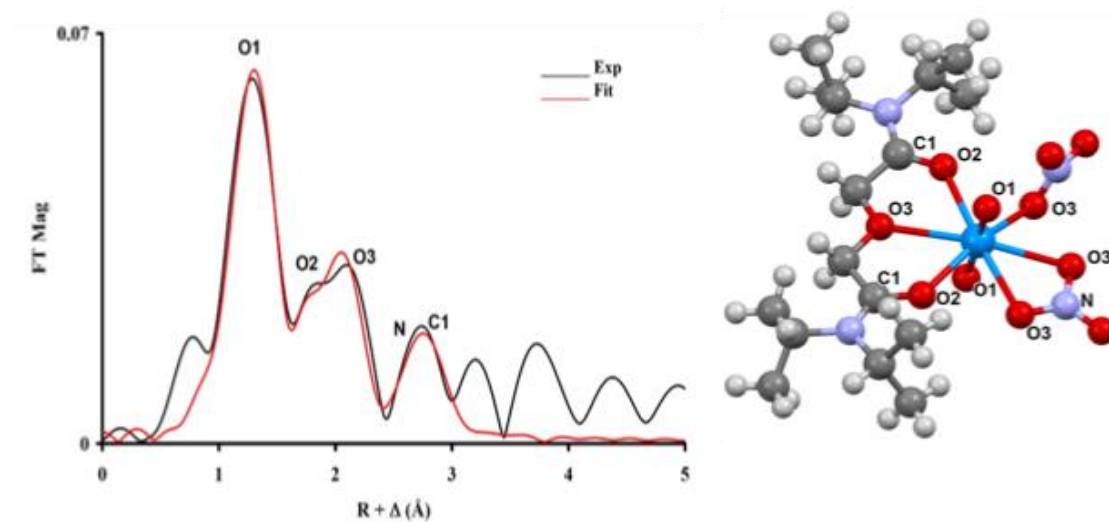


Figure 2. EXAFS fit and the proposed structure of $\text{UO}_2(\text{NO}_3)_2\text{T2EHDGA}$

Horizon 2020 PuMMA: Studies Considering Reprocessing of 40–45 %Pu Fast Reactor MOx

Chris Maher^{1*}, Nathalie Chauvin², Francisco Álvarez³, Martin Giraud², Jessica Gunning¹, Victoria Hayter¹, Rebecca Sanderson¹, Nathalie Reynier-Tronche², Eva de Visser Týnová⁴.

¹ National Nuclear Laboratory, UK, ² CEA France, ³ CIEMAT Spain, ⁴ NRG Netherlands

*Correspondence: author: chris.j.maher@uknnl.com

PuMMA is an EU Horizon 2020 project titled “Plutonium Management for More Agility” including 20 organizations (R&D, Industries, Universities and Safety Authorities) and has a budget of 7 M€ [1]. The project aims to consider the impacts of using high plutonium (Pu) content mixed oxide (MOx) fuels on the nuclear fuel cycle. This includes work packages on reactor safety and performance to consider different options for Pu management in Generation IV nuclear reactors. Pu management in Gen IV reactors will contribute to safer, more efficient and sustainable nuclear energy production. As part of these work packages Pu-active practical studies and modelling studies are being undertaken. The work focusses on fuel performance evaluation, including an extensive review of historic material test (MTR) and fast (FR) reactor irradiation studies, post irradiation examination of Trabant and CAPRIX irradiation studies, and reactor simulation studies. Practical studies to determine fundamental data, such as thermal diffusivity, which is used to refine high plutonium content reactor simulation studies, aim to consider extensive multi-recycling of Pu in ISO or burner fast reactor operating modes. To support these extensive reactor and fuel cycle studies key reprocessing studies are underway and are discussed herein.

The focus of the reprocessing work package (WP5) is to consider the feasibility and impacts of reprocessing fuels with high plutonium content (above 40–45 %Pu) and fuels used in mainstream fast reactor operations (plutonium content of 20–35 %Pu). There are many aspects that will ultimately need to be considered to develop a reprocessing flowsheet and operating plant. PuMMA studies have focused on two key areas: fuel dissolution and the radiation impact on the solvent. A key issue for reprocessing of high plutonium content fuels is the refractory nature of PuO₂ that slows the dissolution rate of MOx as the Pu content is increased [2]. An increased Pu content also increases the alpha radiation dose to the chemical separation solvent used in reprocessing. This work package has been divided into the following tasks:

1. Coordination of MOx dissolution studies
2. Unirradiated MOx dissolution studies
3. Irradiated MOx dissolution studies
4. Evaluation of solvent dose

A summary of the studies are detailed below:

Coordination of MOx dissolution studies

To understand how each series of dissolution experiments will be conducted and maximize comparability of results.

Unirradiated MOx dissolution studies

Two types of studies have been carried out:

- MOx powder dissolutions at low concentrations to improve understanding of the effect of Pu content on dissolution chemistry. A series of dissolution tests have been conducted using with 27, 53 and 80 %Pu MOx powders and different nitric/nitrous acid concentrations and temperatures. Temperature has been observed to be the main factor in increasing the dissolution rate of higher (53 and 80 %Pu) MOx powders.
- MOx pellet dissolutions at process concentrations to select dissolution conditions for irradiated MOx dissolution studies and allow comparison with irradiated MOx samples. These dissolution tests used unirradiated MOx pellets

(CAPRA) under refluxed 8 and 10 mol/l nitric acid conditions and very slow dissolution were observed on the timescales of a working day.

Irradiation MOx dissolution studies

Two series of irradiated MOx dissolution studies are underway:

- Small-scale Trabant 2 dissolutions are being carried out under chemical conditions that are known to accelerate the dissolution of Pu-rich oxides. These include nitric acid based silver(II) and fluoride catalyzed processes. Initial results show an improvement in plutonium recovery [3].
- CAPRIX dissolution studies have applied primary nitric acid dissolution, secondary silver(II) plutonium recovery dissolution and residue characterization (fusion) methods to high flux and upper rod region irradiated fuels. The primary nitric acid dissolution which was carried out over 10 hours was incomplete but much more rapid compared to unirradiated dissolution tests. The dissolution of Pu-rich residues from this primary dissolution stage using silver(II) was successful, but required long time scales (multiple days). The fusion method has allowed characterization of the residues from silver(II) dissolution. The results of the full flux region are published [4] and work on upper flux region is underway.

Evaluation of solvent dose

Increasing the Pu content, and therefore minor actinide content, of MOx fuel increases the alpha dose from the MOx fuel because these radionuclides have shorter half-lives and as such decay more rapidly than uranium. This leads to increased radiation dose to the solvent used in the chemical separation process. Work to develop new modelling tools is underway to evaluate the absorbed dose to solvent and initial results show that a moderate increase in dose occurs upon increasing the plutonium content to 45 %Pu. Further studies are planned, which will contribute to the development of strategies to manage solvent lifetime and quality.

Summary

PUMMA reprocessing studies aim to assess the feasibility of reprocessing 40–45 % Pu content MOx fuels using hydro-reprocessing methods. Initial work demonstrates good feasibility and highlights the challenges of the design of a dissolver cycle for high Pu content MOx and highlights areas for further work.

References

- [1] "Plutonium Management for More Agility," [Online]. Available: <https://pumma-h2020.eu/>.
- [2] D. Vollath, H. Wedemeyer, H. Elbel and E. E. Gunther, "On the dissolution of (U,Pu)O₂ solid solutions with different plutonium contents in boiling nitric acid," *Nucl. Tech.*, vol. 71, no. 1, pp. 240–248, 1985.
- [3] E. E. de Visser – Týnová, K. Kottrup, M. Stijkel and A. Booi, "Dissolution of irradiated MOx fuel with high Pu content," in *Radchem 2022*, Mariánské Lázně, Czech republic, 15–20 May 2022.
- [4] M. Giraud, N. Reynier-Tronche and E. Buravand, "Effects of irradiation on the insolubility of sodium fast reactor (U,Pu)O₂ mixed oxide with a very high amount of plutonium," *Journal of Nuclear Materials*, vol. 587, p. 154727, 2023.

First-Principles Study of a New TODGA Degradation Compound

Lucas Zubillaga-Maharg^{1,2,3}, Iván Sánchez-García⁴, Hitos Galán⁴, J. Manuel Perlado^{1,2},

Emma del Río^{1,2}

¹Universidad Politécnica de Madrid, Instituto de Fusión Nuclear Guillermo Velarde, C/José Gutiérrez Abascal, 2, Madrid 28006, Spain

²Universidad Politécnica de Madrid, E.T.S.I. Industriales, Dpto. Ingeniería Energética, C/José Gutiérrez Abascal, 2, Madrid 28006, Spain

³University of Chicago, 5801 S Ellis Ave, Chicago, IL 60637, United States

⁴Centro de Investigaciones Energéticas, Medioambientales y Tecnológicas (CIEMAT), Avda. Complutense, 40, Madrid 28040, Spain

As a low greenhouse gas emitter, fission-based nuclear energy is a necessary component of our energetic transition. Yet, one cannot ignore the radiotoxic waste produced from this energy source – especially High Level Waste (HLW). Although deep geological repository is a long-term solution for storing used nuclear fuel (UNF), its extensive period of safety management raises serious concerns at the public level. Current Generation III reactors use less than 10% of the fuel's potential energy; thus, a closed, sustainable nuclear fuel cycle presents a more attractive approach, increasing the energy extracted while reducing the volume of HLW generated and the amount of uranium mined. Current efforts focus on recovering U and Pu to create mixed oxide (MOX) fuel, which is fed back into the reactor. A step further would be to reprocess the minor actinides (MA) – such as Am, Cm, and Np – which are responsible for the majority of the UNF's radiotoxicity. [1]

Two techniques to recover MA from UNF under research are pyrometallurgical (non-aqueous) and hydrometallurgical (aqueous) reprocessing. The former is based on high temperature electrolytic or electrorefining methods. The main drawback is that their complete industrialization has not been achieved. The latter (hydrometallurgical/aqueous reprocessing) is based on liquid-liquid extraction. This process has been implemented industrially for many years, mainly through PUREX (Plutonium and Uranium reduction extraction), recovering U and Pu which are used in the production of MOX fuel. Thus, many new advanced reprocessing methods are aqueous-based.

An important factor in the development of these aqueous processes is the extractant molecule's resistance to hydrolysis and radiolysis. The extractant solution contains a high concentration of nitric acid and a considerable number of radionuclides. These extreme conditions may degrade the extractant molecule, causing changes in its composition, affecting the separation efficiency and physiochemical properties of the solvent, and leading to an increase in secondary waste. Moreover, this could affect the safety and economy of future reprocessing plants. Therefore, it is of utmost importance to study the performance, stability, and byproducts of these extractant molecules and possible setbacks under highly acidic and radioactive conditions.

One of the most promising extractants is *N,N,N',N'*-tetraoctyldiglycolamide (TODGA), a lipophilic molecule used for the extraction of MA and Lanthanides (Ln). TODGA is under consideration for several processes, such as *i*-SANEX [2] or EURO-GANEX [3] (a possible option for the second cycle of the GANEX process). TODGA's hydrolytic and radiolytic stability have been extensively studied by several authors and up to nine degradation compounds (DCs) have been detected and characterized [4]. Recent studies, conducted under more realistic conditions, have led to the detection of three new DCs [5]. Little is known about these compounds except for their mass spectra (the mass-to-charge ratios or *m/z* are 256, 476 and 518). Experimentalists have proposed 2-D structures for these new TODGA DCs, with *m/z* = 518 having four possible isomers (see Fig. 1 a-d).

Continuous advancements in supercomputing have made quantum chemistry software a useful tool to complement experimental data. In many cases, simulations can help determine a reaction mechanism and the relative thermodynamic stability of reaction products. In this study, we performed first-principles calculations to analyze the *m/z* = 518 structures proposed by experimentalists in Fig. 1 (a-d). Additional structures were proposed and analyzed after a literature review on the preferred reactivity sites of diglycolamides (see Fig. 1 e-j). Calculations were performed with ORCA 5.0.3 code at the DFT (Density Functional Theory) level. The B3LYP hybrid functional with the def2 Karlsruhe basis set group was used for the geometry optimization, characterization, and Gibbs Free Energy calculations. All the geometries were characterized as

minima by positive vibrational frequencies. However, due to the large size of the molecules – and thus the large number of rotating σ -bonds – its potential energy function is quite flat; to take this into account, a small spatial distribution test was performed. Additionally, *cis* and *trans* forms (*cis* refers to both carbonyl oxygens facing the same direction in a plane, and vice versa for *trans*) were considered for all structures.

Our study found that the most favorable bonding sites for $m/z = 518$ were the carbonylic carbons, the etheric carbons, and the first carbon of the octyl chain. Simulated infrared (IR) spectra were computed as possible reference material for the confirmation of the DCs structures.

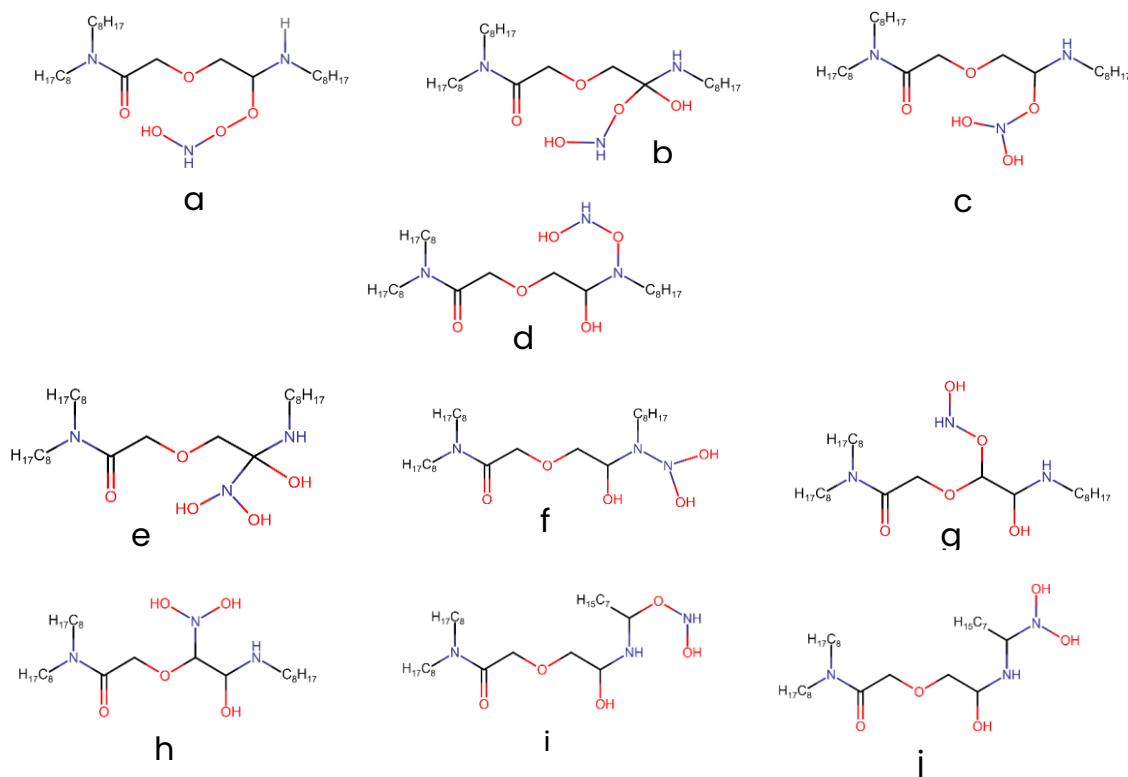


Figure 1: Initial (a-d) [5] and additional (e-i) proposed 2-D structures for the new $m/z = 518$ TODGA degradation compound

1. Poinssot, C. et al. Prog. Nucl. Energy **92**, (2016) 234–241
2. Wilden, A. et al. Procedia Chem. **7**, (2012) 418–424.
3. Malmbeck, R. et al. Radiochim. Acta **107**, (2019) 917–929
4. Sugo, Y. et al. Radiochim. Acta **90**, (2002) 161–165
5. Sánchez-García et al., Radiation Physics and Chemistry, **177**, (2020) 109094

Demonstration of the Single Cycle Am(III) Separation AmSEL Process in Laboratory-scale Annular Centrifugal Contactors

Andreas Wilden^{1*}, Fynn S. Sauerwein¹, Vincent Vanel², Andreas Geist³, Giuseppe Modolo¹

¹ Forschungszentrum Jülich GmbH, Institut für Energie – und Klimaforschung – Nukleare Entsorgung (IEK-6), 52428 Jülich, Germany, ² Commissariat à l'Energie Atomique et aux Energies Alternatives (CEA), 30207 Bagnols-sur-Cèze cedex,, France, ³ Karlsruhe Institute of Technology (KIT), Institute for Nuclear Waste Disposal (INE), 76021 Karlsruhe, Germany.

*Corresponding author: a.wilden@fz-juelich.de

Future fast nuclear reactor fuel cycles allow for the multi-recycling of Pu and possibly Am. Life cycle assessment studies show that Am recycling could significantly decrease the required high-level waste repository surface area for a given amount of electricity produced, and thus allow for a more efficient use of a deep geological repository.^[1] The selective separation of Am(III) from a PUREX high-active raffinate solution is therefore envisioned to implement an industrial process compatible with the industrialized PUREX separation. Due to the complex mixture of minor actinides, fission and corrosion products in the PUREX raffinate, the Am(III) separation process demands a highly selective separation system. In the previous European projects, the innovative-SANEX process was developed, using a TODGA (Figure1) based solvent to extract An(III) and Ln(III) together, and selectively back-extract Am(III) and Cm(III) using SO₃-Ph-BTP.^[2] Using the innovative-SANEX system as a reference, the AmSEL process was developed within the previous EU SACESS and GENIORS, and the current EU PATRICIA projects. The AmSEL process is based on the innovative-SANEX process and uses the same solvent composition, but the more Am(III) selective SO₃-Ph-BTBP (Figure1) ligand for back-extraction by exploiting the inverse Am/Cm selectivity of TODGA and SO₃-Ph-BTBP.^[3]

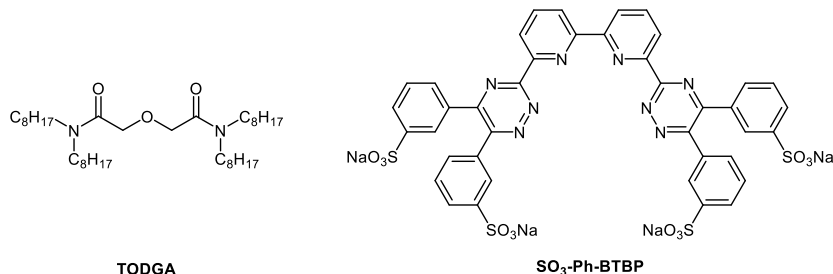


Figure 1.: Chemical structures of TODGA and SO₃-Ph-BTBP.

The chemical system was optimized, and kinetics data were measured in single centrifugal contactor experiments. These data were used to develop an AmSEL process flow sheet using the PAREX+ simulation code.^[4] The flow sheet was optimized regarding the available number of 16 centrifugal contactors and maximizing Am recovery rate and Am/Cm decontamination factors, while limiting Am recycling in the process stages. As the AmSEL system was based on the already demonstrated innovative-SANEX process, a loaded solvent was prepared by batch extractions. The same PUREX raffinate solution as tested in the innovative-SANEX process was used, and analyses of the loaded solvent showed comparable composition to the one produced in the centrifugal contactor demonstration.^[2] This loaded solvent was used as organic feed for the centrifugal contactor test. Figure 12 shows the final flow sheet of the AmSEL process, comprising 12 stages for selective Am(III) stripping and four stages for Cm(III) and Ln(III) re-extraction.

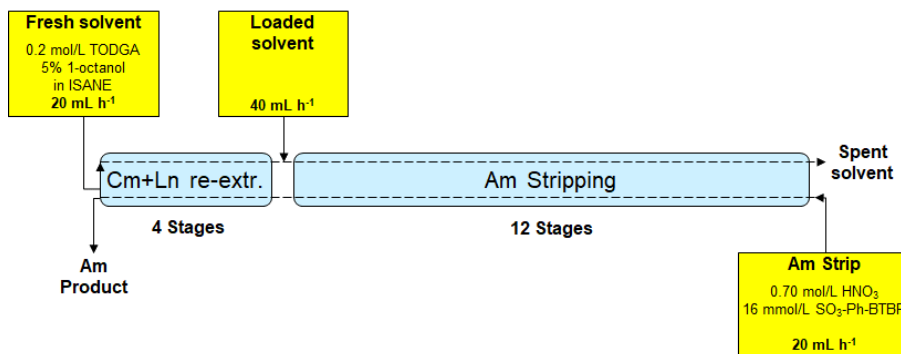


Figure 1. AmSEL process flow sheet tested in centrifugal contactors.

The AmSEL centrifugal contactor test was run for ca. 9.5 h until sampling and quick α and γ analyses of the effluents showed constant ^{241}Am , ^{244}Cm and ^{152}Eu concentrations. Then, the test run was stopped, and the content of the mixing was analyzed. Figure 2 shows the ^{241}Am , ^{244}Cm and ^{152}Eu concentration profiles. An Am(III) product containing 45% Am(III) and only 5% Cm(III) was obtained. The remaining Am(III), Cm(III) and Ln(III) were routed to the spent solvent. The separation from Ln(III) was very good with high decontamination factors. However, significant recycling of Am(III) occurred, which needs to be addressed in further process optimizations. More centrifugal contactor stages are required to improve Am(III) recovery and the Am/Cm decontamination factor.

The results of the AmSEL demonstration test will be presented and discussed. Also, further developments from the PATRICIA project regarding a sulfur-free alternative Am(III) stripping agent will be presented.

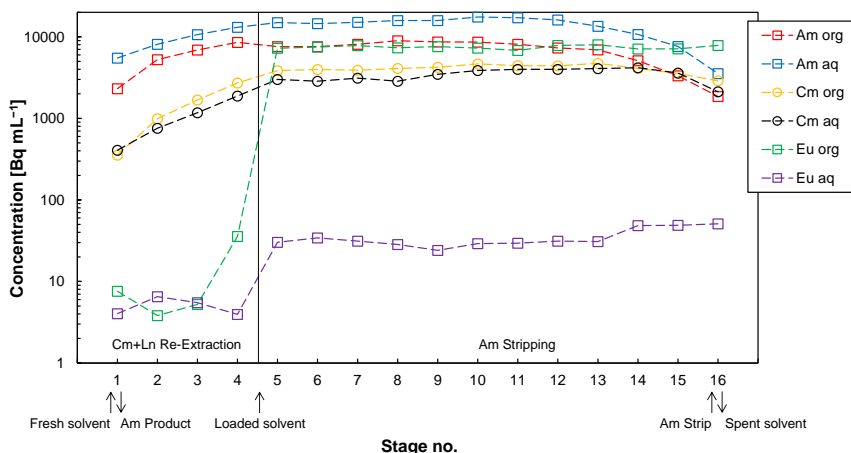


Figure 2.: ^{241}Am , ^{244}Cm and ^{152}Eu concentration profiles.

Acknowledgments

This project has received funding from the Euratom research and training programme 2019-2020 under grant agreement No 945077 (Partitioning And Transmuter Research Initiative in a Collaborative Innovation Action (PATRICIA) project).

References

- [1] J. Serp, C. Poinssot, S. Bourg, *Energies* **2017**, *10*, 1445.
- [2] A. Wilden, G. Modolo, P. Kaufholz et al., *Solvent Extr. Ion Exch.* **2015**, *33*, 91-108.
- [3] C. Wagner, U. Müllich, A. Geist et al., *Solvent Extr. Ion Exch.* **2016**, *34*, 103-113.
- [4] J. Bisson, B. Dinh, P. Huron et al., *Procedia Chem.* **2016**, *21*, 117-124.

Flowsheets for the Validation of the Reference AmSEL System

Vincent Vanel^{1,*}, Andreas Wilden², Giuseppe Modolo², Andreas Geist³, Marc Montuiri¹

¹ CEA, DES, ISEC, DMRC, Univ Montpellier, Marcoule, France, ² Forschungszentrum Jülich GmbH, Institut für Energie – und Klimaforschung – Nukleare Entsorgung (IEK-6), 52428 Jülich, Germany, ³ Karlsruhe Institute of Technology (KIT), Institute for Nuclear Waste Disposal (INE), 76021 Karlsruhe, Germany.

* Corresponding author: Vincent.vanel@cea.fr

Recycling americium (Am) from spent nuclear fuels is an important option considered for the future nuclear fuel cycle as americium is the main contributor to the long-term radiotoxicity and heat power of the ultimate waste. In this framework, the AmSEL flowsheet aims at recovering and purifying americium from a PUREX raffinate. This separation can be achieved by co-extracting lanthanide(III) (Ln) and actinide(III) cations (Am(III) and Cm(III)) into an organic phase containing the TODGA extractant (*N,N,N',N'*-tetraoctyldiglycolamide in Figure 1), and then strip Am(III) selectively towards curium and lanthanides (Wilden et al., Solvent Extr. Ion Exch. 2015, 33, 2, 91-108). The water-soluble ligand SO₃-Ph-BTBP (6,6'-bis(5,6-dialkyl-1,2,4-triazin-3-yl)-2,2'-bipyridine in Figure 1) is used to selectively strip Am from the loaded organic phase.

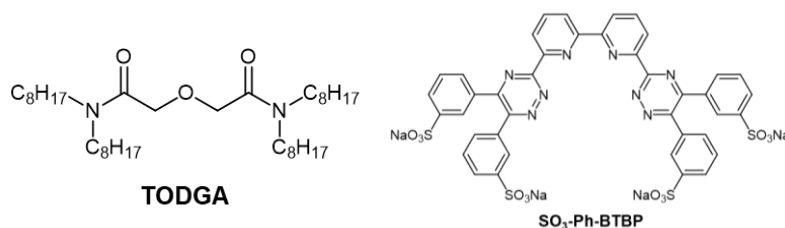


Figure 1. Chemical structures of TODGA and SO₃-Ph-BTBP

The objective of this work is to design a flowsheet for the Am stripping and Cm re-extraction steps to recover americium selectively from Cm and Ln, with TODGA as extractant and SO₃-Ph-BTBP as complexing reagent. The extraction and scrubbing steps of the process were already tested in a former project and will be used as it is.

Based on an extraction model by TODGA previously developed in the framework of the SACESS project (Vanel et al., Procedia Chem. 2016, 21, 223-230), a model is implemented in the PAREX+ code to simulate the complexation of americium and curium by SO₃-Ph-BTBP (Dinh et al., GLOBAL 2013 conference, Salt Lake City, September 29th – October 3rd 2013). The model evaluates five series of tests run in a single-stage centrifugal contactor correctly. The determined complexation constants at equilibrium are consistent with those found in literature (Wagner et al., Dalton Trans., 2015, 44, 17143; Wagner et al., Solvent Extr. Ion Exch. 2016, 34, 2, 103-113). The main limitations of the model are the small range of acidity (0.7 M – 0.8 M HNO₃) of the experimental data and the simplified SO₃-Ph-BTBP speciation (data at 10 mM SO₃-Ph-BTBP).

With this model, different configurations of flowsheets are studied. Depending on the separation factor between Am and Cm, Am recovery rate and decontamination factor between Am and Cm can be hardly achieved simultaneously, and the flowsheet is highly sensitive to experimental parameters. A flowsheet was proposed and implemented by the Jülich team in August 2023 (see figure 2).

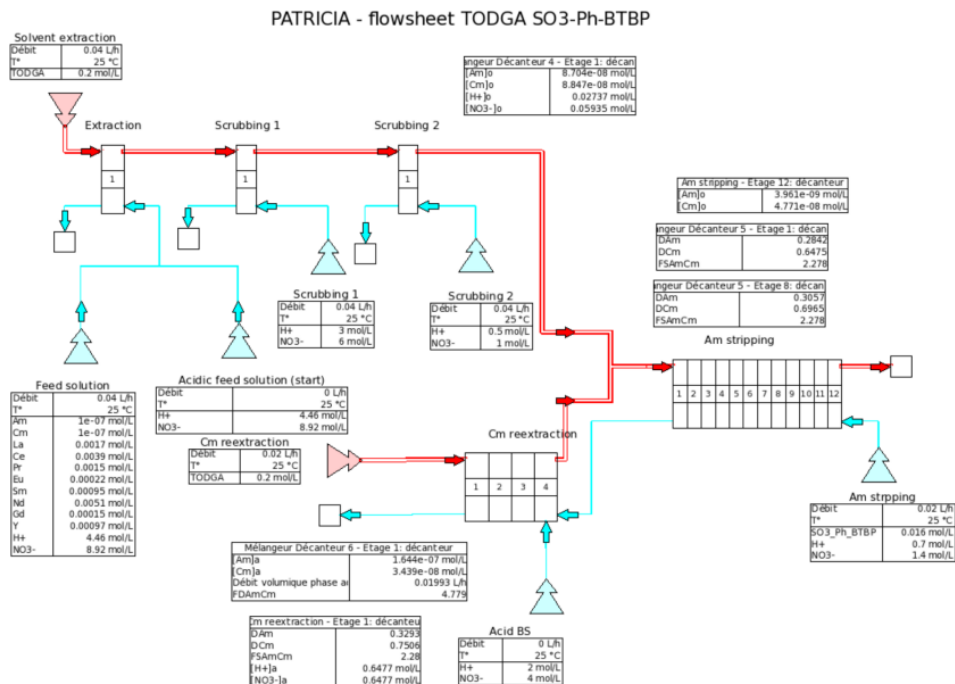


Figure 2. The AmSEL flowsheet

At the end of this test, it was possible to recover 45% of americium in the Am production flow, with a decontamination factor between Am and Cm around 9. The first exploitation of the Jülich test shows it is necessary to adapt the SO₃-Ph-BTBP speciation constant (flowsheet at 16 mM SO₃-Ph-BTBP) and the acidity profile. With these adaptations, it is possible to simulate the Am and Cm profiles correctly (see figure 3). These results will be used to design the flowsheet implemented at>NNL in February 2024.

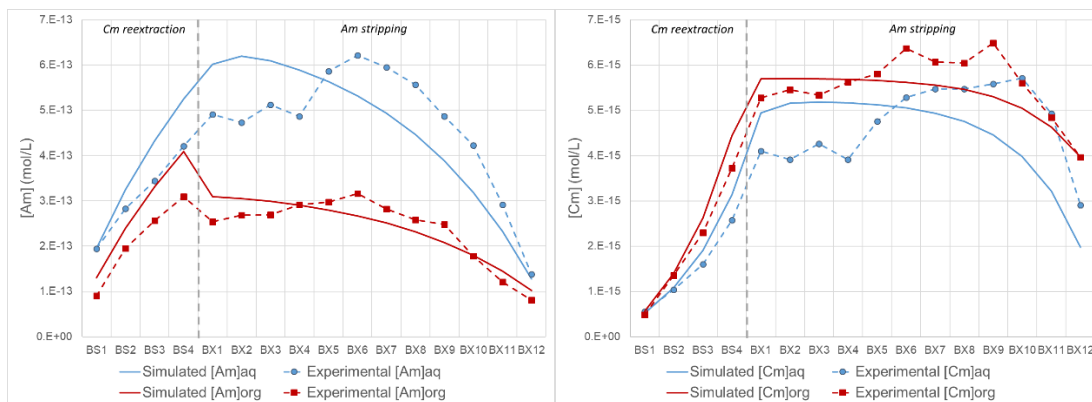


Figure 3. Simulation of the Jülich test profiles

Acknowledgments

Funding for this research was provided by the European Commission through the Partitioning And Transmuter Research Initiative in a Collaborative Innovation Action (PATRICIA) project, grant agreement number 945077.

Novel Water-soluble and CHON-compliant Ligands for Selective Americium Separation from PUREX Raffinate

Elena Macerata¹, Alberto Arici,¹ Giulia Firenze,¹ Letizia Di Matteo,¹ Fabrizio Piromalli,² Andrea Salomone,¹ Gabriele Magugliani,¹ Eros Mossini,¹ Mario Mariani,¹ Alessandro Sacchetti²

¹Department of Energy, Politecnico di Milano, Milano 20133, Italy

²Department of Chemistry, Chemical Engineering and Materials, Politecnico di Milano, Milano 20133, Italy

The management of spent nuclear fuel (SNF) is still a challenge for modern society, impacting on the social acceptance of nuclear energy. The advanced recycling of SNF by hydrometallurgical processes could lead to several benefits, above all the significant reduction of the long-term radiotoxicity and heat load of nuclear waste, strongly impacting on waste management and repository requirements.

In this perspective, the efficient separation of Am from Cm is a key point. Indeed, once removed U and Pu from SNF by PUREX process, Am isotopes are the main responsible for the long term radiotoxicity of nuclear waste. Cm isotopes are inevitably co-extracted with Am, due to their identical chemical behavior, but their relevant neutron emission and heat load make them undesired presence in the fuel fabrication step. Therefore, the separation of only Am from PUREX raffinate could facilitate the fabrication of Am-bearing fuel that could be fruitfully transmuted into shorter-lived isotopes by using proper reactors.

The experimental work focused on the development of new water-soluble ligands, made only of carbon, hydrogen, oxygen and nitrogen, able to selectively keep Am in the aqueous phase while Cm is removed into the organic phase within AmSel (Americium Selective separation) like processes [1]. In particular, the research reported in the present study would like to improve the knowledge about two new classes of hydrophilic ligands recently developed for the hydrometallurgical reprocessing of SNF, namely the bis triazolyl bipyridines and the bis triazolyl phenanthrolines [2, 3].

Three new derivatives belonging to these two classes, referred in the following BTzBP 1, BTzBP 2 and BTzPhen 1, were synthesized following a procedure reported in literature. The ligands' structure is characterized by a tetradentate nitrogen-based complexing core functionalized with different lateral chains to try to improve the limited solubility of these classes of water-soluble ligands [2, 3]. The work done highlighted the complexity in producing high purity compounds with good yields, and synthetic efforts were devoted to improving the yields while keeping a suitable purity. Despite characterization by NMR and ESI-MS techniques did not evidence relevant differences in the different ligand batches, differences were observed in the batch solubility and extracting behaviour. The introduction of a longer ethoxy-ethanol chain on the triazole in BTzBP 1 and BTzPhen 1 succeeded in achieving an excellent solubility in diluted nitric acid solutions (130 mM in [HNO₃] > 0.2M for BTzBP1; 100 mM in [HNO₃] > 0.1M for BTzPhen1). Conversely, a branched lateral chain resulted in an improvement in solubility at a lower extent (50 mM in [HNO₃] > 0.4M for BTzBP 2).

The ligand affinity for Am over Cm were studied under AmSel process conditions and taking into consideration the most relevant parameters. Different series of liquid-liquid extraction experiments were performed with organic phases composed of TODGA in kerosene containing 5% of 1-octanol and aqueous phases containing the ligand and representative cations (²⁴¹Am, ²⁴⁴Cm, ¹⁵²Eu in trace amount and La). Aqueous phase acidity and extractants concentrations were optimized to achieve a satisfactory Am separation from Cm. The most promising results were obtained for BTzBP 1 and BTzPhen 1 that enable to separate Am from Cm in a narrow range of acidity (around 0.3M HNO₃ for BTzPhen 1 and 0.4-0.5M HNO₃ for BTzBP 1) and with a separation factor for Cm over Am around 2, comparable to what achieved in the AmSel process. Am extraction is not substantially affected by temperature in the range (22-32°C) and extraction kinetics resulted to be rapid. Phase aging and stability towards gamma radiation were considered: the behavior of the ligands after ageing and gamma irradiation at low dose (25kGy) seems to be encouraging, but irradiation experiments at high absorbed doses (>100 kG) are still in progress.

Overall, based on the experimental results collected, it is worth to further investigate the extracting behavior of BTzBP1 and BTzPhen 1. They could be potential CHON alternative to SO₃-Ph-BTBP ligand, the current reference ligand in AmSel process

for Am selective stripping. Indeed, the here reported ligands are comparable to the reference one in terms of Am selectivity and extraction kinetics, but are more soluble, enabling a greater process flexibility, and CHON-compliant, facilitating the secondary waste management.

Funding for this research was provided by the European Commission through the PATRICIA project, grant agreement number 945077.

1. Wagner, C.; Müllich, U.; Geist, A.; Panak, P. J., Selective extraction of Am(III) from PUREX raffinate: the AmSel system. *Solvent Extr. Ion Exch.* **2016**, *34* (2), 103–113.
2. Weßling, P.; Maag, M.; Baruth, G.; Sittel, T.; Sauerwein, F. S.; Wilden, A.; Modolo, G.; Geist, A.; Panak, P. J., Complexation and extraction studies of trivalent actinides and lanthanides with water-soluble and CHON-compatible ligands for the selective extraction of americium. *Inorg. Chem.* **2022**, *61* (44), 17719–17729.
3. Edwards, A. C.; Mocilac, P.; Geist, A.; Harwood, L. M.; Sharrad, C. A.; Burton, N. A.; Whitehead, R. C.; Denecke, M. A. *Chem. Commun.* **2017**, 53, 5001–5004.

Extraction and Speciation Studies of New Diglycolamides with Varying Alkyl Chains for Selective Americium Partitioning

Filip Kolesar [1,2], Karen Van Hecke [2], Ken Verguts [2], Cécile Marie [3], Laurence Berthon [3], Koen Binnemans [1], Thomas Cardinaels [1,2]

[1] KU Leuven, Department of Chemistry, Leuven, Belgium

[2] Belgian Nuclear Research Centre (SCK CEN), Institute of Nuclear Energy Technology, Mol, Belgium

[3] Univ Montpellier, CEA, DES, ISEC, DMRC, Marcoule, France

filip.kolesar@sckcen.be

Since the first synthesis of diglycolamides by Sasaki *et al.* in 2001, much research has been devoted to the synthesis and testing of new diglycolamide derivatives for minor actinide partitioning from spent nuclear fuels [1]. One of the most promising extractants to come out of this research is *N,N,N',N'*-tetraoctyldiglycolamide (TODGA). TODGA shows excellent extraction properties, good resistance to hydrolysis and radiolysis, and it is compliant with the CHON principle. Research into its extraction properties culminated with the testing of a TODGA-TBP system for minor actinide recovery from a genuine PUREX raffinate [2]. TODGA extraction is considered as the first step in several selective actinide or selective americium separation systems, such as *i*-SANEX and AmSel processes [3, 4]. In parallel, new diglycolamide analogues with varying alkyl chains were synthesized to obtain "unsymmetrical diglycolamides" (UDGAs). Although a number of different structures have been synthesized, extraction experiments have so far mainly focused on separation of adjacent lanthanides or actinide-lanthanide separation and only a handful have been tested for their Am-Cm selectivity.

One diglycolamide with good extraction performance is *N,N*-di-isopropyl-*N',N'*-didodecyldiglycolamide (iPDdDGA, Figure 1). Extraction studies showed much more efficient extraction than what was observed for TODGA. During the GENIORS project, demonstrations in combination with TPAEN and SO₃-Ph-BTBP showed an improved separation between Am and Cm compared to TODGA. Although the influence of steric hindrance of the alkyl chains on the extraction properties of diglycolamides has already been investigated in previous studies, the effects of introducing a different symmetry into diglycolamide structures is not fully understood yet [5]. In order to gain more insight into these effects, new extractants similar in structure to iPDdDGA, keeping the same diglycolamide core and varying alkyl chains, were synthesized and tested. They were then evaluated through batch extraction tests with the AmSel system (TODGA + SO₃-Ph-BTBP) as a reference. Furthermore, a number of experimental speciation techniques were performed to probe the complexes formed in the organic phase.

In this work, five new diglycolamides were synthesized via the two-step synthesis method described by Mossand [6]. In the first step, didodecylamine was added onto diglycolic anhydride, which was then followed by substitution of a second diamine onto the molecule with the coupling agent (1-cyano-2-ethoxy-2-oxoethylidenaminooxy)dimethylamino-morpholino-carbenium hexafluorophosphate (COMU). The synthesized diglycolamides were *N,N*-dipropyl-*N',N'*-didodecyldiglycolamide (PDdDGA), *N,N*-dibutylamine-*N',N'*-didodecyldiglycolamide (BDdDGA), *N,N*-di-isobutyl-*N',N'*-didodecyldiglycolamide (iBDdDGA), *N,N*-dipentyl-*N',N'*-didodecyldiglycolamide (PnDdDGA), and *N*-pipiperidiny-*N',N'*-didodecyldiglycolamide (pipDdDGA), and are presented in Figure 1 [4]. In the original AmSel system, a first extraction step is performed whereby the trivalent lanthanides and actinides are co-extracted with TODGA dissolved in a kerosene diluent from a 3 mol/L nitric acid solution. This is then followed by a second step where americium is selectively stripped with 16 mmol/L of the SO₃-Ph-BTBP complexant dissolved in a 0.7 mol/L nitric acid solution. In this study, TODGA was replaced with the newly synthesized diglycolamides. Distribution ratios of lanthanides as well as ¹⁵²Eu, ²⁴¹Am, and ²⁴⁴Cm tracers were measured for both the loading and stripping steps, while focusing on the separation factors between Am and Cm and how these compare to those obtained for TODGA and iPDdDGA. The extraction experiments were followed up by a speciation study whereby ESI-MS, UV/VIS, and FTIR spectroscopy were employed to determine the stoichiometry of the formed complexes, characterize the complexes, and compare the different extractants.

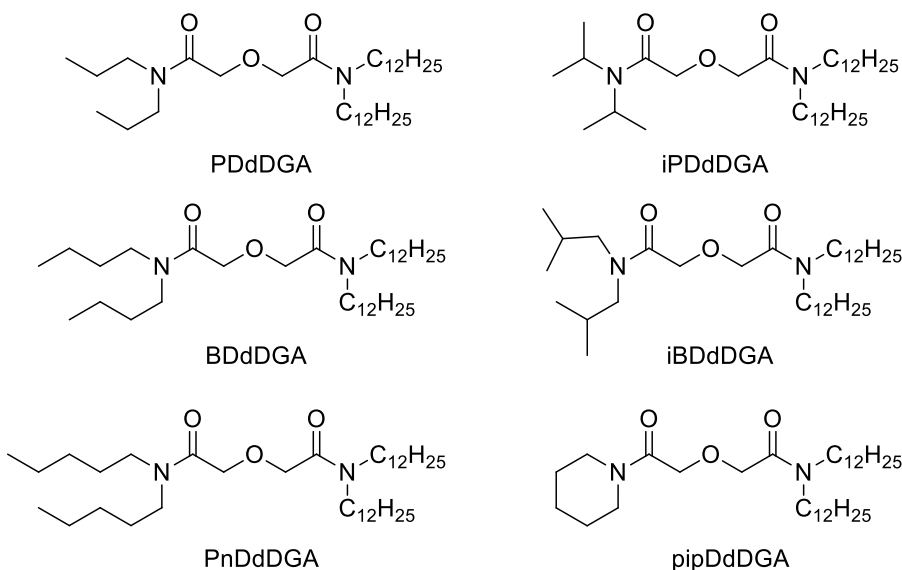


Figure 1: iPDdDGA (top right) and the newly synthesized diglycolamides

- [1] Sasaki, Y.; Sugo, Y.; Suzuki, S.; Tachimori, S. The novel extractants, diglycolamides, for the extraction of lanthanides and actinides in HNO_3 -n-dodecane system. *Solvent Extr. Ion Exch.* **2001**, *19* (1), 91-103. DOI: 10.1081/sei-100001376.
- [2] Magnusson, D.; Christiansen, B.; Glatz, J. P.; Malmbeck, R.; Modolo, G.; Serrano - Purroy, D.; Sorel, C. Demonstration of a TODGA based Extraction Process for the Partitioning of Minor Actinides from a PUREX Raffinate. *Solvent Extr. Ion Exch.* **2009**, *27* (1), 26-35. DOI: 10.1080/07366290802544726.
- [3] Wilden, A.; Modolo, G.; Sypula, M.; Geist, A.; Magnusson, D. The Recovery of An(III) in an innovative-SANEX process using a TODGA-based solvent and selective stripping with a hydrophilic BTP. *Atalante 2012 International Conference on Nuclear Chemistry for Sustainable Fuel Cycles* **2012**, *7*, 418-424. DOI: 10.1016/j.proche.2012.10.065.
- [4] Wagner, C.; Mullich, U.; Geist, A.; Panak, P. J. Selective Extraction of Am(III) from PUREX Raffinate: The AmSel System. *Solvent Extr. Ion Exch.* **2016**, *34* (2), 103-113. DOI: 10.1080/07366299.2015.1129192.
- [5] Stamberga, D.; Healy, M. R.; Bryantsev, V. S.; Albisser, C.; Karslyan, Y.; Reinhart, B.; Paulenova, A.; Foster, M.; Popovs, I.; Lyon, K.; et al. Structure Activity Relationship Approach toward the Improved Separation of Rare-Earth Elements Using Diglycolamides. *Inorg. Chem.* **2020**, *59* (23), 17620-17630. DOI: 10.1021/acs.inorgchem.0c02861.
- [6] Mossand, G. Recherche de nouveaux ligands pour l'extraction sélective de l'uranium et des terres rares. Ph.D. Dissertation, Université Grenoble Alpes, Grenoble, 2017. <https://tel.archives-ouvertes.fr/tel-03086901>.

Selective Americium Separation: New insights into the Complexation of SO₃-Ph-BTBP with Trivalent *f*-Elements

Fynn S. Sauerwein^{1,*}, Thomas Sittel², Andreas Geist², Andreas Wilden¹, Giuseppe Modolo¹

¹ Forschungszentrum Jülich GmbH, Institut für Energie- und Klimaforschung – Nukleare Entsorgung (IEK-6), 52428 Jülich, Germany, ² Karlsruhe Institute of Technology (KIT), Institute for Nuclear Waste Disposal (INE), 76021 Karlsruhe, Germany.

*Corresponding Author: f.sauerwein@fz-juelich.de

Recycling of minor actinides from PUREX raffinate solution is a decisive step towards closing the nuclear fuel cycle. A major challenge is the separation of Am(III) from Cm(III) and other trivalent fission lanthanides (Ln(III)). The Americium Selective (AmSel) process^[1] was designed for this task combining the water-soluble tetradentate N-donor ligand SO₃-Ph-BTBP (tetrasodium-3,3',3'',3'''-([2,2'-bipyridine]-6,6'-diylbis(1,2,4-triazine-3,5,6-triyl))tetrabenzene-sulfonate, Figure 1) with the well-known An(III)/Ln(III) coextracting agent TODGA (*N,N,N',N'*-tetra-*n*-octyl diglycolamide, Figure 1).

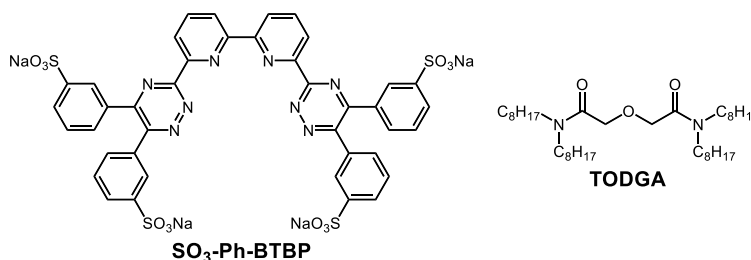


Figure 1: Chemical structures of SO₃-Ph-BTBP and TODGA.

Due to the preferential affinity of BTBP-type ligands for Am(III) over Cm(III)^[1-2], selective Am(III) stripping is possible from an organic An(III)/Ln(III)-loaded TODGA solution into a nitric acid solution containing SO₃-Ph-BTBP. The separation of Am from Cm and the light Ln (La-Gd) is achieved by adjusting the nitric acid concentration to approx. 0.8 mol L⁻¹ HNO₃ to reach distribution ratios $D_{Am(III)} < 1$ and $D_{Cm(III)}, D_{Ln(III)} > 1$ (Figure 2, left).

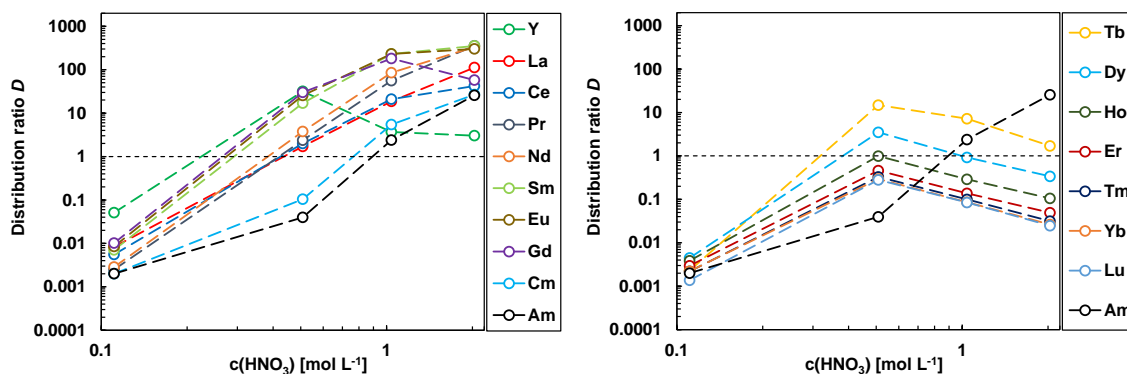


Figure 2: Distribution ratios of Am(III), Cm(III) and the Ln(III) (w/o Pm, incl. Y) for a batch extraction with 0.2 mol L⁻¹ TODGA in *n*-dodecane and 0.01 mol L⁻¹ SO₃-Ph-BTBP in 0.1 – 2 mol L⁻¹ HNO₃, shaking for 15 min at 22°C ±1°C with 2500 rpm.

As hydrophilic N-donor ligands are known for their susceptibility against protonation in acidic solutions competing with metal complexation^[3], and due to the extraction properties of TODGA, increasing distribution ratios with increasing nitric acid concentrations are expected. However, a significant drop in distribution ratios of the heavy Ln (Tb–Lu) and Y can be observed for $\geq 1 \text{ mol L}^{-1} \text{ HNO}_3$ ^[1] (Figure 2, right) indicating a strong complexation of these ions with $\text{SO}_3\text{-Ph-BTBP}$. Wagner et al. considered this remarkable behavior of the heavy Ln to originate from the formation of $\text{SO}_3\text{-Ph-BTBP}$ complexes in the aqueous phase with a composition other than the already known 1:2 metal-to-ligand complexes.^[1,4] Since fundamental understanding of the complexation mechanism of soft N-donor ligands is necessary for future design of optimized ligands, the complexation of $\text{SO}_3\text{-Ph-BTBP}$ with different Ln was further elucidated by different spectroscopic methods (UV/Vis, NMR) as well as ESI-MS. At low nitric acid concentrations ($10^{-3} \text{ mol L}^{-1} \text{ HNO}_3$), $\text{SO}_3\text{-Ph-BTBP}$ complexation is observed for all lanthanides. Remarkably, at high nitric acid concentrations ($3 \text{ mol L}^{-1} \text{ HNO}_3$), $\text{SO}_3\text{-Ph-BTBP}$ only forms complexes with the heavy, smaller ionic radii Ln ions, e.g., Ho^{3+} (Figure 3, left). Regardless of the nitric acid concentration, NMR studies of $\text{SO}_3\text{-Ph-BTBP}$ complexes with heavy Ln always showed the formation of the same complex species (allegedly the 1:2 complex). This surprising observation refutes the assumption of the existence of complexes with a composition other than 1:2.^[1] Apparently, $\text{SO}_3\text{-Ph-BTBP}$ is able to form complexes with the smaller heavy Ln ions in a deprotonated form even at high nitric acid concentrations.

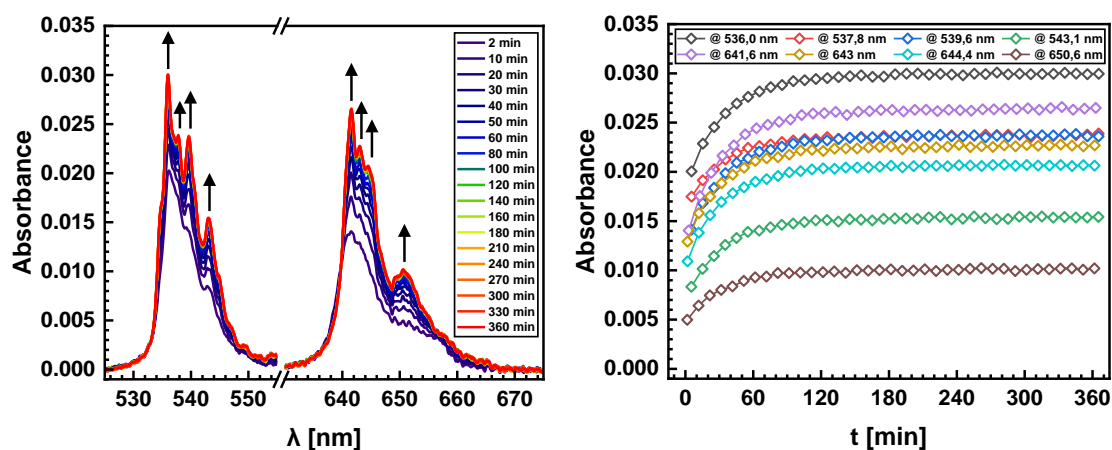


Figure 3: UV/Vis spectra of Ho^{3+} at $3 \text{ mol L}^{-1} \text{ HNO}_3$ recorded within 360 min after adding $\text{SO}_3\text{-Ph-BTBP}$ solution with a molar metal-to-ligand ratio of 1:2 (left). Absorbance at specific wavelengths as a function of time (right).

Complexation equilibrium for the light Ln is reached very fast. In contrast, equilibrium for the heavy Ln is reached between 90 min at $10^{-3} \text{ mol L}^{-1} \text{ HNO}_3$ to 4 h at $3 \text{ mol L}^{-1} \text{ HNO}_3$ (Figure 3, right). This effect was also confirmed by kinetic batch extraction studies and is presumably caused by the kinetically inhibited (de)complexation of the $[\text{Ln}(\text{SO}_3\text{-Ph-BTBP})_2]$ complexes. However, the mechanism is not yet understood and requires further studies.

Acknowledgements

Financial support for this research was provided by the European Commission through the Partitioning And Transmuter Research Initiative in a Collaborative Innovation Action (PATRICIA) project, grant agreement number 945077, and the German Federal Ministry of Education and Research through the *f*-Char project under grant numbers 02NUK059A and 02NUK059D.

References

- [1] C. Wagner, U. Müllich, A. Geist et al., *Solvent Extr. Ion Exch.* **2016**, 34(2), 103–113
- [2] A. Geist, C. Hill, G. Modolo et al., *Solvent Extr. Ion Exch.* **2006**, 24(4), 463–483
- [3] P. Weßling, M. Trumm, E. Macerata et al., *Inorg. Chem.* **2019**, 58(21), 14642–14651
- [4] C. Wagner, U. Müllich, A. Geist et al., *Dalton Trans.* **2015**, 44(39), 17143–17151

Purification of Neptunium and Plutonium by Ion Exchange for Plutonium-238 Production at Oak Ridge National Laboratory

Laetitia H. Delmau, David W. DePaoli, Brad N. Tinker, Dennis E. Benker, and Robert M. Wham

¹*Oak Ridge National Laboratory, Oak Ridge, TN 37931*

Plutonium-238 production capabilities have been reestablished in the United States through efforts conducted at Oak Ridge National Laboratory. After irradiation in the High Flux Isotope Reactor, neptunium-237 targets are transferred to the Radiochemical Engineering Development Center, where they are dissolved and processed to separate plutonium-238 and neptunium-237. Solvent extraction is the first process used to obtain separate plutonium and neptunium streams, and the fission products are discarded. However, that robust process does not provide streams with the purity required for the plutonium product to be used in radioisotope thermoelectric generators nor for recycling neptunium. The main issue for the plutonium lies in the presence of phosphorus (from tributyl phosphate breakdown products), thorium, and remaining neptunium because these species are present in levels that exceed the plutonium product specifications. As for the neptunium recycle stream, the presence of phosphorus may create physical abnormalities in the recycle neptunium pellets upon firing, whereas the presence of trace plutonium-238 (at levels greater than a few tens of parts per million in the neptunium) imposes added constraints for target preparation and handling. As a result, ion exchange has become an indispensable method to purify neptunium and plutonium. The plutonium stream is purified using anion exchange, a process that eliminates thorium, phosphorus, and other potentially lingering fission products. Also, a better understanding of the various redox behaviors of neptunium and plutonium on the column has led to a plutonium product essentially free of neptunium, already meeting product specifications. However, further purification is achieved using a cation exchange resin. A change in the valence of any trace of neptunium still present leads to a species that is not retained on the column while the plutonium is immobilized on the resin before calcination. Plutonium oxide obtained during the third plutonium-238 production campaign at Oak Ridge National Laboratory met all the desired product specifications. Results for the purity of the plutonium oxide produced during the fourth campaign are pending. The neptunium stream also undergoes a purification step using anion exchange, but again, better understanding of the behavior of the redox species provided a much cleaner neptunium product. The last step before being able to provide neptunium adequate for recycling is a purification through a cation exchange column. Large amounts of neptunium can be processed at once through a relatively small cation exchange column by using an adequate valence adjustment, leading to a neptunium product that meets all conditions for trace plutonium, thorium, and, primarily, protactinium. The removal of this last element is key to keeping the dose level low enough for production personnel.

Experimental Studies and Molecular Modeling of the Physico-chemical Properties of Pure Monoamides Extractants

Abderrazak Masmoudi, Dominique Guillaumont, Philippe Guilbaud

CEA, DES, ISEC, DMRC, Univ Montpellier, Marcoule, 30207 Bagnols sur Cèze, France

For several years now, research groups around the world have been looking for alternative processes to the PUREX process to treat spent nuclear fuel.¹ PUREX uses tributyl phosphate (TBP) as selective extractant to recover the reusable elements. Molecules from the monoamide family appear to be the most promising candidates as extracting agents to develop a new process.² They allow complete incineration thanks to their chemical composition, which consists solely of C, H, O and N atoms. They also enable U and Pu to be separated during the partitioning step, without the redox step of reducing Pu(IV) to Pu(III) required in the case of TBP.

Although monoamides have been widely studied as extractants, their intrinsic physico-chemical properties such as viscosity, solubility, density and surface tension are not well understood. A better understanding of these intrinsic properties would lead to a better understanding of the extraction solvent, which is often a monoamide diluted in a diluent such as hydrogenated tetrapropylene (TPH), and therefore better control of the system on an industrial scale. For this reason, in our work, we focus on investigating the physico-chemical properties of monoamides extractants as pure i.e. without diluent. This is done by coupling molecular modeling using molecular dynamics simulations³ and the COSMO-RS approach⁴ with experimental measurements to determine the viscosity, solubility and density of a large number of monoamide molecules. Our results have shown that molecular modelling reproduces experimental data qualitatively, and that the intrinsic properties of monoamides molecules can be modulated by modifying the alkyl chain lengths and branching. We have also found that external parameters such as extraction of nitric acid, U-loading and temperature have a major influence on these properties.

(1) Manchanda, V. K.; Pathak, P. N. Amides and Diamides as Promising Extractants in the Back End of the Nuclear Fuel Cycle: An Overview. *Sep. Purif. Technol.* **2004**, 35 (2), 85–103. <https://doi.org/10.1016/j.seppur.2003.09.005>.

(2) Rodrigues, F.; Ferru, G.; Berthon, L.; Boubals, N.; Guilbaud, P.; Sorel, C.; Diat, O.; Bauduin, P.; Simonin, J. P.; Morel, J. P.; Morel-Desrosiers, N.; Charbonnel, M. C. New Insights into the Extraction of Uranium(VI) by an N,N-Dialkylamide. *Mol. Phys.* **2014**, 112 (9–10), 1362–1374. <https://doi.org/10.1080/00268976.2014.902139>.

(3) Zhang, Y.; Otani, A.; Maginn, E. J. Reliable Viscosity Calculation from Equilibrium Molecular Dynamics Simulations: A Time Decomposition Method. *J. Chem. Theory Comput.* **2015**, 11 (8), 3537–3546. <https://doi.org/10.1021/acs.jctc.5b00351>.

(4) Eckert, F.; Klamt, A. Fast Solvent Screening via Quantum Chemistry: COSMO-RS Approach. *AIChE J.* **2002**, 48 (2), 369–385. <https://doi.org/10.1002/aic.690480220>.

Development of Integrated Actinide Chemistry Application, AACE, for Acceleration of Actinide Chemistry Experiments

Masahiko Nakase^{1,2}, Takahiro Nishihara^{1,2}, Fauzia Hanum Ikhwan¹, Tomohiro Okamura^{1,2}, Kota Matsui³

Laboratory for Zero-Carbon Energy, Institute of Innovative Research, Tokyo Institute of Technology

2. NEUChain Technology

3. Department of Biostatistics, Graduate School of Medicine, Nagoya University

Expanding nuclear energy utilization is inevitable to realize a zero-carbon society by 2050. Some innovative reactors have been developed, and there is also a growing focus on the multi-purpose use of nuclear energy. These will increasingly require accelerated reprocessing and waste research. Research on this separation remains essential because the amount of MA present will also increase because of the reprocessing of high burnup fuel and spent MOX fuel in the next generation of reprocessing. Separating Minor Actinide (MA) from High-Level-Liquid-Waste (HLLW) can minimize the waste repository. However, we must still explore the efficient extractants for MA/Lanthanide(Ln) separation for practical use. Extractants must meet all the necessary criteria, such as a high distribution ratio of trivalent MA but low for Ln, high solubility into the organic phase, no third phase formation, fast extraction kinetics, easy to synthesis (low cost), radiation resistance, and so on. We have been seeking a suitable solvent for a practical MA extraction system. We are mainly focusing on fluorinated solvents or mixture solvents of fluorinated solvent and long-chain alkyl acid for such purpose, and we are developing the scheme of how to find the excellent solvent not only by experiments but also through the chemoinformatic scheme. However, because of the constraints of synthetic effort, limitations of cost, and the generation of radioactive experimental waste, the policy of preparing a large amount of training data, as is usually the case in machine learning, may be more costly. Therefore, we find it needed some scheme of informatics and tools suitable for actinide chemistry, especially in our case, extraction work. Upon such circumstances, we developed an integrated machine-learning application named AACE (Acceleration of Actinide Chemistry Experiment) to make the sequential and repeated experimental activity to find suitable molecules more efficient. The typical functions and the design concepts are illustrated in Figure 1.

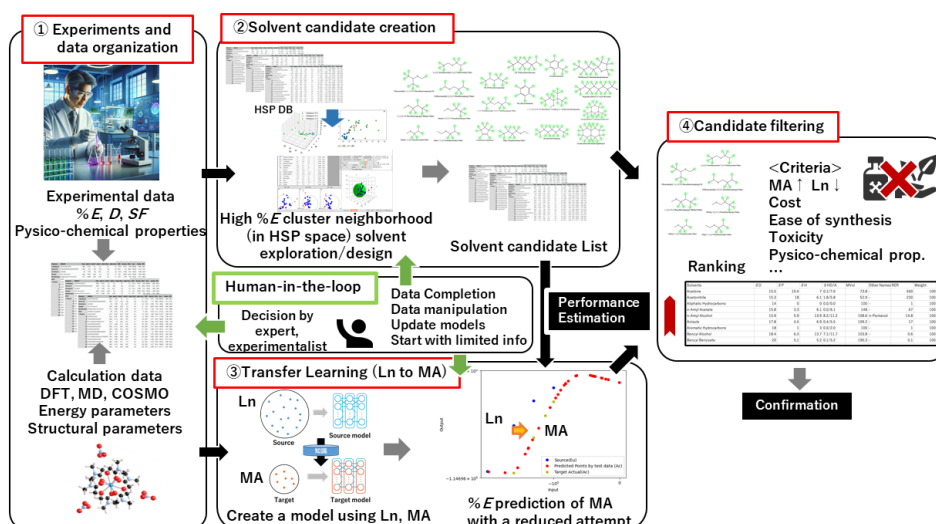


Figure 1 The concept of how to find a suitable solvent with the aid of Machine learning.

The AACE application is hand-made and designed to help experimentalists in actinide chemistry through its multiple functions, such as data organization, solvent candidate creation, transfer learning, and candidate filtration (ranking). Since this is an application, not a command line-based program, users can proceed with the attempt of chemoinformatics. Also, the AACE has the capability of one of the most important concepts, "human-in-the-loop (HITL)," to adjust data (e.g., remove outliers, omit suspect data) and make model updates and modification decisions. This HITL concept enables the chemoinformatic approach to start with less experimental data by considering the expert's experience and previously reported knowledge. The "Transition learning" is also an important concept for the acceleration of actinide chemistry experiments. Experiments with Nd and Eu are often performed to simulate Am behavior in the initial stage. By modeling the correlation between experimental data from the simulant of Am and actual data of Am, it can be possible to predict the Am data. It can greatly reduce the experimental attempts to understand the experimental behavior of Am. Some issues remain, such as evaluating the predicted extrapolated data by transfer learning. Still, the AACE program can predict the behaviors of the target element depending on the quality of the regression models generated from the simulant. By using this application, we are finding novel solvents and extractants with higher extraction performance of MA. The presentation will show the basic concept of the AACE program and some solvent exploration results, as well as the mechanistic insight of the solvent effects on the MA extraction performance.

This study is supported by the MEXT Innovative Nuclear Research and Development Program Grant Number JPMXD0221459189. Actinide extraction experiments were done at the International Research Center for Nuclear Material Science, Institute of Material Research, Tohoku University (Proposal number; 202211-IRKAC-0037, 202212-IRKAC-0413, 202112-IRKAC-0026, 202012-IRKAC-0019, and 20F0023)

Actinide Oxide Dissolution in Tributyl Phosphate

Jarrod M. Gogolski, Chelsea M. Goetzman, Robert J. Lascola, Tracy S. Rudisill

Savannah River National Laboratory, Aiken, South Carolina, USA

An alternative to dissolve used nuclear fuel (UNF) in an acidic solution during reprocessing is to use an organic solution. The flowsheet for this potentially less expensive alternative is first to voloxidize the UNF to remove fission product gases and form an oxide or nitrate mixture; depending on the gases used during voloxidation. After voloxidation, the UNF is dissolved in an organic solution containing an extractant, for example tributyl phosphate mixed with an aliphatic diluent and pre-equilibrated with nitric acid. The organic solution then goes through a solvent extraction process to recover the uranium and/or other desired radionuclides. This work prepared multiple oxides containing varying amounts of uranium, transuranics, and surrogate fission products to determine their dissolution characteristics in the organic solution. The nitrate forms of the oxides were co-precipitated with a hydroxide and then calcined. The calcined solids were then dissolved in a reaction vessel using an air sparging technique to promote mixture and determine scalability of dissolution design. The co-precipitation process produces solid solutions like materials made during the voloxidation of UNF. We studied the dissolution mechanism of the calcined solids using UV-visible-near IR absorbance. Trivalent cations are poorly extracted by TBP within a conventional solvent extraction process; however, the trivalent cations will readily complex the TBP in the absence of an aqueous phase. Additionally, material that is otherwise difficult to dissolve in nitric acid, like PuO_2 or its surrogate CeO_2 , will readily dissolve after being co-precipitated with other elements.

Direct Extraction of Uranium from Used Nuclear Fuel with DEHiBA

Gabriel B. Hall, Nathan P. Bessen, Daria Boglaienko, Gregg J. Lumetta

Pacific Northwest National Laboratory, Richland, WA, USA

With increased focus on advanced reactors which will utilize High Assay Low Enriched Uranium (HALEU), the economic incentive for reprocessing used nuclear fuel (UNF) may increase due to the need to recapture uranium with its residual ^{235}U enrichment. For this reason, Pacific Northwest National Laboratory (PNNL) has been investigating N,N-di-2-ethylhexyl-isobutyramide (DEHiBA, Figure 1) for a uranium (U) only recycle strategy.^{1,2} DEHiBA is selective for hexavalent actinides which offers proliferation resistance by routing Pu with the high activity waste. DEHiBA also adheres to the CHON principle, allowing incineration of secondary organic waste.

The traditional head-end for reprocessing used nuclear fuel is to chop the fuel and dissolve it in hot nitric acid. This is then followed by solvent extraction to recapture desirable components. Directly dissolving the fuel into process solvents (primarily tributyl phosphate, TBP) was first envisioned in the 1960s,³ but has received relatively little attention in the interim.^{4,5} Several advantages can be envisioned including providing a preliminary separation during dissolution, reducing plant footprint, simplifying the process by combining two operations (dissolution and extraction) and reducing corrosion to equipment due to more benign dissolution conditions. Given its known selectivity for hexavalent actinide ions, we have sought to extend this idea to the direct extraction of U from commercial used nuclear fuel.

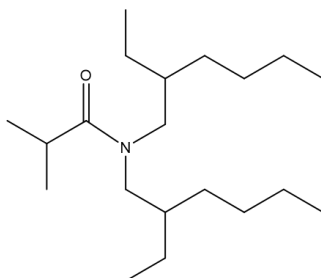


Figure 1. Chemical structure of DEHiBA

Direct extraction of U from three uranium oxides (U_3O_8 , UO_3 , and nitrated uranium oxide) into 1.5 M DEHiBA in *n*-dodecane is examined. The three uranium oxides examined represent three possible feed materials produced in an upstream voloxidation process. For direct extraction of U from the U_3O_8 and UO_3 phases, the DEHiBA solvent is first loaded with nitric acid (HNO_3). For U_3O_8 , the HNO_3 is necessary for oxidation, and for UO_3 the HNO_3 is necessary to form uranyl nitrate. When U has already been nitrated during the voloxidation process, it dissolves without the need for HNO_3 . Sufficiently high loading of U in the organic phase is achieved for all three chemical forms of U, however radiological degradation of the solvent during direct extraction at high concentration is a concern that must be examined in the future. Experiments performed with simulated fuels containing select fission products indicate the direct extraction of the lanthanide elements into the process solvent is suppressed for DEHiBA compared to 30% TBP in *n*-dodecane. Rhenium which was used as a surrogate for technetium is found to significantly dissolve in both TBP and DEHiBA based systems. The fuel simulant which utilized the nitrated uranium oxide showed significant dissolution of fission products negating the initial separation which makes direct extraction attractive.

Direct U extraction experiments were also conducted with Np and Pu doped into a solid solution of U_3O_8 . When the Np-doped U_3O_8 was contacted with the HNO_3 loaded DEHiBA solvent, 48% of the Np accompanied the U into the DEHiBA solvent. Under similar conditions, only 3% of the Np was directly extracted into the solvent when pure NpO_2 was the Np source. This suggests that the loss of lattice stabilization energy by comparison to the pure transuranic oxide caused a higher dissolution rate. A similar experiment conducted with Pu-doped U_3O_8 indicated 30% of the Pu accompanied the U into the DEHiBA phase.

Distribution ratio measurements of the dissolved Np and Pu (Figure 2) suggest that the dissolved transuranics exist as a mixture of oxidation states after dissolution. This contrasts with traditional expectations of DEHiBA which suggest it only extracts the hexavalent actinides.

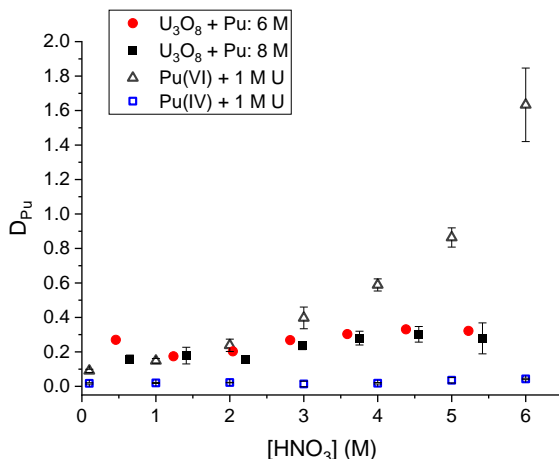


Figure 2. Stripping distribution ratio of Pu after direct dissolution into 1.5 M DEHiBA precontacted with either 6 or 8 M HNO₃. Compared against the distribution ratios obtained from the forward extraction of pure valence Pu in the presence of 1 M uranyl nitrate. Concentration of U after direct dissolution was nominally 0.42 M.

1. Extraction of Nitric Acid and Uranium with DEHiBA Under High Loading Conditions, Hall, G.B.; Campbell, E.L.; Bessen, N.P.; Graham, T.R.; Cho, H.; RisenHuber, M.; Heller, F.D.; Lumetta, G.J., *Inorganic Chemistry* Vol. 62(17), pg. 6711, **2023**
2. Extraction of Zirconium, Technetium, Neptunium, Plutonium, and Americium by Di-(2-ethylhexyl)-iso-butyramide at High Metal Loadings, Hall, G.B.; Bessen, N.P.; Zalupski, P.R.; Campbell, E.L.; Grimes, T.S.; Peterman, D.R.; Lumetta G.J., *Solvent Extraction and Ion Exchange* Vol. 41(5) pg. 545, **2023**
3. Tomijima, H.; Tsukui, K.; Okoshi, Y. Direct Dissolution of Water Insoluble Uranium Compounds by Contact with Neutral Organic Solvents Pretreated with Nitric Acid. US3288568A, November 29, 1966.
4. Dissolution of Used Nuclear Fuel Using a Tributyl Phosphate/n-Paraffin Solvent, Rudisill, T. S.; Shehee, T. C.; Jones, D. H.; del Cul, G. D. *Sep Sci Technol*, 54 (12), pg. 1904, **2019**
5. Kinetics of UO₃ dissolution in nitric acid saturated 30% TBP in a hydrocarbon diluent. Dorda, F.A.; Lazarchuk, V.V.; Matyukha, V.A.; Sirotkina, M.V.; Tinin, V.V., *Radiokhimiya*, 52(5): pg. 397, **2010**

New Monoamide Based Extractants for U(VI) and Pu(IV) Efficient Separation

Cécile Marie¹ Pape Diabate,¹ Audrey Beillard¹

¹ CEA, DES, ISEC, DMRC, Univ. Montpellier, Marcoule, Bagnols sur Cèze 30207, France

Uranium (VI) and plutonium (IV) are separated from spent nuclear fuels at the industrial scale by the PUREX solvent extraction process, using tri-*n*-butyl phosphate (TBP) as extractant. Although TBP has been used for decades as an extractant, it has some drawbacks like its non-incinerability and the formation of undesirable degradation products caused par radiolysis. In addition, the separation of U(VI) from Pu(IV) involves the reduction of Pu(IV) to Pu(III), which requires the use of reducing and stabilizing agents such as U(IV) and hydrazinium nitrate. In order to develop a new extraction system allowing to reprocess MOX fuels in one single cycle and with respect of the CHON principle (i.e. ligands comprising carbon, hydrogen, oxygen and nitrogen atoms only), we have focused our research in recent years on the development of numerous monoamide based extractants [1-3]. Cyclic amine monoamides were recently designed, which are so far very promising molecules to achieve efficient separation of U(VI) and Pu(IV) without reducing agent [4]. In fact, their cycle structure gives them high extraction yields for U(VI) and Pu(IV) in highly acidic medium and allows a very good separation of the latter at lower nitric acid concentration.

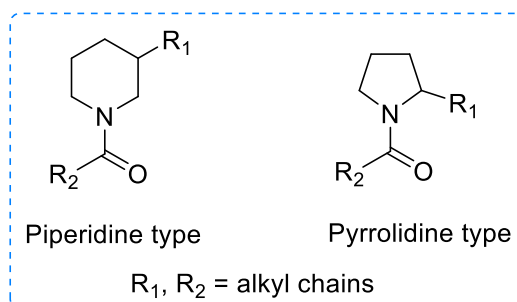


Figure 1: Structures of cyclic monoamide extractants

The impact of structural modifications (alkyl chains length and branching) on extraction efficiencies (U and Pu distribution ratios, U/Pu selectivity) and physicochemical properties (viscosity and loading capacity) was investigated. Specifically, the alkyl chains length (total number of carbon atoms on the molecule) was adapted to provide sufficient lipophilicity preventing from third phase formation, while maintaining a reasonable viscosity (compatible with a good hydrodynamic behaviour). In order to study the complexes formed with U(VI) and Pu(IV) in the organic phase, a speciation study was performed using UV-Visible spectrophotometry.

The authors acknowledge ORANO and EDF for financial support

- [1] Milanole G., Russello E., Marie C., Miguiditchian M., Sorel C., Patent 2018, WO2018138441.
- [2] Miguiditchian M., Baron P., Lopes Moreira S., Milanole G., Marie C., Patent 2017, WO2017/017193.
- [3] Marie C., Berger C., Mossand G., Russello E., Andreiadis E., Guillaumont D., Miguiditchian M., Sorel C., Patent 2019, WO2019002788.
- [4] Marie C., Beillard A., Aloin V., Sorel C. Patent 2023, WO2023067273.

Efficient Manufacture of DEHiBA through Industry 4.0

Tom Shaw, Prof. Bruce Hanson, Prof. Richard Bourne

*Institute of Process Research and Development, School of Chemistry & School of Chemical and Process Engineering,
University of Leeds, LS2 9JT, UK.*

Advanced nuclear reprocessing flowsheets are heavily reliant on specialised organic ligands for their selective chelation properties that facilitates the extraction and recovery of troublesome and valuable radionuclides from used nuclear fuel. This reduces the burden of radiotoxic waste whilst enhancing the sustainability of nuclear fission through the recycle of elements from across the periodic table. The specialist nature of highly tailored ligands such as DEHiBA, TODGA, DMDOHEMA, and BTBPs lends them to being high-cost research materials. This cost barrier is restrictive to researchers, especially when considering the required volumes for pilot-plant testing of advanced flowsheets to further the technology readiness level. The rise of industry 4.0 enhances the optimisation of chemical processes, streamlining the development of chemicals by integrating machine-learning with automated manufacture platforms to maximise key process metrics in minimal time.

By exploiting the power of machine-learning and automated flow chemistry, this work employs an automated, self-optimising flow reactor platform to facilitate the optimisation of process metrics such as reagent cost and productivity for the manufacture of ligands like DEHiBA and TODGA. This approach has identified an optimal, scalable, cost effective manufacture route to DEHiBA (*N,N*-di-(2-ethylhexyl)isobutyramide), through the optimisation and comparison of multiple synthetic pathways and purification routes. This technology facilitates the rapid optimisation of chemical transformations in as little as a day. The resulting product of these optimisations is a synthetic route that offers production rates upwards of 70 kg L⁻¹ h⁻¹ of DEHiBA and product yields of 99.7%, furthermore no solvent is needed to control this reaction, granting a process mass intensity of 1.29 g g⁻¹. We therefore have a methodology applicable to other ligands of interest, granting access to these ligands at a more affordable price (<£100 per litre of DEHiBA) and on demand. We now have the capability to manufacture litres of DEHiBA in house at the Institute of Process Research and Development in the University of Leeds.

Ultimately, this has facilitated our ability to test the performance of DEHiBA for the extraction of uranium across a range of scales and conditions both in batch and flow with pilot plant equipment such as the annular centrifugal contactors in the active lab at Leeds. Thus, confirming that the performance of our DEHiBA matches the data in the literature. This talk discusses and builds on work in our recent publication.¹

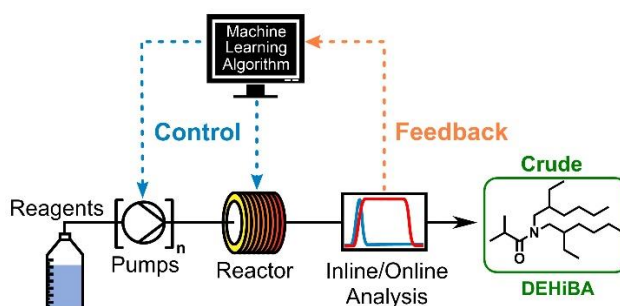


Figure 1. An illustration of a self-optimising flow reactor platform for the automated process optimisation of chemical reactions, such as the synthesis of DEHiBA.

1. T. Shaw, A. D. Clayton, R. Labes, T. M. Dixon, S. Boyall, O. J. Kershaw, R. A. Bourne and B. C. Hanson, *Reaction Chemistry & Engineering*, 2024.

Interinstitutional Study of the New EURO-GANEX Process Resistance by Gamma Irradiation Test Loops

Ivan Sanchez-Garcia,¹ Xavier Heres,² Dean. R. Peterman,³ Hitos Galan,¹ Sylvain Costenoble,² Sylvain Broussard,² Johann Sinot,² Travis S. Grimes,³ Kash Reid Anderson,³ Santa Jansone-Popova,⁴ Maria Chiara Gullo,⁵ Alessandro Casnati,⁵ Andreas Wilden,⁶ and Andreas Geist⁷

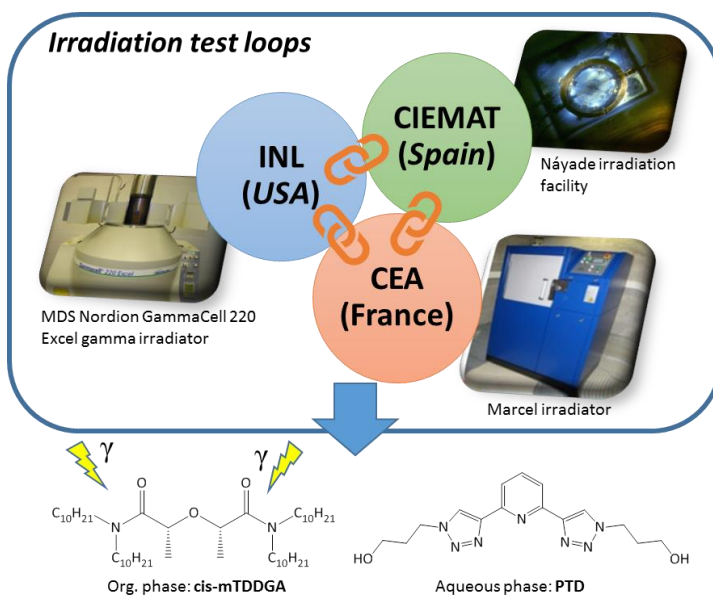
¹Centro de Investigaciones Energéticas, Medioambientales y Tecnológicas (CIEMAT), Avda. Complutense 40, 28040, Madrid (Spain) - ²CEA/DES/ISEC/DMRC-Montpellier University, Marcoule, BP 17171, 30207 Bagnols sur Cèze (France) -

³Center for Radiation Chemistry Research, Idaho National Laboratory, 1955 N. Freemont Ave., Idaho Falls, 83415 (United States) - ⁴Chemical Sciences Division, Oak Ridge National Laboratory, 1 Bethel Valley Rd, Oak Ridge, 37831 (United States)

- ⁵Dept. of Chemistry, Life Sciences and Environmental Sustainability, University of Parma, Parco Area delle Scienze 17/a, 43124 Parma (Italy) - ⁶Forschungszentrum Jülich GmbH (FZJ), Institut für Energie- und Klimaforschung, Nukleare Entsorgung (IEK-6), 52428, Jülich (Germany) - ⁷Karlsruhe Institute of Technology (KIT), Institute for Nuclear Waste Disposal (INE), 76021, Karlsruhe (Germany).

Future advanced nuclear fuel cycles are currently under development around the world with the purpose of increasing nuclear fuel cycle sustainability and reducing the long-term radiotoxicity and heat load of nuclear waste by means of separation and transmutation of the transuranic elements (TRU), specifically the minor actinides (MA: Np, Am, Cm), that together with Pu, have the highest contribution to the long-term radiotoxicity of spent nuclear fuel [1-3]. With this aim, new separation processes based on solvent extraction for the recovery of TRU are being developed globally, which could follow the heterogeneous or homogeneous strategy for the actinides recycling [3-5].

As part of the homogeneous actinide recycling strategy, the EURO-GANEX process is one of the most promising options to achieve the goal of minor actinides recovery. Improvements made to EURO-GANEX system have resulted in the emergence of the so-called New EURO-GANEX process, where the composition of the solvent has been modified by replacing TODGA and DMDOHEMA with *cis*-mTDDGA in the organic phase and SO₃-Ph-BTP with PyTri-Diol in the aqueous phase in order to resolve important issues such as the use of compounds that do not comply with the CHON principle. The objective of this work is 2-fold: evaluate the gamma radiolytic resistance of the new EURO-GANEX process by dynamic irradiation conditions simulating the three main steps of the process and validate the design of CIEMAT Náyade, CEA Marcel, and INL irradiation loop devices since each of them mimics different aspects of the real process. For that reason, this work is involved as part of an inter-institutional collaboration between CEA (*Commissariat à l'énergie atomique et aux énergies alternatives*) in France, INL (*Idaho National Laboratory*) in the United States, and CIEMAT (*Centro de Investigaciones Energéticas, Medioambientales y Tecnológicas*) in Spain. For this collaboration, each research centre employed its irradiation loop device to evaluate the resistance of the New EURO-GANEX process to gamma radiolytic degradation using similar conditions and same solutions. In particular, the Náyade and INL loops could irradiate the organic and aqueous phases together, whereas in the CEA loop, the irradiated solvent is recycled continuously inside a platform with several stages of mixer-settlers containing aqueous flows simulating the three main steps of the process. The extraction performances and changes in the composition of the solvent have been analyzed during the irradiation experiment by different techniques: gamma spectrometry and ICP-MS/OES for cations or radioactive tracer extraction and HPLC-MS to identify and quantify the degradation compounds. Despite some differences between the three irradiation facilities, this interinstitutional study shows that these three comparative tools provide similar trends in the radiolytic stability of a liquid-liquid extraction system. Favorable extraction results for the different steps are obtained according to the static irradiation studies found in literature. However, the degradation of *cis*-mTDDGA is appreciable leading to degradation compounds, some of which form precipitates and produce substantial changes in viscosity, important aspects that must be addressed prior to the successful industrial application of the new EURO-GANEX process.



Acknowledgment

The work carried out by CIEMAT was developed and funded under the framework of the European H2020 GENIORS Project (Contract n: 755171) and Spanish SYTRAD II project (National R&D program: "Retos de la Sociedad", reference number: ENE2017-89280-R). The studies carried out in MARCEL loop test was funded by the CEA, Energy Division, Research Department on Mining and Fuel Recycling Processes, under contract EUR857755171. The experimental work conducted by D. R. Peterman at the Idaho National Laboratory was supported by the Nuclear Technology Research and Development Program, Office of Nuclear Energy, DOE Idaho Operations Office, under contract DE-AC07-05ID14517. The synthesis efforts by S. Jansone-Popova at Oak Ridge National Laboratory were supported by the Nuclear Technology Research and Development Program, Office of Nuclear Energy, U.S. Department of Energy. A. Casnati and M. Chiara. Gullo are grateful for the use of facilities acquired in the framework of the COMP-HUB and COMP-R initiative by the Departments of Excellence Program of MUR, Rome, Italy, 2018-2022 and 2023-2027.

REFERENCES

- [1] Poinssot, C. et al., Comparison between closed and open fuel cycles. *Energy* 2014, 69, 199-211.
- [2] Poinssot, C.; et al., Improving the nuclear energy sustainability by decreasing its environmental footprint. Guidelines from life cycle assessment simulations. *Prog. Nucl. Energy*. 2016, 92, 234-241.
- [3] Assessment of Partitioning Processes for Transmutation of Actinides; International Atomic Energy Agency (IAEA), 2010.
- [4] Joly, P.; Boo, E. ROADMAP-Actinide Separation Processes; Euratom Research and Training Programme on Nuclear Energy within the Seventh Framework Programme, 2015.
- [5] Baron, P. et al., A review of separation processes proposed for advanced fuel cycles based on technology readiness level assessments. *Prog. Nucl. Energy* 2019, 117, 103091.

Americium Separation Processes Developed within the European PATRICIA Project

Christian Sorel,¹ **Andreas Geist**,² Giuseppe Modolo,³ Laure Ramond,¹
Christian Ekberg,⁴ Hitos Galán,⁵ Bruce Hanson,⁶ Gregory Leinders,⁷
Elena Macerata,⁸ Cécile Marie,¹ Petra J. Panak,^{2,9} Mark Sarsfield,¹⁰
Dan Whittaker,¹⁰ Andreas Wilden³

¹French Alternative Energies and Atomic Energy Commission, CEA, DES, ISEC, DMRC, Univ. Montpellier, Marcoule, Bagnols sur Cèze 30207, France

²Karlsruhe Institute of Technology (KIT), INE, Karlsruhe, Germany

³Forschungszentrum Jülich GmbH (FZJ), IEK-6, Jülich, Germany

⁴Nuclear Chemistry, Chalmers University of Technology, Gothenburg, Sweden

⁵Centro de Investigaciones Energéticas, Medioambientales y Tecnológicas (CIEMAT), Madrid, Spain

⁶School of Chemical and Process Engineering, Faculty of Engineering and Physical Sciences, University of Leeds, UK

⁷Institute for Nuclear Energy Technology, Belgian Nuclear Research Centre (SCK-CEN), Mol, Belgium

⁸Department of Energy, Politecnico di Milano, Milano, Italy

⁹Institute of Physical Chemistry, Heidelberg University, Heidelberg, Germany

¹⁰National Nuclear Laboratory, Central Laboratory, Seascale, UK

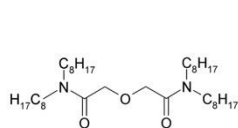
PATRICIA (Partitioning and Transmuter Research Initiative in a Collaborative Innovation Action) is a EURATOM Research and Innovation Action project. In PATRICIA the efficient separation of Am from spent fuel and the behaviour of Am bearing fuel under irradiation is studied, fuel performance codes are developed, and safety related research supporting the licensing process of MYRRHA is performed. For the first time, three R&D communities, partitioning, transmutation, and MYRRHA development, are collaborating in a dedicated project.

Regarding the separation of Am, PATRICIA will see the development and testing (on the lab scale) of processes to extract Am from a PUREX raffinate solution and convert it into a solid precursor material suitable for target or fuel fabrication. This work programme is divided into three Work Packages:

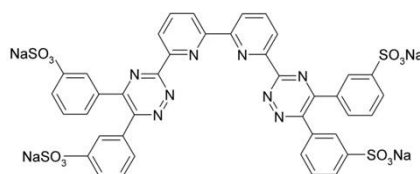
WP1 Basic data acquisition addresses the synthesis and assessment of new CHON compliant ligands for selective Am(III) back-extraction, the determination of liquid-liquid distribution data for Am(III), Cm(III), Ln(III) and key fission products, and the assessment of the radiolytic stability of the chemical systems involved.

The current reference system¹ for Am separation was initially developed in the previous SACSESS project. It uses SO₃-Ph-BTBP to selectively strip Am from a TODGA solvent loaded with Am(III), Cm(III), and Ln(III). Its radiolytic stability was investigated in detail, proving the system's applicability from a stability point of view. Some hitherto unexplained behaviour of heavy lanthanides could be explained by spectroscopic studies.

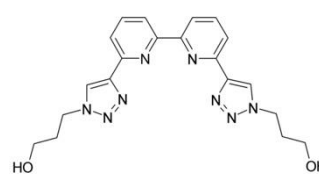
TODGA shows unwanted co-extraction of some fission products other than Ln(III), most notably, Zr(IV), Mo(VI), and Tc(VII). To develop efficient decontamination strategies, the extraction of these fission products was studied.



TODGA



SO₃-Ph-BTBP



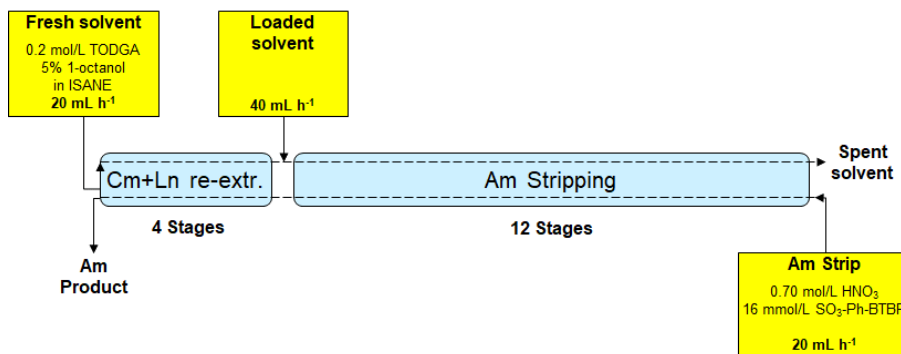
ProH-BPTD

The sulphur content of SO₃-Ph-BTBP creates issues with secondary waste management. Consequently, an alternative stripping agent, ProH-BPTD, was developed in PATRICIA.² This molecule consists only of C, H, O, and N atoms, making it

compatible with secondary waste management. Initial studies proved the TODGA/PROH-BPTD system's feasibility even with nominal concentrations (several mmol/L) of Am(III). When irradiated to relevant doses, the TODGA/PROH-BPTD system maintains its properties. Hence, this system is proposed to replace the TODGA/SO₃-Ph-BTBP system.

WP2 *Process development* tests the above systems by running lab-scale process tests. Flow sheets for process validation are developed using data obtained in WP1, and these flow sheets are then tested using miniature centrifugal contactor rigs.

A flow sheet based on the TODGA/SO₃-Ph-BTBP system was developed and consequently tested with a 16-stage counter-current centrifugal contactor rig using a surrogate PUREX raffinate solution spiked with Am(III) and Cm(III). First results are promising; however, some fine tuning of the flow sheet is needed to improve the decontamination factors.



TODGA/SO₃-Ph-BTBP process flow sheet tested in centrifugal contactors.

In addition to the laboratory trials, process models were developed of the whole flowsheet to investigate operation at full scale and identify critical parameters and their sensitivity on overall Am recovery.

WP3 *Conversion* investigates different liquid-to-solid conversion processes to obtain minor actinide-doped precursor materials suitable for fuel or target fabrication. Both fissile/fertile matrices and inert matrix compounds are being considered. Particular emphasis is on the effect of the Am(III) stripping agent (SO₃-Ph-BTBP or PROH-BPTD) on the conversion steps and on the quality of the final product. Additionally, by studying the hydrolysis behaviour of minor actinide elements in aqueous nitrate solutions, the suitability of sol-gel processes to fabricate microspheres has been evaluated.³

This is an overview of the work carried out in PATRICIA related to the development of Am separation processes. Further details will be presented in dedicated contributions to the ATALANTE 2024 conference.

Funding for this research was provided by the European Commission through the PATRICIA project, grant agreement number 945077.

1. Wagner, C.; Müllich, U.; Geist, A.; Panak, P. J., Selective extraction of Am(III) from PUREX raffinate: the AmSel system. *Solvent Extr. Ion Exch.* **2016**, 34 (2), 103–113.
2. Weßling, P.; Maag, M.; Baruth, G.; Sittel, T.; Sauerwein, F. S.; Wilden, A.; Modolo, G.; Geist, A.; Panak, P. J., Complexation and extraction studies of trivalent actinides and lanthanides with water-soluble and CHON-compatible ligands for the selective extraction of americium. *Inorg. Chem.* **2022**, 61 (44), 17719–17729.
3. Leinders, G.; Acevedo, B.; Jutier, F.; Colak, G.; Verwerft, M., Speciation and ammonia-induced precipitation of neptunium and uranium ions. *Inorg. Chem.* **2023**, 62 (25), 9807–9817.

Radiolytic Stability of Metal (IV) Phosphonate Sorbents Designed for Minor Actinide–Lanthanide Separations

Taren Cataldo¹, Jessica Veliscek–Carolan², Nicholas Bedford¹, Sophie Le Caër³

¹*School of Chemical Engineering, University of New South Wales, Sydney, New South Wales 2052, Australia*

²*ANSTO, New Illawarra Rd, Lucas Heights NSW 2234, Australia*

³*NIMBE, IRAMIS, CEA, CNRS, Paris–Saclay University, CEA Saclay, 91191 Gif sur Yvette Cedex, France*

Nuclear power is an intrinsically clean source of energy. However, improvements in nuclear waste treatment are required. The minor actinide (MA) elements in nuclear waste are problematic due to their radiotoxicity and long half-lives. In principle, minor actinides (MAs) in nuclear waste could be recycled. However, the chemical similarity of MAs and the lanthanide fission products also found in nuclear waste means that separating and recycling MAs is extremely challenging. Hence, there is a need for materials that can selectively separate MAs from lanthanides in nuclear waste, whilst also possessing the necessary acid and radiation resistance required to function in nuclear waste conditions.

Metal (IV) phosphonates, such as titanium or zirconium phosphonates, are a type of material with promising potential for MA–lanthanide separation applications. Metal phosphonates are a coordination polymer: a material in which inorganic metal cations are structurally joined together by organic ligands via coordinate bonds. The hybrid inorganic–organic nature of metal phosphonates allows for a variety of chemical and physical properties. In the context of MA–lanthanide separations, the phosphonate component allows for the intramolecular incorporation of organic ligands that provide selectivity and efficiency for MA sorption. Furthermore, the strong M(IV)–O–P bonding of the inorganic component provides stability and resistance to acid and radiation damage. Post-synthesis, metal phosphonates are collected as a porous, solid powder; hence, they can be employed as a solid-phase phase sorbent in MA–lanthanide separations. Previous studies on zirconium (IV) phosphonate materials have demonstrated promising sorption capacity, selectivity for MA over lanthanides, and excellent stability^{1,2,3}. Therefore, further study and optimization of these materials presents a potential pathway for solving the challenges of MA separation and recycling.

In this study, a zirconium phosphonate sorbent that intramolecularly incorporates the MA-selective 2,6-bis(1,2,3-triazol-4-yl)pyridine (PTP) ligand was synthesised. The sorbent (ZrPTP) was irradiated with high energy electron radiation to doses of 2 MGy to study its radiation stability. Since ZrPs are highly amorphous, synchrotron light sources were employed to accurately assess the average local structure before and after irradiation using x-ray absorption spectroscopy (XAS) and atomic pair distribution function (PDF). Gas chromatography, solid-state NMR and infrared spectroscopy were also used to support the characterisation. Lastly, the MA-selectivity of ZrPTP before and after irradiation was compared using americium and europium. It was found that ZrPTP possessed excellent radiation stability for doses up to 2 MGy. Characterisation of ZrPTP exhibited only small amounts of radiation damage to its Zr–O bonds, aliphatic C–H bonds, and its N bonds in the triazole groups. Furthermore, ZrPTP demonstrated maintained selectivity for americium over europium even after a 2 MGy dose. Overall, the results extensively demonstrate the viability of metal phosphonate sorbents for nuclear waste treatment applications in terms of their radiation stability.

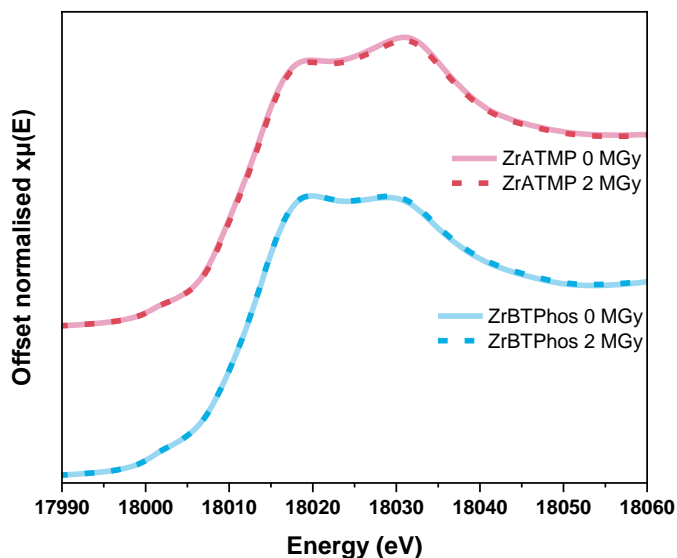


Figure 1. Zr K-edge XANES of unirradiated (0 MGy) and irradiated (2 MGy) ZrATMP and ZrBTPhos

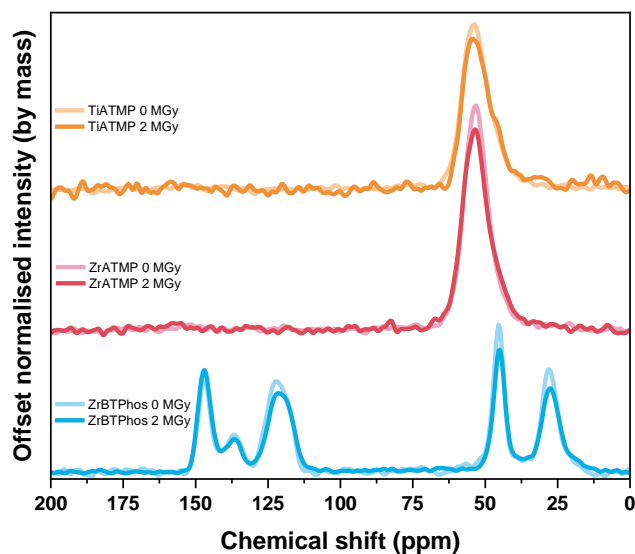


Figure 2. ¹³C MAS solid-state NMR spectra of ZrBTPhos, ZrATMP and TiATMP at a radiation dose of 0 and 2 MGy

References:

1. Veliscek-Carolan, J.; Rawal, A., Zirconium bistriazolylpyridine phosphonate materials for efficient, selective An(iii)/Ln(iii) separations. Chemical Communications 2019, 55 (8), 1168-1171.
2. Veliscek-Carolan, J.; Rawal, A.; Oldfield, D. T.; Thorogood, G. J.; Bedford, N. M., Nanoporous Zirconium Phosphonate Materials with Enhanced Chemical and Thermal Stability for Sorbent Applications. ACS Applied Nano Materials 2020, 3 (4), 3717-3729.
3. Luca, V.; Veliscek Carolan, J., New Insights into the Radiolytic Stability of Metal(IV) Phosphonate Hybrid Adsorbent Materials. Physical Chemistry Chemical Physics 2020, 22.

Optimization of Minor Actinides Recovery Conditions by Combining Mathematical Analysis and Process Simulation

Yuichi Sano¹, Akane Kojima², Tomoyuki Yajima², Yoshiaki Kawajiri²

¹Japan Atomic Energy Agency, Japan, ²Nagoya University, Japan

To recover minor actinides (MA) from dissolver solution or high level liquid waste (HLLW), several processes, e.g. solvent extraction and extraction chromatography techniques using various extractants and adsorbents, have been proposed. It is important for the implementation of these MA recovery processes in practical use to optimize the separation condition and select the most efficient and stable process. When designing the MA recovery process based on various separation methods, process simulations are used to optimize design variables such as equipment conditions (types, sizes, numbers, etc.) and operating conditions (compositions and flowrates of various solutions fed to the equipment, etc.) so that multiple objective variables such as MA recovery yields and purities, waste volumes, etc.) show target values. The MA recovery process, however, has a lot of design and objective variables, so a huge number of simulations are required to optimize all design variables simultaneously, making manual optimization difficult. In this study, we introduced the optimization method combining mathematical analysis and process simulation to efficiently determine the design variables at the lowest computational cost for obtaining the appropriate objective variables.

Four different processes, Np recovery from dissolver solution by the solvent extraction using 30 vol% TBP-n-dodecane (nDD), MA(III) (Am and Cm) recovery from HLLW by the solvent extraction using 50 vol% TBP-nDD, and MA(III) / lanthanides (Ln) separation by the extraction chromatography with the fixed bed (FB) or the simulated moving bed (SMB) using HONTA adsorbents, were discussed. The simulation codes for these processes were described in the previous reports [1-2]. The design variables in each process were changed and optimized by using the Optuna library [3] with Bayesian optimization or evolutionary algorithms. In addition, the scipy.optimize library with the Nelder-Mead algorithms, and the Python-based_SMB_Optimizer [4] were also used to optimize the design variables in MA(III) / Ln separation processes by FB and SMB respectively.

In the Np recovery process, Np is extracted with U and Pu by TBP, and co-stripped with Pu and a part of U. In the calculation, the concentration of nitric acid and reductants in the stripping solution, and its flowrate were changed as design variables under the consideration of the effects on objective variables, such as Np, Pu recovery yields, and U/Pu ratio in the product solution. These design variables could be optimized to take the lowest values in the condition where the objective variables met the target values through hundreds of trials. The MA(III) recovery process needs to achieve higher MA(III) recovery yields with higher decontamination factor (DF) of fission products (FP), especially Zr and Pd which are strongly adsorbed on HONTA adsorbents in the following MA(III) / Ln separation process. Therefore, the optimization of design variables such as the nitric acid concentration in the stripping solution and the TBP-nDD solvent, and their flowrates were carried out to obtain the maximum in the objective variables, e.g. MA(III) recovery yields and DF of FP. The calculation results showed the significant contribution of the nitric acid concentration in the TBP-nDD solvent and the flowrates of the stripping solution to the objective variables, and suggested that the target values of the objective variables could be achieved by selecting the appropriate Pareto solution. For the MA(III) / Ln separation process by FB, the column length, the nitric acid concentration in the eluent and its flowrate were changed and optimized to obtain the target MA(III) recovery yields and DF of Ln with the minimum volume of eluent. In addition to these design variables, the flowrates of the product and recycle solution, and switching time were considered in the MA(III) / Ln separation process by SMB. Based on these optimization results, the productivities (= feed volume / column volume / operational time) and the ratio of the eluent to the feed volume) were calculated. All These values implied the superiority of SMB over FB.

We will have some MA recovery experiments based on these optimized conditions, and select the most preferable process for practical use.

References

- [1] M. Naito, T. Sudo, K. Asakawa, E. Kashiwagi, "A Computer code for simulating the PUREX solvent extraction process", JNC-TN8400-99-005, 1999 (in Japanese).
- [2] Y. Sano, A. Sakamoto, M. Nakahara, S. Watanabe, K. Morita, T. Emori, Y. Ban, T. Arai, K. Nakatani, H. Matsuura, S. Kunii, "Process simulation study on a hybrid process combining solvent extraction and low pressure loss extraction chromatography for a reasonable MA(III) recovery process", 16th Information Exchange Meeting on Actinide and Fission Product Partitioning and Transmutation (16IEMPT), Boulogne-Billancourt, France, Oct. 2023.
- [3] T. Akiba, S. Sano, T. Yanase, T. Ohta, M. Koyama. "Optuna: A Next-generation Hyperparameter Optimization Framework", In Proceedings of the 25th ACM SIGKDD International Conference on Knowledge Discovery & Data Mining (KDD '19), Association for Computing Machinery, New York, NY, USA, 2623-2631, 2019, <https://doi.org/10.1145/3292500.3330701>.
- [4] K. Suzuki, Python-based_SMB_Optimizer, https://github.com/suzuki1969/Pythonbased_SMB_Optimizer.git, 2020.

Recent Results from Lab Scale Testing of Advanced Aqueous Separation Processes for the Future Recycling of Spent Nuclear Fuels

Robin Taylor¹, Dan Whittaker¹, Mark Sarsfield¹, Michael Carrott¹, Billy Keywood¹, Rebecca Sanderson¹, David Woodhead¹, Kate Wallace¹, Hongyan Chen², Clint Sharrad³

¹National Nuclear Laboratory, Central Laboratory, Sellafield, Seascale, CA20 1PG, UK

²Department of Chemical Engineering, the University of Manchester, Oxford Road, Manchester, M13 9PL, UK

³Dalton Nuclear Institute, The University of Manchester, Manchester, M13 9PL, UK

For the future recycling of spent nuclear fuels, reprocessing options that are more efficient, flexible, economic and proliferation resistant will be needed. Additionally, these processes will have to generate less wastes at source and have an overall lower environmental impact. This certainly means that the current PUREX process used for reprocessing nuclear fuels at the industrial scale will have to significantly evolve and may mean new separation processes, not based on tributyl phosphate as the extracting ligand, will be needed [1]. This is certainly the case if the recycling of minor actinides, as well as uranium and plutonium, is a serious goal for advanced closed nuclear fuel cycles.

Recently, a series of laboratory scale tests of innovative separation processes have been carried out with the aims to underpin specific aspects of flowsheet design and validate process models. All the tests used lab scale centrifugal contactor cascades and realistic concentrations of actinides together with fission product simulants.

For the heterogeneous recycling option [2] the lead concept uses an Advanced PUREX process using the ligand aceto-hydroxamic acid (AHA) to only partially separate U, Np and Pu followed by an innovative (or i-) SANEX process. These two solvent extraction cycles have been tested with simulant feeds with representative concentrations on actinides in our laboratories. The key issues tested were for:

- Control of technetium and zirconium in the Advanced PUREX flowsheet
- Co-separation of uranium and plutonium in a 1:1 ratio using a complexant (aceto-hydroxamic acid) rather than a reducing agent in the Advanced PUREX flowsheet
- A test of the full i-SANEX cycle with a new CHON stripping agent ('py-tri-diol')

Further work is underway, in collaboration with the European PATRICIA project, to replace the i-SANEX cycle with a solvent extraction cycle that only recovers americium rather than americium and curium.

For the homogeneous recycling option [3] the lead concept is based on GANEX (Grouped Actinide Extraction). This comprises two cycles to (i) separate the bulk uranium and (ii) recover all the transuranic actinides as a group. Building on past work under the European GENIORS project, the two GANEX solvent extraction cycles have been tested with simulant feeds with representative concentrations on actinides in our laboratories. The aims of the tests were to:

- Increase uranium loading and improve neptunium and technetium stripping in the GANEX first cycle
- Make a test of the second (i.e. "EURO-GANEX") cycle with a new CHON stripping agent ('py-tri-diol')

In parallel, open-source process models were developed for the Advanced PUREX cycle to simulate the results of the flowsheet tests and validate the models so that they can be used in optimizing future flowsheet designs.

An overview of the key results from these tests and the flowsheet simulations will be presented.

References:

1. Taylor, R., Mathers, G., Banford, A., The development of future options for aqueous recycling of spent nuclear fuels, Progress in Nuclear Energy (2023) 164, 104837.

2. Geist, A., Adnet, J.-M., Bourg, S., Ekberg, C., Galán, H., Guilbaud, P., Miguirditchian, M., Modolo, G., Rhodes, C., Taylor, R. An overview of solvent extraction processes developed in Europe for advanced nuclear fuel recycling, part 1 – heterogeneous recycling, *Separation Science and Technology* (2020) 56, 1866-1881.
3. Lyseid Authen, T., Adnet, J.-M., Bourg, S., Carrott, M., Ekberg, C., Galán, H., Geist, A., Guilbaud, P., Miguirditchian, M., Modolo, G., Rhodes, C., Wilden, A., Taylor, R. An overview of solvent extraction processes developed in Europe for advanced nuclear fuel recycling, Part 2 – homogeneous recycling, *Separation Science and Technology* (2022) 57, 1724-1744.

Research on Sustainable Nuclear Energy Use with Actinide Management: Scenario Study on High-Level Waste Generation with MA Separation and Intermediate Storage Technology Implementation

Tomohiro Okamura¹, Ryo Takahashi², Takashi Shimada², Nakase Masahiko¹,
Tomoo Yamamura³ and Kenji Takeshita¹

1. Laboratory for Zero-Carbon Energy, Institute of Innovative Research, Tokyo Institute of Technology

2. Mitsubishi Heavy Industries, Ltd.

3. Institute of Integrated Radiation and Nuclear Science, Kyoto University

1. Introduction

In pursuit of a sustainable society, the global demand is to secure stable and developing energy while simultaneously achieving carbon neutrality. In Japan, the "GX (Green Transformation) Basic Policy" aimed at transforming the economic and social structure through clean energy was decided in a Cabinet meeting on February 10, 2023. Regarding nuclear power utilization, various methods are envisioned, including light water reactor (LWR), MOX fuel use in LWR, next-generation LWRs, fast reactor (FR), high-temperature gas reactors for hydrogen production, as well as small modular reactor (SMR) and innovative reactors.

On the other hand, the advancement in fuel cycle analysis has revealed three significant challenges, making it clear that sustainable nuclear utilization is difficult without appropriate measures.

- ✧ Challenge I: In the MOX fuel use in LWR, the fissile isotope composition of plutonium (Pu) in spent fuel decreases compared to that in LWR uranium fuel, making MOX fuel use in LWR unsustainable after 2-3 reprocessing cycles.
- ✧ Challenge II: The amount of minor actinide (MA) in spent fuel from MOX fuel used in LWR increases several-fold, leading to an increase in the disposal area per glass matrix. While reprocessing of MOX fuel is assumed to start around 2060, sufficient fast reactor capacity for MA transmutation is not expected until the 22nd century. This implies that for about half a century, there will be no means to transmute MAs generated through reprocessing.
- ✧ Challenge III: The current generation of FR for power generation has limited MA transmutation capability, requiring a large number of reactors to achieve the necessary transmutation capacity.

To address these three challenges and realize sustainable nuclear utilization, a "Fuel Cycle with Actinide Management" that meets the following three functional requirements is necessary.

Therefore, this study analyzes the generation scenarios of high-level waste when MA separation and interim storage technologies are introduced, considering multiple future nuclear utilization scenarios in Japan. In this report, the comparison of total foot-print of geological repository in each scenario was summarized.

2. Scenario & Conditions

2.1. Nuclear Fuel Cycle Simulator: NMB4.0

In this study, we conducted an analysis using the nuclear fuel cycle simulator, Nuclear Material Balance analysis code version 4.0 (NMB4.0), jointly developed and freely published by Tokyo Institute of Technology (TokyoTech) and the Japan Atomic Energy Agency (JAEA) [1]. This simulator models a wide range of processes from the front- to the back-end of the nuclear fuel cycle, with a particularly comprehensive scenario analysis function for the back-end. Therefore, it is an appropriate simulator for this study, which evaluates the generation scenarios of high-level waste.

2.2. Scenarios

As illustrated in Fig1, four future nuclear power generation scenarios (A to D) were assumed. In the "A: LWR cycle Scenario", the fuel cycle is continued solely with LWRs, with the recovered Pu being utilized as MOX fuel, and the LWR multi-cycle is assumed. The "B: FR Coexistence Scenario" envisages the minimum introduction of FRs necessary for the transmutation of recovered MAs and high-order Pu, which become problematic in the LWR multi-cycle. The "C: FR Transition Scenario" and the "D: FR Delayed Transition Scenario" assume a transition to the FR cycle after the realization of FaSLiEE (Fast reactor is Superior to LWR including Economic Evaluation) in 2070 and 2110, respectively.

The operation of the reprocessing plant assumes full-volume reprocessing following the commencement of operations at the Rokkasho Reprocessing Plant (from 2025). For the scenarios involving the introduction of MA separation and interim storage technologies, it is assumed that the Rokkasho Reprocessing Plant will be modified and the implementation will start from 2045. In A Scenario, as MAs cannot be transmuted, it is assumed that the recovered MAs will be interim-stored for 120 years before being vitrified and disposed of in a geological repository. The foot-print of geological repository is calculated based on the total number of high-level waste generated in each scenario and the occupied area. The occupied area is determined based on the thermal analysis of the geological repository, considering the decay heat from the nuclide composition in the vitrified waste. As a point of comparison for the disposal area footprint, the reference case is set at 1.75 km², as equivalent to one geological repository, according to Japan's geological disposal program [2].

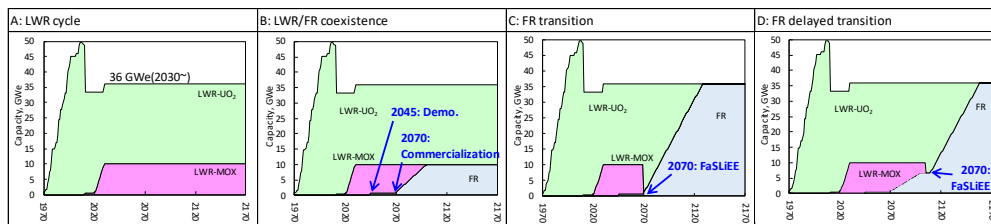


Fig1. Scenarios

3. Result and Discussion

Fig2 presents the total foot-print for each scenario. The introduction of MA separation in each scenario results in a reduction of the foot-print by approximately 80%. With the introduction of MA separation, the foot-print in these scenarios are less than the reference case, making it feasible to bury all vitrified waste generated up to 2170 in the foot-print smaller than one disposal site. In A Scenario, where the recovered MA are interim-stored before vitrification and disposed of in geological repository, there is a reduction in the foot-print by about 25%. In all scenarios, the reduction in foot-print due to the introduction of MA separation and interim storage technologies is confirmed.

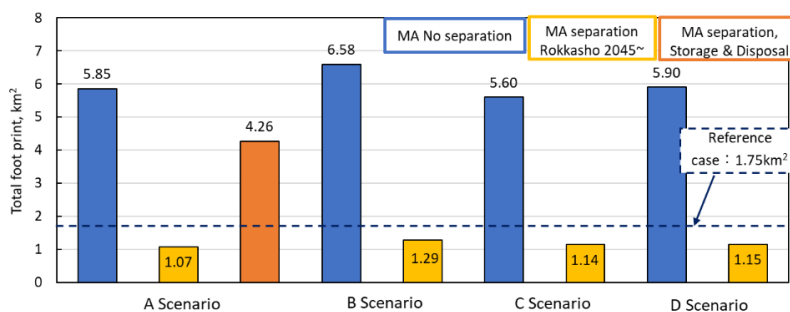


Fig2. Total foot print in each scenario

4. Conclusion

In this study, the effectiveness of reducing high-level waste through the introduction of MA separation and interim storage technologies was evaluated using NMB4.0. The results revealed that in scenarios where FR is introduced, a reduction of approximately 80% was observed. In the LWR cycle scenario, a 25% reduction was achieved when MA were vitrified and disposed of in geological repository after interim storage.

Acknowledgment

This research is a part of the "Research and Development of Nuclear Systems for Actinide Management" project under the "National Projects for Research and Development Promotion" funded by the Ministry of Education, Culture, Sports, Science and Technology, Japan.

References

1. T. Okamura et al., MB4.0: development of integrated nuclear fuel cycle simulator from the front to back-end, *EPJ Nuclear Sci. Technol.* **7**(19), 2021.
2. Nuclear Waste Management Organization of Japan, NUMO Safety Case Report: Realization of Safe Geological Disposal of High-Level Radioactive Waste and TRU Waste in Japan - Development of a Safety Case for the Selection of an Appropriate Site, NUMO-TR-20-03, 2021

Recovery of Strategic High-Value Fission Products from Spent Nuclear Fuel during Reprocessing

Alistair F. Holdsworth^[1], Harry Eccles^[2], Kathryn George^[1], and Clint A. Sharrad^[1]

[1] Department of Chemical Engineering, University of Manchester, Oxford Road, Manchester, UK, M13 9PL;

[2] University of Central Lancashire, Fylde Road, Preston, Lancashire, UK, PR1 2HE;

Corresponding Author: Alistair.Holdsworth@manchester.ac.uk

The Net Zero transition and increasing living standards around the world are placing exponentially increasing demands on scarce natural materials (**Figure 1**) essential for decarbonisation and modern, high-technology applications [1]. As nuclear power has been identified as a key, low-carbon energy source in grid decarbonisation by many nations, expanded use of the technology will inevitably push up demand for the finite natural uranium and thorium reserves [2]. Combined with the high construction costs and long build times for reactors and their supporting infrastructure, a substantial rethink of the nuclear fuel cycle (NFC) to a more holistic, and sustainable approach is needed, incorporating comprehensive resource utilisation and advanced waste management [3].

H																	He
Li	Be											B	C	N	O	F	Ne
Na	Mg											Al	Si	P	S	Cl	Ar
K	Ca	Sc	Ti	V	Cr	Mn	Fe	Co	Ni	Cu	Zn	Ga	Ge	As	Se	Br	Kr
Rb	Sr	Y	Zr	Nb	Mo	Tc	Ru	Rh	Pd	Ag	Cd	In	Sn	Sb	Te	I	Xe
Cs	Ba	*	Hf	Ta	W	Re	Os	Ir	Pt	Au	Hg	Tl	Pb	Bi	Po	At	Rn
Fr	Ra	**	Rf	Db	Sg	Bh	Hs	Mt	Ds	Rg	Cn	Nh	Fl	Mc	Lv	Ts	Og

*Lanthanides	La	Ce	Pr	Nd	Pm	Sm	Eu	Gd	Tb	Dy	Ho	Er	Tm	Yb	Lu
**Actinides	Ac	Th	Pa	U	Np	Pu	Am	Cm	Bk	Cf	Es	Fm	Md	No	Lr

Figure 1: Periodic table of endangered natural resources by element.

Key: **supplies stable**; **supplies at risk**; **supplies endangered**.

The bulk of the 7-11 kilotons of spent nuclear fuel (SNF) produced annually is not reprocessed primarily due to limited capacity brought about by high costs, proliferation concerns, and negative image – most SNF is viewed as a waste rather than a resource [3]. Despite this, reprocessing and responsible management of SNF as a resource will be the key to the long-term sustainability of the NFC.

SNF is not just rich in U and Pu for further energy generation, many fission products (FPs) are valuable resources in their own right, either as the elements or isotopes [1,3]. For example, SNF contains resources such as the platinum group metals (PGMs) Ru, Rh, and Pd, and rare earth elements (REEs) Y, La, Ce, Pr, Nd, Pm, Sm, Eu, Gd, Tb, and Dy at concentrations (kg/t_{SNF}) far higher than in most natural ores (g/t_{ore} , **Figure 2**) [4,5], with approximate values extended from 300,000 USD/ t_{SNF} for the PGMs alone.

Thus, SNF represents an untapped resource of these high-value strategic materials whose recovery would simultaneously offset the high costs of reprocessing and reduce waste volumes, including the demands on deep geological disposal facilities, while simultaneously implementing circular economic principles [3]. Other potential resources such as the noble gases (He, Kr, and Xe) and a range of isotopes useful for medical (e.g. ^{90}Y , ^{106}Ru), sensing (e.g. ^{85}Kr), power generation (e.g. ^{90}Sr), and irradiation applications (e.g. ^{137}Cs) are also present in significant quantities [3,4] and represent further targets

to be considered for recovery. The removal of inactive or low-active species of value from SNF raffinates output from reprocessing operations could serve to reduce waste volumes, reducing the demands on costly deep geological disposal, providing further benefits to the NFC.

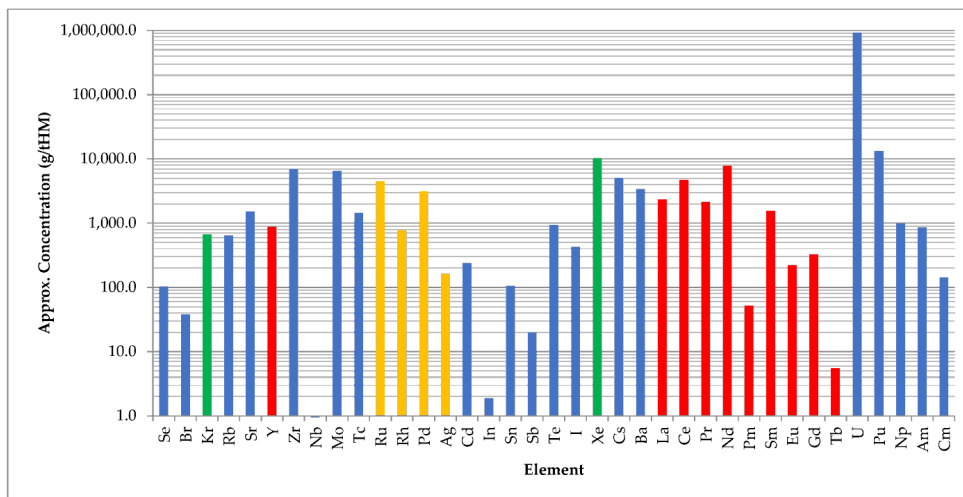


Figure 2: Approximate concentrations of elements in high-burnup (65 GWd/tHM) pressurised water reactor SNF from an EPR-type reactor or similar (5% ^{235}U initial enrichment, 5 year post-reactor cool) [6]. Key: **noble gases**; **platinum group metals**; **rare earths**; **remaining fission products and actinides**.

Although the concept of recovery of FP resources from SNF during reprocessing is not new [4], it is relatively under-developed but has received more attention in recent years and is receiving timely attention in light of recent geopolitical, technological, and climate shifts [3,6]. This presentation will highlight the potential FP resources present in SNF and their value, the likely separation, recovery, and purification routes needed for quantitative recovery with the challenges involved in this [6]. The probable effects on the NFC should this concept be implemented will be discussed in the context of current and likely future NFC implementations in which advanced hydrometallurgical reprocessing is an essential component. The necessity for decay storage and the end-use applications for these materials are also examined [1,3,6].

Focus will be paid to the REEs, targeted to be recovered from SANEX (selective actinide extraction) or GANEX (group actinide extraction) raffinates in advanced reprocessing, and the far more challenging targeted recovery of the REEs, which requires a more comprehensive and complex approach for quantitative recovery. The recycling of additional resources to increase fuel cycle sustainability, such as high-purity Zr cladding, will be also highlighted [7]. Advanced separations to facilitate segregation of high-heat radionuclides (HHRs – e.g. ^{90}Sr , ^{134}Cs , and ^{137}Cs) for decay storage is also compatible with this concept [8,9].

References:

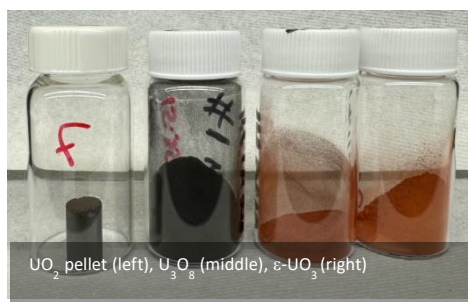
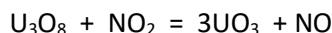
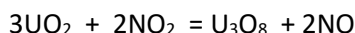
- [1] S. Bourg and C. Poinssot, *Prog. Nucl. Ener.*, **2017**, 94, 222.
- [2] C. Poinssot et al, *Proced. Chem.*, **2012**, 7, 349.
- [3] A. F. Holdsworth et al, *Waste*, **2023**, 1(1), 249.
- [4] C. A. Rohrmann, BNWL-25 Report, Battelle Pacific Northwest National Lab, USA, **1965**.
- [5] A. F. Holdsworth et al, *Progr. Nucl. Ener.*, **2021**, 141, 103935.
- [6] B. J. Hodgson, J. R. Turner, and A. F. Holdsworth, *J. Nucl. Ener.*, **2023**, 4(3), 484.
- [7] E. D. Collins et al, *Proced. Chem.*, **2012**, 7, 72.
- [8] C. W. Forsberg, *Nucl. Tech.*, **2000**, 131(2), 252.
- [9] G. Bond et al, *J. Chromatog. Sep. Tech.*, **2019**, 10, 417.

Demonstration of Advanced Voloxidation and Direct Extraction Using Irradiated UO_2

Peter Tkac¹, Michael Kalensky¹, Sergey Chemerisov²

¹Chemical and Fuel Cycle Technologies Division, ²Experimental Operations and Facilities Division
Argonne National Laboratory, Lemont, IL, 60439, USA

Advanced voloxidation is a novel and promising process option in the recycling of spent nuclear fuel, which addresses the management of volatile fission products. Advanced voloxidation involves oxidation of spent nuclear fuel using NO_2 gas at lower temperatures compared to older voloxidation processes that use air, oxygen and/or ozone. During this process, UO_2 is converted to U_3O_8 and then to UO_3 as a main product (see Figure):



Volatile fission products such as iodine, tritium, xenon, and krypton are released from the fuel and partition into the facility off-gas. The resulting uranium trioxide powder product is suitable for direct extraction by tributyl phosphate (TBP) and *N,N*-di-2-ethylhexyl-isobutyramide (DEHiBA), or it can be dissolved in nitric acid for further processing using traditional solvent extraction. In particular, the upfront removal of iodine and tritium is desired as it eliminates the need for subsequent capturing from several off-gas downstream unit operations in reprocessing facilities, simplifying waste management and emissions control. Produced NO gas can be recycled by reacting with oxygen to form NO_2 .

For this study, UO_2 pellets were irradiated at Argonne using a 55 MeV electron linac to generate fission products with distribution similar to that of spent nuclear fuel. However, due to the short irradiation times (few hours) only short-lived isotopes were produced in quantities that could be analyzed using gamma counting. The release of iodine during voloxidation was monitored by tracking ^{131}I activity. For direct extraction studies, the resulting $\epsilon\text{-UO}_3$ containing the remaining fission products, was contacted with TBP/*n*-dodecane and DEHiBA/*n*-dodecane solvents (pre-equilibrated with nitric acid) to determine partitioning of U and fission products. Limited studies using irradiated simulated spent fuel pellets containing selected lanthanides and transition metals, were also conducted. The iodine partitioning during advanced voloxidation and the observed behavior of select fission products in direct extraction studies will be discussed.

Zirconium Molybdate Rinsing With Carbonate: From R&D to Industrialization in the La Hague Plants

Nicolas Golles^{1*}, Céline Quenault², Pierre Sarrat³, Sandrine Jakab-Costenoble³,
Bénédicte Arab-Chapelet³, Nicolas Vigier⁴, Jean-Luc Emin⁴

¹Orano Recyclage, Châtillon, France, ²Orano Recyclage, La Hague, France, ³CEA, DES, ISEC, DMRC, Univ Montpellier, Marcoule, France, ⁴Orano Projets, St Quentin en Yvelines, France

* Corresponding Author, E-mail: Nicolas.golles@orano.group

Recycling of spent civil nuclear fuel is realized in France since 1966 in successive plants, currently in UP3 and UP2-800 on the La Hague site. During the first step of the process, prior to the PUREX liquid-liquid extraction process, spent fuel rods are sheared and the radioactive material contained in the rods is dissolved in hot nitric acid. Due to the increased burnup of the processed fuel concentrations of molybdenum and zirconium from fission product have steadily increased in the dissolution solution. Coupled with the modification of the process of the UP3 and UP2-800 plant, this lead to an unanticipated large scale precipitation of zirconium molybdate hydrates $\text{ZrMo}_2\text{O}_7(\text{OH})_2(\text{H}_2\text{O})_2$ (ZMH).

The increasing mass of precipitated ZMH in the equipment led to operational difficulties, and thus specific rinsing procedures have had to be implemented. A two-step operation was first put in place to clean the industrial equipment: first sodium hydroxide is introduced to solubilize Mo from ZMH, followed by nitric acid to recover precipitated zirconium hydroxide. This procedure needed strenuous criticality safety management leading to a limited efficiency. The production downtime and the volume of effluents were high, with introduction of large quantities of sodium that led to difficulties in the liquid waste processing units.

Starting in 1997, efforts were undertaken to develop new easier rinsing procedures with the support of the French "Commissariat à l'Energie Atomique et aux Energies Alternatives" (CEA). The main objectives were:

- easier management of criticality and safety: no precipitation of Pu,
- reducing downtime and effluent volume.

A screening of the reagents compatible with the La Hague process was realized, after which active and inactive tests were realized. Sodium carbonate was chosen, even though it introduced high quantity of sodium in the plant. Extensive tests were realized to determine the solubility of ZMH in carbonate solution, the stability of the solution, and all necessary process steps needed to use this new reagent in the existing equipment of the La Hague plant.

The first industrial operations using sodium carbonate were carried out in 2010 at a small scale and with limited carbonate concentration, with a strict control of the safety authority. Thanks to a strong interaction with CEA with tests performed on industrial ZMH, and with a constant interaction with the French safety authority ASN (Autorité de Sécurité Nucléaire), the carbonate concentration has been increased, and the rinsing has been implemented with a recirculation on several equipment, leading to better recovery of ZMH. Carbonate rinsing is now a common operation on the La Hague plant and has shown its efficiency to recover ZMH, with a simplification of rinsing operation and a limitation of effluent volume.

ACTINIDE MATERIALS AND NUCLEAR FUELS

The Potentials of Nano-Scaled Actinide Dioxides

Olaf Walter, Karin Popa

European Commission, DG Joint Research Centre, Directorate G, PO Box 2340, D-76125 Karlsruhe, GER

Nanocrystals (NC's) represent fundamental building blocks in nanoscience and nanotechnology because of their size and shape dependent properties and have attracted high interest. Accordingly NC's of actinide dioxides (AnO_2) have been investigated at the JRC in more detail since now about one decade [1-16].

Our contribution is an overview over our research on highly crystalline AnO_2 NC's obtained via hydrothermal decomposition of the $\text{An}(\text{oxalate})_2 \cdot n\text{H}_2\text{O}$ in hot compressed water at temperatures below 250°C [1-5]. We will compare these results with the ones obtained by solvothermal synthesis leading to monodisperse NC's [8-12]. We will show, what we can learn from AnO_2 NC's in terms of particle growth [15, 16], and how the size of NC's at the end influences on the oxidation state of the metals in the AnO_2 [14].

References

- [1] O. Walter, K. Popa, O. Dieste Blanco, *Open Chem.*, **14**, 170 (2016).
- [2] L. Balice, D. Bouëxière, M. Cologna, A. Cambriani, J.-F. Vigier, E. De Bona, D.G. Sorarù, C. Kübel, O. Walter, K. Popa, *J. Nucl. Mater.*, **498**, 307 (2018).
- [3] K. Popa, O. Walter, O. Dieste Blanco, A. Guiot, D. Bouëxière, J.-Y. Colle, L. Martel, M. Naji, D. Manara, *Cryst. Eng. Comm.*, **20**, 4614 (2018).
- [4] D. Bouëxière, K. Popa, O. Walter, M. Cologna, *RSC Advances*, **9**, 6542 (2019).
- [5] E. De Bona, O. Walter, H. Störmer, T. Wiss, G. Baldinozzi, M. Cologna, K. Popa, *J. Am. Ceram. Soc.*, **102**, 3814 (2019).
- [6] R. Jovani-Abril, R. Eloirdi, D. Bouëxière, R. Malmbeck, J. Spino, *J. Mater. Sci.*, **46**, 5 (2011).
- [7] D. Hudry, C. Apostolidis, O. Walter, T. Gouder, E. Courtois, C. Kübel, D. Meyer, *Chem. Eur. J.*, **18**, 8283 (2012).
- [8] D. Hudry, C. Apostolidis, O. Walter, T. Gouder, A. Janssen, E. Courtois, C. Kübel, D. Meyer, *RSC Advances*, **3**, 18271 (2013).
- [9] D. Hudry, C. Apostolidis, O. Walter, T. Gouder, E. Courtois, C. Kübel, D. Meyer, *Chem. Eur. J.*, **19**, 5297 (2013).
- [10] D. Hudry, C. Apostolidis, O. Walter, A. Janßen, D. Manara, J. C. Griveau, E. Colineau, T. Vitova, T. Prüßmann, D. Wang, C. Kübel, D. Meyer, *Chem. Eur. J.*, **20**, 10431 (2014).
- [11] D. Hudry, J.-C. Griveau, C. Apostolidis, O. Walter, E. Colineau, G. Rasmussen, D. Wang, V. S. K. Chakravadhaluna, E. Courtois, C. Kübel, D. Meyer, *Nano Research*, **7**, 119, (2014).
- [12] R. Jovani-Abril, M. Gibilaro, A. Janßen, R. Eloirdi, J. Somers, J. Spino, R. Malmbeck, *J. Mater. Sci.*, **477**, 298 (2016).
- [13] V. Tyrpekl, J.F. Vigier, D. Manara, T. Wiss, O. Dieste Blanco, J. Somers, *J. Nucl. Mater.*, **460**, 200 (2015).
- [14] J.-F. Vigier, D. Freis, O. Walter, O. Dieste Blanco, D. Bouëxière, E. Zuleger, N. Palina, T. Vitova, R. J. M. Konings, K. Popa, *Cryst Eng Comm.*, **24**, 6338 (2022).
- [15] V. Baumann, K. Popa, M. Cologna, O. Walter, M. Rivenet, *RSC Adv.*, **13**, 6414 (2023).
- [16] D. Bouëxière, K. Popa, O. Walter, M. Cologna, *RSC Adv.*, **9**, 6542 (2019).

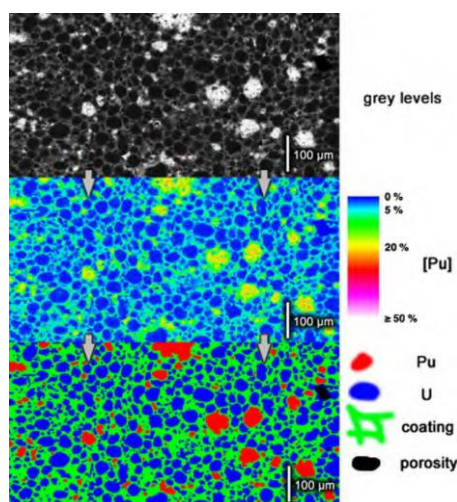
Influence of Uranium Oxide Nature on MOX Fuel Fabrication Process

F. Sauvaire¹, J.-B. Parise¹, A. Delevaque¹, A. Selmil¹, R. Delville², **T. Genevès¹**, V. Garat¹

¹ ORANO site de Melox, BP 93124, 30203 Bagnols-sur-Cèze Cedex - France

² SCK•CEN, Boeretang 200, 2400 Mol - Belgique

The MOX fuel fabrication process implemented in Melox is the MIMAS process (Micronized MASTERblend). It is based in particular on the elaboration of a primary blend (with Plutonium content around 28-30%), consisting of uranium oxide, plutonium oxide and recycled scraps. After ball-milling and sieving, this primary blend is diluted with uranium oxide to obtain the desired plutonium content (typically from ~3 to ~11%). UO_2 powder is thus the major constituent of this powder mixture. MIMAS process results in a dense fuel (~95%TD) with an heterogeneous microstructure where three phases can be identified: a uranium-rich phase (close to 100% U), an intermediate phase and a plutonium rich phase (up to primary blend Pu content) with calibrated primary blend agglomerates.



Evidence of MOX phases (UO_2 phase, matrix phase and primary blend agglomerates) on an X-Ray map of Pu ($M\beta$) acquired by Electron Probe Micro-Analysis [1]

During its existence, the Melox plant underwent several UO_2 powder changes, successively implementing UO_2 ex-ADU (conversion of Ammonium DiUranate), UO_2 DC (Dry Conversion) and UO_2 ex-AUC (conversion of Ammonium Uranyl Carbonate). UO_2 powder characteristics have a significant influence on the powder flowability, pelletizing and sintering properties of MOX fuel. This article aims at illustrating the R&D effort allowing Melox plant to implement these different types of powders while meeting the requirements of our customers. It will cover the description of incoming UO_2 powder, the associated R&D results and the resulting MOX product characteristics.

[1] G.Oudinet et al, "Characterization of plutonium distribution in MIMAS MOX by image analysis", Journal of Nuclear Materials 375 (2008) 86-94.

New Insights in the Structural-Redox Chemistry of Cr, Mn, Fe and V doped- UO_2 Nuclear Fuel Materials

G. L. Murphy [1], Philip Kegler [1], Robert Gericke [2], S. Gilson [2], Martina Klinkgenberg [1], Daniil Sirochii [1], Andrey Bukaemskiy [1], Kristina Kvashnina [2], Volodymyr Svitlyk [2], Christop Henig [2], Peter Kaden [2] and Nina Huittinen [2]

[1] Institute of Reactor and Nuclear Waste Management (IEK-6), Forschungszentrum Jülich GmbH, 52428 Jülich, Germany - [2] Institute of Resource Ecology, Helmholtz-Zentrum Dresden-Rossendorf, Bautzner Landstraße 400, 01328 Dresden, Germany - g.murphy@fz-juelich.de

Transition metal (TM) doped- UO_2 nuclear fuels have drawn considerable interest from industry and researchers alike due to the improved in-reactor performance properties they possess over classical non doped UO_2 . Of the TMs, Cr has endured the most attention due its frequent use in both North American and European fuel blends [1]. Concurrently, researchers have explored and proposed other TMs such as Mn, Fe, V etc. as they have been calculated to potentially possess even more improved fuel properties than that of Cr [2]. The addition of Cr, or other TM dopants is understood to increase the grain size of the fuel matrix and density leading to improvement of fission gas retention resulting in enhanced thermal properties of fuel [3]. However, the small size of TMs compared to the U^{4+} results in extremely low solubility at the ppm in the fuel matrix which is sensitive to preparation conditions including oxygen potential and temperature. With lattice matrix incorporation [3], TMs can readily form additional phases in the bulk fuel structure such as metallic, eutectic and oxide compositions. This chemical complexity in the bulk state has stifled attempts to precisely describe the complete structural dopant chemistry, particularly in the case of Cr-doped UO_2 , due the variety of chemical states present which inhibits reliable bulk characterisation methods and has created intense debate in literature. To resolve these long-standing chemical debates, our group has generated representative single crystal specimens of Cr, Mn, Fe and V doped UO_2 and cross examined these against bulk materials using high resolution synchrotron X-ray diffraction, spectroscopy and electron microscopy [4]. In all cases we are provide conclusively resolved measurements of the Cr, Mn, Fe and V chemical states within the UO_2 matrix, assigning both valence and local structure behaviour. We have further systematically examined the microstructural and ceramic properties of Mn, Fe and V-doped UO_2 against Cr-doped UO_2 to gauge potential application of these TMs as an alternative improved dopant for fuels. The results of these investigations will be presented in detail in particular regard to the chemistry of these materials and the potential impact they have upon fresh and spent nuclear fuels.

1. Arborelius, J., et al., *Advanced Doped UO_2 Pellets In LWR Applications*. Journal of Nuclear Science and Technology, 2006. **43**(9): p. 967-976.
2. Cooper, M.W.D., C.R. Stanek, and D.A. Andersson, *The Role Of Dopant Charge State On Defect Chemistry And Grain Growth Of Doped UO_2* . Acta Materialia, 2018. **150**: p. 403-413.
3. Kegler, P., et al., *Chromium Doped UO_2 -Based Ceramics: Synthesis and Characterization of Model Materials for Modern Nuclear Fuels*. Materials, 2021. **14**(20): p. 6160-6178.
4. Murphy, G.L., et al., *Deconvoluting Cr states in Cr-doped UO_2 nuclear fuels via bulk and single crystal spectroscopic studies*. Nature Communications, 2023. **14**(1): p. 2455.

ESEM-Monitored Dissolution of (U,Th)O₂ Heterogeneous Mixed Oxides for Spent Fuel Modeling

L. Claparede [2], C. Hours [1], I. Viallard [3], N. Reynier-Tronche [1], N. Dacheux [2]

[1] CEA, DES, ISEC, DMRC, Univ Montpellier, Marcoule, France [2] ICSM, CEA, CNRS, ENSCM, Univ Montpellier, Marcoule, France [3] CEA, DES, IRESNE, DEC, Cadarache, France.

Sodium-cooled fast neutrons reactors (SFR) are among the concepts of reactors developed in the Generation IV International Forum. The capacity of these reactors to split transuranic elements allows for better resources management, for control of plutonium stocks and for the reduction of waste toxicity. Fuels for these SFR reactors are Mixed OXide with higher plutonium content than in the MOX fuels dedicated to LWR reactors. They induce significant challenges for the reprocessing step due to the refractory nature of plutonium dioxide in nitric acid medium.

One part of the research developed on these SFR MOX fuels relies on the development of modeling codes able to reproduce the dissolution behavior of these mixed oxides. In particular, Pu-enriched heterogeneities present in small quantities in the SFR oxide fuels are expected to significantly participate in the final balance of residues of dissolution. Furthermore, SFR spent fuels also contain refractory metallic inclusions (mainly composed by Ru, Rh, Pd, Tc and Mo) which can impact the dissolution at the solid/liquid interface and in solution.

For these reasons, characterization of such Pu enriched heterogeneities and metallic inclusions was required in order to study their impact on the dissolution behavior of SFR oxide fuels and then to improve the current modeling codes regarding dissolution.

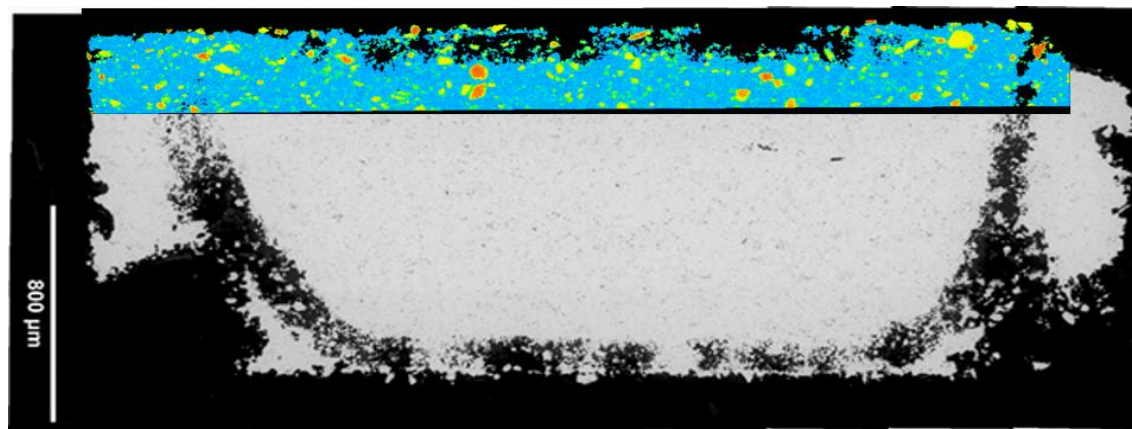


Figure 1: Micrographs coupled with X-EDS analyzes of heterogeneous model compounds (U,Th)O₂ with a dissolution rate of 30%

Using thorium as a plutonium surrogate, heterogeneous U_{1-x}Th_xO₂ samples including platinum group elements (Ru, Rh, Pd) and Mo have been synthesized by wet chemistry route. Indeed samples containing various thorium contents have been prepared by hydroxide precipitation from mixtures of cations in solution [1]. The powders were mixed then sintered through a two-step procedure involving uniaxial pressing at room temperature followed by a heat treatment at 1600 °C under reducing atmosphere. Through this sintering step, metallic inclusions were formed in the materials while the pellets also contained heterogeneities in terms of U/Th mole ratios.

The heterogeneity, microstructure and metallic inclusions spatial distribution were then characterized using image analysis and statistical tools (a set of mathematical techniques well suited for image analysis of spatialized phenomena like heterogeneities distribution [2]) to confirm their ability to mimic SFR spent fuel.

Dissolution experiments are performed in static condition in concentrated nitric acid and associated to operando ESEM-monitored dissolution tests. Images obtained from ESEM-monitoring were then used to reconstruct the observed surface in 3D and determine a localized dissolution behavior [3]. This dual approach allows a better understanding of the dissolution of these heterogeneous compounds with the development of cavities within the pellet (Figure 1). The evolution of the solid-solution interface is then very dependent on the amount of heterogeneity and directly impacts the pellet dissolution kinetics.

- [1] J. Martinez *et al.*, « An original precipitation route toward the preparation and the sintering of highly reactive uranium cerium dioxide powders », *J. Nucl. Mater.*, n° 462, p. 173-181, 2015.
- [2] M. A. Oliver et R. Webster, « A tutorial guide to geostatistics: Computing and modelling variograms and kriging », *CATENA*, vol. 113, p. 56-69, févr. 2014.
- [3] R. Podor *et al.*, « 3D-SEM height maps series to monitor materials corrosion and dissolution », *Mater. Charact.*, vol. 150, p. 220-228, avr. 2019.

Defect Chemistry, Thermal Oxidation, and Thermodynamics of metal-doped UO_2

Xiaofeng Guo¹, Juejing Liu¹, Shinhyo Bang¹, Lorenzo Callejon^{1,2}, Romain Sicard^{1,2}, Sam Karcher¹, John McCloy¹, Hongwu Xu³, Arjen van Veelen³, Nicolas Clavier², Nicolas Dacheux²

¹Washington State University, Pullman WA 99164 US

²ICSM, Univ Montpellier, CNRS, CEA, ENSCM, Bagnols-sur-Cèze, France

³Los Alamos National Laboratory, Los Alamos NM 87545 US

Metal-doped uranium dioxides have many applications in nuclear energy, including tailored design of advanced fuels and simulating high-burnt up fuels. Both needs are demanding for continuing developing more efficient and safer nuclear energy, especially after Fukushima, to bridge the gap between energy demands and sustainable energy supply. Cr- UO_2 has been known as one of the enhanced fuels to lead to smaller grains and thus retention of fission gas that can be used for extended burnt-up.^{1,2} Then Zr and Ln (lanthanides) doped UO_2 have potentials to be mixed-oxide fuels (MOX).³ and have been often used to simulate fission product inclusion in burnt-up fuels or fuels that are resulted from nuclear reactor disasters.⁴⁻⁶ UO_2 crystallizes in the cubic space group ($Fm\bar{3}m$) and exhibits a fluorite structure. While vacancy and O/U defects are better understood in UO_2 in the long-range,^{7,8} their local features were not well understood. The interplay between charge-coupled $\text{M}^{3+}-\text{U}^{4+/5+}$, $\text{M}^{4+}-\text{U}^{4+}$ speciation and oxygen vacancies can result in distinct thermodynamic properties that impact their thermal oxidation or dissolution behaviors,⁹⁻²¹ which are critical for spent fuel storage and processing. Then potential local ordering features of defects may also introduce enthalpic and entropic stabilization to the matrices.²² In recent years, increasing work has been reported for fundamental understanding of defects, stoichiometry, thermophysical and thermochemical behaviors of metal doped UO_2 . However, knowledge gaps still exist in correlating dopant chemistry in UO_2 to its fuel characteristics and thermodynamics, crucial for predicting fuel performance criteria.

In this work, I will present a summary of our recent experimental efforts on multiple metal doped uranium dioxides (Cr- UO_2 , Zr- UO_2 , and Ln- UO_2) to understand their local structures, thermal expansion and thermal oxidation behaviors, and potential non-ideal mixing thermodynamics. These studies were achieved by coupled synchrotron, in-house techniques, and calorimetry. First, we employed Ln L_{III} -edge and U L_{III} -edge X-ray absorption fine structure (XAFS) on Ln- UO_2 . Each composition of Ln- UO_2 has been synthesized under two conditions (non-reducing vs. reducing),²³ resulting in two sets of defect structures. Ce- UO_2 has shown to be less susceptible to changes from preparation conditions due to accessibility to 4+ in the UO_2 structure, while Nd or Gd being only 3+ during substitution induced high-degree disordering in the first U coordination, including both interstitial and vacancy oxygen (summarized in **Figure 1**). Second, high temperature structures of Cr- and Ln- UO_2 studied by in situ high temperature XRD up to 700 °C. Samples were sealed with inert gas inside quartz tubes and heated in diffraction beamlines in synchrotron. We are able to determine the second-order temperature-dependent unit cell parameters and first-order thermal expansion coefficient of these doped UO_2 in comparison to those of stoichiometric UO_2 . Third, thermal oxidation of Ln- and Zr- UO_2 were

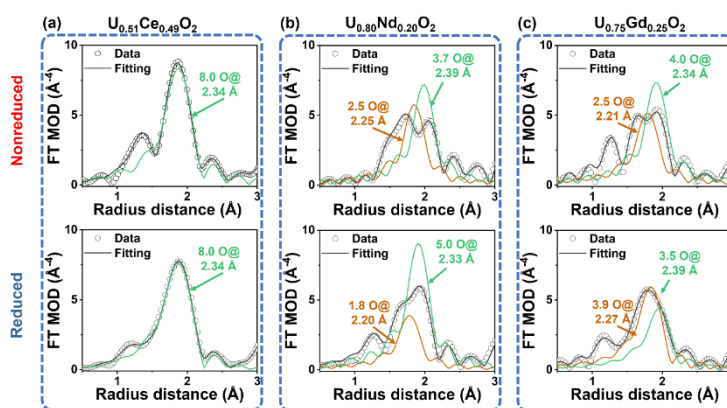


Figure 1. Fitting results and major U-O scattering peaks in RDF function from all Ln- UO_2 samples. (a) to (c) Results from $\text{U}_{0.51}\text{Ce}_{0.49}\text{O}_2$ (a), $\text{U}_{0.80}\text{Nd}_{0.20}\text{O}_2$ (b), and $\text{U}_{0.75}\text{Gd}_{0.25}\text{O}_2$ (c) sample prepared from nonreduced and reduced environment

studied by differential scanning calorimetry coupled with thermogravimetric analysis (DSC-TGA),^{13,16} in situ high temperature Raman¹⁶ and XRD up to 500 ~ 1000 °C. Inclusion of Ln dopants has scattered impacts on the thermal oxidation resistance of UO₂. For Zr-UO₂, a significant decrease in oxidation resistance was identified, with the greatest reduction in low Zr contents, possibly resulting from thermodynamic competition between the oxidized phases, such as Zr-U₃O₈. Lastly, we studied the enthalpies of formation of metal doped UO₂, and the enthalpies of mixing of U-metal in the UO₂ structure, by performing high temperature oxide melt drop solution calorimetry. Thermochemical results will be discussed in accordance with the above structural investigations.

We hope this work can benefit the nuclear fuel community by providing important insights into molecular structure of U-bearing fuel fabrication, defect structure and formation, dopant/fission incorporation mechanism, and the structural-thermodynamic relationship of metal-doped UO₂. This support is crucial for designing future enhanced fuels and predicting spent nuclear fuel evolution in dry/wet storages or geologic repositories.

References

- ¹Goldner, F. J. *et al.* The US Accident Tolerant Fuels Program—Update on a National Initiative. (2021). ²Kegler, P. *et al.* Chromium doped UO₂-based ceramics: synthesis and characterization of model materials for modern nuclear fuels. *Materials* **14**, 6160 (2021). ³Bairiot, H. & Deramaix, P. MOX fuel development: yesterday, today and tomorrow. *Journal of nuclear materials* **188**, 10-18 (1992). ⁴Kirishima, A. *et al.* Structure, stability, and actinide leaching of simulated nuclear fuel debris synthesized from UO₂, Zr, and stainless-steel. *Journal of Nuclear Materials* **567**, 153842 (2022). ⁵Lewis, B., Thompson, W. & Iglesias, F. 2.20-fission product chemistry in oxide fuels. *Comprehensive Nuclear Materials* **2** (2012). ⁶Soldi, L. *et al.* Simulation of the Melting Behavior of the UO₂-Zircaloy Fuel Cladding System by Laser Heating. *Nuclear Science and Engineering* **197**, 351-363 (2023). ⁷Lee, S. M., Knight, T. W., Voit, S. L. & Barabash, R. I. Lattice parameter behavior with different Nd and O concentrations in (U_{1-y}Nd_y) O_{2+x} solid solution. *Nuclear Technology* **193**, 287-296 (2016). ⁸Rittman, D. R. *et al.* Structure and bulk modulus of Ln-doped UO₂ (Ln= La, Nd) at high pressure. *Journal of Nuclear Materials* **490**, 28-33 (2017). ⁹Pavlov, T. R. *et al.* Measurement and interpretation of the thermo-physical properties of UO₂ at high temperatures: the viral effect of oxygen defects. *Acta Materialia* **139**, 138-154 (2017). ¹⁰Zhang, L., Shelyug, A. & Navrotsky, A. Thermochemistry of UO₂-ThO₂ and UO₂-ZrO₂ fluorite solid solutions. *The Journal of Chemical Thermodynamics* **114**, 48-54 (2017). ¹¹Prieur, D. *et al.* Aliovalent Cation Substitution in UO₂: Electronic and Local Structures of U_{1-y}La_yO_{2+x} Solid Solutions. *Inorganic Chemistry* **57**, 1535-1544 (2018). ¹²Bès, R. *et al.* New insight in the uranium valence state determination in U_yNd_{1-y}O_{2+x}. *Journal of Nuclear Materials* **507**, 145-150 (2018). ¹³Olds, T. A., Karcher, S. E., Kriegsman, K. W., Guo, X. & McCloy, J. S. Oxidation and anion lattice defect signatures of hypostoichiometric lanthanide-doped UO₂. *Journal of Nuclear Materials*, 151959 (2019). ¹⁴Vinograd, V. L., Bukaemskiy, A. A., Modolo, G., Deissmann, G. & Bosbach, D. Thermodynamic and structural modelling of non-stoichiometric Ln-doped UO₂ solid solutions, Ln={La, Pr, Nd, Gd}. *Frontiers in chemistry* **9** (2021). ¹⁵Dalger, T., Claparede, L., Szenknect, S., Moisy, P. & Dacheux, N. Dissolution of ThO₂. 25UO₂. 75O₂ sintered pellets: Impact of nitrate ions and nitrous acid. *Hydrometallurgy* **204**, 105717 (2021). ¹⁶Karcher, S. *et al.* Benefits of using multiple Raman laser wavelengths for characterizing defects UO₂. *Journal of Raman Spectroscopy* **in press**. (2022). ¹⁷Vazhappilly, T. & Pathak, A. K. Structure, mechanical and thermo-physical properties of lanthanide fission product doped UO₂ in U (V) state: A density functional study. *Solid State Communications* **347**, 114739 (2022). ¹⁸Potts, S. K. *et al.* Structural incorporation of europium into uranium oxides. *MRS Advances*, 1-7 (2023). ¹⁹Kegler, P. *et al.* Accelerated dissolution of doped UO₂-based model systems as analogues for modern spent nuclear fuel under repository conditions. *MRS Advances* **8**, 255-260 (2023). ²⁰Hours, C. *et al.* Dissolution of (U, Th) O₂ heterogeneous mixed oxides. *Journal of Nuclear Materials* **586**, 154658 (2023). ²¹Vinograd, V., Bukaemskiy, A., Deissmann, G. & Modolo, G. Thermodynamic model of the oxidation of Ln-doped UO₂. *Scientific Reports* **13**, 17944 (2023). ²²Marcial, J. *et al.* Thermodynamic Non-ideality and Disorder Heterogeneity in Actinide Silicate Solid Solutions. *npj Material Degradation* **5**, 1-14 (2021). ²³Massonnet, M. *et al.* Influence of Sintering Conditions on the Structure and Redox Speciation of Homogeneous (U, Ce) O₂+δ Ceramics: A Synchrotron Study. *Inorganic Chemistry* **62**, 7173-7185 (2023).

Heat Capacity Measurements of Self-Damaged Mixed Actinide Oxides: a Method to Assess Defects in Spent Fuels

Thierry Wiss¹, Rudy Konings¹, Dragos Staicu¹, Alessandro Benedetti¹, Jean-Yves Colle¹, Emilio Maugeri², Zeynep Talip², Emanuele De Bona³, Oliver Dieste⁴, Gianguido Baldinozzi⁵, Christine Guéneau⁶

¹ European Commission, DG Joint Research Centre, Karlsruhe, P.O. Box 2340, 76125 Karlsruhe, Germany

² Paul Scherrer Institute, Forschungsstrasse 111, 5232 Villigen PSI, Switzerland

³ European Commission, DG Energy, 10, rue Robert Stumper, 2557 Luxembourg

⁴ University of Trento, Department of Industrial Engineering, Via Sommarive, 9, Povo, 38123 Trento, Italy

⁵ Université Paris-Saclay, CentraleSupélec, CNRS, SPMS, 91190 Gif-sur-Yvette, France

⁶ Université Paris-Saclay, CEA, Service de Recherche en Corrosion et Comportement des Matériaux, 91191, Gif-sur-Yvette, France

The heat capacity of actinides mixed oxides samples having cumulated alpha-decay damage was measured during thermal annealing. Calorimetric measurements of samples undergoing alpha-damage (see Figure 1), showed that the annealing of non-equilibrium defects produces a measurable heat. As first recognized by Wigner in 1946 [1], a significant fraction of the energy released in a radiation process in a material can be stored as atomic defects and extended imperfections. Calorimetry is a well suited technique for the analysis of radiation damage recovery because it is continuous as a function of temperature and it uses a constant heating rate. The excess of heat released from various defect recovery stages was measured in the reported study. Results from Transmission Electron Microscopy, helium thermal desorption, thermal diffusivity, and XRD post-annealing studies were used to support quantitatively the microscopic origin of radiation damage to heat capacity. Electron microscopy is typically unable to detect the smallest defects that also represent the majority of defects induced by irradiation, whereas other techniques display specific sensitivity to a specific and limited subset of defects (e.g. Positron Annihilation Spectroscopy probes essentially atomic vacancies). It was shown that different defect annealing stages could be singled out as depicted in Figure 1. It could also be evidenced that the excess of energy stored by defects tends to saturate at rather low damage levels but, with increasing radiogenic helium production, another contribution of stored energy emerges and that can be attributed to the formation of helium-defect complexes that cannot annihilate until high temperatures are reached.

Table 1: simplified defects annealing temperature ranges for actinide dioxides and correspondance with nuclear facility operational temperatures.

Stage	T, K	Mechanisms	engineering temperatures
I	400-800	O _i migration, U _i	Wet storage clad. max 473 K Dry storage clad. max 673 K
II	700-1100	U _v , Pu _v migration O _v migration	Fuel operation in LWR
III	≥1000	Helium desorption from extended defects	Fuel operation in FR

Some correlations were established with spent nuclear fuel ageing processes. These results are useful in order to provide information on the evolution of the state of spent fuel under interim and final storage conditions. A practical application of these results is that the stored energy in spent-fuels can be expected to increase during the disposal timeframe, potentially leading to changes in properties. Time range of interest for forecasting the fate of spent fuels can vary from decades to millenarities. This has been (partially) covered by the level of equivalent damage of the studied samples. Another interest of

the assessment of the damage effects, in particular in (U, Pu)O₂ samples, lies in the challenges related to multi-recycled plutonium in MOx fuel. In this case, compared to the standard MOX, the isotopic composition of the plutonium will be enriched in ²³⁸Pu, ²⁴⁰Pu, and ²⁴¹Pu, which have much higher specific activities than the ²³⁹Pu isotope, meaning that those fuels will be subjected to strong self-irradiation before being irradiated in a reactor.

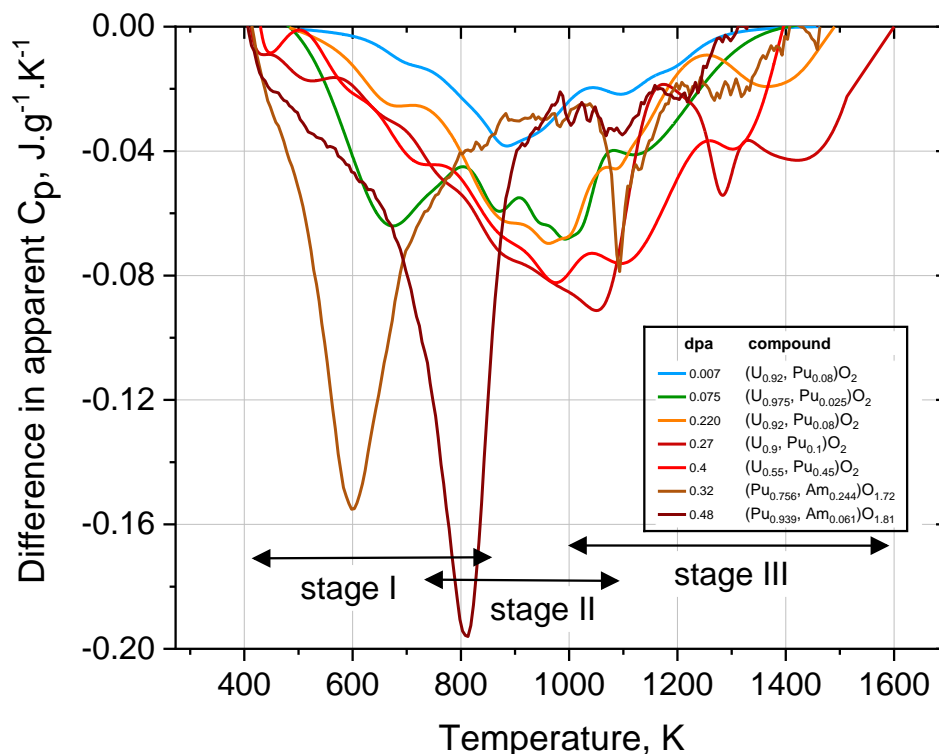


Figure 1: Apparent C_p^* obtained by DSC for 7 selected actinide oxides samples representing different compositions, damage (dpa) and stoichiometry

With full knowledge of the characteristic temperatures of elementary mechanisms, it could enable to predict the relevant macroscopic technological properties (as shown in Table 1). Whereas in wet storage condition there should be no damage recovery it can be expected that in dry storage conditions the oxygen defects could be recovered. This would however not impact the formation of extended defects, on the contrary as observed in ion-irradiation performed at 773 K [3] or at 873K [4].

References:

- 1 Wigner, E.P., Theoretical Physics in the Metallurgical Laboratory of Chicago. Journal of Applied Physics, 1946. 17: p. 857-863
- 2 Staicu, D., Wiss, T., Rondinella, V.V., Hiernaut, J.-P., Konings, R.J.M., Ronchi, C., Impact of auto-irradiation on the thermophysical properties of oxide nuclear reactor fuels. Journal of Nuclear Materials, 2010. 397(1-3): p. 8-18.863.
- 3 Haddad, Y., et al., In situ characterization of irradiation-induced microstructural evolution in urania single crystals at 773 K. Nuclear Instruments and Methods in Physics Research Section B: Beam Interactions with Materials and Atoms, 2018. 435: p. 25-30.
- 4 He, L.-F., et al., In situ TEM observation of dislocation evolution in Kr-irradiated UO₂ single crystal. Journal of Nuclear Materials, 2013. 443(1-3): p. 71-77.

Conversion of U(VI) and Pu(IV) by Peroxide Precipitation and Hydrothermal Treatment

L. Muller^{a,b}, P. Estevenon^a, C. Tamain^a, N. Dacheux^b, N. Clavier^b

^a CEA, DES, ISEC, DMRC, Univ Montpellier, Marcoule, France

^b ICSM, Univ Montpellier, CEA, CNRS, ENSCM, Marcoule, France

With the development of Fast Neutrons Reactors (FNR) and of Mixed Oxide (MOx) fuel multi-recycling policy, opportunities are opening to move toward a closed nuclear fuel cycle. Within this framework, some modifications of the different industrial steps are required. In particular, the MOx fuel synthesis has to be reconsidered as the oxide properties will have to meet different specifications. More specifically, the homogeneity of the cation distribution will have to be improved to allow the use of higher Pu content and subsequently, the further reprocessing of spent MOx fuel.

In this context, new innovative ways of converting uranium and plutonium in nitric solution into actinide oxides (UO_2 , PuO_2 and mixed $(\text{U,Pu})\text{O}_2$) are studied. On the one hand, the plutonium peroxide precipitation is known as an interesting way since the Manhattan project [1] and its thermal decomposition into PuO_2 has also been studied [2]. On the other hand, uranium dioxide synthesis by peroxide pathway is currently developed at an industrial scale [3]. Moreover, uranium and plutonium co-precipitation by hydrogen peroxide is possible [4], however, its development has been hampered by the impact of the particle morphology on the separation step and the risks associated with handling dry peroxide phases. One of the potential innovative pathway to rule out these difficulties consists of hydrothermal conversion with hydrogen peroxide as a precipitating agent. The first stage of the process involves the direct and simultaneous precipitation of both uranium (VI) and plutonium (IV) by H_2O_2 in nitric acid (in their most stable oxidation state in this medium), as uranium (VI) peroxide and plutonium peroxide. Then, actinide peroxide decomposition is achieved under mild hydrothermal conditions ($100 < T < 250^\circ\text{C}$ and self-generated pressures of 1 to 50 bars) instead of conventional heat treatment. This step allows to safely manage the peroxide decomposition reaction without handling powdered materials. Moreover, the oxides obtained exhibit a very low carbon content, as only carbon-free reagents are used.

During actinide peroxide precipitation, the effect of the initial acidity or the initial peroxide concentration on the yield and nature of the precipitate was investigated. Although the influence of these parameters is different for uranium and plutonium, quantitative precipitation conditions have been determined for both actinides (Figure 1). Moreover, specific morphologies for uranium (VI) peroxide were obtained as a function of initial chemicals conditions. As far as plutonium peroxide phases are concerned, new structural characterizations using synchrotron radiation, never performed before, allow a deeper understanding of the synthesized peroxo-nitrate phase.

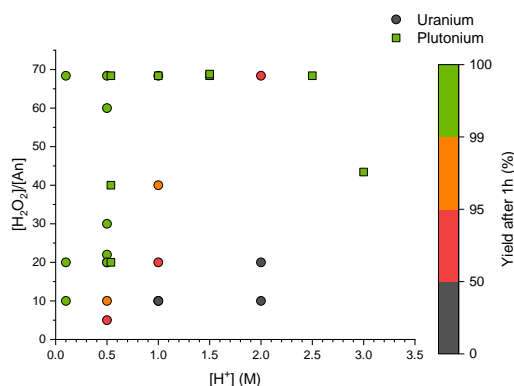


Figure 1: Precipitation yield of pure uranium and plutonium peroxide depending on the initial acidity and molar ratio between actinide and hydrogen peroxide ; $[\text{U(VI)}]_{\text{ini}} = [\text{Pu(IV)}]_{\text{ini}} = 0.068 \text{ M}$

The second part focuses on the hydrothermal conversion of these peroxy-phases to form the corresponding oxide. For the first time, plutonium oxide has been synthesized by this original and novel conversion route (Figure 2, left). For the conversion of uranium (VI) peroxide, a U(VI) oxo-hydroxo phase commonly called “dehydrated schoepite” was obtained (Figure 2, right). Its formula was calculated to be $(\text{UO}_2)\text{O}_{0.17 \pm 0.01}(\text{OH})_{1.66 \pm 0.01}$. For both actinides, the effect of initial acidity, treatment temperature and time on the yield and nature of the powder was investigated. These results provided the first key insights into the mechanisms involved in the hydrothermal conversion of peroxy-phases. These results were compared to those obtained for uranium/plutonium mixtures.

Initial conclusions on the feasibility of this new conversion route will be presented.

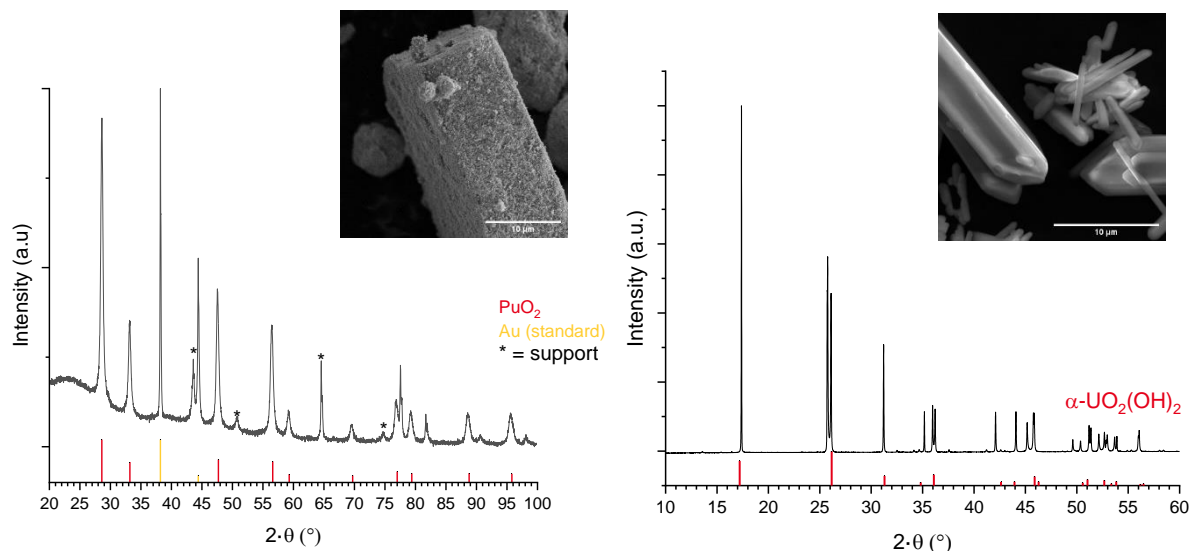


Figure 2: X-ray patterns and SEM micrographs of plutonium oxide (left) and dehydrated schoepite (right) obtained by hydrothermal of U(VI) and Pu(IV) peroxide, respectively.

- [1] Hamaker, J. W. et al. *Paper 6.02 - A Study of the Peroxides of Plutonium*. The transuranium Elements - Research papers. Seaborg, G. T., Katz, J. J., Manning, W. M., Eds. 1949. Vol. 14B-part I, 666–681.
- [2] Hibert, N. *Synthèse et Caractérisation Structurale Des Complexes de Plutonium à Base de Peroxyde*. Thèse, Université de Lille (2018–2021), 2020.
- [3] *Le traitement-recyclage du combustible nucléaire utilisé: la séparation des actinides application à la gestion des déchets*; Commissariat à l'énergie atomique et aux énergies alternatives, Ed.; E-dén; Éd. "Le Moniteur" CEA: Paris Gif-sur-Yvette, 2008.
- [4] Hibert, N. et al. *Coprecipitation of Actinide Peroxide Salts in the U-Th and U-Pu Systems and Their Thermal Decomposition*. Dalton Trans. 2022, **51** (34), 12928–12942.

Densification Study of Cr-doped UO₂ Fuel Pellets with Addition of Fission Products Surrogates

Antonin De Azevedo¹, Fabienne Audubert¹, Nathalie Moncoffre², Jacques Lechelle¹

¹ CEA, DES, IRESNE, DEC. Cadarache F 13108 Saint Paul Lez Durance, France

² Univ Lyon, Univ Claude Bernard Lyon 1, CNRS/IN2P3, IP2I Lyon, UMR 5822, F 69622, Villeurbanne, France

In current nuclear power plant reactors, energy is produced by the fission of uranium and/or plutonium isotopes, contained in oxide pellets made of single phase UO₂ or polyphase (U,Pu)O₂ (MOX). The fission reaction creates fission products that are contained inside the fuel. Those fission products are liable to be released out of the reactor in case of severe accident. The released amount depends on the thermodynamic conditions during the accident and on the chemical state of the fission products. This is why a deep knowledge of the fission products behavior in the fuel in case of accident is absolutely needed in order to anticipate and estimate the consequences of the accident. Some studies have been carried out to identify the chemical state and quantify the release of fission products in irradiated UO₂ and MOX fuels under different thermodynamic conditions [1], [2], [3], [4], [5]. However, irradiated fuels are highly radiotoxic, so their characterization is very complex due to the need of biological protections (shielded hot cells, remote manipulators...). In order to overcome these constraints, an innovative approach consists to synthesize simulated fuels (SIMFUELS), using virgin UO₂ and stable isotopes as fission product surrogates. Then the release of fission products under different thermodynamic conditions is studied with the same approach as for irradiated fuels [3], [6], [7].

UO₂ fuel doped with chromium is part of "E-ATF" (Enhanced Accident Tolerant Fuel). It is studied for its optimized behavior in case of accidents (power ramp) due to a larger grain size compared to a classic UO₂ fuel. Nevertheless, the added chromium is likely to react with some fission products and form volatile species that would not be present in non-doped UO₂ fuel. The speciation of fission products in a Cr-doped SIMFUEL is under study within the framework of the BENEFICIA (BEhavior of New Fuels In Case of Incidents and Accidents) project, supported by the ANR (French National Research Agency).

Therefore, the sintering process of Cr-doped UO₂ has been studied in order to control the microstructure of the pellets. Thus, some pellets have been synthesized under different conditions. The effect of chromium concentration and thermodynamic conditions during sintering on the pellet's microstructural characteristics will be discussed and compared to literature. Then, the addition of fission product surrogates (Ba, Ce, La, Mo, Sr, Y, Zr, Rh, Pd, Ru, Nd) into Cr-doped UO₂ pellets has been done by conventional sintering. The characteristics of the pellets thus obtained as well as the fission products phases will be also presented.

References

- [1] H. KLEYKAMP, « The chemical state of the fission products in oxide fuels », *Journal of Nuclear Materials*, Amsterdam, p. 221-246, 1985.
- [2] Y. Pontillon, G. Ducros, et P. P. Malgouyres, « Behaviour of fission products under severe PWR accident conditions VERCORS experimental programme—Part I: General description of the programme », *Nuclear Engineering and Design*, vol. 240, n° 7, Art. n° 7, juill. 2010,
- [3] C. Le Gall, « Contribution to the study of fission products release from nuclear fuels in severe accident conditions : effect of the pO₂ on Cs, Mo and Ba speciation ». Thèse, Université Grenoble Alpes, 2019
- [4] C. Le Gall *et al.*, « Fission product speciation in the VERDON-3 and VERDON-4 MOX fuels samples », *Journal of Nuclear Materials*, vol. 530, p. 151948, mars 2020
- [5] E. Geiger *et al.*, « Fission products and nuclear fuel behaviour under severe accident conditions part 2: Fuel behaviour in the VERDON-1 sample », *Journal of Nuclear Materials*, vol. 495, p. 49-57, nov. 2017
- [6] E. GEIGER, « Study of fission products (Cs, Ba, Mo, Ru) behaviour in irradiated and simulated nuclear fuels during severe accidents using X-ray absorption spectroscopy, SIMS and EPMA » Thèse, Université Paris-Saclay, 2016.
- [7] L. Balice, « Nuclear fuels in severe accidents : caesium speciation in simulated UO₂ fuels densified by SPS », Thèse, Université Grenoble Alpes, 2022

Hydrothermal Reducing Conversion of Uranium(VI) Oxalate into Oxides

S. Benarib ¹, M. Munoz ¹, I. Kieffer ², J. L. Hazemann ³, N. Dacheux ¹, **N. Clavier** ¹

¹ ICSM, Univ Montpellier, CEA, CNRS, ENSCM, Marcoule, France

² OSUG, Université Grenoble-Alpes, CNRS, Grenoble, France

³ Université Grenoble Alpes, CNRS, Institut Néel, Grenoble, 38042, France

The development of future nuclear reactor technologies is leading us to consider innovative methods for manufacturing (U,Pu)O_{2+x} MOx fuels. In this frame, wet processes are being examined in particular to improve the cationic homogeneity of powders and control their morphology. These methods are generally based on the precipitation of precursors at low temperature, followed by their conversion by heat treatment at high temperature. However, the resulting oxides may still contain traces of carbon that are detrimental to sintering, and their morphology is often unsuitable for densification. In this context, the conversion of oxalate compounds into oxides under hydrothermal conditions now appears to be a promising alternative [1-3]. It retains the advantages of oxalate precipitation (rapid and quantitative precipitation of cations), while allowing the morphology of the final powder to be controlled and carbon impurities to be effectively eliminated.

To date, the work reported in the literature has involved compounds incorporating one or more tetravalent actinides [4]. In order to consider the co-conversion of uranium and plutonium, a recent study also looked at the U(IV)-Ce(III) system, as a model of the U(IV)-Pu(III) couple [5]. However, another method could be to consider U(VI)-Pu(IV), which involves the stabilized oxidation states at the end of the PUREX process. Hydrothermal conversion then inevitably requires the reduction of uranyl ions. In this respect, the scientific literature provides geochemical studies on the reduction of uranyl ions by organic compounds in a natural environment under hydrothermal conditions. In particular, Nakashima *et al.* have undertaken several studies on the reduction of uranium(VI) by organic matter leading to the formation of UO_{2+x} under mild hydrothermal conditions (T = 100-200°C) [6,7]. These studies revealed that the reduction of uranyl ions and the formation of UO₂ in the presence of lignite, R₁R₂CHOH, or a secondary alcohol, e.g. propan-2-ol, is even possibly quantitative at T = 200°C, following :



Drawing on this work, it is possible to envisage the use of oxalates, not only as precipitating agents, but also as organic species capable of quantitatively reducing uranyl ions, which could enable the development of an innovative synthesis route for the mixed oxides of interest.

With this in mind, a preliminary study was undertaken regarding the hydrothermal conversion of a mixture composed of uranyl and oxalate ions to obtain uranium(IV) dioxide. It demonstrated that it was possible to convert uranyl molecular ions into uranium(IV) oxide and made it possible to specify the experimental conditions influencing the physico-chemical properties of the samples obtained. The pH was found to present a considerable effect on the reduction of uranium, the nature of the precipitated uraniferous phases and their precipitation yield, the latter varying drastically over a very narrow pH range. Indeed, at T = 250°C and pH = 0.8, the characteristic fluorine structure of UO₂ was obtained as a pure phase, while at pH = 1, the formation of UO₂ (containing only tetravalent uranium) and α-U₃O₈, consisting of a U(V)/U(VI) mixture, was obtained. From pH = 1.2, the precipitate obtained was composed of α-U₃O₈ and meta-schoepite, with the formula (UO₂)₃O₂(OH)12-10H₂O (fully hexavalent uranium). Optimum conditions for quantitative hydrothermal conversion of the reaction mixture into UO_{2+x} were thus identified, with a conversion time of more than 72 hours to ensure a quantitative precipitation, and an initial pH of 0.8.

In order to gain a better understanding of the redox mechanisms involved in the hydrothermal conversion of uranium(VI) to UO_{2+x} by oxalates, *in situ* XANES analyses at the U-L_{III} edge were carried out on the BM30-FAME beamline at the ESRF synchrotron. The study focused on monitoring the degree of oxidation of uranium in solution and within the precipitate formed rapidly during hydrothermal treatment. The study of the solution revealed an almost complete reduction in uranium(VI), as well as a change in uranium complexation, probably caused by the decomposition of oxalate ions under the effect of the pressure-temperature couple. In parallel, the drop in uranium fluorescence intensity in solution was explained by rapid uranium precipitation. Furthermore, uranium(IV) appears to precipitate directly in the form of UO_{2+x}, and

no variation in the degree of oxidation of uranium within the solid could be detected under the analytical conditions. These data then allowed to propose a first mechanism for the reductive hydrothermal conversion of U(VI) into UO_{2+x} (figure 1).

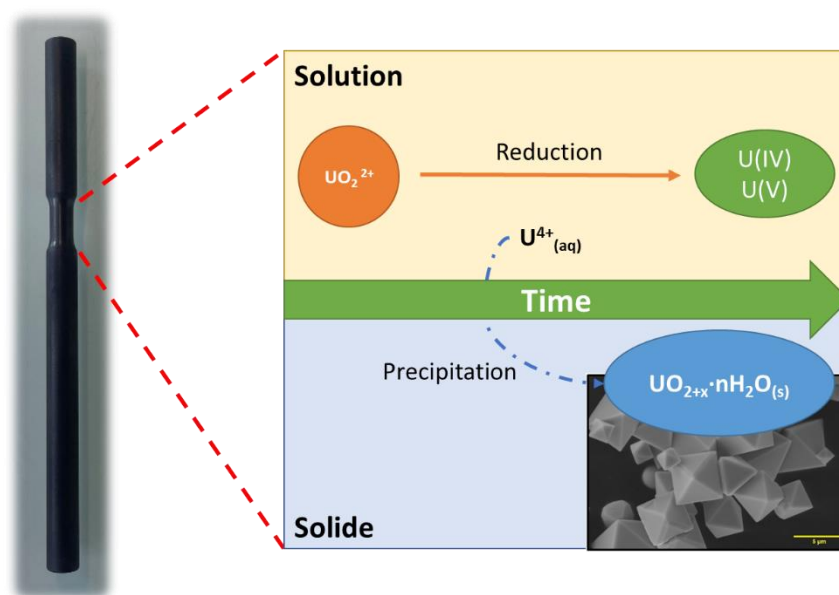


Figure 1: Schematic representation of the hydrothermal conversion of a uranyl solution into hydrated uranium(IV) dioxide.

References

1. O. Walter, K. Popa, and O. D. Blanco, "Hydrothermal decomposition of actinide(IV) oxalates: A new aqueous route towards reactive actinide oxide nanocrystals," *Open Chem.* **14** (2016) 170–174.
2. J. Manaud *et al.*, "Hydrothermal Conversion of Uranium(IV) Oxalate into Oxides: A Comprehensive Study," *Inorg. Chem.* **59** (2020) 3260–3273.
3. J. Manaud *et al.*, "Hydrothermal Conversion of Thorium Oxalate into $\text{ThO}_2 \cdot n\text{H}_2\text{O}$ Oxide," *Inorg. Chem.* **59** (2020) 14954–14966.
4. K. Popa *et al.*, "A low-temperature synthesis method for AnO_2 nanocrystals (An = Th, U, Np, and Pu) and associate solid solutions," *CrystEngComm*, **20** (2018) 4614–4622.
5. S. Benarib *et al.*, "Hydrothermal conversion of mixed uranium(IV)–cerium(III) oxalates into $\text{U}_{1-x}\text{Ce}_x\text{O}_{2+\delta} \cdot n\text{H}_2\text{O}$ solid solutions," *Dalton Trans.* **52** (2023) 10951–10968.
6. S. Nakashima *et al.*, "Experimental study of mechanisms of fixation and reduction of uranium by sedimentary organic matter under diagenetic or hydrothermal conditions," *Geochim. Cosmochim. Acta* **48** (1984) 2321–2329.
7. S. Nakashima, "Kinetics and thermodynamics of U reduction by natural and simple organic matter," *Org. Geochem.* **19** (1992) 421–430.

Actinide Thioamidates as Precursors For Actinide Sulfide Nanomaterials

Sheridon N. Kelly^{ab}, Dominic R. Russo^{ab}, Appie A. Peterson^b, Erik T. Ouellette^a, Michael A. Boreen^a, Jacob A. Branson^{ab}, S. Olivia Gunther^b, Patrick W. Smith^b, John Arnold^a, Stefan G. Minasian^b.

^aDepartment of Chemistry, University of California, Berkeley, Berkeley, California 94720, USA.; ^bChemical Sciences Division, Lawrence Berkeley National Lab, Berkeley, California 94720, USA.

Actinide sulfide materials have been historically understudied, particularly in comparison to their more commonly-studied counterparts, the actinide oxides. However, desirable properties such as higher thermal conductivity and elevated melting points make such materials as uranium and plutonium sulfide appealing as alternative nuclear fuel materials.¹ Still, the physical properties of these materials are not well-documented. Beyond the physical properties, the actinide sulfides are interesting to study from a fundamental standpoint, due to the softer nature of sulfide promoting novel electronic structure. We hypothesize that the closer energy match between the actinide and sulfide valence orbitals² will lead to increased covalency and unique properties as compared to the oxides.

Here, we report the synthesis of uranium and neptunium thioamidate molecules designed as single source precursors to uranium and neptunium sulfide materials. Following isolation of the homoleptic complex, the uranium thioamidate was pyrolyzed, and analysis of the byproducts suggests that the decomposition mechanism is consistent with that reported for analogous amidate complexes.³ The pyrolysis product was characterized by elemental analysis, PXRD, and X-ray absorption spectroscopy to confirm the decomposition of the precursor molecule into uranium disulfide. This marks the first use of a single-source precursor towards an actinide chalcogenide material other than an oxide, and opens up simpler, more accessible pathways to generating US_2 than has previously been reported. Similar studies on the isolated neptunium thioamidate complex towards neptunium sulfide, as well as synthesis of a related plutonium thioamidate, are ongoing.

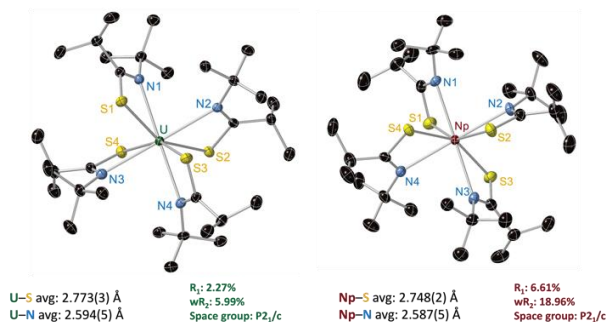


Figure1. X-ray crystal structure of $U(ITA)_4$ (left) and $Np(ITA)_4$ (right) with all atoms represented at 50% probability thermal ellipsoids and hydrogens omitted for clarity.

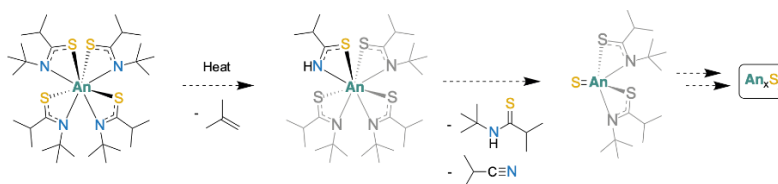


Figure2. Proposed decomposition mechanism of $An(ITA)_4$ into An_xS_y based on similar oxide experiments.

REFERENCES

- (1) *Nuclear Applications*, **1965**, 1:2, 168-175.
- (2) *Inorg. Chem.* **2016**, 55, 9989-10002.
- (3) *Angew. Chem. Int. Ed.* **2019**, 58, 5749.

Synthesis of PuO₂ and (U,Pu)O₂ Solid Solution by Citric Acid Assisted Combustion Synthesis

A. Hautecouverture [1,2], **P. Estevenon** [1], C. Rey [2], X. Deschanel [2]

[1] CEA, DES, DMRC, Site de Marcoule, Bagnols-sur-Cèze, France.

[2] ICSM, Univ Montpellier, CNRS, CEA, ENSCM, Bagnols-sur-Cèze, France.

Within Generation IV International Forum framework, new routes to prepare nuclear fuel and more specially MOx fuel have been studied. In this context, the Syntheses by Combustion in Solution (SCS) have been considered to prepare plutonium oxide or directly uranium and plutonium mixed oxides. The SCS reactions are a family of processes known since the 1970's which enable the formation of transition elements oxide phases [1]. They are based on the preparation of an aqueous mixture of the transition element nitrate salt and a specific reactive organic compound. This solution is then heated leading to its dehydration and the gelation of the mixture. The final step of this reaction corresponds to an ignition of the reactive mixture and its combustion thanks to an exothermic self-propagating phenomenon leading to the formation of the expected oxide phase. The interest of these reactions is that they are based on ignition generally occurring at low temperature (~200°C) with a high flame temperature (beyond 1000°C) and a reaction over a very short period of time. In the context of actinide oxide synthesis for the nuclear fuel cycle, these characteristics might be an asset in the formation of oxide species with low residual carbon content.

To reach these conditions, the selection of an organic specie with a good affinity with the nitrate salt precursor is crucial. The transposition of SCS reactions to actinide chemistry and more specifically to uranium oxide synthesis allowed to identify citric acid as a promising reactant [2-6]. Therefore, in order to produce uranium and plutonium mixed oxide fuel, the SCS reactions nitric solution with Pu(IV) and then U(VI) + Pu(IV) mixture have been studied [7,8].

After preliminary studies on surrogates for actinides and uranium carried out in the Separative Chemistry Institute in Marcoule, experiments on plutonium and uranium and plutonium mixture were carried out on the ATALANTE facility. The experimental methodology was based on the one hand on a parametric study which singled out the optimal conditions of synthesis for the different systems and on the other hand on advanced characterization performed at the different steps of the reaction (aqueous solution, gel and oxide) using Raman, infrared and UV-visible spectroscopies, PXRD, SEM observation and XAS techniques.

The experiments performed on PuO₂ synthesis by citric acid assisted SCS at 300°C proved the feasibility of that reaction. The optimal conditions for its synthesis were determined through parametric experiments and corresponds to a citric acid/plutonium molar ratio of 1.1 (Figure 1a), starting with Pu(IV) nitrate as a reagent. In said conditions, the solid phase obtained presents characteristics which demonstrate that the temperature reached by the sample (due to SCS exothermicity) is the highest in the range of conditions explored: high crystallinity, low carbon content, SCS characteristic morphology.

The compilation of the optimized treatments previously identified for uranium and for plutonium allowed to perform syntheses with U(VI) and Pu(IV) nitric acid solutions in order to synthesize mixed oxide phases. These experiments evidenced the synthesis of over-stoichiometric oxide solid solution phases, (U,Pu)O_{2+x}, for several Pu/U ratio in optimal conditions by this pathway (Figure 1b). HERFD-XANES characterizations performed on ROBL and MARS beamlines on these samples allowed to confirm these results. Moreover, the characterizations made on the precursor gel phase, prior to the combustion reaction and for both pure U/Pu and mixed compounds, gave a better understanding of the reaction mechanism.

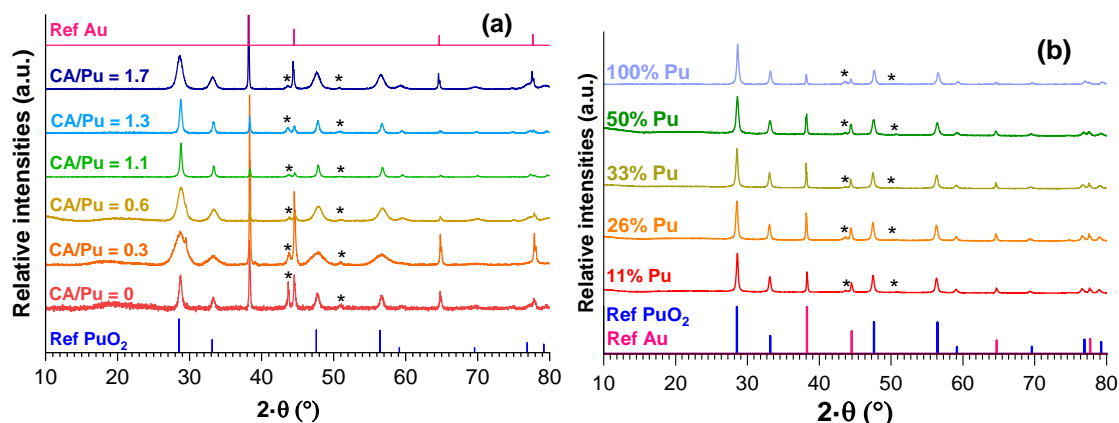


Figure 1: PXRD of oxide phases obtained by citric acid assisted SCS reaction, for different citric acid/plutonium molar ratio (a) and in optimal conditions for different Pu/(U+Pu) molar ratio (b). Gold was used as an internal standard and star-marked diffraction peaks represent to the sample holder.

Finally, the preparation of a MOx fuel pellet has been directly achieved from a mixed uranium and plutonium sample obtained by SCS. These experiments evidenced that SCS originated powders, sintered at low temperature. This behavior is characteristic of nanocrystalline powder. Moreover, they logically exhibit a very high cation homogeneity (Figure 2) since the SCS reaction produce directly a solid solution. All these results allow us to take a first step towards the applicability of SCS reactions for MOx fuel synthesis.

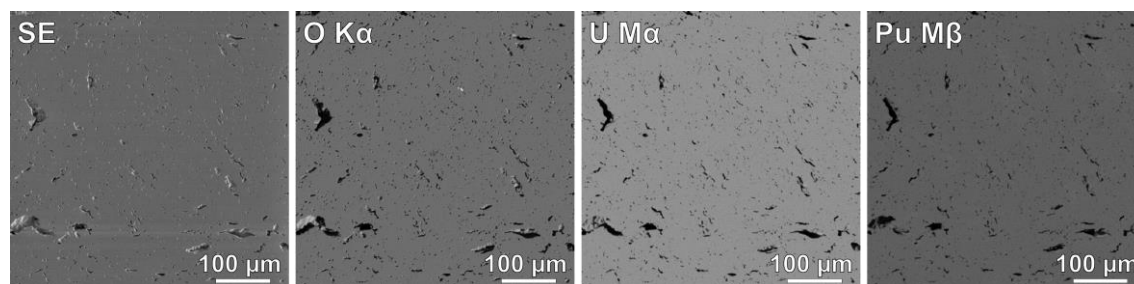


Figure 2: Microprobe analysis of a MOx fuel pellet prepared from mixed oxide prepared by citric acid assisted combustion synthesis.

References:

- [1] A. E. Danks, Material Horizons 2016, 3, 91-112
- [2] J. Monnier, Ph.D. Thesis, 2019, Montpellier University
- [3] S. Anthonyamy, Journal of Nuclear Materials 2000, 278, 346-357
- [4] A. Jain, Journal of Nuclear Materials 2005, 345, 245-253
- [5] D. Maji, Journal of Nuclear Materials 2018, 502, 370-379
- [6] J. M. Roach, Inorganic Chemistry 2021, 60, 18938-18949
- [7] A. Hauteceuvre, Journal of Nuclear Materials 2023, 586, 154694
- [8] A. Hauteceuvre, Ph.D. Thesis, 2023, Montpellier University

Phase Separation in Fluorite-Related $U_{1-y}Ce_yO_{2-x}$: New Insights via Variable Temperature Neutron Diffraction

David Simeone¹, Xavier Deschanel², Philippe Garcia³, Maxim Avdeev⁴, Timothy Ablott⁵,
Gordon J Thorogood⁶

1. Université Paris-Saclay, CEA, DES-Service de Recherche Métallurgie Appliquée, 91191, Gif-sur-Yvette, France

2. Univ. Montpellier, ICSM, CEA, CNRS, ENSCM, Marcoule, France

3. CEA, DES, IRESNE, DEC, Cadarache F-13108 Saint-Paul-Lez-Durance, France

4. Australian Nuclear Science and Technology Organisation, New Illawarra Road, Lucas Heights, NSW 2234, Australia;
School of Chemistry, The University of Sydney, Sydney 2006, Australia.

5. Australian Nuclear Science and Technology Organisation, New Illawarra Road, Lucas Heights, NSW 2234, Australia.

6. Australian Nuclear Science and Technology Organisation, New Illawarra Road, Lucas Heights, NSW 2234; Department of
Nuclear System Safety Engineering, Nagaoka University of Technology, 1603-1 Kamitomioka-machi, Nagaoka-shi, Niigata,
Japan,

The phase separation in the $U_{1-y}Ce_yO_{2-x}$ system for values of y between approximately 0.34 and 0.5 observed at low temperatures (below circa 600 K) purportedly involves only fluorite structures [1,3]. Therefore, to confirm this assumption it is logical to employ high resolution diffraction techniques that can track the progression of the oxygen-sub lattice and resolve peaks that may be overlapping. In this study, the phase separation in the $U_{0.54}Ce_{0.46}O_{2-x}$ system has been revisited using variable temperature high resolution neutron diffraction on samples that are sealed under Ar to prevent a change in oxidation state when heated.

As neutron scattering lengths for U_{tot} and O do not differ to a large degree, U coherent cross section 8.903 barn vs O coherent cross section 4.232 barn, information about the oxygen sub lattice can be obtained from neutron diffraction patterns. This is not the case for X-ray diffraction which has been used for the bulk of the studies on this system.

Below a critical temperature, the existence of two fluorite related structures in the miscibility gap is confirmed: a stoichiometric $U_{0.54}Ce_{0.46}O_2$ phase and an oxygen-deficient $U_{0.54}Ce_{0.46}O_{2-x}$ phase. Although the former is indeed a fluorite, we show that the other end-member phase has a C-type bixbyite structure, Figure 1.

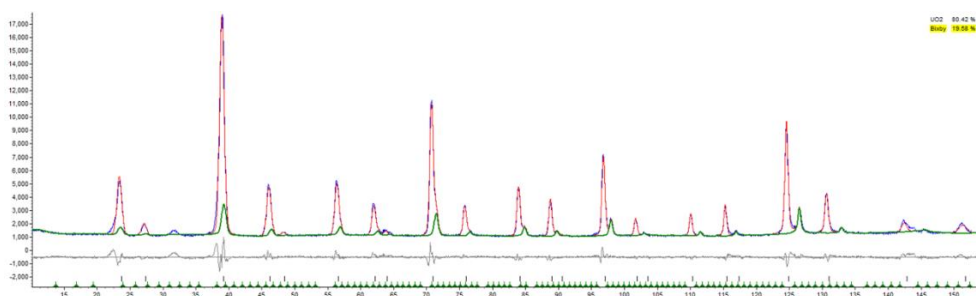


Figure 1. High-resolution neutron diffraction pattern acquired at 300K, C-type bixbyite phase is highlighted in green showing overlap of the two phases.

This would suggest that the oxygen-deficient phase can be described as a bixbyite over the entire cerium composition range (see Figure 2). In this work, we present some recent developments executed to understand the phase transformation in this material and try to relate this with the defects produced by the oxygen deficiency in the anionic sub lattice. The

ultimate goal of this approach is to simulate this phase transformation within the Phase Field as it approaches phase transition.

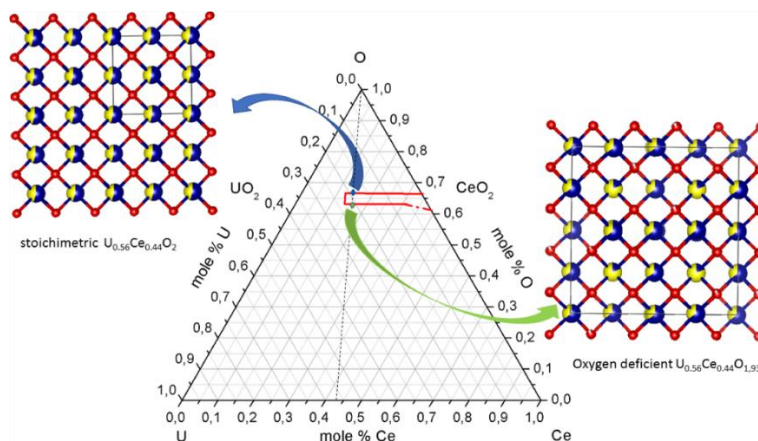


Figure 2: Schematic description of two ended phases produced during the phase transformation of $(U,Ce)O_{1-x}$ ($x=0.07$).

- [1] Markin, T.; Street, R.; Crouch, E. The uranium-cerium-oxygen ternary phase diagram. J. Inorg. Nucl. Chem. 1970, 32, 59-75.
- [2] Lorenzelli, R.; Touzelin, B. Sur le système UO_2 - CeO_2 ; etude cristallographique à haute température. J. Nucl. Mater. 1980, 95, 290-302.
- [3] Vauchy, R.; Belin, R. C.; Richaud, J.-C.; Valenza, P. J.; Adenot, F.; Valot, C. Studying radiotoxic materials by high temperature X-ray diffraction. Applied Materials Today 2016, 3, 87-95.

Fabrication and Dissolution of Americium Plutonium Oxide Fuels

Eva de Visser-Týnová, Jessica Bruin, Frank Oud

Nuclear Research and consultancy Group (NRG), Westerduinweg 3, 1755 LE Petten, the Netherlands

Oxide fuels for Generation IV systems and IMF may contain high concentrations (up to 50%) of plutonium and minor actinides. High concentrations of plutonium in oxide fuels strongly limit the solubility in nitric acid. However, the effect of the MA-content (specifically Am) on the dissolution capability is still not very well known. Yet this effect forms a crucial aspect in the design of a reprocessing flow-sheet for oxide fuels for Generation IV systems, as well as for Inert Matrix Fuels. It is the objective to study the basic dissolution properties of oxide fuels with a high concentration of minor actinides. This enables establishing a relationship between Am-content and dissolution capability, addressing open issues concerning the maximum achievable Minor Actinide content in fuels and targets for transmutation purposes.

The composition of actinides in spent fuel for various P&T scenarios has been calculated with the SERPENT Monte Carlo code[1]. The calculated fraction of plutonium in the oxide phase of the fuel at EOL exceeds 40%, which may constitute an issue for the dissolution performance. Dissolution tests of (Pu,MA)₂O₃ samples with a Pu fraction of up to 50% therefore should be carried out to assess the solubility limit of this fuel composition.

Americium Plutonium oxide pellets have been fabricated by the powder metallurgy method [2], two types pellets were prepared:

	AmO ₂ (wt%)	PuO ₂ (wt%)	Density (% of TD)
Type I	28.4	52.4	75.1 ±3.2
Type II	71.6	47.6	71.1 ±0.8

The pellets have been sintered up to 1600 °C with a dwell of 6 hours. The pellets are about 3 mm high with a diameter of 4.5 mm, each pellet is about 0.45 g. The density of the pellets is determined by immersion in ethanol. Both, the raw powders and the pellets are checked by XRD.

These pellets were prepared for the subsequent dissolution studies. Due to its high plutonium content, this fresh fuel is expected to dissolve slowly with high residues poorly in standard nitric acid (PUREX process) dissolution steps. Therefore, a series of dissolution experiments with varying conditions are proposed: i) Dissolution in hot concentrated nitric acid, ii) Dissolution in hot concentrated nitric acid with fluoride as a catalyst and iii) Oxidation with in-situ chemically generated Ag(II). During the dissolution experiments sub-samples will be taken and analysed for Am and Pu content to get information on the dissolution rates. The residues will be analyzed as well.

All this work is performed in a dedicated glovebox in the actinide laboratory, the radiological aspects of these experiments will be presented as well.

References:

- [1] Janne Wallenius: ASGARD Deliverable D 2.2.1 Modelling study on the composition of spent fuel for various P&T scenarios, 2013
- [2] Eva de Visser-Týnová et al: ASGARD Deliverable D2.2.2 Report on fabrication of Americium Plutonium oxide pellets, 2016

This research was performed as a part of the European project "Advanced fuels for Generation IV reActors: Reprocessing and Dissolution (ASGARD, Grant agreement ID: 295825)" and European project "Fuel Recycle and Experimentally Demonstrated Manufacturing of Advanced Nuclear Solutions for Safety (FREDMANS, Grant agreement ID: 101060800)". The Dutch ministry of economic affairs and climate is acknowledged for the financial support of this research.

Fission Products Speciation in Irradiated MOx Fuel During Interim Storage Accidental Scenarios

R. Caprani¹, Ph. Martin¹, J. Martinez¹, D. Prieur², F. Lebreton¹, K. Kvashnina², E. Bazarkina², D. Menut³, N. Clavier⁴

¹ CEA, DES, ISEC, DMRC, Univ Montpellier, Marcoule, France – ² Helmholtz Zentrum Dresden Rossendorf (HZDR), Dresden, Germany – ³ Synchrotron SOLEIL, L'Orme des Merisiers, Departementale 128, 91190 Saint-Aubin, Gif-sur-Yvette, France –

⁴ Institut de Chimie Séparative de Marcoule, Univ Montpellier, CEA, CNRS, ENSCM, Marcoule, France

Depending on each country fuel cycle strategies, spent MOx fuel assemblies could be either stored for several years into dedicated pools in which the residual heat is removed by water – and then reprocessed and recycled, or directly stored under air into long-term underground deposits. In case of an accidental scenario (loss of coolant, contact with air and / or water, etc.) with loss of coolant, the spent fuel would oxidize rapidly due to its self-heating and the surrounding oxidative environment, inducing therefore a transformation in its physico-chemical properties. Exploring these scenarios is then of the utmost importance to assess the safety of the nuclear fuel cycle over the entirety of its life cycle [1,2].

Considering both high radiotoxicity and complex chemical composition of the spent fuel, model materials called SIMfuel have been developed in the last decades [3-5]. These materials have been shown to be representative of real spent fuel, but with several advantages. First, SIMfuels are constituted by fresh fuel doped with stable FP isotopes, thus significantly reducing the associated radiological risk during the experimentation. Furthermore, the FPs chemical inventory of these materials can be adjusted to study specifically the effect of selected FPs. Until now, only UO₂ based SIMfuel have been studied, so their applicability to spent MOx fuel is limited. In the past years we have developed a synthesis route for MOx-SIMfuels (SIMMOx) samples, as detailed in [6,7].

The type of MOx fuel employed in commercial reactors has heterogeneous nature (MIMAS), consisting in three phases: U-enriched phase, (U,Pu)O₂ matrix, and Pu-enriched phase. This latter reaches the maximum burnup, producing the largest amount of Fission Products (FP) which are known to induce significant changes in the physico-chemical behaviour of the material.

Following the process described in [6,7] we synthesized samples representative of Pu-enriched areas of MIMAS MOx irradiated fuel corresponding to a local burnup of 119 Gw.d/t (13 at.%). Three batches with different compositions has been synthesized in order to separate the effect of three families of FP:

- Batch called “S”: U_{0.74}Pu_{0.26}O₂ + the “soluble” FP (Ce, La, Nd, Sr, Y, Zr)
- Batch called “SM”: U_{0.74}Pu_{0.26}O₂ + the “soluble” FP (Ce, La, Nd, Sr, Y, Zr) + the FP present in metallic inclusions (Mo, Ru, Rh, Pd)
- Batch called “SMB”: U_{0.74}Pu_{0.26}O₂ + the “soluble” FP (Ce, La, Nd, Sr, Y, Zr) + the FP present in metallic inclusions (Mo, Ru, Rh, Pd) + Ba who is related to the formation of perovskite-like phases.

After sintering, thermal treatments corresponding to different accidental scenarios were applied to follow the evolution of the chemical behaviour of both actinides (U, Pu, Am) and fission products (Ba, Ce, La, Mo, Nd, Pd, Rh, Ru, Sr, Y, Zr). The thermal treatments were performed under flowing air at temperatures of 250° C and 310° C, for 110 hours.

The samples were fully characterized following a multi-scale approach, composed of several complementary techniques. XRD and EPMA showed that before the thermal treatment, the material presents a globally monophasic and homogeneous (U,Pu)O₂ with various FP-based precipitates. Figure 1 shows that during the thermal treatment the material oxidizes transforming from monophasic (phase A in Figure 1) to biphasic (phases A and B in Figure 1).

Through the coupling of EPMA with Raman microscopy, we were able to correlate the local FPs enrichment with the changes in the Raman spectra (and thus in term of local symmetry) on a µm scale. Raman microscopy highlighted the important kinetic effect of the oxidation processes, showing how the oxidation starts from cracks and open porosity, moving slowly towards the bulk of the material.

Synchrotron XAS experiments performed at ESRF-ROBL (Figure 2), supplied crucial information on the fission products speciation, determining the prevalent chemical form of each dopant in the samples. HERFD-XANES allowed for a precise determination of the chemical form of some FP (Ba + Lanthanides), and the actinides oxidation state, thus providing the

O/M ratio. Furthermore, a strong change in behaviour is observed for the Lanthanides, which could be related to a highly disordered atomic environment arising as a consequence of the oxidation treatment.

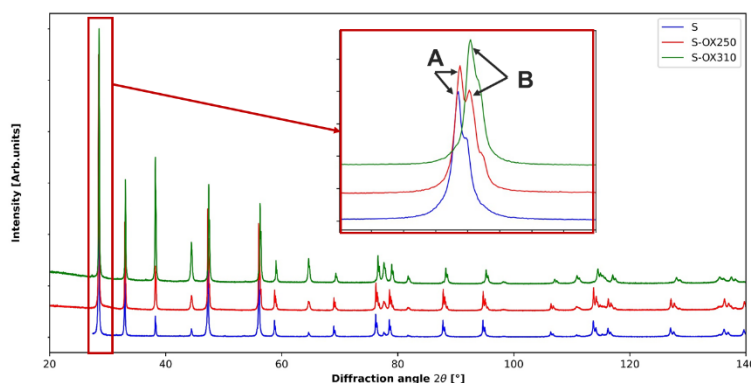


Figure 1 X-ray diffraction pattern of three SIMMOx samples with same composition (batch "S"), before (blue) and after two thermal treatments (250° C and 310° C under flowing air for 110 hours) simulating interim storage accident conditions (red and green). The sample before oxidation is monophasic (blue) showing only phase A, while phase B appears during the thermal treatments. The data are the superposition of the pattern obtained with the Cu K α and K β lines.

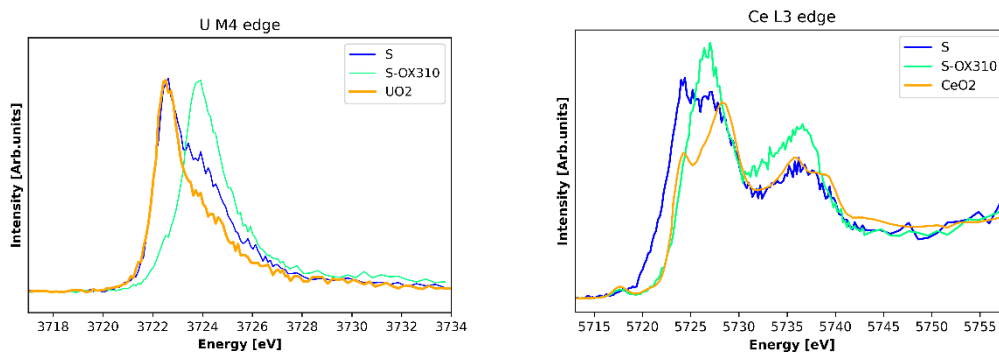


Figure 2 Examples of HERFD-XANES spectra collected at the U M₄-edge and Ce L₃-edge of SIMMOx samples before (blue) and after (green) the thermal treatment, with a reference compound (orange) for U and Ce. In both cases, U and Ce are shown to heavily oxidize during the thermal treatment. Ce chemical environment seems to also shift towards a less ordered system.

- [1] Y. Guerin, Compr. Nucl. Mater., Elsevier, Oxford, 2012.
- [2] K. Samuelsson et al., J. Nucl. Mater. 532, 2020, 151969.
- [3] C. Le Gall, PhD Thesis, Université Grenoble Alpes, 2018.
- [4] E. Geiger, PhD Thesis, Université Paris-Saclay, 2016.
- [5] P.G. Lucuta et al., J. Nucl. Mater. 178, 1991, 48-60.
- [6] R. Caprani et al., J. Nucl. Mater. 585, 2023, 154607.
- [7] R. Caprani, PhD thesis, Université de Montpellier, 2023.

Synthesis and Characterisation of CeO_2 and PuO_2 Pellets with Representative Microstructure for General Purpose Heat Sources

Jérémie Manaud, Walter Bonani, Jacobus Boshoven, Marco Cologna, Michael Holzhäuser, Karin Popa, Sorin-Octavian Vălu, Daniel Freis
European Commission, Joint Research Centre (JRC), Karlsruhe, Germany

The goal of the Horizon Europe project "PU-238-coupled dynamic power system for SpAce exploRation and beyond" (PULSAR) is to evaluate the feasibility to establish within the next decade a European production capability for Pu-238 radioisotope sources for compact, lightweight and high-power electricity generators such as Radioisotope Thermoelectric Generators (RTG) [1]. The JRC-Karlsruhe has broad expertise in all aspects of actinide oxide processing, including handling of highly active Pu-238 although in smaller proportions than those required for RTG. Of particular interest to the present project, is the expertise in microstructure engineering with e.g. manufacturing of solids with ultrafine or ultralarge grains.

Building on global experiences and available literature, the JRC Karlsruhe has replicated a preparation route for PuO_2 pellets involving oxalate precipitation, several intermediate process steps and a hot pressing step [2], emphasizing a specific microstructure crucial for safe helium outgassing during alpha decay in operational and accidental scenarios. Furthermore, this microstructure shall ensure a minimum particle size above inhalable limits in hypothetical release scenarios, preventing environmental dispersion. The developed methodology explores powder production routes compatible with the Np/Pu separation process.

In the first stage of the project, cerium was used as an inactive surrogate for plutonium. The reported relative density for the $^{238}\text{PuO}_2$ pellets was of 82-86 % theoretical density, with a network of fine porosity within the granules and larger, interconnected porosity around the granules [2]. The exact replication of the density and microstructure of the pellets was unlikely for the use of cerium, due to the different chemical nature of cerium and plutonium and the physical behaviour of the associated oxides. However, the characterisation of the sintered pellets has demonstrated the technical capability of JRC infrastructure to replicate the production procedure (Figure1). In addition, conventional sintering of the pellets followed by thermal treatment under two different atmospheres was evaluated as an alternative to the hot-pressing stage.

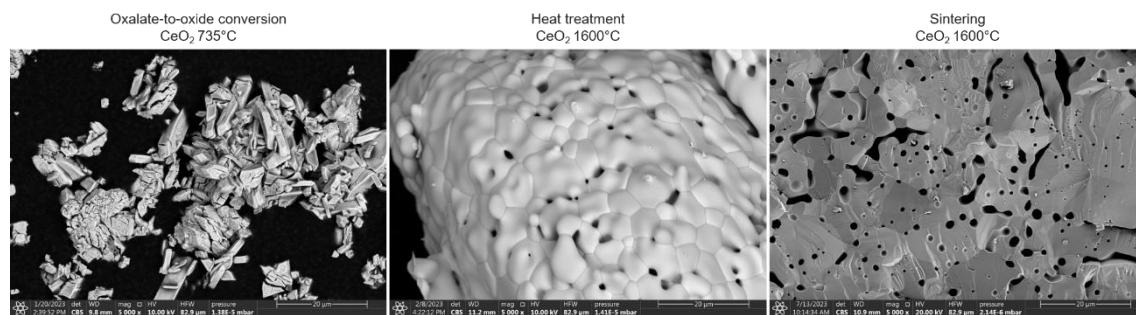


Figure1. SEM images of the CeO_2 powders at two different steps of the process and the final sintered pellet.

In light of the preliminary findings and the lessons learned over the progress of this preliminary study, we have decided on the activities using reactor grade plutonium in active laboratories and the production of PuO_2 pellets is currently proceeding.

References:

[1] <https://cordis.europa.eu/project/id/101061251>

[2] M. Borland, S. Frank, B. Patton, B. Cowell, K. Chidester, "An evaluation of alternative production methods for Pu-239 general purpose heat source pellets", Proceedings of Nuclear and Emerging Technologies for Space 2009, Atlanta, GA, June 14-19, 2009, Paper 203585.

Incorporation of Fission Products into Oxide Nuclear Fuel: Towards a New Paradigm?

L. Desgranges

CEA.DES.IRESNE.DEC, Cadarache F 13108 St Paul Lez Durance

The way fission products are incorporated in uranium dioxide fuels is a long-standing question in nuclear science. Because the microstructure of UO_2 nuclear fuel remains nearly unchanged up to local burn-up as high as 60 GWd/tM, researchers hypothesized that fission products were immobilized in the UO_2 crystalline lattice. This immobilization would be most likely in substitution of uranium for rare-earth elements because of their ionic radius and charge. Consequently, Omichi ^[e] proposed that the unit cell of lanthanide doped UO_2 would be the sum of the weighted ionic radius of each element. In such description, the ionic electroneutrality imposed that the incorporation of trivalent elements should be compensated by other ionic charges in the $\text{U}^{4+}\text{O}^{2-}_2$ lattice. These ionic charges can be either U^{5+} , U^{3+} or oxygen vacancies with an electric charge or not. More EXAFS and XANES results provided the vacancy and charge inventory in some doped UO_2 (see for example ^[f]). These results confirmed the existence of U^{5+} and confirmed the substitution hypothesis. However, recently some new characterization became available about the dynamic local environment in UO_2 crystalline structure that could shade this historical interpretation.

The existence of disorder in UO_2 crystalline structure was first reported by Hutchings ^[g], who proposed to explain changes in the intensity of UO_2 diffraction peaks by the formation of different types of oxygen interstitial clusters. Later on, some authors considered that UO_2 thermodynamic properties could be explained by point defect creation, either polarons ^[h] or oxygen vacancies ^[i], but this would imply a 10% percent concentration of such defects above 2500K ^[j], confirming the idea of grouped defects initially proposed by Hutchings and consistent with some more recent calculations ^[k]. In the last decade, both experimental ^[l] and theoretical ^[m] studies evidenced that, at high temperature, the cubic coordination polyhedron of uranium atom could change symmetry and become octahedral at the local scale. Two different distortion schemes were proposed to account for a non-cubic local symmetry. The fit of experimental neutron PDFs led to the choice of Pa-3 local symmetry ^[n], while the analysis of atomic positions calculated by molecular dynamics led to a distortion path in two steps first from Fm-3m to $P4_2/nmc$ and then to Pbcn ^[m]. All these data are an indication for the existence of a kind of internal disorder in UO_2 at high temperature, because of which the local environment and the charge of regular uranium atom could be different from 4+ and cubic, respectively.

In this presentation, we will consider the implications of such state of disorder on the incorporation of rare-earth element in UO_2 lattice. The basic underlying idea consists in the following hypothesis: rare-earth element would incorporate in a

^e T. Ohmichi et al. 'On the relation between lattice parameter and O/M ratio for uranium dioxide-trivalent rare earth oxide solid solution', J. Nucl. Mater., vol. 102, no. 1, pp. 40-46, Nov. 1981.

^f R. Bès et al., 'New insight in the uranium valence state determination in $\text{UyNd}_{1-y}\text{O}_{2+x}$ ', J. Nucl. Mater., vol. 507, pp. 145-150, Aug. 2018.

J. Chem. Soc. Farad. Trans. 2, 83 (7) (1987), p. 1083, 10.1039/f29878301083

^h P. Ruello et al., Heat capacity anomaly in UO_2 in the vicinity of 1300 K: an improved description based on high resolution X-ray and neutron powder diffraction studies, Journal of Physics and Chemistry of Solids 66 (2005) 823-831

ⁱ R.J.M. Konings, O. Beneš, The heat capacity of NpO_2 at high temperatures: The effect of oxygen Frenkel pair formation, Journal of Physics and Chemistry of Solids, Volume 74, Issue 5, 2013, Pages 653-655, <https://doi.org/10.1016/j.jpcs.2012.12.018>.

^j T.R. Pavlov et al., Full length article Measurement and interpretation of the thermo-physical properties of UO_2 at high temperatures: The viral effect of oxygen defects T.R. Pavlov et al. / Acta Materialia 139 (2017) 138-154

^k H Zhang et al. Superionic UO_2 : A model anharmonic crystalline material Cite as: J. Chem. Phys. 150, 174506 (2019); <https://doi.org/10.1063/1.5091042>

^l Desgranges L et al. 2017 "What is the actual local crystalline structure of uranium dioxide, UO_2 ? A new perspective for the most used nuclear fuel" Inorg. Chem. 56 321-6

^m Fossati PCM, Chartier A and Boule A (2021) Structural Aspects of the Superionic Transition in AX_2 Compounds With the Fluorite Structure. Front. Chem. 9:723507. doi: 10.3389/fchem.2021.723507

ⁿ Lionel Desgranges, et al., Understanding Local Structure versus Long-Range Structure: The Case of UO_2 , Chem. Eur. J. 2018, 24, 2085 – 2088

dynamic local environment a high temperature and then be quenched to room temperature. At high temperature, cationic local environment in UO_2 is not only cubic but also octahedral. Most of the crystalline structures of rare-earth oxides have an octahedral environment for the rare-earth cation, therefore we will assume that at high temperature rare-earth element would have octahedral environment. Because uranium atoms can have both cubic and octahedral environment, we imagine that domains would exist in which both uranium and rare-earth element have an octahedral environment, while the remaining domains would be made of uranium only. When quenching this would lead to a biphasic microstructure instead of a homogenous microstructure that is predicted by the historical interpretation.

Figure1 presents a Nd doped UO_2 that was heat treated at 1700°C during 72 hours under reducing atmosphere. The TEM results clearly evidenced different domains, the ones containing Nd, the others with uranium only. This result would be in favor of the disorder interpretation and not of the historical interpretation.

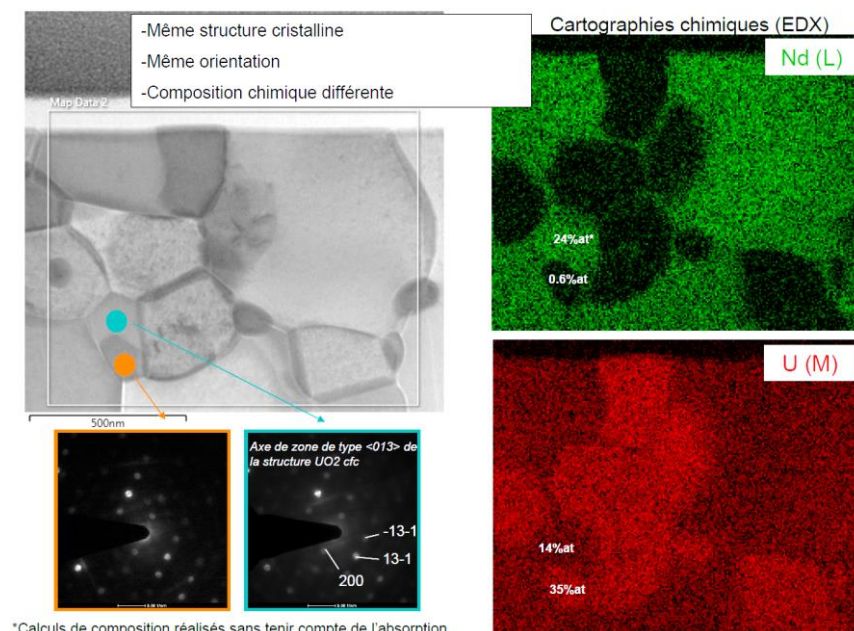


Figure 1: TEM characterization of an Nd doped UO_2 after 72 hours heat treatment at 1700°C under reducing atmosphere

Quantification of the Morphology and Roughness of Oxide Powder Particles In Relation to their Manufacturing History and Flow Properties

Christophe D'Angelo¹, Solène Bertolotto¹, Anne-Charlotte Robisson¹ and Christelle Duguay¹

¹CEA, DES, IRESNE, DEC, SA3E, LCU, Cadarache F-13108 Saint-Paul-Lez-Durance, France

In a nuclear fuel fabrication process, knowledge of flow properties is essential. Fuel production is based on successive powder metallurgy stages (grinding, sieving, stirring, pressing and sintering), which require good flowability. This good flowability minimizes retention phenomena during transport between the various operations and contributes to the manufacturer's productivity. In the literature, powders are the subject of studies aiming at establishing the link between their flow properties and their physical characteristics. The impact of parameters such as the size, density, morphology and texture of the particles making up the powder has been studied in various fields such as food processing [1] and pharmaceuticals [2]. Studies have also been carried out on actinide powders [3], but only the influence of particle size on flow properties has been quantitatively demonstrated.

In this work, we propose to establish a quantitative link between the morphology and roughness of oxide powder particles and their flow properties. To this end, model uranium dioxide powders have been fabricated to obtain a controlled particle size distribution and shape. A method has been developed to characterize particle morphology. This method is based on ImageJ's Shape Filter module [4] and analyzes the images resulting from the 2D projection of each aggregate. The morphological parameters used to characterize the powder are elongation, circularity and solidity. These images can be obtained by different ways: a morphogranulometer (using dry or liquid dispersion), a digital-optical microscope (using dry dispersion) or a scanning electron microscope (using resin-coated particles). Rheological properties are obtained using an FT4 powder rheometer: the powder undergoes different tests (permeability, compressibility, shear, etc.) to quantify its flowability. Finally, two optical methods are used to characterize roughness. The first one is based on the use of a gray-level co-occurrence matrix analyzing images of the particles making up the powder. The second method, derived from existing work [5], is based on a fractal analysis of the particle contour. Finally, we establish a link between these different properties.

[1] Fu, X., Huck, D., Makein, L., Armstrong, B., Willen, U., & Freeman, T. (2012). Effect of particle shape and size on flow properties of lactose powders. *Particology*, 10(2), 203–208.

<https://doi.org/10.1016/j.partic.2011.11.003>

[2] Kaialy, W., Alhalaweh, A., Velaga, S. P., & Nokhodchi, A. (2012). Influence of lactose carrier particle size on the aerosol performance of budesonide from a dry powder inhaler. *Powder Technology*, 227, 74–85. <https://doi.org/10.1016/j.powtec.2012.03.006>

[3] Madian, A., Leturia, M., Ablitzer, C., Matheron, P., Bernard-Granger, G., & Saleh, K. (2020). Impact of fine particles on the rheological properties of uranium dioxide powders. *Nuclear Engineering and Technology*, 52(8), 1714–1723. <https://doi.org/10.1016/j.net.2020.01.012>

[4] Wagner, T., & Lipinski, H.-G. (2013). IJBlob: An ImageJ Library for Connected Component Analysis and Shape Analysis. *Journal of Open Research Software*, 1(1), e6. <https://doi.org/10.5334/jors.ae>

[5] Guida, G., Viggiani, G. M. B., & Casini, F. (2020). Multi-scale morphological descriptors from the fractal analysis of particle contour. *Acta Geotechnica*, 15(5), 1067–1080. <https://doi.org/10.1007/s11440-019-00772-3>

Field Assisted Sintering of UO₂ Based Nuclear Fuels

R.W. Harrison¹, J. Morgan¹, J. Buckley¹, T. Abram¹, D. Pearmain², S. Bostanchi², C. Green², R. White²,
D. Goddard³, N. Barron⁴

¹ Nuclear Fuel Centre of Excellence, The University of Manchester, Manchester, M13 9PL, UK

² Lucideon Limited, Queens Road, Stoke-on-Trent, ST4 7LQ, UK

³ National Nuclear Laboratory, Springfields, Preston, PR4 0XJ, UK

⁴ National Nuclear Laboratory, Sellafield, Seascale, CA20 1PG, UK

Field assisted sintering (FAS) techniques such as spark plasma sintering (SPS) and flash sintering (FS) have received increasing attention for the manufacture of uranium-based nuclear fuels over the last decade. Conventionally, UO₂ is manufactured by cold uniaxial pressing followed by pressure-less sintering in a reductive atmosphere at hold temperatures of ~1700°C for 5–10 hours to achieve the required density, microstructure and stoichiometry. SPS and FS offer the possibility to dramatically decrease the sintering hold time and temperatures required to produce dense fuel pellets. The reduced sintering temperatures and times make these techniques of interest to UO₂ and mixed uranium-plutonium oxide (MOx) fuels for thermal and fast reactors. However, there are still challenges to address with both techniques to demonstrate controllability, repeatability and scale-up as well as understanding the effect of shorter hold times and sintering temperatures on the pellets microstructure when considered against the fuel specification, particularly plutonium distribution in the MOx fuel, which has consequences on fuel performance and reprocess-ability. To examine the effects of the shorter hold times and sintering temperature on the pellet microstructure and “Pu distribution” in MOx fuel we have manufactured UO₂ and (U_{0.93}Ce_{0.07})O₂ as a MOx fuel surrogate using FS, SPS and conventional sintering (CS) at the Nuclear Fuels Centre of Excellence (NFCE), chemical maps from SPS and CS Ce-MOx are shown in Figure 1 [1]. This has involved collaborative work with the National Nuclear Laboratory (NNL) and Lucideon Limited to develop, install and commission a bespoke uranium active FS furnace at the NFCE. The optimisation of this novel active FS system (shown in Figure 2 [2]) for UO₂ and Ce-MOX pellet manufacture. Alongside this, results of the effect of sintering technique/parameters on the pellet microstructures and chemical homogeneity from XRD, SEM-EDS and Raman microscopy characterisation will be presented with an outlook for exploiting the benefit of FAS techniques for the manufacture of uranium oxide bearing fuels to achieve the fuel specifications. Trials have been performed in the temperature range of 500–1300°C and pellet densities of >95% TD and grain sizes of ~ 5µm have been achieved for the optimised SPS and FS programmes which represents a up to ~50% reduction in both the sintering temperature and sintering cycle time compared to CS techniques.

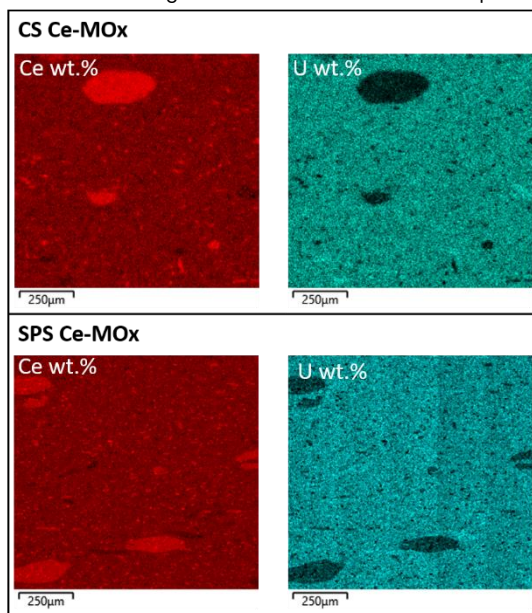


Figure 2. EDS maps of U and Ce in conventional sintered (CS) and spark plasma sintered (SPS) (U,Ce)O₂ samples

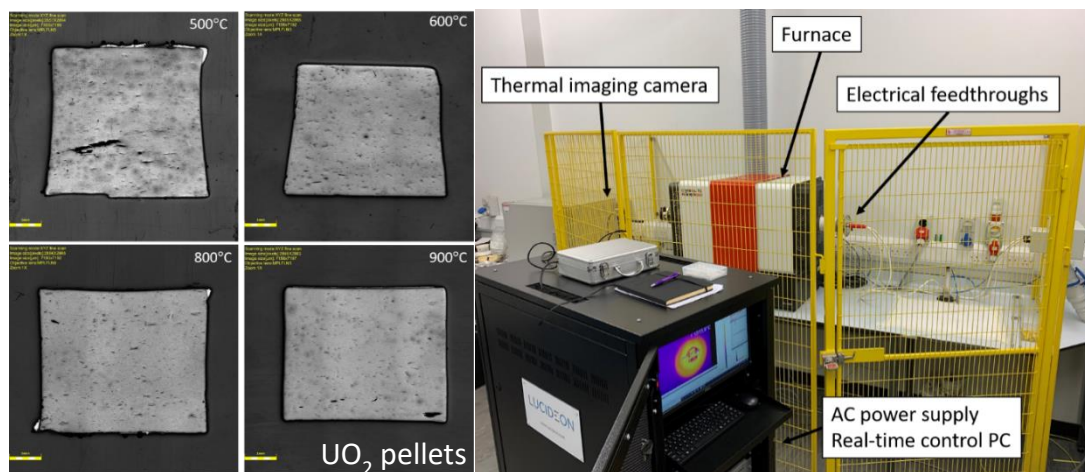


Figure 3. Left - UO_2 pellets manufactured by FS in range of 500–900°C furnace temperature and Right - uranium active flash sintering furnace at the University of Manchester

References;

- [1] R.W. Harrison, J. Morgan, J. Buckley, T. Abram, D.T. Goddard, N.J. Barron, Spark Plasma Sintering of $(\text{U,Ce})\text{O}_2$ as a MO_x Nuclear Fuel Surrogate, J. Nucl. Mater. (2021) 153302. doi:<https://doi.org/10.1016/j.jnucmat.2021.153302>.
- [2] R.W. Harrison, J. Morgan, J. Buckley, S. Bostanchi, C. Green, R. White, D. Pearmain, T. Abram, D.T. Goddard, N.J. Barron, Development and comparison of field assisted sintering techniques to densify CeO_2 ceramics, J. Eur. Ceram. Soc. 42 (2022) 6599–6607. doi:<https://doi.org/10.1016/j.jeurceramsoc.2022.06.079>.

Characterization of the Phases Formed During the High Temperature Oxidation of (U,Pu)O₂ Mixed Oxides

Priscilla Berenguer-Besnard^{a,b}, Philippe Martin^a, Loïc Marchetti^a, Loïc Favergeon^b

^a CEA, ISEC, DMRC, Univ Montpellier, Marcoule, France

^b Mines Saint-Etienne, Univ Lyon, CNRS, UMR 5307 LGF, Centre SPIN, F-42023 Saint-Etienne, France

priscilla.berenguer-besnard@cea.fr, Philippe-m.martin@cea.fr, Loic.marchetti@cea.fr, favergeon@emse.fr

Keywords: Oxidation, Uranium, Plutonium, Synchrotron, characterizations

Introduction

The widespread use of Mixed Oxide (MOX) fuel in Pressurized Water Reactor associated with a plutonium multi-recycling is an option currently studied in France. Such strategy has gained increasing attention as a way to stabilize the plutonium inventory. The dissolution of spent fuel in nitric acid is one of the main step of the nuclear fuel recycling. However, a decrease in (U,Pu)O₂ dissolution kinetics with the increase in Pu content is observed^{1,2}. An innovative process is currently being studied to enhance MOX reprocessing at industrial rates. This process consists of extracting the fuel from its cladding upstream the dissolution, in order to increase the fuel surface area in contact with concentrated nitric acid and thus facilitate its dissolution. Currently, the most promising solution involves high temperature oxidation of the MOX spent fuel, which induces phase transformations leading to the collapse of the ceramic into a more reactive powder.

As illustrated by figure 1, the microstructure of a MIMAS MOX fuel consists of three (U,Pu)O₂ “pseudo phases⁰”: U-rich agglomerates, Pu-rich agglomerates and a coating phase^{3–5}. Due to their different plutonium contents, these “pseudo phases” are expected to behave differently during oxidation. Therefore, the understanding of the mechanisms occurring during the oxidation of MOX fuel, implies first studying the oxidation of the different “pseudo phases” constituting its microstructure.

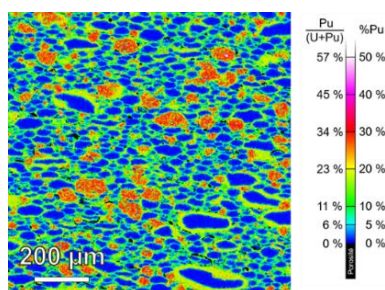


Fig. 1 Electron probe micro analysis (EPMA) mapping obtained on an unirradiated MIMAS MOX pellet with a Pu/(U+Pu) ratio of 9.6 wt.%.

Experimental approach

The aim of the present study is to investigate the oxidation behavior of model compounds simulating the “pseudo phases” present in the MIMAS MOX microstructure: UO₂, U_{0.89}Pu_{0.11}O₂ and U_{0.72}Pu_{0.28}O₂. To complete our understanding of the phenomena, a compound with a higher Pu content (U_{0.55}Pu_{0.45}O₂) is also being studied. Such an understanding requires the study of the effects of Pu content, temperature and pO₂ on the nature of the phases formed during high temperature oxidation, i.e. their crystallographic structure, the oxidation states and local environment of U and Pu in each phase. To achieve this goal, a multimodal and multi-scale approach is used, employing a wide range of characterization techniques: X-ray Diffraction (XRD, sample-scale), μ -Raman spectroscopy (μ m-scale), Scanning Electron Microscopy (SEM) and X-Ray absorption spectroscopy (HERFD-XANES and EXAFS).

⁰ Hereafter, the term “pseudo-phase” will be used to distinguish fractions of the material with different plutonium concentrations.

The oxidation experiments were carried out between 350 °C and 500 °C under controlled atmosphere (Ar-O₂ mixture containing 20 % to 80 % O₂). The starting and resulting materials were first characterized at the ATALANTE facility (CEA Marcoule). The X-ray Diffraction pattern of the U_{0.89}Pu_{0.11}O₂ starting sample shows only peaks belonging to a fluorite structure (*Fm* $\bar{3}$ *m* space group 225), with a lattice parameter of $a = (5.466 \pm 0.001) \text{ \AA}$ (Fig. 2-b). This pattern is compared with that of the U_{0.89}Pu_{0.11}O₂ sample oxidized for 3 hours at 500 °C in an Ar-80 % O₂ mixture. An increase in weight of about 3.7 % and the appearance of numerous supplementary diffraction peaks confirm the formation of over-oxidized phases (Fig. 2-a). These peaks are attributed to an orthorhombic (U,Pu)₃O₈ phase and a fluorite phase. For the latter, a decrease in the lattice parameter compared to the starting material is illustrated by a shift towards larger diffraction angles compared is observed. This could be caused either by an excess of oxygen (presence of (U,Pu)O_{2+x} or (U,Pu)₄O₉ phase) or by an increase in the Pu content in this phase.

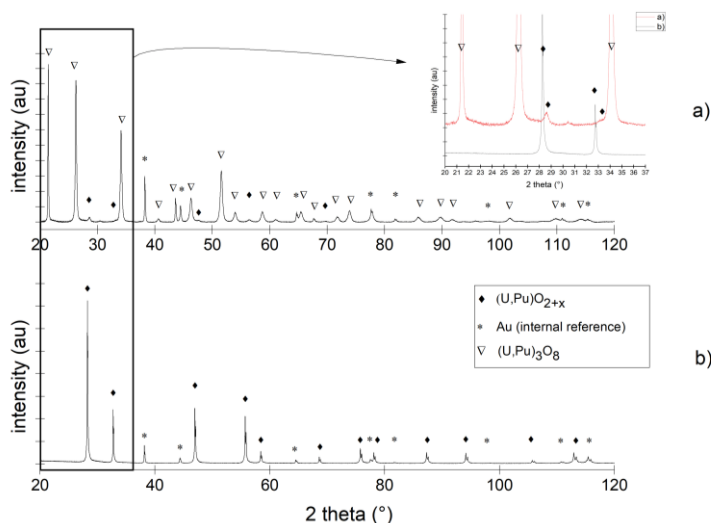


Fig. 2 XRD pattern of the U_{0.89}Pu_{0.11}O₂ sample oxidized at 500 °C under Ar-80 % O₂ mixture for 3 hours (a), compared to the U_{0.89}Pu_{0.11}O₂ starting sample (b). The star (*) identifies the peaks from the Au internal reference, the diamond (♦) identifies the peaks attributed to a fluorite type phase and the inverted triangle (▽) identifies the peaks attributed to the orthorhombic (U,Pu)₃O₈ structure.

However, considering the detection limit of laboratory XRD (a few percent), transmission synchrotron Powder X-Ray Diffraction (SPXRD) was performed in December 2023 to achieve a comprehensive identification of the oxidized phases formed. Thanks to a better signal to noise ratio, such measurements also provide information on the nature and the crystallographic structure of the minority phases formed during oxidation. Moreover, due to its ability to reveal information at the molecular level (local range order and oxidation states of each cation⁶), HERFD-XANES and EXAFS experiments at M_{4,5} and L_{2,3} edges of Pu and U are planned in March and April 2024. These analyses will be carried out at BM20-ROBL (ESRF, Grenoble, France) and MARS beamlines (SOLEIL, Saint-Aubin, France) thanks to their ability to accept highly radioactive samples..

Acknowledgements : The authors would like to thank Orano and EDF for their financial support.

References

1. D. Vollath, H. Wedemeyer, H. Elbel, E. Günther, *Nuclear Technology*. 71:1 (1985) 240-245.
2. Y. Ziouane, B. Arab-Chapelet, G. Leturcq, *Hydrometallurgy*. 198 (2020) 105504.
3. G. Oudinet, I. Munoz-Viallard, L. Afore, M.J. Gotta, J.M. Becker, G. Chiarelli, R. Castelli, *Journal of Nuclear Materials*. 375 (2008) 86-94.
4. Z. Talip, S. Peugeot, M. Magnin, M. Tribet, C. Valot, R. Vauchy, C. Jégou, *Journal of Nuclear Materials*. 499 (2018) 88-97.
5. O. Kahraman, F. Lebreton, P. Martin, M. Mermoux, *Journal of Applied Physics*. 132 (2022) 115106.
6. R. Caprani, P. Martin, D. Prieur, J. Martinez, M. O.J.Y. Hunault, F. Lebreton, M.M. Desagulier, C. Aloin, L. Picard, M. Alibert, G. Gabriel, P. Signoret, N. Clavier, *Journal of Nuclear Materials*. 585 (2023) 154607.

Fundamental Insights into Defect Generation and Transport Phenomena at Grain Boundaries in Nuclear Fuel

S. Finkeldei¹, J. Proctor¹, O. Lori¹, S. Dillon¹, J. White², Y. Wang², M. Cooper²,
D. Andersson²

¹University of California, Irvine, CA, United states; ²Los Alamos National Laboratory, NM, United States

Nuclear power provides the only broadly deployable source of stable, 24/7, carbon-free energy and currently supplies ~20% of electricity in the United States. Next-generation reactors such as small modular reactors, are expected to operate for longer time spans as well as under more extreme conditions regarding temperature and irradiation dose. The utilization of advanced fuels, such as doped UO₂ fuels is underway for the current reactor fleet, and highly likely to be implemented in advanced reactors. An in-depth understanding of how extreme conditions, e.g. radiation damage, effect the fuel properties will enable future mechanism-informed design of advanced nuclear fuel candidates.

Combined experimental and computational results about fission gas diffusion at grain boundaries in surrogate materials, UO₂ and doped UO₂ will be presented. The effect of irradiation and fission gas accumulation in doped-UO₂ is analyzed by *in-situ* electrochemical impedance spectroscopy during Xe and Kr implantation at LANL's Ion Beam Materials Laboratory with a strong emphasis towards understanding grain boundary responses/alterations. These results are compared to irradiation experiments of doped UO₂ fuel candidates at UCI's TRIGA reactor with subsequent microscopic analysis of irradiation effects on defects in these complex oxides. Finally, new mechanistic insights from experimental and computational studies on diffusional creep models in UO₂ and doped UO₂ will be presented.

Impact of Ru, Rh, Pd and Mo Metallic Particles on the Dissolution Kinetics of UO₂.

Kaczmarek T.¹, **Szenknect S.**¹, Le Goff X.¹, Podor R.¹, Dacheux N.¹

Institut de Chimie Séparative de Marcoule, Univ Montpellier, CEA, CNRS, ENSCM, (ICSM). Bagnols sur Cèze, France.

Although a spent nuclear fuel (SNF) is composed of about 96 wt. % of UO₂, its composition and microstructure display an extreme complexity due to the presence of more than 30 fission products (FP). Fission products found as metallic precipitates are mainly composed of noble metals Ru, Rh, Pd, Mo. The first step of the spent nuclear fuel reprocessing is the dissolution in a concentrated nitric acid solution. In this context, this work focuses on the impact of metallic FP on the kinetics of dissolution of the UO₂ matrix.

Model samples of UO₂ incorporating separately 3 mol. % of Ru, Rh, Pd or Mo were prepared using a wet chemistry route [1]. The obtained powders were sintered at high temperature under reducing atmosphere [2]. The speciation, morphology as well as the spatial distribution of the elements were determined in the sintered samples from Scanning Electron Microscopy (SEM) and Transmission Electron Microscopy (TEM) analyses. Then, the prepared samples were submitted to various dissolution tests in order to quantify the impact of the metallic particles on UO₂ dissolution rate. Dissolution experiments were carried out under dynamic conditions representative of the reprocessing of SNF (4 M HNO₃, 80°C). Additionally, specific dissolution experiments in static and less aggressive conditions (0.1 M HNO₃, 60°C) were designed to identify the mechanism involving each element of interest. The elemental concentrations in solution were determined by Inductively Coupled Plasma Optical Emission Spectroscopy or Mass Spectroscopy (ICP-OES or ICP-MS). HNO₂ concentration was measured in the dissolution medium using UV-vis spectrometry and the Griess method. The dissolution rate of UO₂ and metallic particles of FP were then determined for each model compounds. At microscopic scale, the evolution of the solid/liquid interface was monitored by Environmental-SEM.

The density of the prepared pellets was found similar. However, the introduction of metallic particles of FP influenced significantly the UO₂ grain size. The Ru, Rh, Pd and Mo particles were nanosized and evenly distributed at the surface of the pellets (**Figure 1-a**). Their average diameter was 10, 50 nm, 200 nm and 50 nm, respectively. The TEM-EDS analysis of the ultra-thin slides cut in the synthesised compounds confirmed the presence of particles inside the pellets, the metallic nature of the FP particles and the absence of these elements in the UO₂ matrix. The dissolution experiments (**Figure 1-b**) revealed that the presence of Ru, Rh or Pd metal particles increased the dissolution rate of UO₂ by a factor of 1.8 to 4.0 in 4 M HNO₃ at 80°C. The mechanism responsible for this effect does not drastically alter the rate of nitrous acid production, since the ratio of uranium and HNO₂ concentrations remains close to unity, as predicted by the balance equations for the autocatalytic dissolution of UO₂ in nitric acid [3]. On the other hand, the presence of Mo metallic particles decreased the dissolution rate of UO₂ by a factor of 1.3. The dissolution rates of platinum elements and molybdenum were also evaluated and can be classified according to the sequence: Rh < Ru << Mo < Pd. This difference in chemical durability results in a different final distribution of the FP between the solution and the dissolution residues.

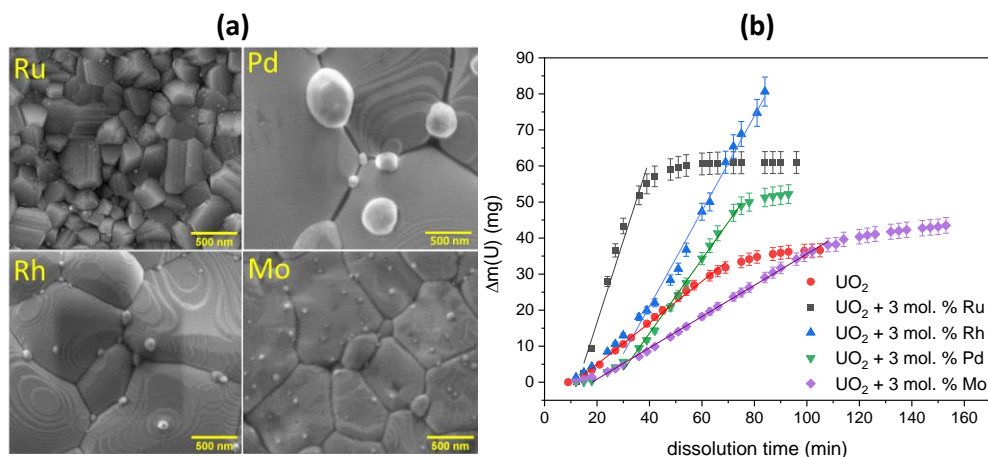


Figure 1: SEM micrographs (SE mode) of UO_2 pellets with 3 mol.% of metallic FP (a); evolution of U mass loss during dynamic dissolution of the pellets in 4 M HNO_3 solution at 80°C (b).

The results obtained under less aggressive conditions (0.1 M HNO_3 60°C), which do not lead to the production of HNO_2 and therefore do not allow the autocatalytic dissolution of UO_2 to take place, showed an even more differentiated effect of metallic particles. Indeed, under these conditions, the presence of Ru^0 and Rh^0 led to an increase in the dissolution rate of UO_2 by a factor of 870 and 140, respectively. The presence of Pd^0 had no effect on the dissolution rate of UO_2 , while the presence of Mo^0 led to a decrease in the rate by a factor of 3. Thanks to the complete set of specific experiments with Ru, we were able to propose a mechanism to explain the impact of the metallic fission product on the dissolution rate of UO_2 [4]. Especially, the catalytic activity of the Ru^0 particles was demonstrated without dissolution of Ru^0 particles and without production of HNO_2 , provided that a solid/solid interface exists between UO_2 and Ru^0 particles. The key phenomenon that supports the catalytic impact of Ru^0 particles is connected to the oxidation of Ru^0 into $\text{Ru}(\text{II})$ entities by nitrate ions and the concomitant reduction of $\text{Ru}(\text{II})$ into Ru^0 at the particle/ UO_2 interface, which leads ultimately to the formation of $\text{U}(\text{VI})$. $\text{U}(\text{VI})$ surface entities are further solubilized as UO_2^{2+} species at the UO_2 /solution interface. The electronic transfer from the solution to UO_2 is promoted by the high electric conductivity of the metallic particles, by their nanometric dimension and by the intimate contact with UO_2 . The monitoring of the pellet interface by ESEM showed that this phenomenon could be further amplified by the increase of the surface covered by Ru^0 nanoparticles during dissolution. This mechanism is also supported by the results obtained with the others metallic FP. Indeed, a strong catalytic effect of Rh^0 was also observed and the same kind of mechanism is made possible thanks to the values of the standard potential of the $\text{Rh}(\text{II})/\text{Rh}^0$ or $\text{Rh}(\text{III})/\text{Rh}^0$ couple. However, the oxidation of Pd^0 by nitrate ions is impossible, thus the formation of $\text{Pd}(\text{II})$ at the particle/ UO_2 interface and the subsequent oxidation of $\text{U}(\text{IV})$ by $\text{Pd}(\text{II})$ cannot occurred, which explains that the Pd had virtually no effect on the UO_2 dissolution rate and was not dissolved itself in 0.1 M HNO_3 solution. Finally, the redox potentials of Mo couples are all lower than the $\text{U}(\text{IV})/\text{U}(\text{VI})$ couples. Thus, Mo^0 acts as a competitor to $\text{U}(\text{IV})$ oxidation by nitrates. The oxidation of Mo^0 by nitrate ions explains also the high dissolution rate of Mo in 0.1 M HNO_3 . In addition, reduction of $\text{U}(\text{VI})$ by Mo^0 is also thermodynamically possible and all these reactions can contribute to slow the UO_2 dissolution kinetics.

- [1] T. Kaczmarek, Impact des éléments platinoïdes et du molybdène dans les mécanismes de dissolution du dioxyde d'uranium, in, Université de Montpellier, 2022.
- [2] T. Cordara, S. Bertolotto, L. Claparede, S. Szenknect, A. Mesbah, R. Podor, C. Lavalette, N. Dacheux, Impact of platinum group metals (Ru, Pd, Rh) on the dissolution of UO_2 , *J. Nucl. Mater.*, 528 (2020) 151836.
- [3] F. Charlier, D. Canion, A. Gravinese, A. Magnaldo, S. Lalleman, G. Borda, É. Schaer, Formalization of the kinetics for autocatalytic dissolutions. Focus on the dissolution of uranium dioxide in nitric medium, *EPJ Nuclear Sci. Technol.*, 3 (2017) 26.
- [4] T. Kaczmarek, S. Szenknect, L. Claparede, M. Cabie, X. Le Goff, A. Mesbah, R. Podor, N. Dacheux, Impact of ruthenium metallic particles on the dissolution of UO_2 in nitric acid, *Npj Mater. Degrad.*, 6 (2022).

Thermal Oxidation and High Temperature Structures of Uranium Carbide: in situ X-Ray Diffraction Studies

Emma C. Kindall, Natalie S. Yaw, Juejing Liu, Malin C. Wilkins, Sam Karcher, Hongwu Xu, Arjen van Veelen, Josh T. White, John McCloy, Xiaofeng Guo
Washington State University, Pullman WA 99164 US; Los Alamos National Laboratory, Los Alamos NM 87545 US

Uranium carbide shares a number of characteristics with industry standard uranium oxide, that make both ceramics well-suited to nuclear fuel applications, including high melting points and high tolerance to irradiation. In addition to this, uranium carbide, along with other non-oxide ceramic fuel candidates, has a higher thermal conductivity and higher fissile density than conventional uranium oxide fuels making them a strong candidate for advanced fuel candidates in emerging Generation IV advanced reactors like very high temperature gas reactors and fast spectrum reactors [1]. Despite the potential advantages carbide fuels possess, their high susceptibility to oxidation is a large hurdle to their practical implementation in the nuclear energy industry. Furthermore, a fundamental understanding of the crystal chemistry and thermodynamic properties of uranium carbide is critical for predicting its behavior under reactor or extreme conditions. More work investigating high temperature structural characteristics and oxidation behaviors of uranium carbide fuels is necessary to continue assessing the viability of this potential fuel.

In this work, uranium monocarbide (UC) was characterized with in situ high temperature synchrotron x-ray diffraction under low and 0.21 atm oxygen partial pressure conditions (labeled as sealed and open-air), with temperatures up to 689 °C and 500 °C respectively. Rietveld refinements were performed using General Structure Analysis System software version II (GSAS-II) to determine unit cell and phase compositions, summarized in figure 1. In the sealed experiments, UC was isolated from oxidizing atmospheric conditions, but even still a small oxygen concentration was present in the sample cell, accounting for the UO_2 growth. An appreciable amount of unoxidized carbide was maintained throughout the course of the experiment enabling continued analysis of its structural parameters. With the progressing partial oxidation, we were able to determine the temperature dependent thermal expansion function for UC from room temperature to 689 °C, with the mean coefficient of thermal expansion at ~689 °C was found to be $11.5 \times 10^{-6} \text{ } ^\circ\text{C}^{-1}$, in good agreement with previously reported values [2-4]. Of interest to note, is the presence of tetragonal $14/\text{mmm } \alpha\text{-UC}_2$ at higher temperatures as seen in figure 1b. The $\alpha\text{-UC}_2$ can be identified by its strong (1 0 1) and (0 0 2) reflections which can be seen in figure 2 around $2\theta \approx 3.42$. Thermodynamically the $\alpha\text{-UC}_2$ phase is not favored to form at this temperature but may be stabilized under similar conditions with low partial pressure of oxygen and/or CO. Computational

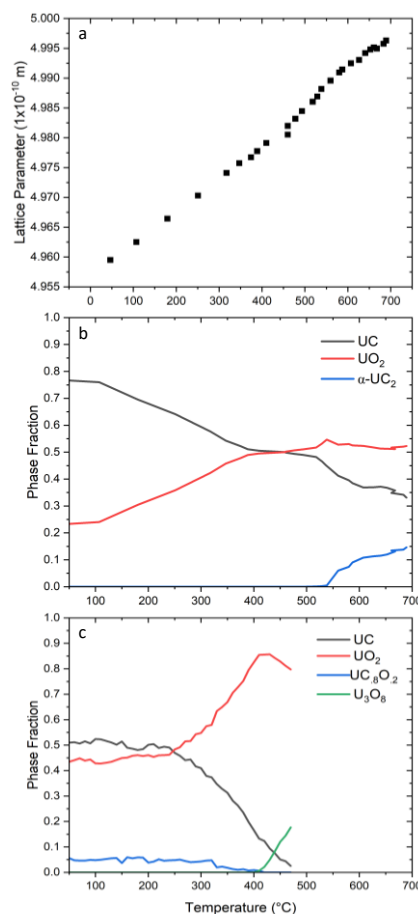


Figure 1. unit cell lattice parameter (a) and phase composition (b) from sealed experiments and phase composition from open-air experiments (c).

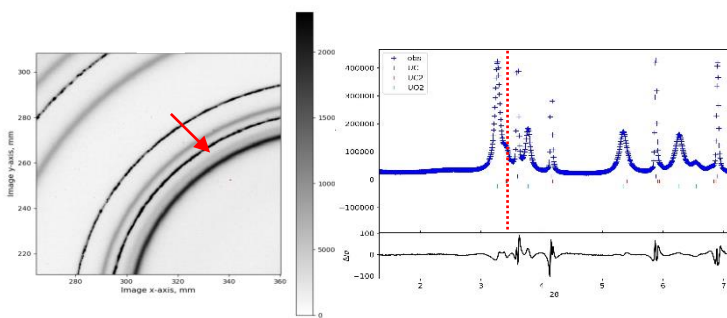


Figure 2. UC 2D powder image and pattern from sealed experiments at 689°C with diffraction around $2\theta = 3.42$, showing presence of $\alpha\text{-UC}_2$

figure 3, shows UC thermal oxidation as a step-wise process [7], the first step of which involves UC oxidizing to composite phases with mas equivalent to UO_3 , evolving gas such as CO_2 . The phase compositions obtained by reitveld refinement from both sealed and open-air experiments indicates the formation of UO_2 as the main intermediate oxide phases (rather than UO_3) with secondary phases such as UC_2 or $\text{UC}_x\text{O}_{1-x}$, followed by the final oxidation to U_3O_8 . This information necessitates the reevaluation of subsequent in situ X-ray diffraction data. This work will provide important insights into the thermal oxidation and other high temperature behaviors of uranium carbide ceramic fuels.

work has theorized the stabilization of this phase with dissolved oxygen substituting into the lattice, forming $\text{UC}_{2-x}\text{O}_x$ rather than pristine UC_2 [5,6]. More detailed thermodynamic studies are needed to correctly predict UC_2 /possible $\text{UC}_{2-x}\text{O}_x$ formation, accounting for it in the U-C-O phase diagram.

The in situ high temperature open-air experiment provides valuable insights into the thermal oxidation of UC. Previous work involving thermogravimetric analysis coupled with differential scanning calorimetry and mass spectrometry (TGA-DSC-MS), shown in

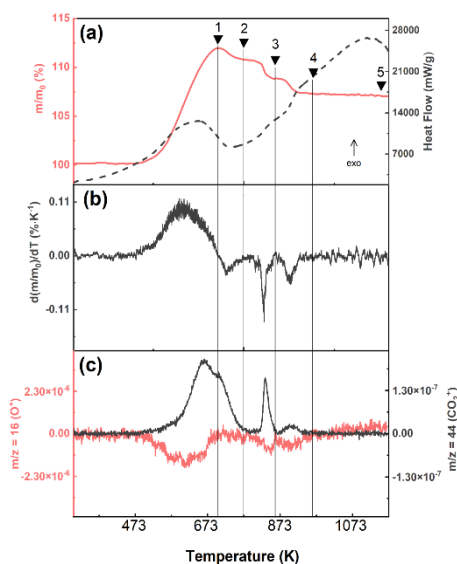


Figure 3. TGA-DSC (a), mass loss derivative (b), and MS ion current signal curves (c) from previous work [7].

References

- [1] Vasudevamurthy, G.; Nelson, A. T. *J. Nucl. Mater.* **2022**, 558, 153145.
- [2] Crane, J. *et al.* The Development of Uranium Carbide as a Nuclear Fuel. Third Annual Report. United States, **1963**.
- [3] Mendez-Penalosa, R; Taylor, R.E. *J. Am. Ceram. Soc.* **1964**, 47 (2), 101-102.
- [4] Richards, H. K. *Nucl. Technol.* **1971**, 10, 54-61.
- [5] Besmann, T. M.; Lindemer, T. B. *J Chem. Thermodyn.* **1982**, 14, 419-424.
- [6] Cheik Njifon, I; Torres, E. *J Nucl. Mater.* **2021**, 553, 153046.
- [7] Goncharov, V. *et al.* *J. Nucl. Mater.* **2022**, 569, 153904.

WASTE CONDITIONING AND GEOLOGICAL REPOSITORY

REGAIN project – Recycling of Zirconium from Nuclear Hulls

Mathilde Guilpain, Isabelle Hablot, Bertrand Morel

Orano – Prisme, 125 Avenue de Paris 92320 CHATILLON

The cladding material of the nuclear fuel is composed of a high-tech zirconium-based alloy, which has undergone extensive purification into hafnium and a succession of metallurgical steps.

During spent nuclear fuel processing operations, irradiated fuel assemblies are sheared into sections called hulls, separated from the fuel by a dissolution step, rinsed and then compacted and packaged into CSD-C (French acronym for Standard Container of Compacted Waste) (Fig. 1). They are currently considered as Intermediate Level Waste Long Life (ILW-LL) in the French waste classification and will be stored in the CIGEO French geological disposal.

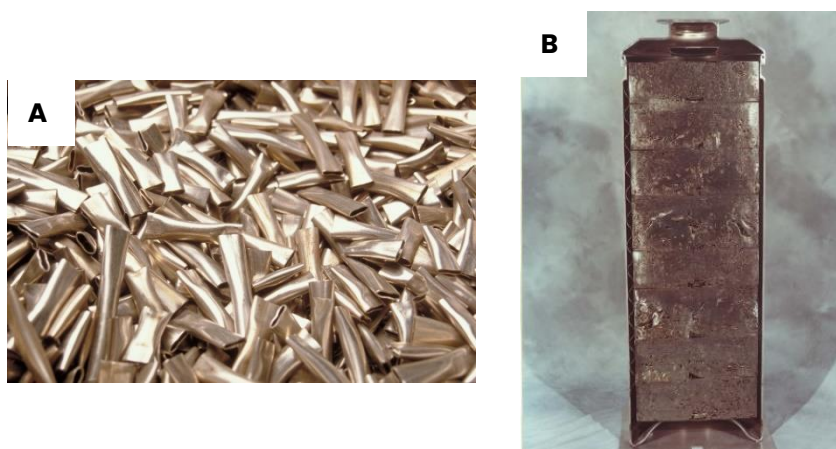


Fig. 1: Picture of A) hulls and B) hulls compacted into CSD-C

The REGAIN project (French acronym for recycling of nuclear hulls) proposes the study of an alternative solution to the process resulting from hull compaction. This solution is based on an innovative and completely disruptive approach, consisting in reducing the radiological source term of the hulls through successive decontamination operations to recover the Zr. Regarding the performance of the developed process, possibility to create a nuclear cycle will be evaluated. Otherwise, the expected results of the project will make possible to define the treatment and conditioning of the hulls with a view to sub-surface even surface storage. In both cases, the volume of final waste to be sent to CIGEO will be limited.

To this end, several innovative technological bricks, of different initial maturity, will be studied and developed. The bricks leading to the highest decontamination performance will be combined into a unique decontamination process. Process studies will be conducted at the laboratory level in inactivity (on non-radioactive simulants), then at the prototype scale in inactivity. For bricks of the highest initial maturity, studies can be continued in an active laboratory to determine decontamination factors from actual spent fuel rod samples.

The first technological bricks considered will concern the decontamination of the hulls with actinides and fission products and the following ones will focus on the purification of zirconium by removing the structural activation products present in the cladding material following its stay in the reactor (Fig. 2). The need to combine or not the two steps to achieve the targeted decontamination factor will also be examined during the project. The technological bricks relating to these two stages of decontamination will be studied in parallel. These studies will make it possible to conclude, depending on the decontamination factors obtained, about the technical possibilities of directing the flow of hulls towards a recycling route, or towards a storage other than CIGEO's Intermediate Level Waste Long Life (ILW-LL) storage. Technical and economic evaluations of each of the industrial-scale bricks, as well as the overall process, will make possible to position the economic

feasibility of a recycling sector for cladding materials optimizing the volume of ILW-LL produced as well as the consumption of mining resources. This study will be accompanied by a life cycle assessment. The aim of this study will be to compare the overall environmental impact of the developed sector with the current production of cladding materials and cladding management after irradiation, *i.e.* from zirconium extraction to deep geological disposal. Finally, technical and economic analyses combined with a social impact analysis will make it possible to assess the economic benefits involved in the development of this new sector on an industrial scale. The REGAIN project consists of a feasibility study to optimize the sector and a business plan can be defined by the industrialists of the consortium at the end of the project studies.

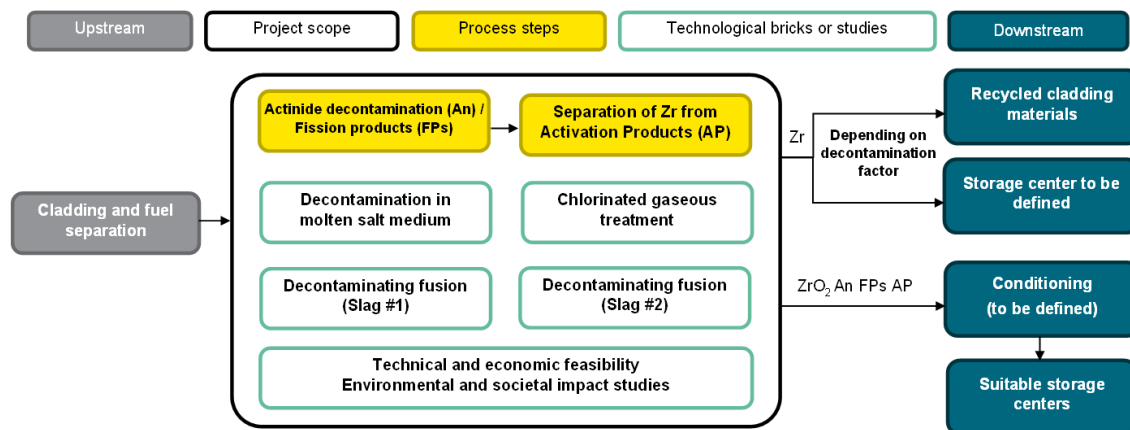


Fig. 2: REGAIN project scope scheme

The upstream (fuel processing) and downstream (cladding manufacturing) stages of the project have been industrial realities for several decades. The recycled zirconium produced by the process and workshop studied in this project would therefore fit into a mature industrial scheme with an existing market. The economic and industrial interest of the project is based on its dual stakes:

The reduction in the volume of Intermediate Level Waste Long Life to be sent to CIGEO limits the cost of storage, and CIGEO's footprint.

The valorization in the nuclear industry of metallic zirconium from the cladding material, which would no longer contain hafnium.

This project is funded by the French government as part as France 2030. Given the technological blocks that will be developed and the objective of the studies, the REGAIN project consortium was logically built around the main industrial players in the French nuclear industry (Framatome and Orano) and leading research organizations in the field of energy (CEA and CNRS).

Successful Lasergrammetry Operation in an ATALANTE Hot Cell: First Step for Deploying Digital Technologies on Hot Cells In Operation

Caroline Chabal ^{(1)*}, Michaël Gauthier ⁽¹⁾, Julien Delrieu ⁽¹⁾, Thibaud Durand ⁽¹⁾, Christian Père ^{(2)**}

⁽¹⁾ French Alternative Energies and Atomic Energy Commission (CEA), DES, ISEC, DPME, Univ. Montpellier, Marcoule – France, ⁽²⁾ GAMBI-M, 30200 Bagnols sur Cèze, France

*corresponding author: caroline.chabal@cea.fr - **corresponding author: christian.pere@gambi-m.com

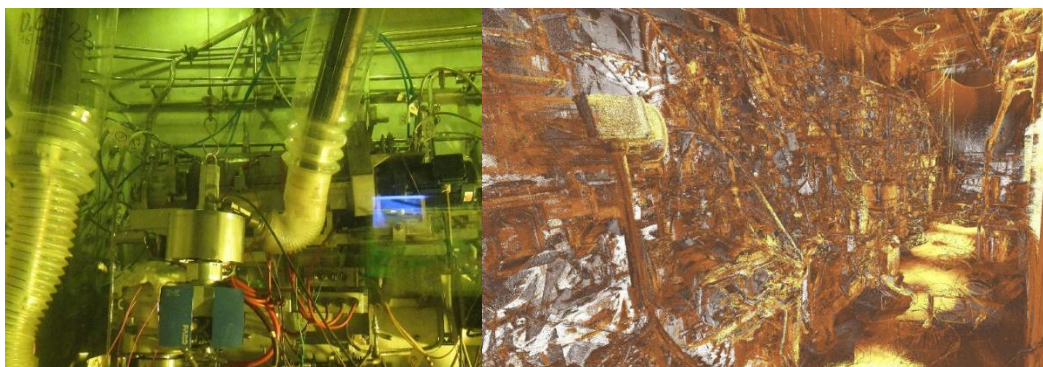
The SOSIE project, co-funded by the Occitanie region, is a research project between the CEA and GAMBI-M. Starting in June 2022 and lasting 2 years, it aims at developing digital twins of two CEA calcination-vitrification processes, including VESPA process at the ATALANTE facility. To achieve this, an initial laser survey is required to reconstruct a 3D model of the interior of the hot cell. Based on this 3D model, a visual, augmented and intelligent digital twin will be implemented, including Virtual Reality, Augmented Reality and Machine Learning technologies. The ultimate aim is to provide tools to assist the management of these complex processes, based on digital technologies.

The laser scanning operation was carried out in June 2023 in the ATALANTE facility. It consisted in introducing a laser scanner into the cell to obtain a point cloud and panoramic photos. The scanner, suspended from the bridge crane, carried out around twenty stations, during which it was held by a remote master-slave manipulator to improve the device's stability.

The use of scanners in hot cells is still little developed, due to the technical constraints to be met in cells of this type. The technical solution implemented is the result of close collaboration between various CEA teams and the Gambi-M company, and requires adaptations of the scanner to allow wired communication, via a PLC box and a wired power supply for the scanner. This operation generated point clouds of adequate quality.

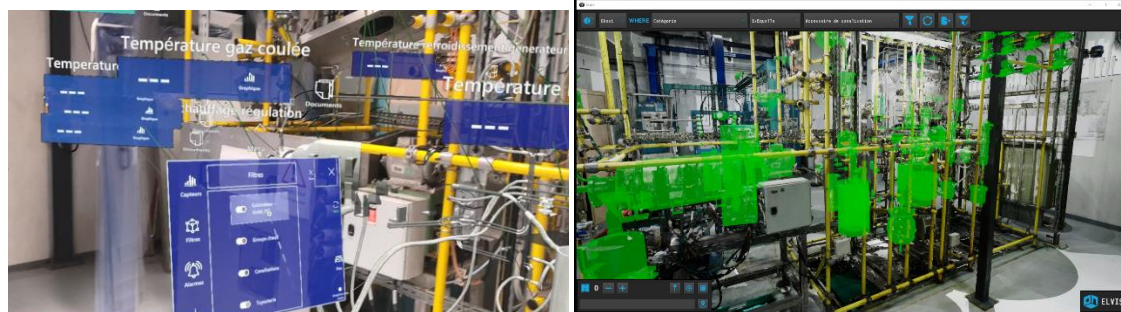
From the point cloud obtained, a 3D model of the cell is being reconstructed, from which the digital twins will be developed.

The proven technical solution has been qualified and can be reused for further investigations on ATALANTE, or elsewhere.



Implementation of the scanner in the cell (left) and point cloud from the VESPA process (right)

Based on the 3D model generated, developments are underway to create virtual and augmented reality applications to provide assistance to operators in charge of process operation: whether for maintenance assistance, process control assistance, training or communication tools, proofs of concept have been developed to demonstrate the benefits of using digital technologies for such complex processes. Initial results are already available on a first calcination-vitrification process and will be deployed on the hot cell very soon.



First results on implementation of mixed reality applications

Effects of Radiolysis Products and Acidic Media on the Aggregation Behaviour of Nuclear Fuel Debris Nanoparticle Simulants via Stochastic Simulations

Miguel Pineda¹, Cong Chao¹, Yiwei Zhang^{1,2}, Takehiko Tsukahara², Panagiota Angeli¹,
Eric S. Fraga¹

¹ThAMes Multiphase and Sargent CPSE, Department of Chemical Engineering, University College London, WC1E 7JE, London, UK; ²Laboratory for Zero-Carbon Energy, Institute of Innovative Research, Tokyo Institute of Technology, 2-12-1-NI-6, Ookayama, Meguro, Tokyo 152-8550, Japan.

One of the most important challenges for decommissioning the damaged reactors of the Fukushima-Daiichi Nuclear Power Plant is the safe retrieval and storage management of the fuel debris. This challenge involves understanding the behaviour of the debris while it is being processed. As a result of manipulation, bulk-scale debris fragments and various types and sizes of nanoscale particles are produced. Because of nanoscale effects, these nanoparticles could behave differently than their macroscopic counterparts. This potential difference in behaviour must be understood to manage fuel debris retrieval and storage properly. Particularly, elucidating the impact of water radiolysis products and acidic media on these nanoparticles' dissolution, denaturalisation, and aggregation/agglomeration behaviour in aqueous solutions is of relevance because these fuel debris are typically subjected to contact with water, ionising radiation, and acidic conditions.

In this work, we investigated computationally the effects of water radiolysis products (e.g., H₂O₂) and acidic media (e.g., HNO₃) on the aggregation kinetics of metal oxide nanoparticles analogous to nanoscale particles generated by fuel debris retrieval (e.g., CeO₂ and ZrO₂ nanoparticles) in aqueous solution. Our computational approach is based on a dynamic version of the so-called Monte Carlo (MC) simulation approach in conjunction with the classical and extended versions of the Derjaguin-Landau-Verwey-Overbeek (DLVO) theory for nanoparticle aggregation in suspensions and Brownian diffusion. In comparison with other simulation methods of particle aggregation (e.g., Molecular dynamics or Brownian dynamics), the DLVO-MC approach allows us to treat the simulation domains as statistical particle ensembles where each interaction event has a probability of occurrence quantified via transition rates (or frequency functions) calculated based on particle-particle interaction energetics. The time evolution of the aggregation diameter (AD) and its corresponding particle size distribution (PSD), which can be directly compared to dynamic light scattering experiments, are the main outcomes of our computational approach. We focused on nanoparticle aggregation kinetics under batch conditions but also continuous ones in microfluidic channels. Apart from the calculation of the AD and PSD for several case studies, a series of sensitivity analyses were carried out to illustrate the influence of various model parameters (e.g., pH, primary nanoparticle diameter, concentrations of water radiolysis products and acidic media, temperature) on aggregation kinetics. Our simulation results suggest that our computational approach has the potential to become an analysis tool for predicting the aggregation behaviour of nanoparticles generated from nuclear fuel retrieval under aqueous conditions.

Insights into Glass Alteration Mechanisms from the Study of Long Term Burial Experiments

Clare L. Thorpe, Garry Manifold, Rachel Crawford and Russell J. Hand

Department of Materials Science and Engineering, University of Sheffield, Sheffield, S10 2TN, UK.

Glass dissolution mechanisms have been well described as far as they relate to nuclear waste type silicate or borosilicate glass exposed to simple solutions. Successive stages of glass alteration are understood to progress from initial ion exchange, inter-diffusion and network hydrolysis, to the formation of secondary alteration phases leading to a rate drop and either a long-term reduction in glass alteration or eventual rate resumption. Understanding how these interrelated processes are affected by glass composition has allowed predictive models to estimate alteration rates within certain limitations. With countries now engaged in site selection for near surface or deep geological disposal facilities for vitrified waste, there is increased interest in understanding glass alteration in more complex systems.

Recent studies of glass alteration in dynamic, open, natural environments highlight the role that external elements, sourced from groundwater and surrounding mineralogy, play in secondary phase formation. In particular, multiple studies show that externally sourced elements are sequestered and have significant effect on alteration layer chemistry. The distribution of these elements within glasses (altered for between 20 and 220 years) offers insight into the processes by which alteration layers grow and evolve over time. Additionally, it has been evidenced that microorganisms can affect glass alteration indirectly by controlling the local chemical environment, particularly the speciation of Fe and the availability of P. Results of these unique field experiments expand on the currently accepted model for silicate/borosilicate glass alteration and pose questions for further research.

Impact of Lanthanide and PGM Elements on the Chemical Durability and Surface Modifications during the Leaching Tests of FP Doped Pellets Mimicking Interim Repository

P.H. Imbert, L. Claparede, S. Szenknect, **N. Dacheux**

ICSM, Univ Montpellier, CNRS, CEA, ENSCM, Site de Marcoule, Bagnols-sur-Cèze, France

Managed by ANDRA, the European collaborative research program EURAD aims to federate research efforts and to share scientific and technical knowledge in the field on the long-term management of radioactive waste. In this context, ICSM is interested in studying the chemical durability of spent nuclear fuels under interim storage conditions (mimicking their stay in cooling pool). Due to the complex structure and microstructure of spent nuclear fuels, the global understanding of their behavior when leaching is very difficult to analyze, although it appears as a very important task. In this study, the role of two fission products families: lanthanide elements dissolved in the structure of UO_2 , on the one hand, and PGM elements (Ru, Rh, Pd) forming separated metallic inclusions [1,2], on the other hand, has been particularly examined.

As part of the experiments carried out in this work, several types of sintered materials representative of used fuels were prepared by wet chemistry route (hydroxide precipitation [3]) and then sintered at high temperature. The results showed that the lanthanide ions (Nd, Ce, La, Pr and Y) were incorporated quantitatively into the fluorine structure, leading to a slight decrease in the lattice parameter. On the other hand, the platinum elements (Ru, Rh, Pd) and molybdenum were not incorporated in the structure. They formed metallic alloys inclusions that have been clearly revealed by X-EDS analysis. Using this method, dense samples with densification rates of between 89 and 97% of the calculated density were obtained. The developed surface areas, determined by image analysis (SESAM method) were between 2×10^{-2} and $10^{-1} \text{ m}^2 \cdot \text{g}^{-1}$. They were ≈ 100 times greater than the geometric surface area of the pellets (i.e. $3 \times 10^{-4} \text{ m}^2 \cdot \text{g}^{-1}$).

A dual approach combining microscopic and macroscopic analyses was thus developed to study the long-term behavior of the prepared pellets. At the macroscopic scale, various leaching tests were developed on all the prepared pellets in conditions mimicking an interim storage, i.e. in distilled water, in a solution containing boric acid (2500 ppm, i.e. $2.3 \times 10^{-4} \text{ mol L}^{-1} \text{ H}_3\text{BO}_3$, pH = 5) and in a solution containing boric acid and lithin ($2.3 \times 10^{-4} \text{ mol L}^{-1} \text{ H}_3\text{BO}_3$, LiOH, pH = 7). Two temperatures (50 °C and 70 °C) were considered.

Leaching tests performed on UO_2 and $(\text{U,Ln})\text{O}_2$ at pH = 7 revealed the existence of a slope break when plotting the evolution of the normalized leaching $N_i(\text{U})$. The normalized dissolution rates decreased by a factor of 3 for UO_2 after 100 days. This break appeared earlier for $(\text{U,Ln})\text{O}_2$ (i.e. for $t > 60$ days) and was stronger (decrease by a factor of 12 to 30), leading to very low normalized dissolution rates (typically in the range of $5\text{--}8 \times 10^{-6} \text{ g} \cdot \text{m}^{-2} \cdot \text{d}^{-1}$). This suggests a beneficial impact of Ln elements on the chemical durability of the prepared ceramics. No slope break was observed for UO_2 :PGM ceramics until 250 days, after which a plateau suggested the formation of neoformed phase. Due to the catalytic properties of PGM elements, enhancing oxidation of U (IV) to U (VI), a much higher concentration of U at saturation was obtained compared to that obtained in the case of $(\text{U,Ln})\text{O}_2$ solid solutions.

Leaching tests of $(\text{U,Ln})\text{O}_2$ and UO_2 :PGM sintered pellets, at pH = 7, revealed the formation of neoformed phases, that was confirmed by operando monitoring of the solid/solution interface by ESEM. For $(\text{U,Ln})\text{O}_2$ solid solutions (with 6 mol % Ln) leached at 50°C and pH = 7, small nodules (less than a few tens of nanometres in size) were formed. Due to the too small size of these nodules, their identification remained impossible even after 450 days of leaching. Conversely, operando monitoring by ESEM during leaching of UO_2 :PGM samples at 50 °C and pH = 7 revealed the formation of platelets type crystals onto the surface of the leached material (Figure 1). These crystals covered the entire surface of the sample after 550 days of leaching. The characterization of these crystals was performed with the help of XRD, ESEM and Raman spectroscopy. XRD analysis suggested the formation of Li-compreignacite $\text{Li}_2[(\text{UO}_2)_6\text{O}_4(\text{OH})_6] \cdot 8\text{H}_2\text{O}$ (Figure 2). All the bands associated to compreignacite were observed by Raman spectroscopy, especially that corresponding to the $\nu_3(\text{U-O})$ vibration (830 cm^{-1}), characteristic of the uranyl group. From the correlation proposed by Bartlett *et al.* [4], the $\text{d}(\text{U-O})$

distance was evaluated to 1.7808 Å, which appeared in good agreement with the value associated to the becquerelite's family structure.

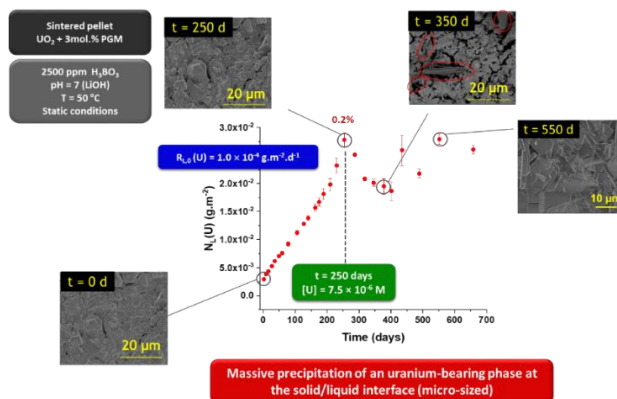


Figure 1 : Operando monitoring of the evolving surface of $\text{UO}_2\text{:PGM}$ obtained at 50°C, at pH =7, in the presence of H_3BO_3 and LiOH

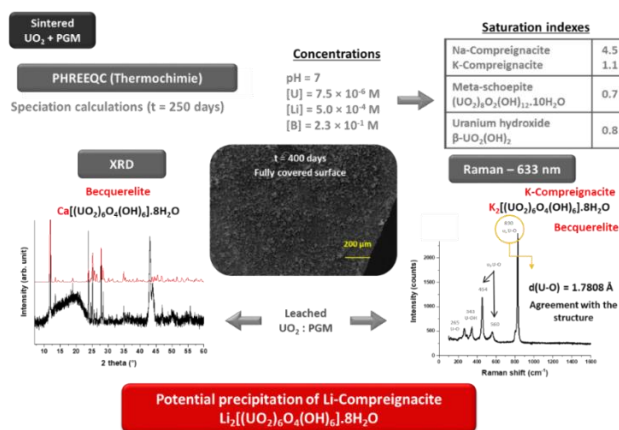


Figure 2 : Characterization of the neoformed phase obtained during leaching tests of $\text{UO}_2\text{:PGM}$ obtained at 50°C, at pH =7, in the presence of H_3BO_3 and LiOH ($t > 400$ days)

Leaching these samples at pH = 5 revealed the formation of meta-schoepite $(\text{UO}_2)_6\text{O}_4(\text{OH})_6 \cdot 10\text{H}_2\text{O}$ or U hydroxide $\beta\text{-UO}_2(\text{OH})_2$. Raman spectrum obtained after leaching confirmed this point with the existence of a strong doublet near to 860 cm^{-1} , characteristic of the uranyl group in the meta-schoepite structure. The crystal neoformed at the surface of the samples appeared bigger than that observed for Li-compreignacite. Speciation calculations showed that both systems were oversaturated related to Compreignacite (saturation index of 4.5 considering the solubility constant of Na-Compreignacite, no data being available for Li-Compreignacite) on the one hand, and to meta-schoepite (saturation index of 0.6 to 0.7), on the other hand. This confirmed the existence of saturation conditions in the obtained leachates.

Dissolution tests are currently being extended to increase the quantity of neoformed phase for the several systems or to grow the crystals for others. Finally, once they have been produced as pure phases, the solubility products of Li-compreignacite and meta-schoepite will be evaluated based on concentrations obtained under saturation conditions.

- [1] T. Cordara et al., *Hydrometallurgy*, 188 (2019) 182-193.
- [2] T. Kaczmarek et al., *npj Materials Degradation*, 6 (2022) 39.
- [3] J. Martinez et al., *Journal of Nuclear Materials*, 462 (2015) 173-181.
- [4] J. R. Bartlett, R. P. Cooney, *Journal of Molecular Structure*, 193 (1989) 295-300.

The Impact of Hot Isostatic Pressing on U Speciation and Local Coordination in Simulant Pu Ceramic Wasteforms

Aidan Friskney¹, Ewan R. Maddrell², Claire L. Corkhill³ and Lewis R. Blackburn¹

¹Immobilisation Science Laboratory, Department of Materials Science and Engineering, University of Sheffield, Mappin Street, S1 3JD, UK

²National Nuclear Laboratory, Workington, CA14 3YQ

³School of Earth Sciences, The University of Bristol, Bristol, BS8 1RJ

The United Kingdom currently holds the world's largest civil inventory of plutonium, with 113 tHM equivalent PuO₂ currently in storage as a result of continued reprocessing operations.^[1] It is accepted that at least some portion of this inventory may be designated for immobilisation in a suitable wasteform prior to permanent disposition within a geological disposal facility (GDF). Zirconolite-structured ceramics (CaZrTi₂O₇) processed via hot isostatic pressing (HIP) are candidate wasteform materials for the disposition of separated UK plutonium, evaluated on the basis of high aqueous durability and radiation stability. Previous work has demonstrated the potential for Pu accommodation alongside neutron absorbing and charge modifying additives. Pu³⁺ and Pu⁴⁺ can be feasibly accommodated between either Ca²⁺ and/or Zr⁴⁺ sites depending on the targeted substitution regime, permitting a waste loading up to ~ 20 wt. % Pu.^{[2]–[4]}

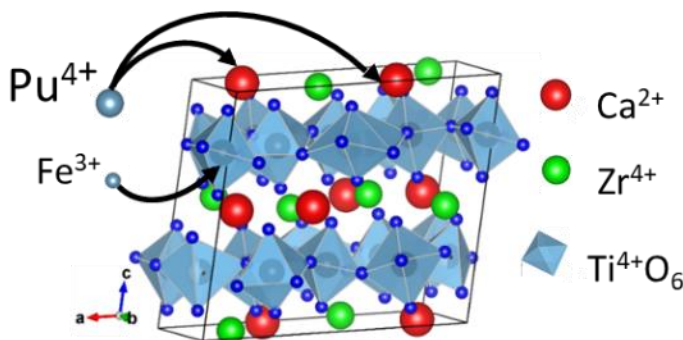


Figure 1: Zirconolite-2M crystal structure (space group C2/c)^[5]

Uranium has been previously utilised as a Pu surrogate, with the view to evaluate the viability of wasteform compositions and act as a basis from which to inform future Pu validation trials. In order to ascertain the feasibility of potential Pu-zirconolite solid solutions, the local coordination environment and prevailing oxidation states of the U surrogate fraction must be well characterised. When targeting formulations whereby U⁴⁺ is nominally substituted into the Ca²⁺ site, a suitable charge modifier must be substituted in appropriate molarity onto the Ti⁴⁺ site. The present study utilised the unique radiological HIP capability at the University of Sheffield to fabricate U-zirconolite materials containing Fe as a charge modifying cation. Conventional bulk measurements probed the pre-edge region of the Ti and Fe K edges, showing the impact of the partial O₂ pressure inside the HIP can on the charge compensator Fe³⁺ incorporation and Ti³⁺ formation. Bulk measurements at the U L₃-edge informed U oxidation state analysis alongside Extended X-Ray Absorption Fine Structure analysis (EXAFS). Understanding the incorporation mechanisms of U in the zirconolite system is key to underpin and inform future Pu validation trials.

[1] Nuclear Decommissioning Authority (NDA), "2022 UK Radioactive Material Inventory," 2022, [Online]. Available: <https://ukinventory.nda.gov.uk/wp-content/uploads/2023/02/2022-Materials-Report-010223.pdf>.

[2] B. D. Begg, R. A. Day, and A. Brownscombe, "Structural Effect of Pu substitutions on the Zr site in Zirconolite," *Mater. Res. Soc. Symp. Proc.*, vol. 668, pp. 1–8, 2001.

[3] E. R. Vance *et al.*, "Actinide and rare earth incorporation into zirconolite," *Journal of Alloys and Compounds*. 1994.

- [4] L. R. Blackburn *et al.*, "Review of zirconolite crystal chemistry and aqueous durability," *Advances in Applied Ceramics*, vol. 120, no. 2. Taylor and Francis Ltd., pp. 69–83, 2021, doi: 10.1080/17436753.2021.1877596.
- [5] H. Rossell, "Zirconolite: A fluorite related superstructure," *Nature*, vol. 283, pp. 282–283, 1980.

Impact of Gamma Dose Rate on the Alteration of Nuclear Glass in Geological Disposal Conditions

M. Taron [1, 2], H. Aréna [1], F. Chupin [1], K. Ressayre [1], R. Podor [2], M. Tribet [1], S. Peugeot [1]

[1] CEA, DES, ISEC, DPME, Université de Montpellier, Marcoule, Montpellier, France

[2] Institut de Chimie Séparative de Marcoule, ICSM, CEA, CNRS, ENSCM, Univ Montpellier, Marcoule, France

In France, the chosen containment option for long-lived high-level radioactive waste from spent fuel reprocessing is vitrification in a borosilicate glass matrix. Contact with groundwater is the main source of release of radionuclides contained in glass. The latter are responsible for the self-irradiation of the glass which modifies its alteration kinetics [1]. The aim of R&D studies is to predict the long-term behavior of nuclear glass, in order to help justify the safety of the repository. The physical and chemical stability of glass on a geological timescale therefore needs to be studied, which requires assessing the response of glass to radiation emitted by nuclear waste, as well as its behavior when subjected to alteration by water.

Among the radioactive wastes contained in glass, fission products lead to beta decays and gamma transitions, while minor actinides generate alpha decays. Several methods are available to study the effects of irradiation on glass alteration. Alteration experiments are often carried out on samples pre-irradiated with ions or electrons to simulate the damage created by the different decays and transitions on the material. However, it is also important to study the effects of irradiation on the alteration solution and the possible impact of its radiolysis on alteration kinetics. To this end, experiments are being carried out at the Gammatec facility (STERIS, Marcoule), combining underwater alteration and gamma dose rate. Unitary titanium containers containing glass and water are placed in a temperature-controlled enclosure at 90°C, near to a ⁶⁰Co source that generates a gamma dose rate of around 1,200 Gy/hr. At regular intervals, containers are sampled and solution and solid analyses are performed to assess the effects of the gamma dose rate on alteration kinetics.

This presentation will cover the study methodology and the experimental system used, and will be completed by an illustration of some results currently being acquired on a non-radioactive glass chemically simulating the nuclear glass used in France.

[1] Peugeot, S., et al., Radiation effects in ISG glass: from structural changes to long term aqueous behavior. npj Materials Degradation, 2018. 2:23.

Low-Temperature Condensation and Solidification of Radioactive Liquid Waste by Freeze Drying

Akihiko Kajinami¹, **Sou Watanabe**²

¹Faculty of Engineering, Kobe University, 1-1, Rokko-dai cho, Nada, Kobe, Hyogo, 657-8501 Japan

²Nuclear Fuel Cycle Engineering Laboratories, Japan Atomic Energy Agency, 4-33, Muramatsu, Tokai-mura, Naka-gun Ibaraki 319-1194, Japan

Nuclear facilities such as laboratories have generated various radioactive liquid wastes containing not only radioactive species but also reactive chemicals, and those have been accumulating inside the facilities due to difficulty in handling and treatment. Japan Atomic Energy Agency is conducting fundamental studies for treatment of those liquids in **S**ystematic **T**reatment of **R**adioactive liquid wastes for **D**ecommissioning (STRAD) project.

Immobilizing radioactive species and various chemicals is an indispensable technology in the project. One of the promising immobilization technologies is solidification such as vitrification, cementation, etc. Vitrification is a commercially available technology employed in reprocessing plants. However, the technology cannot be easily introduced in existing facilities due to the required high temperatures. The technology is also unsuitable for volatile elements and chemicals. Cementation is also a common technology for immobilization of elements and can be done at a lower temperature. However, resistance against the leaching of elements and chemicals into the water cannot be expected. Therefore, a new immobilization technology that can be applied to various chemical species is required to be developed.

Our group is focusing on a new technology to condense radioactive liquid and encapsulate chemical species simultaneously using a freeze-drying method, where ingredients of a matrix for the encapsulation are added into a target liquid before the condensation. After the freeze-drying condensation, species in the liquid are trapped in the matrix. Our preliminary test on a metal ion solution succeeded in the separation of water and solutes and the encapsulation of the solute in the matrix. In this study, components of the matrix were parametrically changed in the solidification tests on metal ions in nitric acid solutions, and solidification performance was evaluated through structural analyses of the product by XRD and EXAFS, and leaching tests to show the fundamental performance and mechanism of this technology. The applicability of the technology to the solution containing various chemicals was also examined.

An appropriate combination of the matrix was selected from Al, P, Fe, B, and Si, and systems with Al + Si or Fe + Si were revealed to be stable. The product had an amorphous structure, and cations were shown to be adsorbed on the matrix by electrostatic force. The leaching speed from the product was almost the same as that of the vitrified glass. Relatively large size chemical species such as ammonium ions and sulfamic acid molecules were also immobilized in the matrix. The new immobilization technology developed by this study is promising for the treatment of various radioactive liquid wastes stored in the facilities. The applicability of this technology for organic liquid wastes will also be investigated soon.

A part of this study is financially supported by Chubu Electric Power Co.

Investigation of Cement-Based Materials with Dihydrogen Sequestration Properties

H. Danis¹⁾, C. Cau Dit Coumes¹⁾, P. Antonucci¹⁾, I. Pointeau²⁾, T. Cordara²⁾, N. Macé³⁾, S. Savoye³⁾

¹⁾ CEA, DES, ISEC, DPME, SEME, LFCM, Univ. Montpellier, Marcoule, France

²⁾ CEA, DES, DDS, DFDE, SECC, LECD, Cadarache, France

³⁾ Université Paris-Saclay, CEA, Service de Physico-Chimie, 91191, Gif-Sur-Yvette, France

Corresponding author: Hugo Danis, email: hugo.danis@cea.fr

Mitigating dihydrogen release is an important issue for the disposal of certain types of cemented waste packages, containing for instance reactive metals or highly irradiating waste. The dihydrogen production results from corrosion of the metals encapsulated in the cement matrix, and/or radiolysis of water.

A solution under investigation consists in dispersing an inorganic getter in the cement matrix. The selected getter, which was first described by Kozawa *et al.* in the 1980s [1], comprises γ - MnO_2 , a random inter-growth of ramsdellite and pyrolusite (Figure 1), as well as small amounts of Ag_2CO_3 . The H_2 trapping mechanism involves $MnOOH$ formation in the allotropic forms of groutite (H in 2x1 tunnels) at first, and then of manganite (H in 1x1 tunnels) [2]. Ag_2CO_3 acts as a promoter by increasing the sequestration rate of dihydrogen, but can also be reduced into Ag metal, with concomitant production of water and carbon dioxide, following a secondary route.

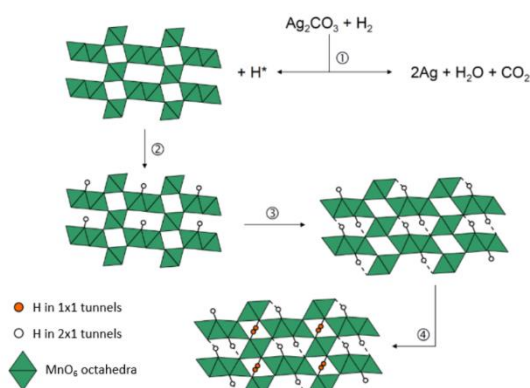


Figure 1 - Selected inorganic getter and trapping mechanism [2]

Complementary to the getter addition, the cement composition is also optimized to minimize adverse cement-waste interactions. For instance, Portland cement (CEM I, following EN197-1 standard) and composite cement (CEM V) are widely used for the stabilization/solidification of evaporator concentrates or coprecipitation sludges [3]. Magnesium potassium phosphate cements, yielding a pore solution with reduced pH (close to 8-9), may be an interesting candidate to encapsulate Al metal [4], and calcium sulfoaluminate cements have been shown as promising binders for the conditioning of borated waste [5], or incineration ashes with high contents of heavy metals [6].

This work investigates the chemical evolution of the getter in these different cementitious environments and its influence on the sequestration properties of hydrogen. For safety assessment studies, it is indeed important to determine whether the getter keeps its performance under such specific conditions of use.

The getter is thus equilibrated with cementitious suspensions or synthetic solutions mimicking the pore solution of the different binders. After separation, the solid and liquid phases are characterized using a large panel of techniques (X-ray diffraction, X-ray fluorescence, SEM/EDX, XPS, ICP-AES). γ - MnO_2 is shown to exhibit some reactivity in wet environment, due to the hydroxylation of its surface, leading to the sorption of ions (Ca^{2+} , K^+) released by the dissolution of cement phases.

Besides, partial or total destabilization of silver carbonate into silver oxide or silver phosphate is predicted by thermodynamic calculations, and confirmed experimentally (Figure 2).

Dihydrogen sequestration experiments are then launched with the getter samples previously equilibrated in the different

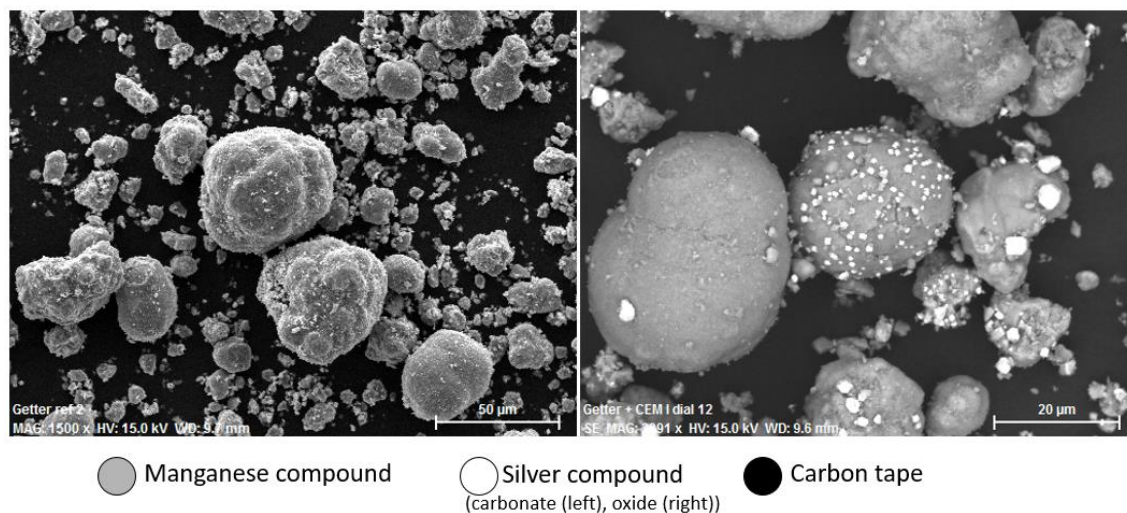


Figure 2 – SEM observation of getter (left) and getter previously equilibrated with a CEMI suspension (right)

cementitious environments. The getter is introduced in a metal reactor that is hermetically sealed, placed under vacuum and filled with a N_2/H_2 gas mixture containing 4% hydrogen. The decrease of the hydrogen content in the headspace of the reactor is determined by gas chromatography analysis. It is shown that both the H_2 sequestration rate and the total capacity of the getter are influenced by its chemical composition. Finally, these results provide a basis for optimizing the design of cemented waste packages (type of cement used, getter content) to limit H_2 outgassing.

This work is supported by BPI as part of the program “Investissements d’Avenir” funded by the French government.

References

- [1] Kozawa A., Kordesch K.V., Silver-catalysed MnO_2 as hydrogen absorber, *Electrochimica Acta* 26 (1981) 1489-1493.
- [2] Galliez K., P. Deniard, C. Payen, D. Lambertin, F. Bart, H.J. Koo, M.H. Whangbo, S. Jobic, Pair Distribution Function and Density Functional Theory Analyses of Hydrogen Trapping by γ - MnO_2 , *Inorg. Chem.* 54 (2015) 1194-1196.
- [3] Cau Dit Coumes, C., and al., Cementation of a Low-Level Radioactive Waste of Complex Chemistry: Investigation of the Combined Action of Borate, Chloride, Sulfate and Phosphate on Cement Hydration Using Response Surface Methodology. *Cement and Concrete Research* 33 (3), 2003, 305-16.
- [4] Cau Dit Coumes, C., and al., Selection of a Mineral Binder with Potentialities for the Stabilization/Solidification of Aluminum Metal. *Journal of Nuclear Materials* 453 (1), 2014, 31-40.
- [5] Champenois, J.B., and al., Influence of Sodium Borate on the Early Age Hydration of Calcium Sulfoaluminate Cement. *Cement and Concrete Research* 70, 2015, 83-93.
- [6] Berger, S., and al., Stabilization of $ZnCl_2$ -Containing Wastes Using Calcium Sulfoaluminate Cement: Cement Hydration, Strength Development and Volume Stability. *Journal of Hazardous Materials*, 194, 2011, 256-67.

Microwave Plasma-Assisted Combustion of Waste Organic Solvents

Shimpei Ohno¹, Atsushi Sakamoto¹, Sou Watanabe¹, Masahiro Nakamura¹, Tsuyoshi Yamamoto²
and Ryou Tanaka³

¹Nuclear Fuel Cycle Engineering Laboratories, Japan Atomic Energy Agency 4-33, Muramatsu, Tokai-mura, Naka-gun Ibaraki, 319-1194, Japan

²Kyushu University 744, Motoooka, Nishi-ku, Fukuoka-shi, Fukuoka, 819-0395, Japan

³Aichi Electric Co., Ltd. 1, Aichi-cho, Kasugai-shi, Aichi, 486-8666, Japan

Japan Atomic Energy Agency (JAEA) started decommissioning of some old hot facilities. However, various kinds of organic solvents still exist in the facilities without treatments due to a lack of potential treatment technologies. These organic solvents containing radioactive elements have to be mineralized, and our group is conducting fundamental studies to develop effective mineralization technologies for organic compounds as a part of the Systematic Treatment of RADioactive liquid wastes for Decommissioning (STRAD) project. One of the promising mineralization technologies is the nonequilibrium plasma-assisted combustion which is expected to supplant the thermal plasma combustion. The nonequilibrium plasmas effectively generate activated chemical species due to their high electron temperature; therefore, chemical reactions for the dissociation of chemical bonds in the organic compounds can be promoted. However, this technology has never been applied to the spent solvent treatment. Not only optimization in plasma conditions for the treatment, but also recovery of radioactive material are challenges for the application. In this study, applicability of the microwave plasma-assisted combustion to the waste solvents treatment was examined on simulated spent solvent comprising normal dodecane, TEHDGA (Tetra2-ethylhexyl diglycolamide), and neodymium (Nd), where Nd was loaded into the solvent through solvent extraction operation from a nitric acid medium and a Nd ion exists as a complex $\text{Nd}(\text{NO}_3)_3(\text{TEHDGA})_2$ in the solvent.

An experimental apparatus consists of a discharge tube, a microwave generator, a rotary vacuum pump, and a solid powder recovery vessel. (Figure 1) An oxygen plasma was generated by 2.45 GHz microwave irradiation, and the simulated spent solvent was introduced into the plasma through a nozzle to form droplets. (Figure 2) Normal dodecane and TEHDGA are composed of only C, H, O, and N elements. Thus, CO_2 , H_2O , and NO_x must be generated if the mineralization is completely progressed. As a result of gas chromatography analysis of the exhaust gas after treatment, it was found that almost all of the carbon in the simulated spent solvent was converted to CO_2 , indicating that it had been mineralized. Nd should be recovered as Nd_2O_3 powder by the treatment. After the experiment, organic liquids did not remain inside the apparatus, and ash were collected in the vessel and vacuum tube. Nd was found in the ash by X-ray fluorescence analysis, and the decomposition of the complex might progress as expected. However, the recovery ratio of Nd was about 35 %, and a residual 65% was in the pump. This is because the particle size of the recovered Nd_2O_3 powder was not large enough. Since the recovery ratio of Nd is poor, optimizations in both operational conditions and the apparatus are underway.

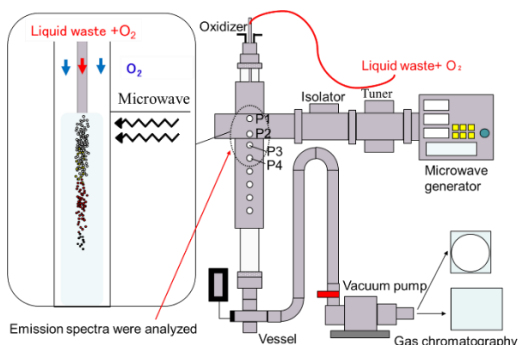


Figure 1 apparatus consist



Figure 2 Combustion test of organic liquids

Search for a Cement Matrix for ITER Beryllium Radwaste Conditioning

Laflotte R.¹⁾, Cau Dit Coumes C.¹⁾, Cannes C.²⁾, Delpech S.²⁾, Haas J.¹⁾, Rivenet M.³⁾

¹⁾ CEA, DES, ISEC, DPME, SEME, LFCM, Univ. Montpellier, Marcoule, France

²⁾ Université Paris-Saclay, CNRS/IN2P3, IJCLab, 91405 Orsay, France

³⁾ Univ. Lille, CNRS, Centrale Lille, Univ. Artois, UMR 8181 – UCCS – Unité de Catalyse et Chimie du Solide, F-59000 Lille, France

The commissioning of the ITER fusion facility will produce low or intermediate-level radioactive waste with significant amounts of neutron-irradiated beryllium metal. In addition to its high toxicity, beryllium can corrode under aqueous environment, with concomitant production of dihydrogen. Cementation is one of the processes under investigation for the conditioning of such waste. Since cemented waste packages must exhibit a very low outgassing rate to be acceptable in a repository, it is of primary importance to select a binder leading to beryllium passivation. The potential-pH diagram of beryllium in water, firstly established by Pourbaix in 1963 [1], was recently revisited [2]. Beryllium presents an amphoteric behavior and its precipitation as $\text{Be}(\text{OH})_2$ is expected to occur for pH values within the range 5.5 – 13.5. By using electrochemical impedance spectroscopy (EIS), Bouhier *et al.* [3] showed that when Be is immersed in NaOH solutions, the Faradaic resistance reaches a maximum at a pH close to 12. The higher this resistance, the less the metal is corroded. Based on these results, this work investigates the corrosion behavior of Be metal into three cement pastes with pore solutions pH falling within the stability domain of $\text{Be}(\text{OH})_2$. Portland cement (PC), which is commonly used for waste conditioning, produces a pore solution pH close to 13, governed by the dissolution of alkalines (Na_2O , K_2O) and portlandite ($\text{Ca}(\text{OH})_2$). The two other binders, referred as B_{40} and CSA_{15} , are designed in order to yield a pore solution pH close to 12. The former (B_{40}) is a binary blend comprising 60% Portland cement and 40% silica fume. The massive addition of silica fume makes it possible to consume portlandite by pozzolanic reaction. The pH is then controlled at ≈ 11.5 by the dissolution equilibrium of calcium silicate hydrates having a low Ca/Si ratio [4]. The latter (CSA_{15}) is made of 85% calcium sulfoaluminate clinker and 15% anhydrite (CaSO_4). Hydration of CSA_{15} mainly yields ettringite ($3\text{CaO} \cdot \text{Al}_2\text{O}_3 \cdot 3\text{CaSO}_4 \cdot 32\text{H}_2\text{O}$), monosulfate ($3\text{CaO} \cdot \text{Al}_2\text{O}_3 \cdot \text{CaSO}_4 \cdot 12\text{H}_2\text{O}$) and gibbsite ($\text{Al}(\text{OH})_3$). The pore solution pH is initially close to 11-12 and raises to 12-13 when anhydrite is fully depleted [5].

The corrosion rate of beryllium in the three cement matrices is investigated with two experimental techniques: measurement of dihydrogen released by corrosion using gas chromatography (GC), and investigation of the electrochemical behavior of Be by EIS. A specific three-electrode cell is designed, comprising two platinum electrodes and one beryllium electrode that are embedded in the cement matrix under investigation. EIS provides information on both the corrosion at the interface metal/cement and the evolution of the matrix over time. After a qualitative analysis of the EIS spectra, a corrosion mechanism of Be is postulated and an equivalent electrical circuit is proposed to fit the impedance spectra. The circuit parameters are adjusted by fitting the impedance spectra. These parameters enable to determine the corrosion current and the corresponding H_2 production (assuming that Be only undergoes aqueous corrosion). The H_2 volume determined in EIS is compared to the H_2 release determined by micro GC. The CSA_{15} matrix appears as the most promising since it leads to reduced corrosion of Be and H_2 release, as compared to the other materials. These results offer new prospects for the conditioning of deleterious waste containing Be metal.

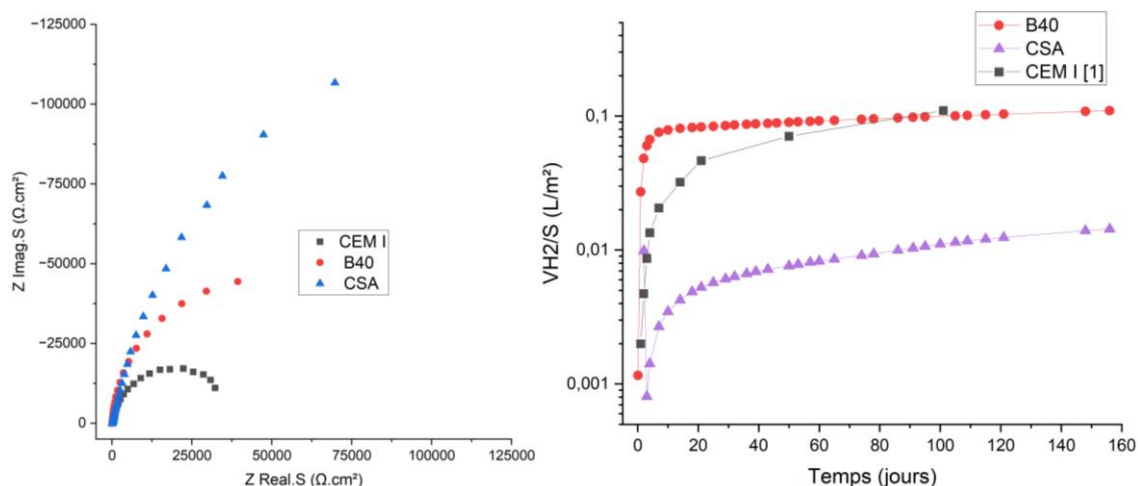


Figure 1: Nyquist diagrams of CEM I, B₄₀ and CSA₁₅ pastes at 2 hours (left) and predicted H₂ volume production from EIS results (right)

References

- [1] M. Pourbaix, « Atlas of electrochemical equilibria in aqueous solutions », *Journal of Electroanalytical Chemistry and Interfacial Electrochemistry*, vol. 13, n° 4, avr. 1967, doi:10.1016/0022-0728(67)80059-7.
- [2] N. Çevirm-Papaioannou, X. Gaona, M. Böttle, E. Yalçıntaş Bethune, D. Schild, C. Adam, T. Sittel, M. Altmaier, « Thermodynamic description of Be(II) solubility and hydrolysis in acidic to hyperalkaline NaCl and KCl solutions », *Applied Geochemistry*, n° 117, 2020, doi:10.1016/j.apgeochem.2020.104601.
- [3] P. Bouhier, C. Cannes, D. Lambertin, C. Grisolia, D. Rodrigues, et S. Delpech, « Evaluation of several conditioning matrices for the management of radioactive metal beryllium wastes », *Journal of Nuclear Materials*, vol. 559, févr. 2022, doi:10.1016/j.jnucmat.2021.153464.
- [4] T. T. H. Bach, C. Cau Dit Coumes, I. Pochard, C. Mercier, B. Revel, et A. Nonat, « Influence of temperature on the hydration products of low pH cements », *Cement and Concrete Research*, vol. 42, n° 6, juin 2012, doi:10.1016/j.cemconres.2012.03.009.
- [5] F. Winnefield et B. Lothenbach, « Hydration of calcium sulfoaluminate cements — Experimental findings and thermodynamic modelling », *Cement and Concrete Research*, vol. 40, n° 8, août 2010, doi:10.1016/j.cemconres.2009.08.014.

Repercussions of Solubility for the Conditioning of Fission Products and Minor Actinides in Borosilicate Glasses

L. Campayo, I. Giboire, S. Schuller, E. Régnier, D. Perret

CEA, DES, ISEC, DPME, Université de Montpellier, Marcoule, 30207 Bagnols-sur-Cèze Cedex, France

The management of nuclear waste is the subject of much research. For the most harmful, France has chosen a storage in a deep geological layer after conditioning in matrices with high confinement performance. This is the case for solutions of fission products and minor actinides resulting from the reprocessing of spent fuels that are currently vitrified in an aluminoborosilicate glass (the so-called R7T7 glass). Apart from insoluble particles such as ruthenium oxide, a homogeneous glass is targeted. This principle of a confinement of radionuclides at a molecular scale involves suitable formulations and conditions for producing such a glass in order to guarantee its homogeneity. This also allows a predictive modelling for the release of radionuclides in a disposal situation to be built.

In this presentation, we will endeavor to describe the specific behavior of certain fission products and minor actinides during the production of a R7T7 type glass and related glasses with particular attention paid to their solubility limit. The solubility limit is indeed an important parameter that must be taken into account both during the step of chemical reactivity between the calcined radionuclides-containing solution and the glass frit additive during the production of the material as well as after extinction of any reactivity.

Four emblematic cases will be considered here: minor actinides and rare earths, molybdenum and iodine.

In the case of rare earths and minor actinides, exceeding the solubility limits can be the source of the emergence of crystallizations in the glass such as apatites [1] or cerianites. By concentrating the activity of alpha emitters in their crystal lattice, these phases are likely to amorphize and mechanically constrain the glass, which can cause a fracturing phenomenon. In addition, the accumulation of alpha particles in the vitreous network can result in the emergence of gas bubbles in the glass and the mobility of helium must then be studied [2, 3]. It is of note that oxidation state can also be an interesting parameter to control to favor solubility of some radionuclides like uranium, U^{VI} being more soluble than U^{IV} in silicate-based melts for instance [4]. This can be useful for the conditioning of uranium-enriched waste.

For molybdenum, an incorporation rate that would result in exceeding its solubility limit at the production temperature will lead to a liquid-liquid phase separation responsible for the appearance of alkaline and/or alkaline earth molybdates after cooling [5]. By grouping together, these alkaline molybdates can be at the origin of the formation of typical microstructures called "yellow phase" which can carry cesium and present a labile character in contact with a vector of dissemination like water.

For its part, iodine is an element that is little retained in the vitreous network of R7T7 type glasses due to its volatility at the temperatures at which these matrices are produced. The same is true for other fission products such as technetium. However, iodine has been the subject of particular attention because of its role in the safety studies of potential disposal sites. Its solubility in glass depends both on the nature of the alkalis and on their overall content [6]. Research is currently being carried out on both glass and glass-ceramics and on new forming conditions to promote its confinement [7, 8].



Example of a “yellow phase” due to a liquid-liquid phase separation coming from a high molybdenum content (courtesy of Dr. S. Schuller)

Radionuclides are not the only species coming with solutions of fission products and minor actinides that have to be taken into account. These solutions may also contain corrosion products that if not radioactive can induce heterogeneities in the final glass. This is the case of chromium of which the solubility in typical aluminoborosilicate melts of interest does not exceed 0.6 wt.% in Cr_2O_3 . Above this limit, chromium-containing crystals are met within the glass [9]. These crystals can play the role of nucleating agents.

Eventually, obtaining a homogeneous glass for all the species that are to be conditioned is a complex topic as each solubility can be the limiting factor and the number of possible interactions increases with the complexity of waste. It is a unique expertise of nuclear industry.

- [1]: A. Kidari et al., Solubility and partitioning of minor-actinides and lanthanides in aluminoborosilicate nuclear glass, *Procedia Chemistry* 7 (2012) 554 – 558.
- [2]: T. Fares et al., Helium Solubility in SON68 Nuclear Waste Glass, *Journal of the American Ceramic Society* 95 [12] (2012) 3854–3862.
- [3]: R. Bès et al., Helium mobility in SON68 borosilicate nuclear glass: A nuclear reaction analysis approach, *Journal of Nuclear Materials* 443 (2013) 544–554.
- [4]: O. Podda et al., Solubility of uranium oxide in ternary aluminosilicate glass melts, *Journal of Non-Crystalline Solids* 595 (2022) 121845.
- [5]: S. Schuller et al., Liquid-liquid phase separation in borosilicate glass enriched in MoO_3 – experimental investigations and thermodynamic calculations, *Journal of Non-Crystalline Solids* 600 (2023) 121997.
- [6]: B. Venague et al., Role of alkalis on the incorporation of iodine in simple borosilicate glasses, *Journal of Non-Crystalline Solids* 576 (2022) 121278.
- [7]: Y. Morizet et al., Predicting iodine solubility at high pressure in borosilicate nuclear waste glasses using optical basicity: an experimental study, *Journal of Materials Science* 57 (2022) 16600–16618.
- [8]: V. Jolivet et al., High-pressure experimental study on iodine solution mechanisms in nuclear waste glasses, *Journal of Nuclear Materials* 533 (2020) 152112.
- [9]: H. Hansen et al., Chromium enriched peraluminous glasses: Incorporation limit, crystalline phase equilibrium and impact of chromium on the rheological properties of the glass, *Journal of Nuclear Materials* 567 (2022) 153802.

Progress towards the Immobilisation of the UK Plutonium Inventory in Titanate Ceramics

Lewis R. Blackburn¹, Amber R. Mason¹, Laura J. Gardner¹, Claire L. Corkhill²

¹Immobilisation Science Laboratory, Department of Materials Science and Engineering, University of Sheffield, UK

²School of Earth Sciences, University of Bristol, UK

The United Kingdom holds a substantial inventory of PuO₂, forecast to reach approximately 140 teHM (tonnes equivalent heavy metal) upon completion of reprocessing. This material presents a unique decommissioning prospect for which there is a need to develop a robust management strategy [1]. Prompt immobilisation and disposal within a geological disposal facility (GDF) is a promising route towards ultimate disposition, yet in order to safely underpin the safety case for the geological disposal of Pu, it is necessary to understand the long-term evolution of candidate wasteform materials in simulated repository environments. Moreover, there is a need to develop suitable wasteform materials capable of co-accommodating Pu, prescribed quantities of neutron poisoning species, trace processing impurities and transition metal cations capable of providing charge balance for non-stoichiometric compositions. Several baseline wasteform formulations derived from zirconolite, pyrochlore and fluorite-type matrices have been proposed on the basis of high chemical durability, radiation stability and moderate ease of processing [2]. Herein, this talk will provide an overview in recent advances in the formulation refinement and fundamental characterisation of candidate wasteform materials for UK Pu. This includes detailed scoping trials aiming to characterise the incorporation of a representative U, Th and Ce surrogate fraction within zirconolite and pyrochlore phases, fabricated by conventional sintering (CPS), hot isostatic pressing (HIP) and reactive spark plasma sintering (RSPS) [3].

[1] N. C. Hyatt, "Safe management of the UK separated plutonium inventory: a challenge of materials degradation," npj Mater. Degrad., vol. 4, no. 28, 2020.

[2] L. R. Blackburn and N. C. Hyatt, "Actinide Immobilisation in Dedicated Wasteforms: An Alternative Pathway for the Long-Term Management of Existing Actinide Stockpiles," in Encyclopedia of Nuclear Energy, 1st ed., E. Greenspan, Ed. Elsevier, 2021, pp. 650–662.

[3] L. R. Blackburn et al., "Hot Isostatically Pressed Zirconolite Wasteforms for Actinide Immobilisation," in IOP Conference Series: Materials Science and Engineering, 2020, vol. 818, no. 1.

Elaboration and Characterization of Iodate and/or Carbonate-Doped Apatites for Long-Lived Radionuclides Conditioning

Olivier Dautain^{a,b}, Céline Cau dit Coumes^b, Christophe Drouet^a, David Grossin^a, Lionel Campayo^b, Christèle Combes^a

^a CIRIMAT, Toulouse INP, Université de Toulouse 3 Paul Sabatier, CNRS, Université de Toulouse, ENSIACET, 4 allée Emile Monso, 31030 Toulouse Cedex 4, France

^b CEA, ISEC DPME, SEME, Marcoule, Univ. Montpellier, F-32027 Bagnols sur Cèze, France

Introduction: Different ways of tackling the issue of non-recyclable long-lived nuclear wastes have been studied over decades. Some countries, like France, made the choice of their disposal in deep geologic repositories. However, some of the waste components from nuclear spent fuel are currently not, or in very marginal proportions, incorporated in conditioning matrices (like borosilicate glasses) used nowadays. It is the case for iodine-129, carbon-14 and chlorine-36, coming from spent fuel reprocessed at La Hague facility (France). Iodine-129 and carbon-14 are currently managed by isotopic dilution and discharged in the Channel, while chlorine-36 is released in the gas phase during the retreatment process. The possibility of new, and more severe, discharge regulations concerning gaseous and aqueous waste streams, and the potential development of 'inland' reprocessing plants, with no access to the sea, constitute two incentives for developing a new way to manage these three radionuclides, by conditioning and storage. The matrix should follow some specifications to limit their release into the environment and exhibit good long-term stability and resistance to aqueous alteration. For example, the half-life of iodine-129 is about 1.57×10^7 years and this radionuclide is expected to have high diffusivity in a deep geologic repository. [1] Modelling showed that iodine-129 and chlorine-36 are among the major contributors to the outlet dose, at a timescale of $10^5 - 10^6$ years. Consequently, the selected matrix should have high durability, which means a very low release rate for these radionuclides in geologic conditions and a specific surface area that should be as low as possible. A high waste incorporation rate would also be desirable to limit the number of packages to be disposed of. Besides, the elaboration process should be compatible with an implementation in nuclear environment. Studies have already been carried out for ^{129}I , ^{14}C and ^{36}Cl conditioning [2] [3]. In particular for iodine-129, low melting point glasses, cements and ceramics have been investigated. Among them, apatites are promising candidates because of their outstanding properties. The structure of these poorly soluble minerals is indeed highly tolerant to cation and anion substitution, which can lead to chemical entrapment of deleterious species. Furthermore, they have the property to anneal radiation damage, which gives them low amorphization susceptibility [4]. In particular, hydroxyapatite (Hap), $\text{Ca}_{10}(\text{PO}_4)_6(\text{OH})_2$, crystallizes in a hexagonal structure, with a peculiar organization: some Ca^{2+} ions are arranged in a tunnel-shaped structure, and OH^- ions are located in those tunnels. The incorporation of iodine as iodate (IO_3^-) and chlorine as chloride (Cl^-) occurs by substitution in the OH^- sites, while carbon as carbonate ions can also substitute in the phosphate sites. However, the incorporation of chloride via an aqueous route is not thermodynamically favored [5] and the synthesis parameters of carbonate- and iodate-substituted hydroxyapatite still need to be optimized to make easier its further shaping process. The objectives of this study are thus to (i) synthesize carbonate and/or iodate-doped apatites through the aqueous precipitation route and the cement route, (ii) optimize the various synthesis parameters and (iii) thoroughly characterize the reaction products.

Materials and methods: Iodate-substituted Hap (Hap-IO_3) and carbonate-substituted Hap (Hap-CO_3) were prepared by precipitation in water, following the protocols of Campayo et al. [2] and Nelson et al. [6], respectively. Syntheses were performed at 90 °C for Hap-IO_3 or 85 °C for Hap-CO_3 , at relatively high pH (Hap-IO_3 : pH = 10; Hap-CO_3 : pH = 9) and with a maturation time of 5 h. We also formulated an apatitic cement based on the reaction between a soluble calcium phosphate phase (brushite) and a metastable calcium carbonate phase (vaterite). Iodate was added either in the mixing solution or as an iodate salt pre-mixed with cement. The synthesized apatite powders, the cement pastes and set cements were characterized by XRD, FTIR, Raman spectroscopy, SEM/EDX and elemental analyses.

Results and discussion: For precipitated Hap-IO₃, we demonstrated the incorporation of iodate in the apatite phase, with a crystallite size of ~ 60 nm, and an incorporation rate of 7% w/w. By varying some parameters (maturation time, concentration of reagents, pH), we were able to maximize the incorporation rate of IO₃⁻ and a significant increase in crystallinity was obtained by raising the maturation time to 24 h. Hap-CO₃ apatite phase was also synthesized by coprecipitation, with an apparent crystallite size equivalent to that of Hap-IO₃ (60 nm). By implementing advanced FTIR analysis [7], we were able to identify the substitution sites for carbonate (OH⁻ sites for A-type Hap-CO₃, and PO₄³⁻ sites for B-type Hap-CO₃) and quantify the extent of substitution. With the cement route, it was shown that the introduction of iodate as an additive during mixing did not inhibit setting and hardening of the material. The determination of the kinetic of the setting reaction and the iodate loading and speciation in the cement matrix still need to be further determined.

These preliminary results on two different routes to synthesize iodate- and/or carbonate-doped apatites pave the way for the development of apatite matrices with tunable compositions and physicochemical properties for ¹²⁹I and ¹⁴C conditioning. Future work will be focused on the challenging synthesis of co-doped apatites with iodate, carbonate and chloride ions.

Acknowledgments: The authors thank Bpifrance – France 2030 program and the European Union – France Relance program for supporting this research.

References:

- [1] ANDRA, Dossier Argile 2005 (2006), Chap.6, 212
- [2] L. Campayo et al., Journal of Materials Chemistry (2011) 17609 – 17611
- [3] P. Lei et al, Journal of Nuclear Materials (2020) 151857
- [4] L. Campayo et al., MRS Online Proceedings Library (2014) 15–20.
- [5] G. Maiti, F. Freund, Journal of Inorganic and Nuclear Chemistry (1981) 2633 – 2637
- [6] D. Nelson et al., Journal of Colloid and Interface Science (1989) 467– 479
- [7] A. Grunenwald et al., Journal of Archaeological Science (2014) 134 –141

The Effect of Cation Substitution and Valency on Formation Energetics of Brannerite Ceramics for Nuclear Waste Applications

Natalie S. Yaw, Chris Dixon Wilkins, Nicolas Dacheux, John McCloy, Xiaofeng Guo

Department of Chemistry, Washington State University, Pullman WA, USA 99163

Transforming used nuclear fuel into highly durable wasteforms prior to geological disposal is one of the current credible options for the long-term immobilization of these materials. Ceramics such as titanate brannerites (AB_2O_6 , prototypically UTi_2O_6) have emerged as an attractive option due to their chemical durability, inertness, and high loading of actinides (1,2). Furthermore, both A and B sites are open to substitutions provided that the average valency of the combined sites is +4. Thus, brannerite ceramics have the advantage of incorporating fission products, neutron absorbers, actinides from mixed oxide fuels, or other charge-balancing elements (3). This flexibility has been exploited in previous studies, including the synthesis of mixed Ce/U/Th brannerites and charge balancing U(V). While these studies demonstrate the feasibility of isolating a wide range of synthetic brannerites relevant to nuclear wastes, little knowledge exists on how the charge-couple substitution and valence changes impact the underlying thermodynamic properties.

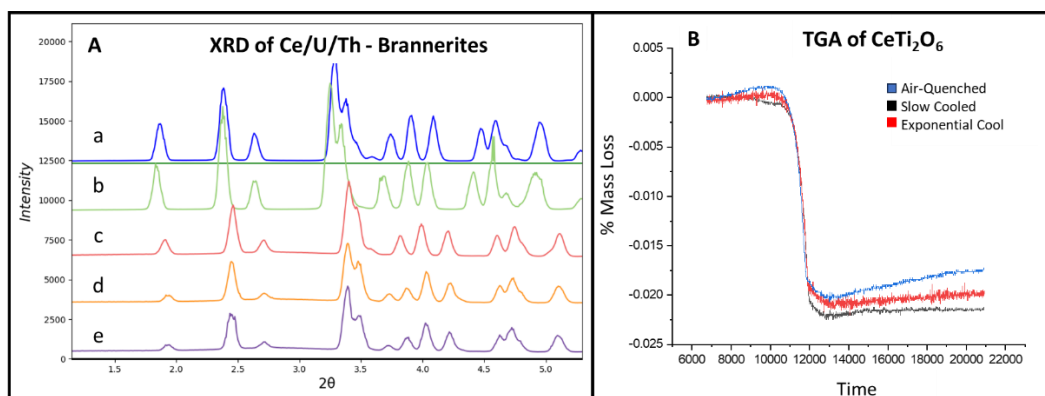


Figure 1- A. X-ray Diffraction of brannerites from this work, taken at the Canadian Light Source (a) UTi_2O_6 , (b) $ThTi_2O_6$, (c) $U_{0.5}Ce_{0.5}Ti_2O_6$, (d) water-quenched $CeTi_2O_6$, and (e) slow-cooled $CeTi_2O_6$. B. TGA/DSC of $CeTi_2O_6$ run under N_2 fully reducing Ce(IV) to Ce(III), demonstrating differing amounts of Ce(III) quenched into matrix.

In this work, the correlation between compositional differences and formation energetics is systematically studied by examining cationic (Ce, Th, U) solid-solution brannerites relevant to its nuclear waste applications. Previous work has established that Ce-, Th-, and U-brannerites (endmembers) have distinct enthalpies of formation, yet do not reflect a clear empirical relation with their unit cell parameters, and no enthalpy of formation reported for phase-pure $PuTi_2O_6$ due to synthesis and handling difficulties (6,7). Designing solid-solutions based ceramic wasteforms is rational considering the multi-elements in the burnt-up fuels and mixed-oxide fuels. We hypothesized that solid-solutions of the endmember brannerites impact and (de)stabilize the brannerite structure, originated from the local arrangement of the mixing elements whether they are random distribution and short-range ordering (SRO). These structural features translate to both enthalpic and entropic impacts, which has not yet been studied. Mixing is not only realized from different elements, but also from different valence states of the same element. Variations in A-site oxidation state, both of pure endmembers and in solid solutions thereof, will have thermodynamic consequences. Recent work has suggested that mixed Ce(III/IV) oxidation states may contribute to the enthalpic stabilization of the Ce brannerite endmember (7,8). This is particularly critical for U, which can be stabilized at higher oxidation states; with higher oxidation states (V, but particularly VI) being significantly more soluble and mobile in aqueous solutions than U(IV), thus making their presence undesirable for nuclear waste

applications and geochemically significant (9). Understanding and controlling when higher valence U is formed, why these phases are stabilized, and how to avoid them if necessary is thus critical in wastefrom design.

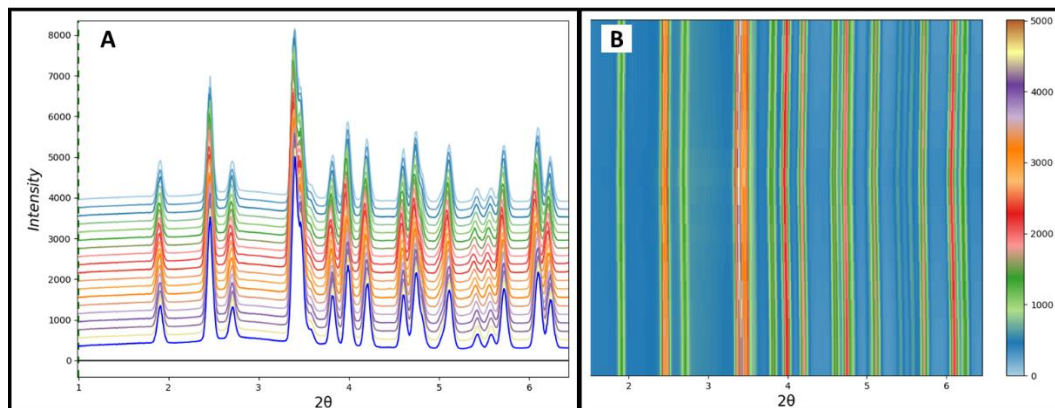


Figure 2- In-situ high temperature X-ray Diffraction of mixed Ce/U brannerite synthesized in this work (A, overlaid peaks from 100-900 °C and back down, B Heatmap of the same scans). XRD conducted at the Canadian Light Source. Phase stability is demonstrated through 900 °C in this scan.

End-member and solid solutions of Ce/U/Th brannerites have been synthesized via solid-state chemistry. Altering the quenching rate and atmospheric composition allowed for brannerites of the same atomic but different valence compositions to be synthesized, including a series of five CeTi_2O_6 with differing ratios of Ce(III)/Ce(IV). Samples have been rigorously characterized both in house and at synchrotron facilities with X-ray techniques to quantify compositional characteristics, and both TGA/DSC and high temperature oxide melt solution calorimetry are being used to interrogate resultant thermodynamic properties (ΔH and ΔS). Future leaching experiments will also be done on the same samples to understanding their dissolution behaviors and chemical durability in the acidic solutions. Our initial results on Ce(III)/Ce(IV) ceramics indicate that increased fractions of Ce(III) correlate to increasing enthalpic stabilization in the brannerite material. Work is ongoing to determine how this finding will impact Ce/U/Th brannerites, especially those with corresponding charge balancing of U(V). Tracking compositional changes onto corresponding changes in entropic and enthalpic properties in this way, we will build out our understanding of cation mixing, critical stability constants, and valence-driven (de)stabilization in these important mixed actinide ceramics.

1. Bailey, MRS Adv. 2017, 2 (10)
2. Yuditsev, Radiochemistry, 2016, 58 (4)
3. Hess, J. Frankl. Inst. 1920, 189 (2)
4. Dixon Wilkins, Inorg. Chem. 2021, 60 (23)
5. Dixon Wilkins, MRS Adv., 2020, 5 (1-2)
6. Helean, J Nucl. Mater. 2003, 320 (3)
7. Dixon Wilkins, Inorg. Chem, 2020, 59 (23)
8. Marcial, Mater. Degrad. 2021, 5 (34)
9. Maher, Inorg. Chem, 2013 52 (7)

Densification of Mesoporous Silicas Induced by Radiation Damage – New Perspectives for the Treatment of Radioactive Effluents

Jun Lin*, Clara Grygiel**, Sandrine Dourdain*, Yannick Guari***, Cyrielle Rey*, Jérémy Causse*,
Olaf Walter****, **Xavier Deschanel***

*ICSM, CEA, CNRS, ENSCM, Univ Montpellier, Marcoule, France

**CIMAP, CEA-CNRS-ENSICAEN-UNICAEN Bd. Henri Becquerel, Caen, France

***ICGM, Univ Montpellier, CNRS, ENSCM, Montpellier, France

****JRC Karlsruhe, Germany

In recent years, mesoporous silicas (SBA15, MCM41) discovered in the 1990s, synthesized by sol-gel process [1-2] have been the subject of numerous studies for various applications in the fields of catalysis, CO₂ encapsulation, or treatment of radioactive effluents [3]. More precisely, a new strategy for this treatment is based on the use of a mesoporous silica functionalized by an organic ligand selective of the RadioNuclides (RN). This hybrid material would allow at the same time the separation of the RN and their encapsulation after collapsing the porosity. This new concept would result in obtaining a primary wasteform matrix. Several ways are being considered to close the mesoporosity: chemical reactions (sol-gel in particular), thermomechanical treatments, and irradiation effects. The collapse of silica mesoporosity by external irradiation (ion and electron) has been demonstrated in several works [4-5]. More recently, the possibility of closing the porosity of a mesoporous silica through self-irradiation damage produced by the presence of the short-lived actinide ²³⁸Pu has been studied in our laboratory. The results of this work will be presented in the talk.

^{238/239}Pu sorption experiments have shown that hybrid silicas grafted with Ac-Phos and Prop-Phos ligands (Figure 1) have a loading capacity of around 10% by weight, enabling significant self-irradiation damage, comparable to an external irradiation experiment, to be achieved in around two years. Our findings are in line with previous results [6]. Small-angle X-ray scattering (SAXS), which is accessible on the SOLEIL synchrotron's MARS beamline, was employed for characterization of these Pu-doped materials. After 17 months of ageing, these measurements show a decrease in the interplanar (100) distance of the hexagonal pore network of mesoporous silica, indicating a densification of around 10% of the pore volume (Figure 2).

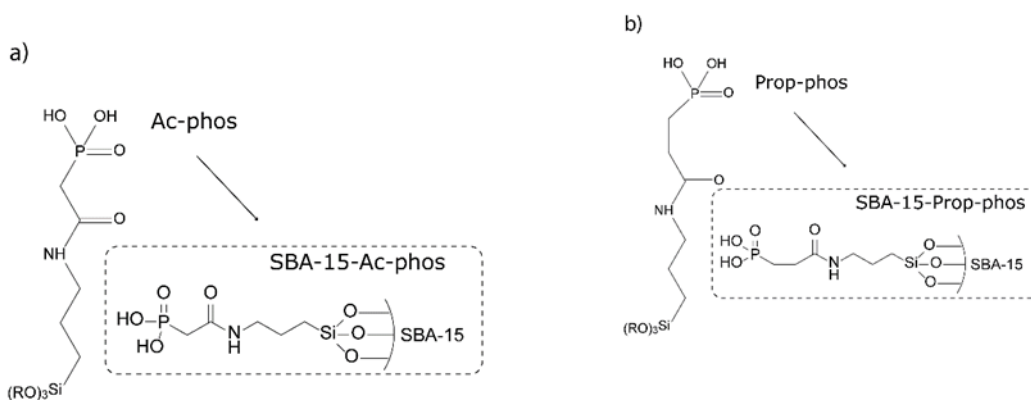


Figure 1: Structure of the starting ligands and the grafted mesoporous silicas. a) Ac-phos ligand and SBA-15-Ac-phos; b) Prop-phos ligand and SBA-15-Prop-phos

The results obtained will be discussed in the light of the differences observed between external irradiation and self-irradiation.

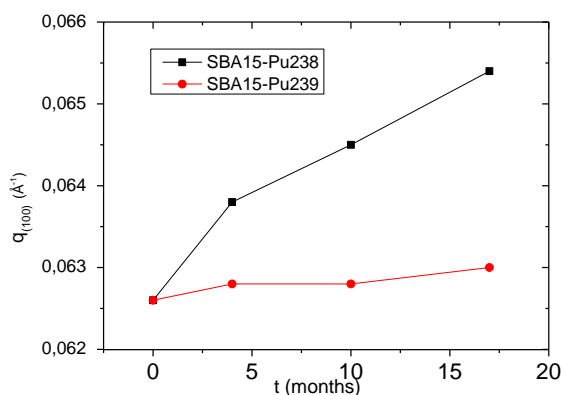


Figure 2 : Comparison of the evolution of interplanar (100) distance of the hexagonal pore network of SBA15-Prop-phos ²³⁸Pu and SBA15-Prop-phos ²³⁹Pu, versus ageing duration

- [1] Beck, J. S., J. C. Vartuli, W. J. Roth, M. E. Leonowicz, C. T. Kresge, K. D. Schmitt, C. T. W. Chu, D. H. Olson, E. W. Sheppard, S. B. Mccullen, J. B. Higgins and J. L. Schlenker, A New Family of Mesoporous Molecular-Sieves Prepared with Liquid-Crystal Templates, American Chemical Society, Vol. 114, 1992, pp. 10834-10843.
- [2] Zhao, D., J. Feng, Q. Huo, N. Melosh, G. H. Fredrickson, B. F. Chmelka and G. D. Stucky, Triblock copolymer syntheses of mesoporous silica with periodic 50 to 300 angstrom pores, Vol. 279, 1998, pp. 548-552.
- [3] P. Makowski, X. Deschanel, A. Grandjean, D. Meyer, G. Toquer and F. Goettmann, New J. Chem., 36 (2012) 531.
- [4] Y. Lou, S. Dourdain, C. Rey, Y. Serruys, D. Siméone, N. Mollard, X. Deschanel, Micropor. Mesopor. Mater., 251 (2017) 146.
- [5] J. Lin, G. Toquer, C. Grygiel, S. Dourdain, Y. Guari, C. Rey, J. Causse, X. Deschanel, « Behavior of mesoporous silica under 2 MeV electron beam irradiation » Microporous Mesoporous Mater. 328 (2021) 111454.
- [6] Fryxell, G. E., H. Wu, Y. Lin, W. J. Shaw, J. C. Birnbaum, J. C. Linehan, Z. Nie, K. Kemner and S. Kelly, Lanthanide selective sorbents: self-assembled monolayers on mesoporous supports (SAMMS), Vol. 14, 2004.

A Historical Overview of Corroded Microstructures and Present-day Best Practices.

Mir Anamul Haq

Microscopes and Ion Accelerators for Materials Investigation Facility, University of Huddersfield, UK

Nuclear wasteforms such as glasses and ceramics when subjected to corrosion undergo a combination of dissolution, leaching and precipitation leaving behind complex microstructures that can provide clues regarding each of these processes. After several years of careful studies of corroded glass microstructures of different compositions using electron microscopy at cryo-temperatures, it appears that in general the alteration layers of glasses corroded at high temperatures consist of more or less five sub layers. Different layers have different sensitivities to electron beam exposure but most of the layers are unstable to electron beam exposures at room temperature with electron exposures of only a few minutes leading to their destruction. The presentation will highlight the necessity of using cryo-temperatures to fully grasp the correct microstructural detail of the alteration layers at nanoscale and the potential role of various sub bands in glass passivation. However, it is worth highlighting that glass microstructures have been studied and documented for hundreds of years starting with optical microscopy and the use of Cryo-TEM in this pursuit is only a recent addition. Therefore, in addition to discussing the recent nanoscale microstructures, the aim of this presentation is to provide a comprehensive historical to present day overview of corroded glass microstructures starting from 1860s work of Sir David Brewster using optical microscopy. This was subsequently followed up by two world renowned physicists, Lord Rayleigh, and C V Raman from 1900s to 1940s and then by several other important works from 1940s to 1980s. The presentation will also discuss the struggles scientists had to endure to study corroded glass microstructures (even with optical microscopy) and give an overview of the present-day best practices in pursuit of studying the microstructures at nanoscale.

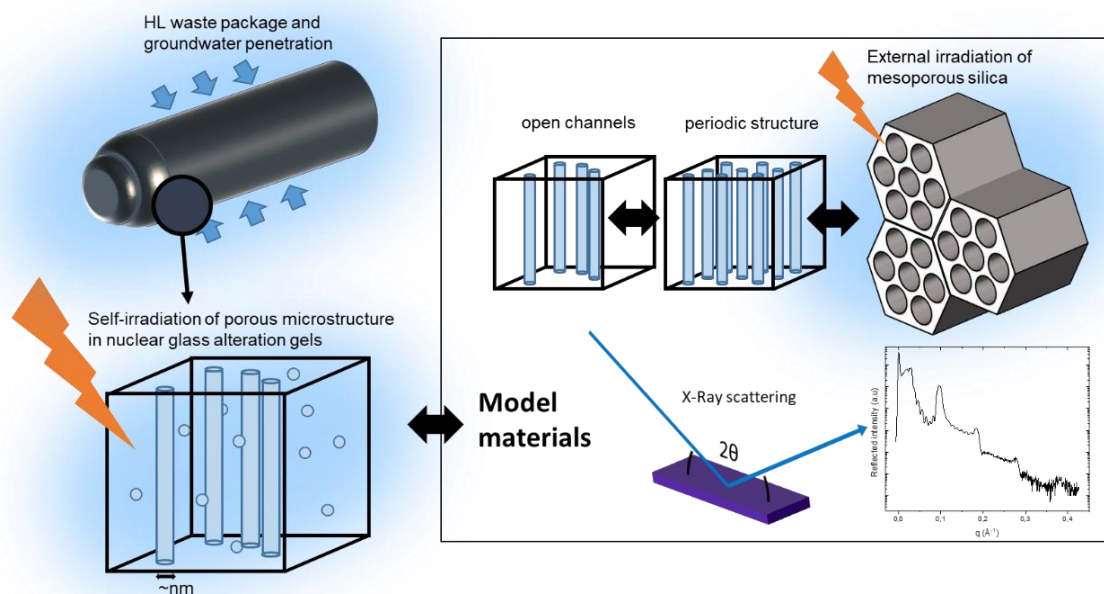
Compared Radiation Stability of Mesoporous Silica and Nuclear Glass Alteration Gels

Pierre De Laharpe^{*}1, Xavier Deschanel¹, Sylvain Peugeot², Helene Arena², Melanie Taron^{1,2}, Jun Lin¹, Bertrand Siboulet¹, Jean-Marc Delaye²

¹ ICSM, CEA, CNRS, Univ. Montpellier, Marcoule, France

² CEA, DES, ISEC, CMPE, Marcoule, France

*pierre.delaharpe@cea.fr



Among the numerous scientific challenges pertaining to high-level nuclear waste vitrification and deep geological burial, the alteration of nuclear glass by groundwater combined with the waste package's self-irradiation are still being studied [1]. Several studies conducted on simplified borosilicate glass compositions (including CJ2: $\text{SiO}_2\text{-AlO}_2\text{-B}_2\text{O}_3\text{-Na}_2\text{O}$) have established that reproducing the damage caused by nuclear collision via external irradiation, prior to aqueous alteration, increases the formation rate of the glass' alteration gel. Its nanometer-scale porosity, which features closed pores as well as open channels, develops faster as well. [2]. This acceleration correlates with higher water mobility across the altered layer, challenging the durability performance of the glass. However, other recent results highlighted the possible collapse of this porous microstructure when irradiating CJ2 alteration gel with a Xe, 600 keV ion beam, where TEM images demonstrated a complete shrinkage of the observed pores [3]. Due to high vacuum and low temperature in the experimental setup, the influence of certain parameters, such as the presence or absence of pore water, remains unclear. Further research is required to rationalize this possible competing process.

To allow some degree of fundamental understanding and experimental practicality, hexagonal mesoporous silica can serve as model materials to perform ion irradiation experiments assessing on nanometer-scale porous structures. X-ray scattering measurement techniques have already been proved appropriate to monitor the pore collapse of SBA-15 and

MCM-41 thin films and powders in several irradiation regimes [4], [5]. Exploratory ion irradiation experiments (Xe, 92 MeV and Ne, 20 MeV) were performed in the past year on SBA-15 and MCM-41 thin films derivatives immersed in water, leading to an overall reduction of pore collapse compared to the dry ones, according to the available analysis tools. (see excerpt on Figure 1)

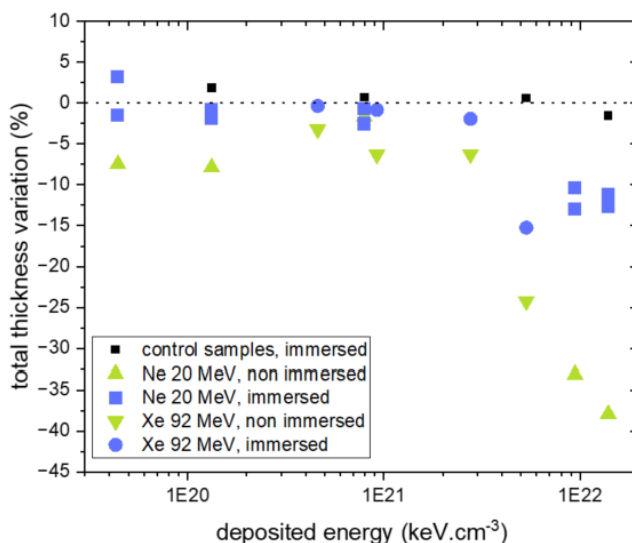


Figure 1 – total thickness reduction of MCM-41 derived thin film irradiated under Ne and Xe ion beams, comparing between dry samples and samples immersed in water prior to irradiation

In this work, we set out to further study this process and assess the comparability between model materials and alteration gels in various irradiation conditions. Dedicated analysis tools are improved to describe the microstructural evolution in both types of materials. Furthermore, radiation-induced displacement cascades are replicated in molecular dynamics simulations in the ballistic regime and compared to the literature [6]. Finally, in comparative experiments, mesoporous silica thin films and alteration gels are irradiated in an environmental TEM apparatus for a more comprehensive description.

- [1] S. Gin, P. Jollivet, M. Tribet, S. Peugeot, et S. Schuller, « Radionuclides containment in nuclear glasses: an overview », *Radiochim. Acta*, vol. 105, n° 11, p. 927-959, nov. 2017, doi: 10.1515/ract-2016-2658.
- [2] A. Jan et al., « Radiation effects on the structure and alteration behavior of an $\text{SiO}_2\text{-Al}_2\text{O}_3\text{-B}_2\text{O}_3\text{-Na}_2\text{O}$ glass », *Int. J. Appl. Glass Sci.*, vol. 14, n° 1, p. 113-132, janv. 2023, doi: 10.1111/ijag.16618.
- [3] A. H. Mir, A. Jan, J.-M. Delaye, S. Donnelly, J. Hinks, et S. Gin, « Effect of decades of corrosion on the microstructure of altered glasses and their radiation stability », *Npj Mater. Degrad.*, vol. 4, n° 1, p. 11, déc. 2020, doi: 10.1038/s41529-020-0115-0.
- [4] Y. Lou et al., « Structure evolution of mesoporous silica SBA-15 and MCM-41 under swift heavy ion irradiation », *Nucl. Instrum. Methods Phys. Res. Sect. B Beam Interact. Mater. At.*, vol. 365, p. 336-341, déc. 2015, doi: 10.1016/j.nimb.2015.08.009.
- [5] J. Lin et al., « A multiparametric study on the behavior of mesoporous silica under electron irradiation », *Materialia*, vol. 32, p. 101903, déc. 2023, doi: 10.1016/j.mtl.2023.101903.
- [6] Y. Lou, B. Siboulet, S. Dourdain, M. R. Rafiuddin, X. Deschanel, et J.-M. Delaye, « Molecular dynamics simulation of ballistic effects in mesoporous silica », *J. Non-Cryst. Solids*, vol. 549, p. 120346, déc. 2020, doi: 10.1016/j.jnoncrysol.2020.120346.

Insights into the Structural and Redox Chemistry of Cr-doped (Ln,U)O₂ Materials

Daniil Shirokiy,¹ Maximilian Henkes,¹ Andrey Bukaemskiy,¹ Kristina O. Kvashnina,² Martina Klinkenberg,¹ Philip Kegler,¹ Dirk Bosbach,¹ and Gabriel L. Murphy,¹

¹ Institute of Energy and Climate Research, Forschungszentrum Jülich GmbH, 52428 Jülich, Germany

² The Rossendorf Beamline at ESRF, The European Synchrotron, CS40220, 38043, Grenoble, Cedex 9, France

Cr-doped UO₂ nuclear fuels have endured sustained interest from industry and researchers due to the superior in-reactor performance they possess over traditional non-doped variants (UO₂). The ubiquitous generation of spent nuclear fuel (SNF) is a challenge that impacts many nations, regardless of fuel type. Direct disposal of SNF into deep geological repositories is the preferred method for nations including German and Finland among many others but requires long-term understanding of the SNF stability that is often ensured for 1 000 000 years according to StandAG §1. Consequently, researching the structural and chemical stability of SNF is crucial aspect of nuclear waste management. Despite high, increased in-reactor performance and reduced in bulk waste generation of Cr-doped UO₂ fuels, their chemistry and structural properties within SNF are still poorly studied. Specifically potential interaction of Cr with trivalent cations of lanthanides (Ln) and minor actinides (MA) (e.g., Nd³⁺, Gd³⁺, Am³⁺, Cm³⁺) and Pu⁺³ may lead to the formation of alteration phases such as perovskite ((Ln³⁺/MA³⁺)Cr³⁺O₃) which may impact stability both in-reactor and as SNF. Accordingly, we have been exploring the formation of such phases via the preparation of model system materials, under conditions that are relevant to Cr-doped UO₂. This involves the systematic synthesis of Cr-doped ((U_{1-x}Ln_x)O₂) for Ln = La, Ce, Pr, Gd, Ho, Lu. These materials have been subject to high resolution structural and redox analysis using synchrotron X-ray powder diffraction (S-PXRD) and high-energy resolution fluorescence diffraction-X-ray absorption near-edge structure spectroscopy measurements (HERFD-XANES) performed at BM20 beamline of the European Synchrotron Radiation Facility (ESRF). These measurements, supported by Raman spectroscopy mapping and scanning electron microscopy, allow the occurrence of specific alteration phases to be observed in Cr-doped UO₂ when encountering lanthanides. These results will be discussed in detail with respect to the current knowledge of Cr-doped UO₂ and classical UO₂ chemistry in the context of nuclear waste management. In summary the findings might potentially have important implications for the long-term performance of nuclear waste repositories and the design of new materials for nuclear applications.

Simulating Auto-Irradiation of Glass Using External Irradiation Beams: Impact on Glasses Structure and Properties

M. Taron ^{1,2}, **H. Aréna** ¹, C. Gillet ¹, F. Perrudin ¹, R. Podor ², M. Tribet ¹, S. Miro ¹, S. Peugeot ¹

¹ CEA, DES, ISEC, DPME, Université de Montpellier, Marcoule, France

² Institut de Chimie Séparative de Marcoule, ICSM, CEA, CNRS, ENSCM, Univ Montpellier, Marcoule, France

In the current context of nuclear waste management, the fission products and minor actinides are vitrified in a borosilicate matrix and intended for long-term disposal in a deep geological repository. After several thousands of years, groundwater is expected to resaturate the clay host, then corrode the metallic canister and encounter the glass packages. The long-term behavior of glass under these conditions needs to be studied to guarantee the efficient containment of radionuclides. Glass self-irradiation is a key parameter because it impacts the glass properties and thereby its behavior¹. Alteration experiments conducted on radioactive glasses are cumbersome to carry out, as they have to take place in hot environments (glove boxes or shielded cells). Therefore, external irradiations are used to simulate the impact of self-irradiations on the glass structure and properties². Nuclear glasses will suffer from both electronic and nuclear damages, due to alpha and beta disintegrations, and to gamma transitions.

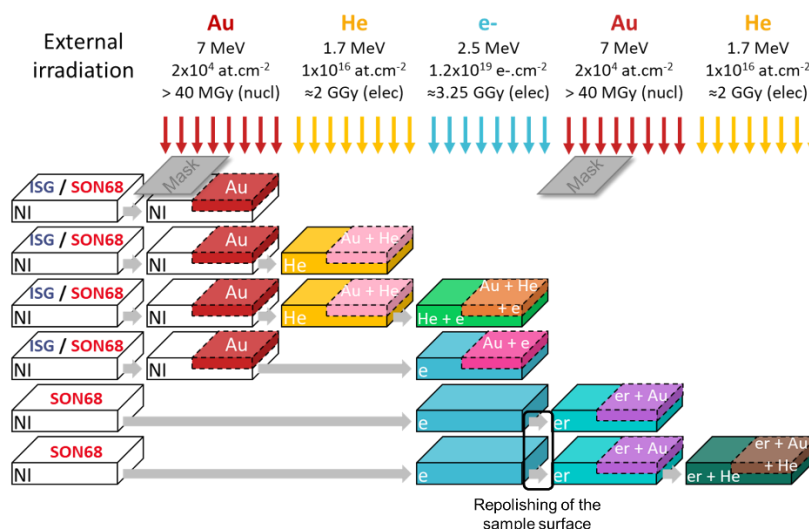


Figure 1: Scheme of the irradiation scenarios performed on the glass coupons.

In this work, the structural changes induced by different irradiation scenarios of a complex SON68 type glass as well as its equivalent simple glass ISG are studied. The effect of various couplings between nuclear and electronic interactions using different electronic stopping power S_e are simulated by Au and He ions and electron irradiations. 2.5 MeV electron irradiations simulate the damage of beta and gamma radiations at saturation of the damage effects. 7 MeV Au irradiations and 1.7 MeV He simulate the damage of the recoil nuclei of alpha decays and alpha particles respectively. Au irradiations induce mainly nuclear interactions with matter while the electron and He irradiations lead to electronic interactions, except at the end of the path for He, but correspond to different stopping powers (higher for He than for electrons). Sequential irradiations are performed to reproduce the coupling effect of these different interactions to mimic the case of self-irradiation in nuclear glasses, leading to 8 to 12 irradiation scenarios (Figure). This work compares the structural damage induced by the various irradiation scenarios to help to understand the coupling effects between nuclear and electronic interactions.

The modifications on the structure and properties of the glass (swelling, hardness) are determined by several characterization technics like Raman spectrometry, Fourier Transform Infrared Spectroscopy, micro-indentation and optical interferometry³.

- 1 Gin, S., Jollivet, P., Tribet, M., Peugeot, S. & Schuller, S. Radionuclides containment in nuclear glasses: an overview. *Radiochim. Acta* **105**, 927-959, doi:10.1515/ract-2016-2658 (2017).
- 2 Mir, A. H. & Peugeot, S. Using external ion irradiations for simulating self-irradiation damage in nuclear waste glasses: State of the art, recommendations and prospects. *J. Nucl. Mater.* **539**, 152246, doi:https://doi.org/10.1016/j.jnucmat.2020.152246 (2020).
- 3 Gillet, C. *et al.* Impact of complex irradiation scenarios on the structure and the properties of the International Simple Glass. *J. Nucl. Mater.* **572**, doi:10.1016/j.jnucmat.2022.154079 (2022).

The Influence of pH, Ionic Strength and Temperature on Cs, Ba, Co, and Eu Sorption on Biotite – Experiments and Modelling

Pawan Kumar, **Stellan Holgersson**, Christian Ekberg

*Department of Chemistry and Chemical Engineering, Division of Nuclear Chemistry
Chalmers University of Technology, Kemivägen 4, SE-41296 Göteborg, Sweden*

Abs The sorption behavior of ^{134}Cs , ^{133}Ba , ^{60}Co and ^{152}Eu , in a mixture, at tracer concentration [$\sim 10^{-8}$ M] on crushed Na-converted biotite (particle size 0.25–0.5 mm) was investigated by the batch sorption experiment with S:L ratio of 1:50 under the inert gas conditions ($[\text{O}_2] < 1\text{ppm}$) for up to two months. The experiment was carried out in triplicate with pH adjusted to 5, 6, 7, 8 or 9 with buffered solutions of 0.001, 0.01 and 0.1 M NaClO_4 at 40 and 60 °C.

Titration experiments on the biotite surface were conducted over a pH range of around 3 to 11 at 40 and 60 °C respectively. The results were modelled to obtain $\text{pK}_{a,1} = -7.10 \pm 0.05$ at 40°C and -6.93 ± 0.32 at 60 °C, $\text{pK}_{a,2} = -4.90 \pm 0.32$ at 40°C, and -5.00 ± 0.13 at 60°C using PHREEQC chemical speciation calculations coupled with an error minimization routine.

Sorption results for the pH-range 5–9 show that for Cs, Ba, Co, and Eu, at 40°C and $I = 0.001\text{M}$ the R_d values were 0.6–2.3, 0.2–3.8, 0.01–4.0 and 2.4–11.3 m^3/kg respectively. Corresponding results for 40°C and $I = 0.01\text{M}$ were $R_d = 0.2$ –0.8, 0.03–5.1, 0.01–10.9 and 0.2–22.3 m^3/kg and for 40°C and $I = 0.1\text{M}$, were $R_d = 0.05$ –0.2, 0.02–0.4, 0.01–8.61 and 2.7–13.63 m^3/kg .

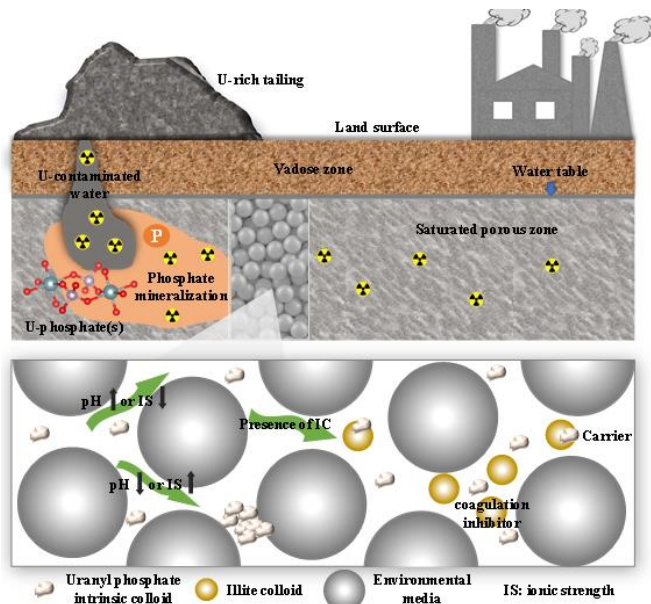
For 60°C and $I = 0.001\text{M}$ the R_d values for Cs, Ba, Co, and Eu were 0.7–7.8, 0.3–4.4, 0.03–5.77 and 3.1–18.3 m^3/kg respectively. Corresponding results for 60°C and $I = 0.01\text{M}$ were $R_d = 0.2$ –3.2, 0.02–8.1, 0.01–19.3 and 0.2–22.9 m^3/kg and for 60°C and $I = 0.1\text{M}$ $R_d = 0.1$ –0.9, 0.1–0.8, 0.01–18.0 and 5.3–30.0 m^3/kg .

The sorption of all four elements is dependent on pH, ionic strength, and temperature. A computer code was developed that coupled PHREEQC geochemical modeling software with PYTHON programming language to fit the sorption experimental data with the compensation for biotite dissolution. Sorption of all metals was successfully modelled with a combination of one amphoteric (i.e. 2- pK_a) surface complexation site and one ion exchange site. The model was fitted to the data without any compensation for electrostatic effects. The modeling result shows that the Cs sorption is primarily governed by two surface species: $\equiv\text{SOCs}$, a surface complex, and CsX , an ion exchange species. However, in the case of Ba, two surface complexes: $\equiv\text{SOBa}^+$ and $\equiv\text{SOBaOH}$ and one ion-exchange species, BaX_2 , mainly contribute to sorption. The Co sorption data was fitted by considering three-surface complexes: $\equiv\text{SOCo}^+$, $\equiv\text{SOCoOH}$, and $\equiv\text{SOCo}(\text{OH})_2^-$ but no ion exchange is involved. The model predicts that Eu is sorbed as three different surface complexes: $\equiv\text{SOEu}^{2+}$, $\equiv\text{SOEuOH}^+$, and $\equiv\text{SOEu}(\text{OH})_2$, and in addition, also one ion-exchange species EuX_3 .

Colloids Pose an Enhanced Transport Risk of Uranium in Saturated Porous Media: A Challenge for Immobilization Remediation of Uranium Contaminated Site

Duoqiang Pan, Xiaoyan Wei, Xinyi Shi, Weixiang Xiao, Zhen Xu, Wangsuo Wu
MOE Frontiers Science Center for Rare Isotopes, Lanzhou University, Lanzhou 730000, China

The occurrence forms and migration behaviors of uranium in the environment are crucial for nuclear environmental safety assessment. Based on the geochemical process of uranium in the environment, strategies including phosphate, bacteria, and redox reagents treatment, have been proposed to immobilize uranium in the contaminated sites, solutes migration models have been constructed as well to describe and predict uranium migration laws and then evaluate the effectiveness of immobilization remediation. However, the migration distance of on-site monitoring is often greater than the predicted migration results, studies have found that colloids play an important role in radionuclide migration. Uranium is prone to form intrinsic colloids under groundwater environment conditions due to the nucleation and crystallization process, and also easily associates with the widely existed environmental colloids to form pseudo colloids. The existence of colloids significantly affects the occurrence mode and migration law of uranium. In this work, aiming at the migration behavior and interface mechanism of typical uranium colloids, the column experiment method was used to reveal the transport law of uranium intrinsic and pseudo colloids, the colloidal interface reaction process and microscopic mechanism were clarified with the aid of advanced spectroscopic technologies, and the migration law of uranium colloids under different environmental conditions was revealed, and a transport model considering colloidal radionuclides was constructed. The retention, distribution, migration, and fate of key uranium colloids in different types of environmental media were elucidated, and the governing strategies for reducing colloids mobility was proposed. Relevant achievements provide theoretical basis and technical support for the migration mechanism of uranium in geological media and the remediation of contaminated site, and provide important reference for nuclear environmental safety assessment.



Processes Driven by Iron Reducing Bacteria on Technetium Immobilization

Cardaio L., Müller K., Cherkouk A., Stumpf T., Mayordomo N.

Institute of Resource Ecology, Helmholtz-Zentrum Dresden-Rossendorf e.V., Dresden

Technetium (Tc) is the element 43 of the periodic table, with the configuration $[\text{Kr}]4d^5s^2$ and an estimated number of 45 isotopes, being ^{99}Tc the most relevant. ^{99}Tc is a β^- emitter with a long half-life ($t_{1/2} = 2.13 \cdot 10^5 \text{ a}$). ^{99}Tc is a fission product of ^{235}U and ^{239}Pu and it can also originate from the decay chain of metastable technetium-99 (^{99m}Tc), a short-lived isotope ($t_{1/2} = 6.01 \text{ h}$) [1]. Thus, the release of technetium in the environment is mainly due to reprocessing of spent nuclear fuel, for example in nuclear plants such as Sellafield (UK) and La Hague; nuclear energy production, nuclear weapon detonation and the wide use of ^{99m}Tc in radiodiagnostic techniques [2].

Technetium can be present in many oxidation states, which range from $-I$ to $+VII$. The most common states in the environment are Tc^{VII} and Tc^{IV} in absence of stabilizing organic ligands. Under oxidizing conditions, technetium would rather occur as Tc^{VII} in the form of pertechnetate ($\text{Tc}^{VII}\text{O}_4^-$), whereas Tc^{IV} prevails under reducing conditions. The high solubility in aqueous phases and poor ability of interactions with mineral surfaces make pertechnetate a very mobile hazardous anion. In contrast, Tc^{IV} mobility in water is limited due to its reduced solubility and interactions with mineral surfaces such as co-precipitation or incorporation in minerals, such as Fe^{II} minerals [3; 4].

Deep geological repositories (DGRs) for the safe long-term storage of hazardous and long-lived radiotoxic waste are conceptualized as multi-barrier systems based on (geo)technical and geologic layers [5]. Bentonite clay, as geotechnical barrier is considered a good candidate to act as buffer material for the retention of radionuclides. The clay harbors indigenous microorganisms as well, such as anaerobic bacteria which, through their natural production of acidic metabolites, can induce highly complex environments, and alter the chemical conditions and the integrity of the materials present in the DGR [6]. Thus, the influence of bacteria and bacterial induced processes on Tc (im)mobilization needs to be understood in detail on a macroscopic and molecular level.

In this work, we have studied the influence of *Desulfitobacterium* sp. G1-2 on Tc mobility. It is a novel isolate extracted from FEBEX bentonite [7]. The *Desulfitobacterium* genus utilizes different forms of ferric iron (e.g. $\text{Fe}^{\text{III}}\text{Cl}_2$, Fe^{III} citrate) as electron acceptor for the external electron transfer of the anaerobic respiratory chain [8; 9].

In the first step, *Desulfitobacterium* sp. G1-2 was grown in a liquid medium in presence of Fe^{III} citrate [10]. The bacterial growth was followed by cell counting, and the consumption of Fe^{III} and production of Fe^{II} was analyzed by ferrozine assay. During the growth of the bacteria, the formation of a white precipitate was observed. Raman microscopy and X-ray diffraction confirmed the identity of the precipitate as vivianite ($\text{Fe}^{\text{II}}_3(\text{PO}_4)_2 \cdot 8\text{H}_2\text{O}$) [11; 12].

In the second step, the biogenic vivianite was extracted and isolated, to study its interaction with Tc as a function of time, pH, ionic strength, and Tc concentration. Sorption experiments were performed to study the yield of Tc retention by biogenic vivianite. In addition, microscopic and spectroscopic methods (Raman microscopy, scanning electron microscopy, X-ray photoelectron spectroscopy, and X-ray absorption spectroscopy) were used to determine the molecular environment of Tc in the solid. It was shown that Tc immobilization by biogenic vivianite is due to the reduction of Tc^{VII} to Tc^{IV} and it is dependent on time, and pH. The Tc activity in solution decreased with more basic environments, reaching the lowest value at pH 11. It was also observed, that at $\text{pH}_{\text{eq}} \approx 8.5$, Tc removal from the aqueous phase in presence of biogenic vivianite reached 94% after seven days of interaction.

References

- [1] Johnstone, E. V., Yates, M. A., Poineau, F., Sattelberger, A. P., Czerwinski, K. R. (2017). Technetium: The First Radioelement on the Periodic Table. *Journal of Chemical Education*, 94(3), 320–326. <https://doi.org/10.1021/acs.jchemed.6b00343>
- [2] Meena, A. H., Arai, Y. (2017). Environmental geochemistry of technetium. In *Environmental Chemistry Letters* (Vol. 15, Issue 2, pp. 241–263). Springer Verlag. <https://doi.org/10.1007/s10311-017-0605-7>
- [3] Schmeide, K., Rossberg, A., Bok, F., Shams Aldin Azzam, S., Weiss, S., Scheinost, A. C. (2021). Technetium immobilization by chukanovite and its oxidative transformation products: Neural network analysis of EXAFS spectra. *Science of the Total Environment*, 770. <https://doi.org/10.1016/j.scitotenv.2021.145334>
- [4] Rodríguez, D. M., Mayordomo, N., Scheinost, A. C., Schild, D., Brendler, V., Müller, K., Stumpf, T. (2020). New Insights into 99Tc(VII) Removal by Pyrite: A Spectroscopic Approach. *Environmental Science and Technology*, 54(5), 2678–2687. <https://doi.org/10.1021/acs.est.9b05341>
- [5] Ruiz-Fresneda, M. A., Martínez-Moreno, M. F., Povedano-Priego, C., Morales-Hidalgo, M., Jroundi, F., Merroun, M. L. (2023). Impact of microbial processes on the safety of deep geological repositories for radioactive waste. *Frontiers in Microbiology*, 14. <https://doi.org/10.3389/fmicb.2023.1134078>
- [6] Matschiavelli, N., Kluge, S., Podlech, C., Standhaft, D., Grathoff, G., Ikeda-Ohno, A., Warr, L. N., Chukharkina, A., Arnold, T., Cherkouk, A. (2019). The Year-Long Development of Microorganisms in Uncompacted Bavarian Bentonite Slurries at 30 and 60 °C. *Environmental Science and Technology*, 53(17), 10514–10524. <https://doi.org/10.1021/acs.est.9b02670>
- [7] Drozdowski, J., Lopez-Fernandez, M., Kluge, S., Cherkouk, A., Institute of Resource Ecology 2018 *Annual report*. HZDR-096 (2019) p. 40. <https://www.hzdr.de/publications/Publ-28898>
- [8] Shelobolina, E. S., Vanpraagh, C. G., Lovley, D. R. (2003). Use of ferric and ferrous iron containing minerals for respiration by *Desulfitobacterium frappieri*. *Geomicrobiology Journal*, 20(2), 143–156. <https://doi.org/10.1080/014904503003884>
- [9] Villemur, R., Lanthier, M., Beaudet, R., Lépine, F. (2006). The *Desulfitobacterium* genus. In *FEMS Microbiology Reviews* (Vol. 30, Issue 5, pp. 706–733). <https://doi.org/10.1111/j.1574-6976.2006.00029.x>
- [10] DSMZ 579, DSMZ - German Collection of Microorganisms and Cell Cultures GmbH. https://www.dsmz.de/microorganisms/medium/pdf/DSMZ_Medium579.pdf; Accessed on 19.12.23
- [11] International Centre for Diffraction Data, <https://www.icdd.com/>
- [12] RRUFF ID: R050076, RRUFF™ Project, <https://rruff.info/Vivianite/R050076>

SAFEGUARDS AND ANALYTICAL CHEMISTRY

Real-Time and Automated Process Control via On-Line Monitoring

Amanda M. Lines,^{1*} Poki Tse,¹ Nathan Bessen,¹ Thomas Serrano,¹ Alyssa Espley,¹ Gilbert Nelson,² Gabriel B. Hall,¹ Jarrod R. Allred,¹ Gregg J. Lumetta,¹ and Samuel A. Bryan¹

¹ Pacific Northwest National Laboratory, 902 Battelle Boulevard, Richland, WA 99352

² College of Idaho, 2112 Cleveland Blvd. Caldwell, ID 83605

Integration of on-line monitoring into nuclear materials processes can enable game-changing benefits to reduce costs, improve safety, allow for material tracking, avoid process upsets and more. Focusing on optical spectroscopy-based monitoring systems will enable chemical characterization and quantification. This approach has the additional benefits of allowing for fast, non-destructive analysis with robust probes capable of handling the harsh environments typical of nuclear applications. These can be and have been applied to a wide range of process types, including aqueous and nonaqueous liquids, gases, solids, and molten salts.¹⁻⁴ Furthermore, optical spectroscopy can be optimized for a wide range of process scales from microscale ($\sim\mu\text{L}/\text{min}$) to macroscale ($>100\text{ L}/\text{hr}$).⁵⁻⁷ Finally, complex process streams will often exhibit similarly complex spectral data that, traditionally, would hinder accurate analysis. The application of advanced, chemical data science in the form of chemometric analysis can allow for successful characterizations of complex, multicomponent reprocessing streams.^{8,9} Overall, optical spectroscopy-based monitoring systems can provide chemical characterization and quantification within a wide range of nuclear applications.

Examples of applications include looking at uranium within molten salts, hydrogen isotopes in the gas phase, and separations of actinides within a co-decontamination (CoDCon) process stream.¹⁰ In all these examples optical tools such as ultraviolet-visible (UV-vis) absorbance and/or Raman spectroscopy were used in conjunction with chemometric analysis to identify and quantify chemical targets within complex chemical systems. This was taken further with the CoDCon separation where optical on-line monitoring was used to enable real-time process control. In this flowsheet operators were aiming to produce a mixture of U and Pu with a U/Pu mass ratio of 7/3. Because real-time process control cannot feasibly be achieved by collecting and analyzing grab samples, on-line monitoring is required. In this demonstration, operators made manual process adjustments based on current product stream composition to produce the desired U/Pu ratio. Note, in this system, sensor fusion was utilized to monitor multiple actinide targets within multiple inlet and outlet streams simultaneously. Targets included Pu(III), Pu(IV), Pu(VI), U(IV), U(VI) and nitric acid.

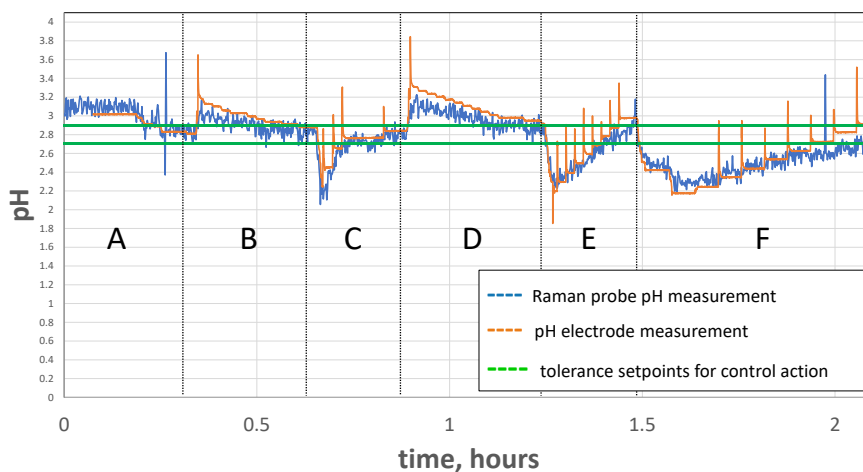


Figure 1: pH response during batch control experiment during 5 control periods, A-F.

More recently, a demonstration of automated process control was completed. This focused on utilizing Raman spectroscopy partnered with chemometric analysis to monitor the pH of a citric acid buffer system. Monitoring output was

fed into custom control software that could then actuate pumps to add in acid or base as needed to achieve target process pH. This was demonstrated in two significant experiments. The first was a simple batch process where a chemical system buffered with citric acid was monitored while pH was perturbed manually by researchers. As pH was pushed outside of the acceptable range set within the control software, the automated system actuated pumps to add acid or base as needed to push the batch back to desired pH, with the pH response demonstrated in Figure 1. Building on this, the second experiment was a repeat experiment looking at a TALSPEAK and Advanced TALSPEAK separations on a bank of centrifugal contactors. Within these repeat systems the aqueous feed consisted of the citric acid buffer system and two non-rad metal targets: neodymium and holmium. The TALSPEAK and Advanced TALSPEAK systems are particularly interesting to explore in this pH control demo because they exhibit pH sensitivity in the separation efficiencies of metal targets. The pH of the aqueous feed was manually perturbed which impacted separation of metal targets. All process inlets and outlets were fitted with both Raman and UV-vis optical sensors to allow operators to characterize separation efficiency in real time. As pH of the feed was manually perturbed outside of ideal operating conditions, changes in separation performance could be observed in the aqueous and organic outlets. However, the automated system successfully detected changes in pH and added needed acid or base to push the feed-back to desired pH. As this occurred, separation of metal targets was seen to reset into original steady-state.

Overall, this work presents a strong case of the utilization of optical monitoring to allow for automated process control of nuclear material processes. This talk will provide an overview of the automated pH control approach and results while also outlining the flexibility and range of application of optical-based monitoring within the nuclear field.

References

1. Casella, A. J.; Ahlers, L. R. H.; Campbell, E. L.; Levitskaia, T. G.; Peterson, J. M.; Smith, F. N.; Bryan, S. A., Development of Online Spectroscopic pH Monitoring for Nuclear Fuel Reprocessing Plants: Weak Acid Schemes. *Anal Chem* **2015**, *87* (10), 5139-5147.
2. Casella, A. J.; Levitskaia, T. G.; Peterson, J. M.; Bryan, S. A., Water O-H Stretching Raman Signature for Strong Acid Monitoring via Multivariate Analysis. *Anal Chem* **2013**, *85* (8), 4120-4128.
3. Schroll, C. A.; Lines, A. M.; Heineman, W. R.; Bryan, S. A., Absorption spectroscopy for the quantitative prediction of lanthanide concentrations in the 3LiCl-2CsCl eutectic at 723 K. *Anal Methods-Uk* **2016**, *8* (43), 7731-7738.
4. Felmy, H. M.; Clifford, A. J.; Medina, A. S.; Cox, R. M.; Wilson, J. M.; Lines, A. M.; Bryan, S. A., On-Line Monitoring of Gas-Phase Molecular Iodine Using Raman and Fluorescence Spectroscopy Paired with Chemometric Analysis. *Environ Sci Technol* **2021**.
5. Nelson, G. L.; Asmussen, S. E.; Lines, A. M.; Casella, A. J.; Bottenus, D. R.; Clark, S. B.; Bryan, S. A., Micro-Raman Technology to Interrogate Two-Phase Extraction on a Microfluidic Device. *Anal Chem* **2018**, *90* (14), 8345-8353.
6. Nelson, G. L.; Lines, A. M.; Casella, A. J.; Bello, J. M.; Bryan, S. A., Development and testing of a novel micro-Raman probe and application of calibration method for the quantitative analysis of microfluidic nitric acid streams. *Analyst* **2018**, *143* (5), 1188-1196.
7. Mattio, E.; Caleyron, A.; Miguiditchian, M.; Lines, A. M.; Bryan, S. A.; Lackey, H. E.; Rodriguez-Ruiz, I.; Lamadie, F., Microfluidic In Situ Spectrophotometric Approaches to Tackle Actinides Analysis in Multiple Oxidation States. *Appl Spectrosc* **2022**, *76* (5), 580-589.
8. Lines, A. M.; Adami, S. R.; Sinkov, S. I.; Lumetta, G. J.; Bryan, S. A., Multivariate Analysis for Quantification of Plutonium(IV) in Nitric Acid Based on Absorption Spectra. *Anal Chem* **2017**, *89* (17), 9354-9359.
9. Lines, A. M.; Nelson, G. L.; Casella, A. J.; Bello, J. M.; Clark, S. B.; Bryan, S. A., Multivariate Analysis To Quantify Species in the Presence of Direct Interferents: Micro-Raman Analysis of HNO₃ in Microfluidic Devices. *Anal Chem* **2018**, *90* (4), 2548-2554.
10. Lines, A. M.; Hall, G. B.; Asmussen, S.; Allred, J.; Sinkov, S.; Heller, F.; Gallagher, N.; Lumetta, G. J.; Bryan, S. A., Sensor Fusion: Comprehensive Real-Time, On-Line Monitoring for Process Control via Visible, Near-Infrared, and Raman Spectroscopy. *Acs Sensors* **2020**, *5* (8), 2467-2475.

Photonic Lab-On-A-Chip, a Versatile and Powerful Tool for R&D Studies on Spent Fuel Reprocessing

Fabrice Lamadie^{1*}, Elodie Mattio¹, Manuel Miguirditchian¹, Amanda M. Lines², Samuel A. Bryan², Hope E. Lackey², Fabrice Onofri³, Isaac Rodriguez-Ruiz⁴

¹ CEA, DES, ISEC, DMRC, Univ Montpellier, 30207 Bagnols-sur-Ceze, Marcoule, France

² Pacific Northwest National Laboratory, Richland, Washington 99352, United States

³ Aix-Marseille University, CNRS, IUSTI, UMR 7343, Marseille, France

⁴ Laboratoire de Génie Chimique - CNRS, UMR 5503, Toulouse, France

* Corresponding Author, E-mail: fabrice.lamadie@cea.fr

The study and development of present and future processes for the recycling of spent nuclear fuels require many steps, from design in the laboratory to setting up on an industrial scale. Analysis and instrumentation are crucial in all of these steps. These developments are increasingly carried out on milli/microfluidic devices for scientific reasons (small-scale studies, control of phenomena, etc.) and to minimize costs, risks, and waste. The logic is the same for the chemical analyses associated with their follow-up and interpretation. Due to this, over the last few years, opto/microfluidic analysis devices adapted to the monitoring of different processes (dissolution, liquid/liquid extraction, precipitation, etc.) have been increasingly designed and developed. This communication will review 5 years of photonic lab-on-a-chip (PhLoC) development and show how this technology (cf. Figure 1) can be a suitable and powerful tool to monitor several steps along the PUREX process (Plutonium Uranium Reduction Extraction).

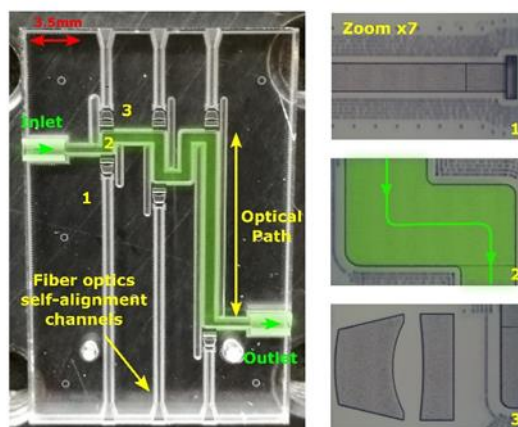


Figure 1: Left, typical picture of a glass made PhLoC with three optical path (1.0, 3.5 and 15mm) – Right, zoom on the main integrated optical elements.

This scientific communication will be organized as follows. First, the PhLoC concept and the integration of optical components at microfluidic scale on lab-on-chips will be reviewed. Second, different manufacturing processes as well as the suitability of the different materials for the harsh environment of nuclear process R&D will be discussed. Finally, based on the design shown in Fig.1, two typical applications will be presented and discussed in detail:

- One on the use of the PhLoC platform has a tool to tackle actinides analysis in multiple oxidation states even in mixtures over wide concentration ranges and above all with the same degree of simplicity and accuracy of a lab-scale UV-Vis spectrometer, but using minute amounts of sample (Fig.2 right).
- One on the measurement of optically diluted colloidal suspensions of silica (SiO_2) and polystyrene nanoparticles, with sizes from 30 nm to 0.5 μm and volume concentrations from 1 to 1000 ppm, for both static and dynamic flow conditions (Fig.2 left).

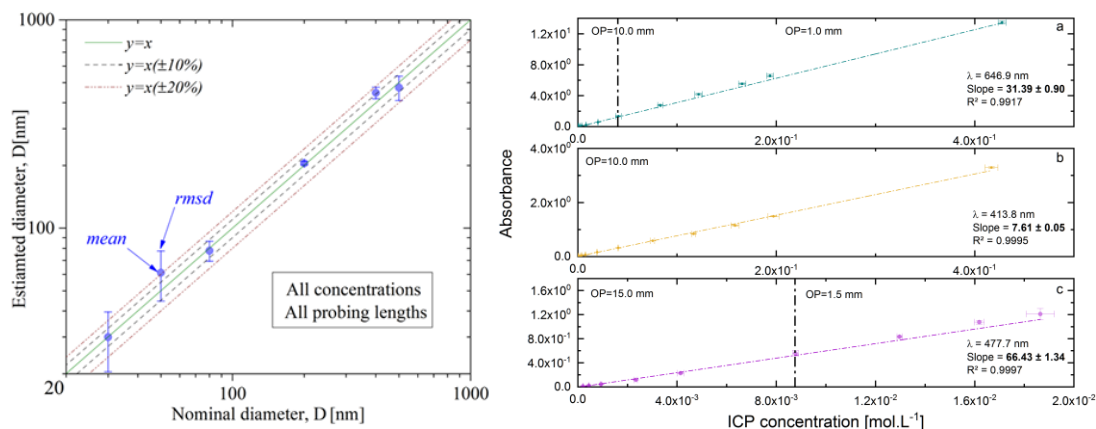


Figure 2: Left, nanoparticles mean diameter measurements for different calibrated suspensions (SiO_2 , Latex); Right, Concentration measurements for three major actinides of the PUREX process, U(IV), U(VI), and Pu(IV).

As a conclusion, some perspectives and examples of future PhLoC design will be drawn, notably with regard to the characterization of more complex solid suspensions or the coupling of measurement techniques (e.g. UV-Vis and Raman spectroscopy).

References

- (1) Rodríguez-Ruiz I, Lamadie F, Charton S., *Uranium(VI) On-Chip Microliter Concentration Measurements in a Highly Extended UV-Visible Absorbance Linearity Range*, Analytical Chemistry 2018; 90: 2456–2460.
- (2) Elodie Mattio, Audrey Caleyron, Manuel Miguiditchian, Amanda M. Lines, Samuel A. Bryan, Hope E. Lackey, Isaac Rodriguez-Ruiz and Fabrice Lamadie, *Microfluidic In Situ Spectrophotometric Approaches to Tackle Actinides Analysis in Multiple Oxidation States*, Applied Spectroscopy 2022, Vol. 0(0) 1–10.
- (3) Mattio E., Lamadie F., Rodriguez-Ruiz I., Cames B., Charton S., *Photonic Lab-on-a-Chip analytical systems for nuclear applications: optical performance and UV-Vis-IR material characterization after chemical exposure and gamma irradiation*, Journal of Radioanalytical and Nuclear Chemistry (2020) 323:965–973.
- (4) Onofri F.R.A., Rodriguez-Ruiz Isaac, Lamadie F., *Microfluidic lab-on-a-chip characterization of nano- to microparticles suspensions by light extinction spectrometry*, Optics Express Vol. 30, No. 2 / 17 Jan 2022.

Real-Time Solution Analysis in Microfluidic Devices using Optical Spectroscopy

Samuel A. Bryan,^{1*} Hope E. Lackey,¹ Gilbert L. Nelson,² Job M. Bello,³ Fabrice Lamadie,⁴ and Amanda M. Lines¹

¹ Pacific Northwest National Laboratory, 902 Battelle Boulevard, Richland, WA 99352

² College of Idaho, Department of Chemistry, 2112 Cleveland Blvd, Caldwell, ID 83605

³ Spectra Solutions Inc. 1502 Providence Highway, Norwood, MA, 02062-4643

⁴ CEA, DES, ISEC, DMRC, Univ. Montpellier, SA2I, 30207 Bagnols-sur-Cèze, Marcoule, France

The advancement of microfluidics and lab-on-a-chip designs has provided a pathway of experimentation that utilizes volumes that are orders of magnitude less than previous techniques. For radioactive applications the benefits of lower dose to workers and equipment, smaller feedstock volumes, and less waste make these techniques of significant interest. With these benefits come the complications of solution analysis, as conventional spectroscopic techniques require much larger volumes. An example is Raman spectroscopy, which has been used extensively for solution analysis; of key interest to the nuclear field is measurement of species such as actinide dioxocations, organic solvent components and complexants, inorganic oxo-anions (NO_3^- , CO_3^{2-} , OH^- , SO_4^{2-} , etc), and pH/acid concentration. Microfluidic devices are a growing field with significant potential for applications to analyzing solutions to minimize waste and dose to equipment and personnel. Much like large scale processing, fast, reliable, and cost-effective means of monitoring streams during processing are needed. Here we apply a novel micro-Raman probe to the on-line monitoring of streams with-in a microfluidic device. For either macro or micro scale process monitoring via spectroscopic response, interfering or confounded bands can obfuscate results. By utilizing chemometric analysis, a form of multivariate analysis, species can be accurately quantified in solution de-spite the presence of overlapping or confounding spectroscopic bands. This is demonstrated on solutions of HNO_3 , NaNO_3 , and $\text{UO}_2(\text{NO}_3)_2$ within micro-flow and microfluidic devices.

Spectroscopy is a common technique that is applied across a range of micro-scale experiments to industrial scale on-line systems.¹⁻³ Typically used for identification and quantification of species, a myriad of spectroscopic techniques are available to isolate the desired analyte signature, including absorbance, fluorescence, infrared, Raman, etc.. In general, spectroscopy is a valuable tool because it provides fast results, employs simple experimental setups, and is nondestructive in nature.

However, spectroscopic analysis can be difficult to apply to complex systems. Analysis of solutions containing multiple species can become difficult when the system exhibits overlapping bands, matrix effects, and baseline shifts.⁴ This is particularly notable when traditional methods of single variate analysis (e.g. Beer's Law) are used to quantify a species based on the spectroscopic response at a single point (e.g. wavelength). The work presented here describes an advanced approach to the analysis of spectroscopic data that allows for accurate and precise identification of species under complex solution conditions. Namely, this work explores the application of multivariate, or chemometric, analysis to the quantification of species in solution where species exhibit confounding bands. This builds on and expands the applicability of previously demonstrated forms of spectroscopic analysis and on-line monitoring.^{3, 5-7}

The instrument that was used to measure Raman from the micro-flow cell employs a fiber optically coupled Raman microscope probe, a 671 nm diode-pumped solids state (DPSS) laser, and a high-throughput volume phase holographic (VPH) grating Raman spectrograph. The Raman microscope probe employs a miniature fiber optic Raman probe with a backscattering optical design and a board level charge coupled device (CCD) video camera for live video imaging of the sample. A dichroic long-pass filter that transmits the 671 nm Raman region and reflects the visible region for imaging is placed in between the CCD camera and the Raman probe. The dichroic filter overlaps the optical axis of the Raman and the video image so that both are focused on the same spot at the sample and thus have a common field of view. A 10x objective lens is used as the focusing lens for the microscope Raman probe, which focuses the laser beam to a very small spot, collects the Raman signal, and also provides a magnified image of the sample. The Raman microscope was packaged in a small handheld probe head with fiber optic connections to the laser and the spectrograph. An Ethernet cable connects the CCD video camera to the computer for live display of the magnified sample image. A custom transmission VPH grating spectrograph with a thermoelectrically (TE)-cooled CCD detector was used to record the Raman signal from the microscope Raman probe. It has a spectral range from 0 cm^{-1} to 3500 cm^{-1} and ~6 cm^{-1} spectral resolution.

This micro-Raman-probe is capable of focusing the laser spot used in Raman spectroscopy to a beam diameter of less than 100 μm . Figure 2 (left) is a photograph of the micro-Raman-probe with the laser excitation beam focused onto a microfluidic flow cell. An image of the laser spot demonstrating a 70- μm beam diameter is shown in Figure 2 (right); this image was acquired using the internal charged couple device (CCD) camera inside the micro-Raman probe.

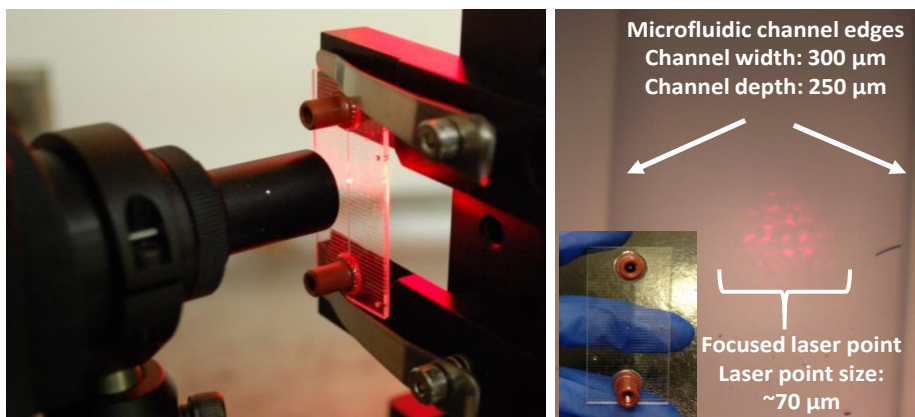


Figure 1: left) Micro-Raman probe with excitation laser focused on a straight path microfluidic device; right) picture taken with on-board camera of micro-Raman probe indicating excitation laser is focused within the solution channel of the microfluidic device.

References

- (1) Casella, A. J.; Ahlers, L. R. H.; Campbell, E. L.; Levitskaia, T. G.; Peterson, J. M.; Smith, F. N.; Bryan, S. A. Development of Online Spectroscopic pH Monitoring for Nuclear Fuel Reprocessing Plants: Weak Acid Schemes. *Anal Chem* **2015**, *87* (10), 5139–5147. DOI: 10.1021/ac504578t.
- (2) Kuswandi, B.; Nuriman; Huskens, J.; Verboom, W. Optical sensing systems for microfluidic devices: A review. *Analytica Chimica Acta* **2007**, *601* (2), 141–155. DOI: 10.1016/j.aca.2007.08.046.
- (3) Nelson, G. L.; Lines, A. M.; Bello, J. M.; Bryan, S. A. Online Monitoring of Solutions Within Microfluidic Chips: Simultaneous Raman and UV-Vis Absorption Spectroscopies. *ACS Sens* **2019**, *4* (9), 2288–2295. DOI: 10.1021/acssensors.9b00736.
- (4) Lines, A. M.; Adami, S. R.; Sinkov, S. I.; Lumetta, G. J.; Bryan, S. A. Multivariate Analysis for Quantification of Plutonium(IV) in Nitric Acid Based on Absorption Spectra. *Anal Chem* **2017**, *89* (17), 9354–9359. DOI: 10.1021/acs.analchem.7b02161.
- (5) Nelson, G. L.; Asmussen, S. E.; Lines, A. M.; Casella, A. J.; Bottenus, D. R.; Clark, S. B.; Bryan, S. A. Micro-Raman Technology to Interrogate Two-Phase Extraction on a Microfluidic Device. *Anal Chem* **2018**, *90* (14), 8345–8353. DOI: 10.1021/acs.analchem.7b04330.
- (6) Lines, A. M.; Nelson, G. L.; Casella, A. J.; Bello, J. M.; Clark, S. B.; Bryan, S. A. Multivariate Analysis To Quantify Species in the Presence of Direct Interferents: Micro-Raman Analysis of HNO_3 in Microfluidic Devices. *Anal Chem* **2018**, *90* (4), 2548–2554. DOI: 10.1016/acs.analchem.7b03833.
- (7) Nelson, G. L.; Lackey, H. E.; Bello, J. M.; Felmy, H. M.; Bryan, H. B.; Lamadie, F.; Bryan, S. A.; Lines, A. M. Enabling Microscale Processing: Combined Raman and Absorbance Spectroscopy for Microfluidic On-Line Monitoring. *Anal Chem* **2021**, *93* (3), 1643–1651. DOI: 10.1021/acs.analchem.0c04225.

The Joint Research Centre's Expertise in Nuclear Safeguards Sample Analysis

A.M. Sánchez Hernández, R. Buda, K. Casteleyn, L. Commin, F. D'Amati, J. Horta, A. Le Terrier, A. Muehleisen, S. Stohr, H. Schorlé, M. Toma, M. Vargas Zuñiga, D. Wojnowski, J. Zsigrai, K. Mayer
European Commission, Joint Research Centre, Directorate Nuclear Safety and Security, Karlsruhe, Germany

The Joint Research Centre (JRC) in Karlsruhe, in partnership with the Directorate General for Energy (DG ENER), plays a critical role in ensuring the accurate analysis of nuclear materials, as mandated by the EURATOM Treaty. The Analytical Service (AS) at JRC Karlsruhe is dedicated to maintaining the highest standards of quality, accuracy, and traceability in its analytical measurements, with a focus on uranium and plutonium content and isotopic composition.

Our laboratory is accredited according to ISO/IEC 17025 and has a proven track record of successful participation in numerous Inter-Laboratory Comparisons (ILCs), demonstrating our expertise and commitment to excellence in nuclear material analysis. We employ a range of analytical methods, including active and passive radiometric techniques and mass spectrometry, to ensure the lowest possible uncertainty in our results.

Our laboratory has consistently achieved top performance in various ILCs, showcasing our ability to deliver high-quality results and our dedication to maintaining the highest standards of accuracy and reliability. This is a testament to our rigorous quality control processes and our commitment to staying at the forefront of nuclear material analysis.

This paper provides insights into the factors that we believe have contributed to our top performance, including our rigorous quality control processes, our commitment to staff training and development, and our investment in state-of-the-art instrumentation. By sharing our experiences and best practices, we aim to contribute to the advancement of nuclear material accounting and control, safeguards verification, and non-proliferation efforts.

A New Plutonium Metal Certified Reference Material at CETAMA: the MP4 Standard

S. Picart¹, M. Crozet¹, Y. Davrain¹, C. Bertorello¹, G. Canciani¹, C. Rivier¹, D. Cardona², G. Legay², G. Bailly², N. Caussignac², C. Zeleny², A. Quemet¹, S. Baghdadi¹, C. Maillard¹, V. Dalier¹, L. Montreuil¹, S. Jan¹, S. Mialle³, C. Cruchet³, H. Isnard³, W. Pacquentin³, F. Doreau¹, P. Estevenon¹, J. Lorino¹, L. Picard¹, S. Richter⁴, Y. Aregbe⁴, A. M. Sanchez Hernandez⁵, H. Schorle⁵, R. Buda⁵, U. Repinc⁶, M. Kohl⁶, J. Hiess⁶, G. Duhamel⁶, M. Sumi⁶.

¹ CEA, DES, ISEC, DMRC, Univ. Montpellier, Marcoule, Bagnols-sur-Cèze, France

² CEA, DAM, Valduc, Is-sur-Tille, France

³CEA, DES, ISAS, DRMP, Univ. Paris-Saclay, Gif-sur-Yvette, France

⁴Joint Research Centre (JRC), European Commission, Geel, Belgium

⁵Joint Research Centre (JRC), European Commission, Karlsruhe, Germany

⁶IAEA, SGAS, NML, Seibersdorf, Austria

The production of high-purity plutonium (Pu) metal standards is the cornerstone of Pu fissile material accountancy, as these standards are needed to calibrate the analytical tools used to characterize Pu-containing materials. The fabrication of Pu metal standards is a complex task because facilities with the capacities to purify and produce high-purity Pu in metal form are very rare, and also because it requires a large analytical workforce to characterize the material and determine the reference values.

More than ten years ago, the Valduc research center and the Commission for the Establishment of Analytical Methods (CETAMA) of the French Alternative Energies and Atomic Energy Commission (CEA) joined forces to launch the MP4 program in order to complete the range of Pu metal certified reference materials (CRMs) in the CETAMA's catalog. The aim was to offer a new CRM in the form of a metal piece with reduced mass compared with the current MP2 CRM (fig. 1).

Manufacturing and packaging took place over the 2017-2019 period and was followed by the material characterization step from 2021 to 2023 through the organization of an interlaboratory comparison (ILC) involving expert laboratories of the CETAMA's network.

The present paper details the data processing which led to the establishment of the certified reference values for several quantities such as Pu isotopic composition and Pu mass fraction. Thanks to its comprehensive set of certified values and reduced mass compared to MP2, this new MP4 material constitutes an outstanding standard, essential for Pu fissile material accountancy and nuclear safeguards activities.

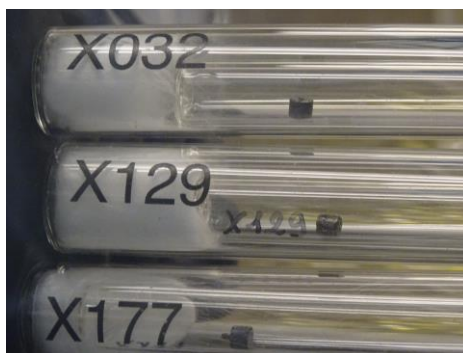


Figure 1: MP4 Pu metal pieces in their sealed glass ampoule.

Development of Uranium Oxide-based Reference Microparticles for Particle Analysis in Nuclear Safeguards

Stefan Neumeier¹, **Shannon Potts**¹, Philip Kegler¹, Giuseppe Modolo¹,
Martina Klinkenberg¹, Simon Hammerich², Dirk Bosbach¹, Irmgard Niemeyer¹

¹Forschungszentrum Jülich GmbH, Institute of Energy and Climate Research – Nuclear Waste Management (IEK-6), 52428 Jülich, Germany

²Heidelberg University, Institute of Earth Sciences, 69120 Heidelberg, Germany

The International Atomic Energy Agency (IAEA) and its worldwide Network of qualified Analytical Laboratories (NWAL) conduct analytical measurements on swipe samples taken during inspections at nuclear facilities to detect the presence or verify the absence of undeclared nuclear materials and activities. These efforts, together with the increasing number of samples (more than 500 in 2022) to be analysed require constant quality control, further advancement of highly sensitive analytical methods incl. the development and provision of tailor-made reference materials.

In 2020, the safeguards laboratories at Forschungszentrum Jülich GmbH (FZJ) were officially qualified as the first member for the provision of microparticulate reference materials to the IAEA's NWAL. These reference particles are applied to strengthen the IAEA's quality control system for particle analyses including analytical instrument calibration, method development and validation as well as their application in interlaboratory exercises.

Recent activities related to the development of microparticulate reference materials, e.g. for age-dating verification measurements will be discussed in this presentation. Therefore, a co-precipitation method was adopted to produce Th-doped bulk-scale materials as a kind of "internal reference materials". These materials allow for investigations with state-of-the-art analytical techniques to unravel the structural incorporation mechanism of Th into uranium oxide crystal structures (UO₃ and U₃O₈) in dependence of the amount of Th-doping. Regarding the transferability of the results to the particle production process, the phase transformation from UO₃ to U₃O₈ is of particular interest. Thus, the pristine materials (Th-doped ammonium diuranate) were investigated with Thermogravimetry – Differential Scanning Calorimetry (TG-DSC) to identify the temperature at which the phase transformation of UO₃ to U₃O₈ for the doped materials occurs. Subsequently, the materials were calcined at the identified temperatures and structurally characterized with X-ray Diffractometry (XRD). The results indicate an incorporation of Th-dopant into the UO₃ and U₃O₈ crystal structure which is an important material property of reference particles for reliable age dating measurements. They help to identify relevant process parameters such as the aerosol heating temperature to produce high quality microparticulate reference materials to the IAEA's NWAL.

Additionally, the activities regarding the investigation of storage and performance conditions of the microparticles will be addressed. Previous studies on structure and shape of uranium oxide microparticles clearly showed alteration process leading to the formation of uranium hydroxide like schoepite. However, the formation of aqueous uranium oxide phases causes analytical challenges, particularly in measurements with LG-SIMS, as the ultra-high vacuum in the device can lead to the decomposition of the aqueous phases and thus to the destruction of the reference particles.

To further investigate and understand this alteration process, a systematic shelf-life study of uranium microparticles (produced at FZJ) was launched in 2021. The first part of this study is related to the evaluation of the influence of different atmospheric conditions on the stability of the microparticles. Microparticles were deposited on Glass-like Carbon Disks (GCDs) and stored in humid air, normal laboratory air, Ar-atmosphere in a desiccator and in a lab furnace at 90°C. The second part of the shelf-life study is dedicated to the long-term stability of the particles in different solvent media (ethanol, 2-propanol, n-butanol, tert-butanol). The uranium oxide particles used in both approaches were periodically measured using Scanning Electron Microscopy (SEM) and μ -Raman Spectroscopy for structural as well as Large Geometry-Secondary Ion Mass Spectrometry (LG-SIMS) for isotopic investigation. The combination of these methods allows to describe the long-term stability of uranium microparticles in suspension and under different atmospheric conditions as well as the effect of alteration on the quality of spectrometric analysis and allows consequently to identify optimal storage conditions for potential reference materials. Recent results of atmospheric and suspension shelf-life studies will be discussed in this presentation.

Laser Ablation- ICP-MS Method Development for a Self-Consistent Calibration in Post Irradiation Examination of Spent Fuels

Peter Zsabka¹, Kyle Johnson²

¹ Studsvik Nuclear AB, Nyköping, Sweden; ² Westinghouse Electric Sweden AB

Laser ablation (LA) is a sampling technique that generates a dry particle aerosol from a sample substrate which can be analyzed with e.g. Inductively Coupled Plasma Mass Spectrometry (ICP-MS). When the logging of the track of the laser beam is performed simultaneously with the measurement, a surface mapping of nuclear fuel becomes feasible at a high spatial resolution, at the typical quantification limits of an ICP-MS. In comparison to the nuclear fuel burn-up analysis performed on dissolved fuel pellets, the distribution of actinides and fission products can be determined across an entire pellet surface. These types of analysis can reveal irradiation induced changes in composition, release of volatile fission products, aggregation of dopants or noble metals fission products, differences in local burn-up etc.

The main challenge in LA, in comparison to the liquid mode of ICP-MS operation, is that the parameters chosen for the laser, as well as the physico-chemical properties of the sample under investigation both determine the efficiency with which the laser beam ablates the matrix. As a result, the comparison of signal intensities obtained from a spent fuel sample with signals obtained from a commercially available reference sample typically cannot provide a sufficiently reliable basis for calibration. A second difference is that there are only a limited number of possibilities to eliminate between isobaric interferences in the dry mode of operation. These properties make LA-ICP-MS a primarily *relative* method, that can reveal local differences in the abundance of compounds as a function of location.

Extracting absolute or “calibrated” nuclide concentrations however is of great importance in the context of benchmarking of nuclear fuel burn-up calculations and criticality analysis. For this reason, a range of tools have been investigated at the Hot Cell Laboratory in Studsvik, in order to approach the accuracy of the LA-ICP-MS method to the accuracy of the ICP-MS technique operated in the liquid mode. On the one hand, matrix-matched, mono- and multi-element doped calibration UO₂ fuel were analyzed together with irradiated nuclear fuel samples. Preparation of such reference samples with surrogate fission products is mostly limited to doping with non-volatile elements, such as lanthanides. For some volatile fission products (Ru, Cs, Rb), the synthesis of doped reference material is very challenging, as during sintering, these nuclides tend to relocate or volatilize. The incorporation of alpha emitter transuranium actinides is challenging due to the radiological hazard posed by the dopants. For this reason, besides the use of matrix-matched reference samples, other techniques were also investigated.

The capturing of laser ablation generated dry aerosol, followed by the dissolution of the captured particles allows *self-consistent and absolute* determination of nuclide contents, with the possibility to use the entire range of calibration methods available for the liquid mode of operation in ICP-MS. In this way, the problem of obtaining matrix-matched reference samples for all fission products of interest is greatly reduced to finding one or more chemically homogeneous area(s) on the sample, from which enough substance can be collected with the laser ablation followed by dry aerosol capture and later liquid measurement.

For the analysis of noble gas fission products, an external calibration method has been developed: based on the use of a dual micro-flow controller system, and a Xe-gas external calibration.

The combination of the various methods described above provides a toolbox for a broad range of samples, alleviating the need to have at hand a matrix-matched reference sample series including and bracketing the concentrations expected in a sample. An example on the application of the range of methods described will be shown on the analysis of a low burn-up, Gd burnable absorber containing samples.

Burnup Determination of Irradiated U-Mo Alloy Fuel by ^{148}Nd Monitor Method

Hyejin Cho, Namuk Kim, Yang-Soon Park, Minjae Ha, Tae-Hong Park, Hye-Ryun Cho, Jai Il Park

Korea Atomic Energy Research Institute, 111 Daedeok-daero-989, Yuseong-gu, Daejeon 34057

The determination of burnup is a crucial step for assessing nuclear fuel performance. Employing both non-destructive and destructive techniques, researchers aim to quantify the number of fissions per heavy atom (mass ≥ 232) initially present in the fuel.

A destructive method was employed to determine the burnup of U-Mo alloy fuel irradiated in the High-flux Advanced Neutron Application Reactor (HANARO) at KAERI. The basic processes for the burnup and isotopic determination are shown in Fig. 1. The dissolution procedure is composed of two-steps for sequential dissolution of cladding material and alloy fuel. The fuel sample can be dissolved completely in 6 M HCl and 14 M HNO_3 - 1 M HF mixture, maintained at 60 ~ 90 °C for 6 hours under reflux conditions. A two-step separation for both the unspiked and spiked sample solutions enabled us to achieve the pure separation of various fission products, including U, Pu, and Nd. The isotopic compositions of U, Pu, and Nd were determined using a thermal ionization mass spectrometer (TIMS) by the isotope dilution mass spectrometric method (IDMS), which employed triple spikes of ^{233}U , ^{242}Pu , and ^{150}Nd . Through precise analysis and measurement, the burnup of the U-Mo alloy fuel was accurately determined.

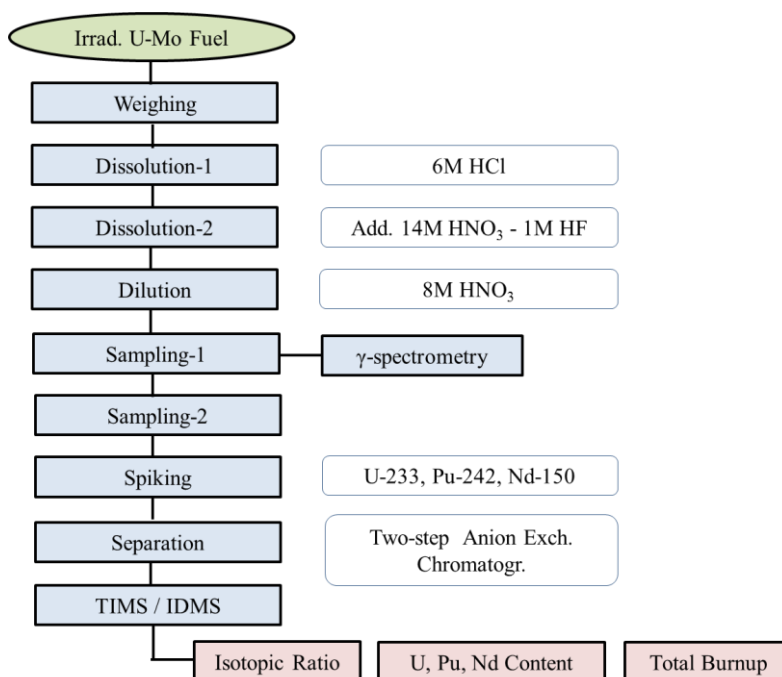


Figure 1. Analytical processes for the burnup determination of irradiated U-Mo alloy fuel

On L-edges X-ray Emission Spectroscopy as a Tool to Study Actinide's Electronic Structure: The Case of Uranium in U_xO_y Compounds

P. Silvenoinnen, I. Prozheev, **R. Bes**

Department of Physics, University of Helsinki, P.O. Box 64, FI-00014 Helsinki, Finland.

The attractiveness of actinides (An) is not only due to their high relevance on safety and economic performance of the nuclear power plant or the sustainability of the nuclear waste management but also from a fundamental point of view. Indeed, such materials show exciting interdependence between their properties and their complex electronic structure. Over the last decade, systematic studies of the relationship between electronic structure and ground state properties have supported our understanding of the metallic compound properties [1]. Those fundamental results have provided opportunities to develop more accurate and predictive theoretical model in 5f chemistry, but the case of oxide remains unclear, despite the tremendous effort carried out using X-ray photoelectron spectroscopy (XPS) [2,3], or High-energy Resolution Fluorescence detected X-ray Absorption spectroscopy (HERFD-XAS) [4-8]. An-4f XPS data are routinely used for determining actinide speciation thanks to significant chemical shift of 4f shells, but its near surface sensitivity is limiting the type of samples one can measure. In addition, HERFD-XAS has demonstrated its bulk sensitivity, especially at An $M_{4,5}$ -edges, but the collected spectra usually suffer from the overlapping of both speciation and local structure effects which are difficult to detangle. Consequently, those effects reduces the overall sensitivity and accuracy of speciation quantification.

X-ray emission spectroscopy (XES) is a promising candidate to probe efficiently the speciation of actinides because XES can overcome the limitation usually encountered in XPS and HERFD-XAS. Given the nature of XES, which is probing the filled electron shells in the hard X-ray regime, one may expect bulk sensitivity with less local order effect while keeping the speciation effects intact. Moreover, the use of polychromatic beam would significantly reduce the detection limit allowing the study of highly diluted materials.

However, while XES studies are becoming more common in the context of 3d elements, only very few are available for actinides. The only example is the recent study of the 5f delocalization on uranium fluorides [9,10]. In order to assess whether XES could be an efficient tool for actinide's electronic structure study, we aim to perform extensive and systematic experiments on actinide samples showing various speciation and local order. As a first step, we have studied the case of U L-edge emission lines, and within this contribution we will discuss the results obtained during an experiment at the ROBL beamline of the ESRF on uranium oxides.

- [1] C.H. Booth et al., PNAS 109(26) (2012) 10205.
- [2] Y.A. Teterin et al., Phys Chem Minerals 7 (1981) 151.
- [3] Y. A. Teterin et al., Russ. Chem. Rev. 73 (2004) 541.
- [4] R. Bes et al., Journal of Synchrotron radiation 29 (2022) 21.
- [5] K.O. Kvashnina et al., Chemical Communications 54 (2018) 9757.
- [6] G. Leinders et al., Inorganic Chemistry 56 (2017) 6784.
- [7] T. Vitova et al. Nature Communications 8 (2017) 16053.
- [8] K.O. Kvashnina et al., Phys. Rev. Letters 111 (2013) 253002.
- [9] J. G. Tobin et al., Appl. Sci. 10 (2020) 2918.
- [10] J.G. Tobin et al., J. Phys. Commun. 4 (2020) 015013.

PYROCHEMISTRY AND CHEMISTRY FOR MOLTEN SALTS

Overview of Plutonium Pyroprocessing By-Products Management

G. Bourgès, S. Faure, O. Lemoine, D. Cardona – Barrau

CEA, DAM, VALDUC, F- 21120 Is sur Tille, France

CEA/DAM has been operating Plutonium pyroprocesses for several decades. These processes generate mainly three types of by-products that may contain significant amounts of plutonium associated with americium: spent salts where the plutonium is trapped in a chloride gangue, metal scraps such as dross and highly impure buttons, metallic and ceramic pieces with both metal and salt adherences. The composition of these by-products varies from one batch to another, according to process and interim storage conditions, and they cannot be discarded as waste. Processes have been developed to recover the plutonium from these products and to decontaminate the substrates in order to meet the requirements for low or middle activity waste discard.

The process baseline is aqueous nitrate polishing including nitric dissolution, purification using ion exchange or solvent extraction, and oxalate conversion to recover plutonium as pure dioxide. For each type of by-product, a front-end process has been developed to produce a plutonium oxide feed material suitable for aqueous nitrate polishing in terms of both efficiency, and waste and effluents management.

Metal oxidation was developed to convert metal scraps to oxide as well as to remove plutonium from refractory metal and ceramic pieces.

The front-end process for chloride spent salts was challenging to develop. The process consists in a pyrochemical oxidation, using carbonate and chlorine to convert plutonium species into oxide, followed by vacuum distillation at high temperature. The high efficiency of the process has been demonstrated in terms of both decontamination factor and plutonium conversion to oxide.

The obtained plutonium oxide products were then suitable for subsequent aqueous nitrate processing using oxidizing or nitro-fluorhydric dissolution processes.

Spent Fuel Reprocessing for Molten Salts Fast Neutron Reactors

A. Handschuh¹, P. Ryckewaert¹, P. Baron¹, S. Delpech², C. Cannes², D. Lambertin¹, T. Kooyman¹

¹NAAREA - 66 allée de corse, Nanterre (92000), France

²Université Paris-Saclay, CNRS/IN2P3, IJCLab, 91405 Orsay, France

Corresponding author: a.handschuh@naarea.fr

Energy is crucial to achieve all 17 Sustainable Development Goals set since 2015 at COP21. That's why the energy of the future needs to be safe, equitable, carbon-free and decentralized.

Nuclear power is seeing renewed interest as a potential energy source due to society's commitment to low-carbon sources to deal with climate change. Molten salts fast neutron reactors are considered as a promising technology in this context, thanks to their greater efficiency in generating electricity and/or heat, in addition to offering advantages in terms of radioactive waste management.

NAAREA's XAMR* (eXtrasmall Advanced Modular Reactor) concept uses long-lived nuclear waste in the form of a ternary NaCl-PuCl₃-UCl₃ salt as fuel to produce safe, abundant, dispatchable, carbon-free and decentralized energy that can be deployed as close as possible to industrial consumers around the world.

Spent fuel still contains valuable materials such as uranium, plutonium and minor actinides that can be used to produce a new molten salt fuel. To do this, the spent fuel must be reprocessed to separate the reusable material from the final waste, which must be packaged in a matrix such as borosilicate glass for long-term storage.

Several reprocessing options are being considered:

- Option 1: Spent fuel salt dissolution in nitric acid to make it compatible with the Orano La Hague spent fuel reprocessing plant. The presence of chlorine must be limited, particularly to avoid corrosion, before mixing the solutions resulting from the dissolution of NAAREA spent fuel salt with the dissolution solutions usually processed at the La Hague plant. Thus, a chlorine precipitation step with silver, for example, could be added before reprocessing.
The presence of sodium should also be limited or, at a minimum, the solutions resulting from the dissolution of NAAREA spent fuel salt must be diluted with solutions from the reprocessing of light water reactor fuels to ensure a sodium content compatible with the vitrification process.
After reprocessing, the uranium and plutonium would be reused for a new fuel salt production and the final waste would be packaged in a glass matrix for long-term storage, as is done for the final waste from the light water reactor (LWR);
- Option 2: Since the spent fuel salt of NAAREA is composed of about 50% by weight of NaCl, and the chlorine could be enriched, it seems interesting to separate the NaCl before reprocessing the spent fuel salt. For this, precipitation of species other than NaCl via the use of a mixture of gas or carbonate directly into molten salt [1] followed by a separation step such as filtration or vacuum distillation [1], [2] could be added. The precipitated and separated species (such as actinides and fission products) would then be dissolved in nitric acid to make them compatible with the Orano La Hague spent fuel reprocessing plant. The spent fuel salt reprocessing, without chloride and sodium, would be simplified. After reprocessing, the uranium and plutonium would be reused for a new fuel salt production and the final waste would be packaged in a glass matrix for long-term storage, as is done for the final waste from the light water reactor (LWR);
- Option 3: Spent fuel salt reprocessing by a pyrochemical process where reusable materials (NaCl, PuCl₃, UCl₃, chlorides of minor actinides) are separated from molten salt and directly reused to produce a new molten salt fuel. Fission products (considered as a final waste) would be encapsulated in a suitable matrix for long-term storage such as borosilicate glass matrix. This treatment could be carried out in the vitrification workshops of the Orano La Hague plant after a nitric acid dissolution step.

Options 1 and 2 do not allow reusable materials to be directly recycled, i.e. it requires the addition of a hydrometallurgical process between 2 molten salt steps (management of used fuel salt and new fuel salt fabrication). However, these options can be deployed in the short to medium term after some research and development studies.

Option 3 seems more optimal because it allows reusable materials to be recycled directly. However its implementation seems possible only in the medium/long term after more substantial research and development.

For ATALANTE 2024, NAAREA will present its progress on the reprocessing of molten salts' studies, in particular the R&D carried out with surrogates.

- [1] C Thiébault, G. Bourgès, D. Lambertin and L. Pescayre, « Plutonium pyrochemistry spent salts treatment by oxidation and distillation », TMS annuel meeting, p. 1021-1025, 2005.
- [2] Gilles Bourgès, S. Faure, B. Fiers, S. Saintignon, O. Lemoine, D. Cardona-Barrau, D. Devillard, « Vacuum distillation of plutonium pyrochemical salts», Procedia Chemistry, vol. 7, p. 731-739, 2012.

Pyrochemical Treatment for Molten Salt Nuclear Reactor

Joelle Costantine¹, Davide Rodrigues,¹ Céline Cannes,¹ Elisa Capelli,² Bertrand Morel,² Sylvie Delpech¹

¹ Université Paris-Saclay, CNRS/IN2P3 IJCLab, 91405 Orsay, France

² Orano, 92320 Châtillon, France

*Corresponding author, joelle.costantine@ijclab.in2p3.fr

Molten salt nuclear reactors are one of the six selected concepts for fourth-generation nuclear reactors [1]. The first molten salt reactor concept developed by Oak Ridge National Laboratory, USA, was designed to operate a fuel salt based on fluorides. These concepts relied on a thermal spectrum conferred by the moderating nature of the graphite core, BeF₂ salt and fluorides. These neutronic and chemical environments are compatible with a Th/U nuclear cycle but not with a U/Pu nuclear cycle, the latter being the French historical cycle. Chloride salts are more suitable to operate a reactor with the U/Pu cycle or for an actinide burner concept [2],[3]. The base salt chosen is NaCl, to which MgCl₂ or ThCl₄ is added to reduce the melting temperature to 460 and 330°C respectively. Therefore, it is interesting to study NaCl-ThCl₄-PuCl₃ salt since it has the lowest melting temperature [4]. Studies were carried out on this salt to investigate its stability, its redox properties and to define methods of treating the spent fuel.

In this context, two lines of research have been developed:

- Thorium chloride-based salt preparation:

Thorium was studied in a chloride medium by oxidizing metallic Th powder. Based on the literature and thermodynamic calculations, the question of the stability of ThCl₂ arises. To answer this question, two oxidizing agents were tested: MgCl₂ and ZnCl₂. The oxidizing power of MgCl₂ is sufficient to oxidize Th metal to ThCl₂ but not to ThCl₄. On the contrary, to form ThCl₄ we need to use ZnCl₂.

Electrochemical measurements show that MgCl₂ was not able to oxidize the metallic Th powder. Meanwhile, electrochemical measurements show the oxidation of Th metallic powder to Th(IV) after the addition of ZnCl₂. In consequence, the experimental results then proved that Th(IV) is the only stable soluble oxidation state in the chloride salt.

- Lanthanides/actinides separation by pyrochemical treatment:

This study focused on investigating the effectiveness and specificity of electrochemical separation of actinides and lanthanides in chloride salt solutions. The process employed an aluminum solid electrode and a liquid aluminum alloy. Cerium was selected to simulate lanthanides, while thorium represented actinides. Electrochemical analysis with aluminum electrodes revealed a shift in the reduction potential for both thorium and cerium. The extraction efficiency, determined through ICP analysis, demonstrated high yields approaching 100% when using aluminum solid electrodes.

REFERENCES

- [1] "Gen IV international forum".
- [2] D. E. Holcomb et al. "Fast Spectrum Molten Salt Reactor Options," 2011.
- [3] E. Merle et al. "Preliminary design assessment of the molten salt fast reactor," 2012.
- [4] T. Dumaire et al., Calphad (2022), vol. 79, 102496.

Feasibility of Lanthanide Extraction Assisted by Electrolysis on Li-Bi Liquid Cathode in Molten Fluorides.

Pierre Chamelot, Mathieu Gibilaro and Laurent Massot

Laboratoire de Génie Chimique UMR-5503, Université de Toulouse III Paul Sabatier, 118 route de Narbonne, 31062
Toulouse cedex 9, France
pierre.chamelot@univ-tlse3.fr

On the six nuclear concepts selected in the frame of Generation IV International Forum (GIF) [1], one concerns the Molten Salt Fast Reactor (MSFR). Based on the MSRE and MSBR developed between 1950 and 1976 by Oak Ridge National Laboratory (ONRL) [2], the MSFR concept has been developed by CNRS in the frame of the French program on nuclear energy-PACEN.

In the development of GEN IV reactor system, the nuclear fuel reprocessing for each concept appears to be one of the key points however, the complete reprocessing scheme for MSR was not fully demonstrated, particularly the lanthanide fission product extraction from the fuel, and thus remains to be studied and optimized.

This study is dedicated to the reprocessing step concerning the Lanthanide fission product extraction from the fuel after Actinide extraction by reductive extraction using Bi pool containing reductive Li reagent.

Two usual electrochemical processes are available for lanthanide extraction from the melt:

- Liquid-liquid extraction (reductive extraction)
- Electrodeposition on inert or reactive cathode (liquid or solid)

To better understand the extraction efficiency of lanthanide extraction on Bi pool with different Li contents, the electrochemical behaviours of the NdF_3 or SmF_3 on Bi and Mo electrodes were studied and compared with the electrochemical behaviours of the reduction of UF_4 and ThF_4 on the same electrode materials.

Then, extractions by electrolysis of NdF_3 , SmF_3 and $\text{NdF}_3 + \text{SmF}_3$ on Bi pool were performed to evaluate the extraction efficiency and the minimum Li content allowing the lanthanide extraction if the extraction is feasible.

- [1] US DOE Nuclear Energy Research Advisory Committee and the Generation IV International Forum, *A technology Roadmap for Generation IV nuclear Energy Systems*, GIF-002-00 (2002).
- [2] H. G. Macpherson, *The Molten Salt Reactor Adventure*, Nucl. Sci. Eng.90-4 (1985) 374-380.

Molten Salts and Pyrochemical Processing Progress at the UK's National Nuclear Laboratory

Ruth Carvajal-Ortiz, **Mike J Edmondson**, Moya Hay

The National Nuclear Laboratory, Chadwick House, Warrington Road, Birchwood Park, Warrington, WA3 6AE

The UK's National Nuclear Laboratory offers infrastructure and capabilities to support research and development programmes for advanced fuel cycles and partitioning and transmutation (P&T). Our world-leading facilities have been widely used as part the UK government funded Advance Fuel Cycle Programme. Part of the programme involved the development of molten salt and pyrochemical processing capabilities including fuel manufacture, salt science, engineering, online monitoring, and fuel cycle integration. This has led to a resurgence of activity in molten salt technologies for nuclear application

Molten salt reactors (MSRs) are receiving increasing attention due to their potential for passive safe, efficient energy production [1]. Combined with pyrochemical processing they offer the potential for closing the nuclear fuel cycle, contributing to energy security and meeting the UK's 2050 Net Zero commitments.

Molten salt reactors come in a variety of models [2] from those using salt purely as a coolant to those with fuel dissolved in the molten salt. The choice salt and fuel, their resultant behaviour in the reactor and the energy extraction methods are all fundamental variables. These choices influence the reactor capabilities and more specifically their application.

The chemistry of MSRs is complex [1]: the varying composition over time as fuel is converted to fission products impact the physical and chemical properties, and neutronics of the system. This leads to challenges in control of corrosion, salt behaviour and the ability to sustain the nuclear reaction. The fact that the fuel is a fluid is both an advantage and disadvantage in this respect. The ability to add to and remove from the salt allows fuel and redox control agents to be added and poisons removed, but it creates added complexity in modelling, assurance measurement and radiation shielding leading to control and regulatory challenges. The treatment of wastes from MSRs is also far from trivial.

While the design and control of the reactor is challenging the promise of a suite of meltdown proof reactors, offering economic benefits (capital and operational cost) over alternatives, with a reduced waste burden means the race to solve this tricky puzzle is on.

References

- [1] "Status of Molten Salt Reactor Technology", Technical Reports Series No. 489, IAEA, 2023.
- [2] "Advances in Small Modular Reactor Technology Developments. A Supplement to: IAEA Advanced Reactors Information System (ARIS). 2022 Edition" IAEA, September 2022 (<http://aris.iaea.org>)

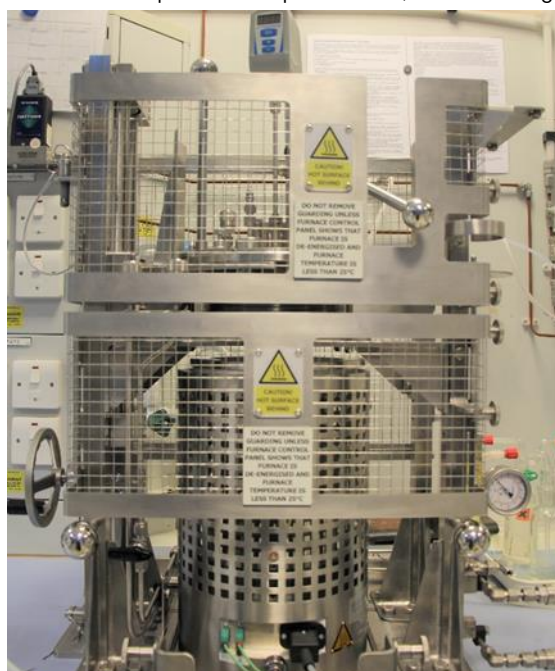


Figure 1: The pyrochemical alpha-active processing apparatus (PAPA), has been developed to handle and investigate the electrochemical and physical properties of actinides (including Pu) in molten salt mixtures

Synthesis of Actinide Chlorides as Fuel for Fast Molten Salt Reactor

P. Chevreux¹, M. Duchateau¹, G. Serve¹, M. Pons¹.

¹. CEA, DES, ISEC, DMRC, Univ Montpellier, 30207 Bagnols-sur-Cèze, Marcoule, France. Email: pierrick.chevreux@cea.fr

The innovative system for actinides conversion (ISAC) project gathering main French contributors within the nuclear field (CEA, CNRS, EDF, Framatome and Orano) focuses on fast molten salt reactor (MSR) dedicated to actinides conversion. The objective of ISAC project is to study the feasibility of minor actinides transmutation, especially Americium, by a MSR concept to reduce the inventory of high-level waste to be stored in deep geological disposal. The reactor system is based on the circulation of the liquid fuel which is the molten salt containing the dissolved actinides as fissile material. A chloride salt was chosen for the use of converter reactor, as it provides low melting point, high solubility of actinides and harder neutron spectrum. Besides, high solubility of chlorides in aqueous solution is consistent with hydrometallurgical treatment and separation processes already used in France. The molten salt is composed of the NaCl-MgCl₂-PuCl₃-AmCl₃ system and its composition has to be carefully controlled with impurity content as low as possible to avoid corrosion and precipitation issues. Producing pure actinide chlorides without contaminants such as oxide, oxychloride, hydroxide and water is still a challenge.

In this work, the synthesis of pure actinide chlorides such as PuCl₃ and AmCl₃ is investigated. Actinide chlorides are synthesized based on a gas-solid reaction between an actinide precursor and a chlorinating agent. Chlorination experiments were carried out in a static bed reactor under flowing gas. The impact of several reaction parameters such as actinide precursor (oxide or oxalate), gas (chlorine or hydrogen chloride), chlorinating time and temperature were studied. The purity of formed products were evaluated first by X-ray diffraction measurements and then by electrochemical measurements and chemical analysis after leaching. Thermodynamic calculations were also performed to support results. The carbochlorination of PuO₂ was conducted in the temperature range of 600 °C to 800°C with chlorine gas as a chlorinating agent and the presence of solid carbon. Results show that conversion efficiency mainly depends on the chlorinating temperature and the contact between the oxide and the chlorinating agent. Volatilization of plutonium was observed with chlorine gas. The hydrochlorination of plutonium oxalate was performed at lower temperature and exhibited a good conversion to PuCl₃.

Americium chloride was synthesized using both carbochlorination and hydrochlorination techniques. Americium seems to be easier to chlorinate than plutonium, since AmO₂ could directly react with HCl gas at 600 °C to form AmCl₃. The purity of actinide chlorides needs further investigations and salt purification and actinide behavior in molten salt is the subject of ongoing studies.



(a)



(b)

Figure 1. Pictures of (a) PuCl₃ and (b) AmCl₃ synthesized using carbochlorination or hydrochlorination reaction.

Molten Salt Spectroelectrochemistry in Chloride Based Eutectic Systems with Uranium

Jessica A. Jackson, Nicole Hege, Jacob Tellez, Jenifer Shafer

Colorado School of Mines, Golden Colorado, USA

With growing interest in clean energy production and environmental stewardship, advanced nuclear reactor production has increased to meet societal demands. In support of this, Molten Salt Reactors (MSR) are an advanced technology actively being pursued for future nuclear energy production. A critical area of need for MSR technologies is the development of materials accountancy capabilities to support responsible utilization of this energy resource. One focus of ongoing research has been the development of online monitoring techniques and spectroscopic techniques which can provide transparency in this area. As part of the research that will be presented, a 3-D high temperature furnace has been constructed that enables simultaneous measurements using Raman and UV-Vis spectroscopy with electrochemical techniques. The electrochemical studies provide diffusion coefficients that improve insight into *f*-element speciation in solution, coupled with classical molecular dynamics modeling. These measurements coupled with UV-Vis or NIR spectroscopy, otherwise referred to as spectroelectrochemistry (SEC), will be used for the quantitative determination of *f*-element metal ion behavior useful for spectroelectrochemical sensor capabilities in MSR systems.

The figure below shows the custom-built small-scale furnace, a quartz cuvette with 1.5 g of molten LiCl-KCl eutectic, and the schematic of the furnace with electrode placement shown relative to the fiber optic cables. Molten salt SEC has many design challenges that have required significant time dedicated to method development. Some of these challenges will be discussed. Electrochemical studies have also been completed on a 50 g scale to help elucidate the source of some difficulties experienced in the 1.5 g scale. Balancing the requirements for spectroscopy with the requirements of electrochemistry at high temperatures in a molten chloride salt eutectic will also be discussed in this presentation. The ultimate focus of this work is monitoring higher concentrations of uranium in the presence of fission products in a molten LiCl-KCl eutectic that are relevant to reactor conditions.

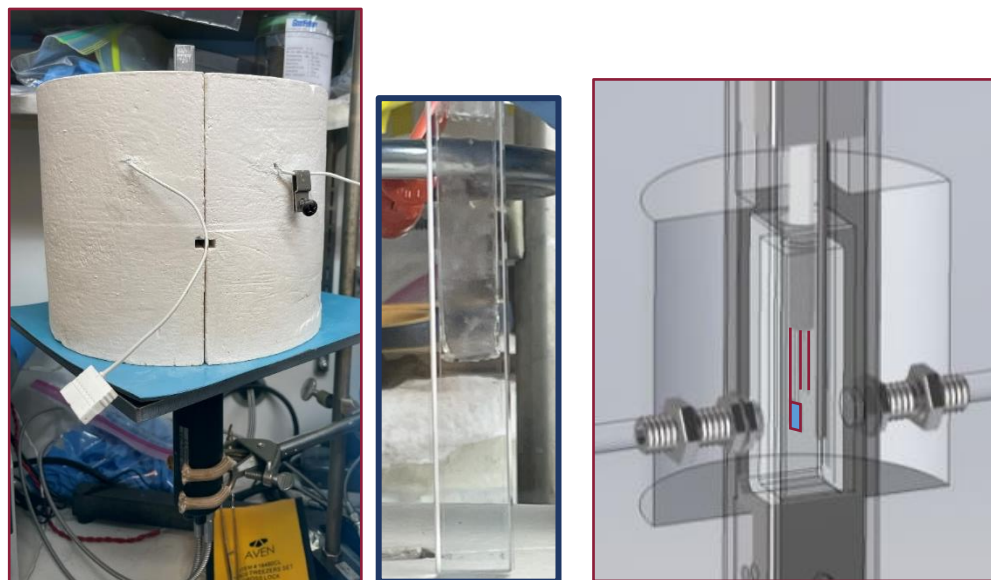


Figure. (Left) Small scale furnace; (Middle) Molten LiCl-KCl eutectic in quartz cuvette; (Right) Schematic showing location of electrodes relative to fiber optics for spectroscopy.

Influence of Nitrogen on Uranium Metal Stability in Molten LiCl-KCl

Théo Caretero¹, Laurent Massot¹, Mathieu Gibilaro¹, Jérémie De Marco², Mehdi Arab², Pierre Chamelot¹

¹Laboratoire de Génie Chimique, Université de Toulouse, CNRS, INPT, UPS, Toulouse, France.

²Hall de recherche de Pierrelatte, Site ORANO du Tricastin, BP 16, 26701 Pierrelatte, France.

Uranium is used primarily as a fuel in the production of nuclear energy. One of the key elements of the fuel cycle is its reprocessing. One possible method of reprocessing is called pyroprocessing. This process uses electrolysis of spent metallic nuclear fuel in a molten chloride melt to separate uranium from transuranium species. This process is initiated by anodic dissolution of the spent metallic nuclear fuel in a LiCl-KCl melt. Uranium is then selectively recovered by electrolysis using a solid cathode. Finally, the transuranium species are recovered on a liquid cadmium electrode. A good understanding of the behavior of the actinides in the media is essential for a proper process operation. Thus, studies were made over the past decades in order to collect data on the behavior of uranium species and the uranium deposition in molten chlorides [1-3]. However, there is a lack of data regarding the stability of uranium in chloride media.

As a result, this research aims to evaluate the effect of different atmospheres of argon with various partial pressures of nitrogen, on the stability of U metal in LiCl-KCl over the 450-550°C temperature range. Experiments showed that nitrogen gas can be dissolved in LiCl-KCl and is electroactive on a nickel electrode.

Thermodynamic data indicate that nitrogen gas can oxidize U to form U(III). Therefore, the oxidation rate of an uranium plate was studied in LiCl-KCl under 5 ppm and 1000 ppm of nitrogen in an argon atmosphere. Chronopotentiometry was used to calculate the amount of U(III) formed in the salt over immersion time and a linear relationship was found. Oxidation rates were obtained for the 450-550°C temperature range and the two atmospheres. It was found that increasing the temperature or nitrogen concentration results in an increase in the oxidation rate of uranium metal.

REFERENCES

- [1] K. Serrano et al., *Journal of applied electrochemistry* (1999), 29 (4), 497-503.
- [2] P. Masset et al., *Journal of The Electrochemical Society* (2005), 152 (6), A1109.
- [3] CH. Lee et al., *Journal of Nuclear Materials* (2017), 488, 210-214.

ACTINIDE AND FISSION PRODUCTS CHEMISTRY

Elucidating the Radiation-Induced Redox Chemistry of Plutonium Under Used Nuclear Fuel Reprocessing Conditions

G. P. Holmbeck, Amy E. Kynman, Jacy K. Conrad, and Travis S. Grimes

Center for Radiation Chemistry Research, Idaho National Laboratory, Idaho Falls, ID, P.O. Box 1625, 83415, USA.

Plutonium plays a critical role in the development of sustainable nuclear fuel cycles, and yet, our fundamental understanding of this element's inherent radiation-induced redox chemistry and associated impacts on nuclear fuel cycle technologies is limited. Unanticipated changes in oxidation state distribution can influence the speciation and transport of plutonium in a given process. Control of these parameters is especially important for used nuclear fuel reprocessing technologies, wherein the separation and recovery of plutonium is typically achieved by the selective formation, maintenance, and complexation of specific oxidation states. Furthermore, plutonium's inherent radiation-induced redox chemistry has the capacity to influence the radiolytic behavior of its complexes, the longevity of which are critical in the design of efficient and cost-effective advanced reprocessing technologies. These radiation-induced processes are unavoidable under fuel cycle conditions owing to the inherency of ionizing radiation fields to the decay of plutonium's isotopes and to the various other radioisotopes generated by nuclear fission and neutron-capture process and the subsequent radioactive decay of their products. As such, mechanistically understanding the response of plutonium's multiple oxidation states to multi-component ionizing radiation fields is essential for predicting the behavior of this critical element under used nuclear fuel reprocessing conditions. Here, through a combination of time-resolved (electron pulse, **Fig. 1A**) and steady-state (alpha and gamma, **Fig. 1B**) irradiation experiments complemented by quantitative, multiscale modeling calculations (**Fig. 1B**), we present advances in our understanding of radiation-induced plutonium redox chemistry!

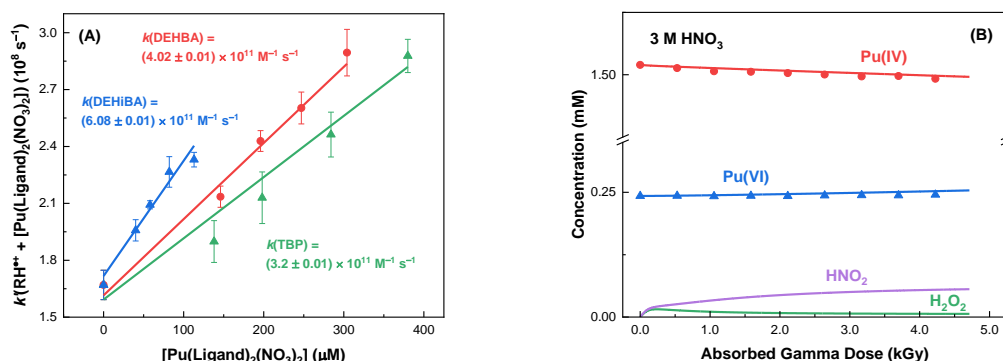


Fig.1. (A) Second-order determination of the rate coefficient (k) for the reaction of the dodecane radical cation ($\text{RH}^{\bullet+}$) with Pu(VI) complexes ($[\text{Pu}(\text{Ligand})_2(\text{NO}_3)_2]$) of tributyl phosphate (TBP), N,N -di-(2-ethylhexyl)butyramide (DEHBA), and N,N -di-2-ethylhexylisobutyramide (DEHIBA). Solid lines correspond to a weighted linear fit, with slopes equal to k . **(B)** Concentration of Pu(IV) and significant ($\geq 1 \mu\text{M}$) radiolysis products as a function of absorbed dose from the gamma irradiation of Pu(IV) in aerated, aqueous 3.0 M nitric acid (HNO_3). Solid curves are predicted values from multi-scale modeling calculations.

How Plutonium “Brown” Peroxo Complex emerges from Aerated Electrolysis Experiments

Quentin Hervy¹, Richard Husar¹, Thomas Dumas¹, Philippe Guilbaud¹, Matthieu Viro²,
Philippe Moisy¹

¹CEA, DES, ISEC, DMRC, Univ Montpellier, Marcoule, France

²Institut de Chimie Séparative de Marcoule, CEA, CNRS, ENSCM, Univ Montpellier

In aqueous solution, the chemistry of plutonium is complex, especially in macroconcentration. First, the plutonium is very sensitive to hydrolysis phenomenon, which can lead to the formation of hydroxides, polymeric or colloidal precipitates at pH above 1. Moreover, in these solutions, the plutonium can coexist under four steady states (+III, +IV, +V and +VI) corresponding to the cationic form Pu^{3+} , Pu^{4+} , PuO_2^+ and PuO_2^{2+} respectively. This coexistence is possible because Pu(IV) and Pu(V) tend to disproportionate. Pu(IV) disproportionate into Pu(III) and Pu(VI) while Pu(V) disproportionate into Pu(IV) and Pu(VI) . These phenomena complicate the redox reactions of plutonium in aqueous solutions and add to side reactions. For instance, the formation of the linear trans-dioxo ions $\text{AnO}_2^{+/2+}$ involves water molecules to form oxo bonds that results in slow kinetics and over potential to be applied in electrolysis experiments. Moreover, the crossed standards potentials for redox couples (Figure 1) often cause steady states equilibrium in which oxidized and reduced plutonium are simultaneously formed¹.

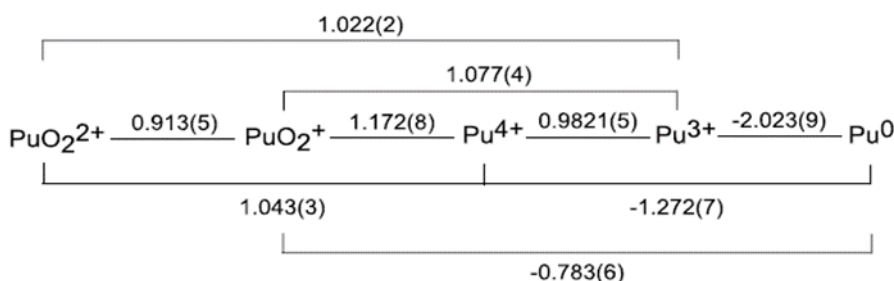


Figure 1: Latimer diagram of redox potentials for selected plutonium couples at 25°C in V vs SHE in 1M HClO_4 .¹

However, the generation of intermediate species during electrolysis may interfere with the studied reactions and lead to disturbing or undesired phenomena. Particularly, hydrogen peroxide may be formed under aerated conditions by direct two electrons oxygen reduction reaction at the catalytic electrode surface². In this work, a spectroelectrochemical approach is used to provide an *in-situ* analytic access to Pu redox reactions. The monitoring of Pu electrolysis reveals the formation of a Transient Plutonium Ion (TPI) formed independently from the applied redox conditions. The isolation of the spectroscopic signature of the TPI by chemometric methods shows an intense absorption signal similar to a dimeric peroxo-bridged complex described seventy years ago as the Plutonium “Brown Complex” by Connick and Mc Vey³. A separate synthesis of the Plutonium “Brown Complex” confirms the nature of the TPI (Figure 2):

The occurrence of this species in plutonium redox reactions that differs from conventional Pu electro-activity concepts will be discussed.

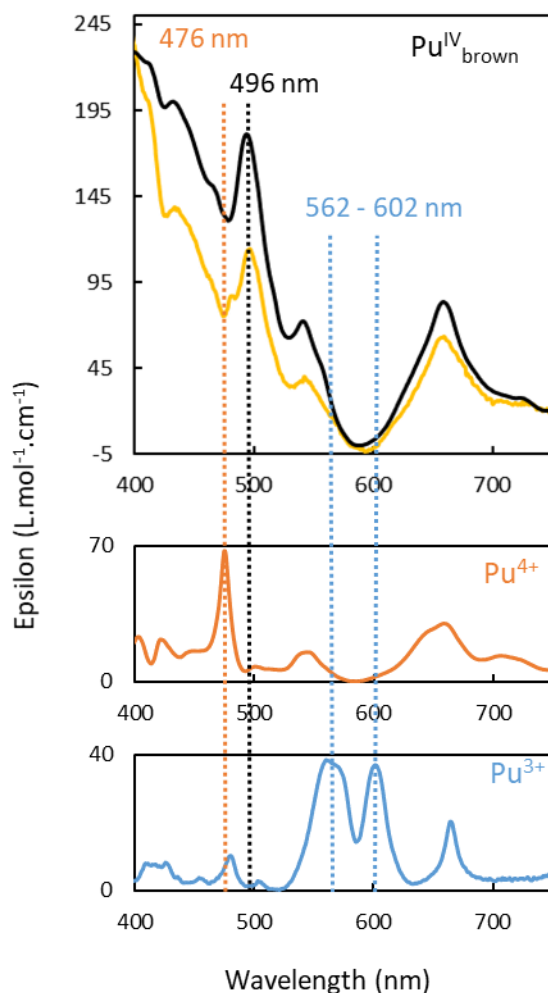


Figure 2 : Shifted molar electronic absorptivity of the TPI (yellow) and references of trivalent (blue), tetravalent (orange) Pu in 0.1 M HNO₃ and plutonium peroxide brown complexe (black).

- [1] Lemire, R. J., Fuger, J., Nitsche, H., Potter, P., Rand, M. H., Rydberg, J., Spahiu, K., Sullivan, J. C., Ullman, W. J., Vitorge, P., and Warner, H. (2001) Chemical 1236 Plutonium Thermodynamics of Neptunium and Plutonium, Elsevier, Amsterdam, The Netherlands, 845 pp
- [2] aI. Katsounaros, W. B. Schneider, J. C. Meier, U. Benedikt, P. U. Biedermann, A. A. Auer, K. J. J. Mayrhofer, *Phys Chem Chem Phys* **2012**, 14, 7384-7391; bG. A. Attard, A. Brew, *J Electroanal Chem* **2015**, 747, 123-129; cG. A. Attard, A. Brew, J. Y. Ye, D. Morgan, S. G. Sun, *Chemphyschem* **2014**, 15, 2044-2051.
- [3] aR. E. Connick, W. H. McVey, *J. Am. Chem. Soc.* **1949**, 71, 1534-1542

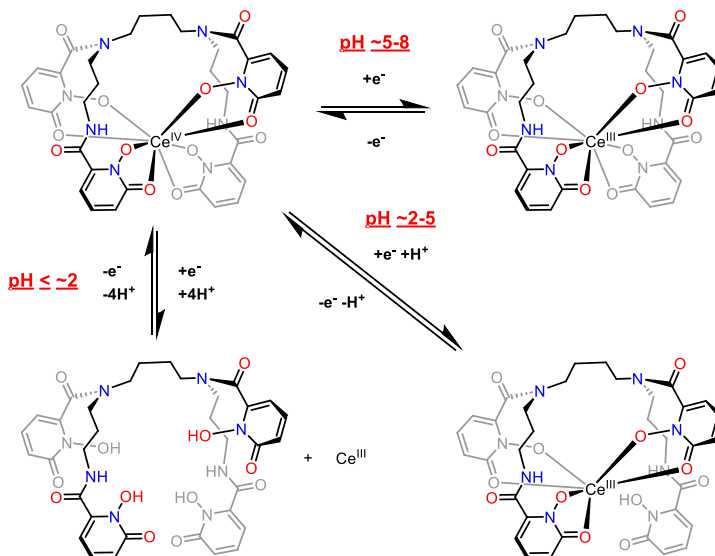
The Redox Chemistry of $[M^{IV/III}(3,4,3-Li(1,2-HOPO))]^{0/-}$ Complexes in Acidic Aqueous Media

Jeffrey R. McLachlan^{ab*}, Andrae A. Tabbs^a, Alex C. Rigby^a, Joshua J. Woods^a,
Rebecca J. Abergel^{ab*}

^a Chemical Sciences Division, Lawrence Berkeley National Laboratory, Berkeley, CA 94720 USA

^b Department of Nuclear Engineering, University of California, Berkeley, CA 94720 USA

3,4,3-Li(1,2-HOPO), abbreviated as HOPO herein, is a biologically inspired octadentate hydroxypyridinone chelator renowned for its propensity to form remarkably strong complexes with tri- and tetra-valent metal ions. This behavior has been exploited in several fields that range from radiopharmacology to fundamental *f*-element science. These endeavors include using HOPO as (1) an actinide decorporation agent, (2) a platform for theragnostic bioconjugates designed for cancer imaging and treatment, (3) a ligand that facilitates the formation of high-valent, non-oxo *f*-element species in aqueous media (e.g., Ce, Np, U, and Bk), and (4) an aqueous holdback agent that facilitate the separation of trivalent actinides from trivalent lanthanides, as well as the purification of tetravalent ions from ions of other valences. In each of these applications, HOPO and its associated chelates are subjected to several strong oxidants and reductants (e.g., metabolites and radiolysis products), as well as ionizing radiation. However, only few studies have focused on the fundamental redox behavior of HOPO and $[M^{IV/III}(HOPO)]^{0/-}$ in solution conditions relevant to biological or spent nuclear fuel reprocessing. Here we show the diverse behavior of HOPO and its complexes from highly acidic to near-neutral conditions using a range of electrochemical and analytical techniques. The redox behavior of HOPO changed significantly upon complexation with redox inactive trivalent (La^{3+}) and tetravalent (Zr^{4+}) metals. The effect of pH on the redox behavior of HOPO coordinated with redox active metals (e.g., $Ce^{4+/3+}$) was studied and primary mechanisms identified (Scheme 1). These findings not only provide insight to the redox behavior of HOPO and its associated complexes but exemplify the importance of assessing the reactivity and behavior of past and future ligands in representative coordination geometries.



Scheme 1: Primary redox pathways for the $[Ce^{IV/III}(HOPO)]^{0/-}$ couple in highly acidic to neutral condition.

Chronicles of Peroxide Plutonium Species: Structural Characterization of New Pu(IV) Green Peroxide

J. Margate [1], M. Virost [1], S. Bayle [1], D. Menut [3] T. Dumas [2], E. Dalodière [1],
C. Tamain [2], P. Estevenon [2], P. Moisy [2], S. I. Nikitenko [1]

[1] ICSM, Univ Montpellier, CEA, CNRS, ENSCM, Marcoule, France

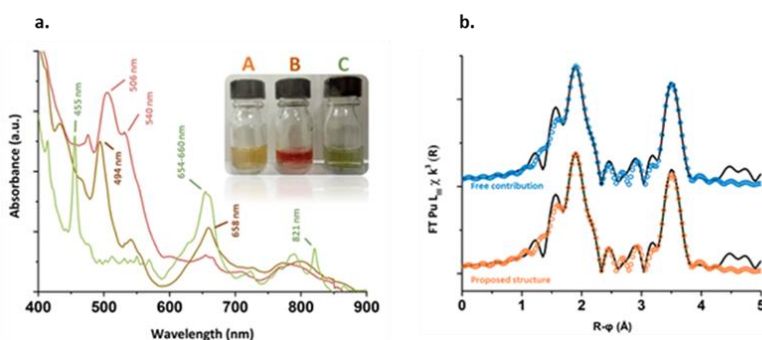
[2] CEA, DES, ISEC, DMRC, Univ Montpellier, Marcoule, France

[3] Synchrotron SOLEIL, L'Orme des Merisiers, Saint-Aubin, France
matthieu.virost@cea.fr

Over fifty years ago, the description of plutonium peroxo complexes started with the addition of hydrogen peroxide to acidic Pu(IV) solutions, forming colored species in solution. The solutions were reported to transition from the brown to the red color as H₂O₂ concentration increased. Several structures have been postulated.[1] The excessive addition of H₂O₂ to Pu(IV) acidic solutions was reported to form green precipitates, used as precursors for the purification of Pu solutions prior to PuO₂ synthesis or for nuclear spent fuel waste management.[2] Nowadays, the literature surprisingly offers only one resolved structure for Pu peroxo compounds: a dimeric peroxo carbonato compound exhibiting bridging $\mu_2\text{-}\eta^2\text{-}\eta^2\text{O}_2$ ligands [3].

In this study, we synthesized a new peroxo compound of tetravalent plutonium by diluting Pu(IV) acidic aliquots into highly concentrated solutions of H₂O₂ (n(H₂O₂)/n(Pu) ratio > 10) at a pH of 1-2. Such a procedure resulted in the formation of a stable green solution devoid of any precipitate. The solution displayed distinct absorption bands at 455 nm and 820 nm with a broader one located in the 654-660 nm region (Fig. 1.a). Upon drying, the solid precipitated as a green compound exhibiting an absorption spectra identical to the stable green species observed in solution. This observation, in combination to laboratory and synchrotron characterization techniques, allowed to clarify the coordination sphere of the Pu atoms and the presence and nature of the peroxo ligands in the structure (Fig. 1.b). The approach allowed us to propose a relevant polynuclear structure agreeing with the clues acquired from the different techniques.

Figure 1(a) Vis-NIR absorption spectra acquired in solution for the (A) brown (495, 541 and 658 nm), (B) red (510 and 530 nm) and (C) green (455, 654-660 and 821 nm) peroxo complexes or compounds of Pu(IV) in nitric media. Insert: photograph of the respective solutions (b) FT of the experimental k^3 -weighted EXAFS spectrum (black) measured on the green peroxo complex in solution (5 mM). Blue and orange circles stand for the fits.



[1] R.E. Connick et al., J. Am. Chem. Soc. 71 (1949)

[2] J.A. Leary et al. Ind. Eng. Chem. 51 (1959) 27-31

[3] W. Runde et al. Chem. Commun. (2007) 1728.

Development of Water-Compatible N_3O_2^- -Pentadentate Planar Ligands for Uranium Harvesting from Seawater

Koichiro Takao,¹ Takumi Mizumachi,¹ Minami Sato,¹ Koma, Ito,¹ Ryuto Nabata,¹ Masashi Kaneko,² Tomoyuki Takeyama,^{1,3} Satoru Tsushima^{4,5}

¹Laboratory for Zero-Carbon Energy, Institute of Innovative Research, Tokyo Institute of Technology, Japan.

²Department of Chemistry, Graduate School of Science, Osaka University, Japan.

³Department of Applied Chemistry, Sanyo-Onoda City University, Japan.

⁴Institute of Resource Ecology, Helmholtz-Zentrum Dresden-Rossendorf, Germany.

⁵International Research Frontiers Initiative, Institute of Innovative Research, Tokyo Institute of Technology, Japan.

E-mail: takao.k.ac@m.titech.ac.jp

Development of sustainable human society that can also coexist with the natural environments cannot be achieved without securing stable and clean electric energy supply. Nuclear power has an overwhelmingly high energy density ($\sim 10^9$ kcal·mol⁻¹), and does not emit greenhouse gases like CO₂ at least during power generation, making it the most powerful baseload energy source distinguishable from others available today. Needless to say, nuclear fuels must be continuously supplied to generate electricity in the power plant. Accordingly, resource security of nuclear fuel materials, most commonly U, is the largest concern for sustainability of the nuclear energy supply [1]. Seawater is dissolving most of naturally occurring elements including U. While its concentration is very small (3.3 ppb = 14 nM), the net amount of U in seawater is approx. 4.5×10^9 tons thanks to the huge volume of seawater (1.35×10^9 km³), which is 10^3 times greater than that in terrestrial mining available. Therefore, U in seawater is one of promising options to resolve the resource security concerns for nuclear fuel materials. However, there are additional challenging aspects arising from concomitance of other metal ions and presence of HCO₃⁻/CO₃²⁻ (2.3 mM in total), which strongly binds to UO₂²⁺ to give its triscarbonato complex, [UO₂(CO₃)₃]⁴⁻, the most predominant form of U dissolved in seawater [2].

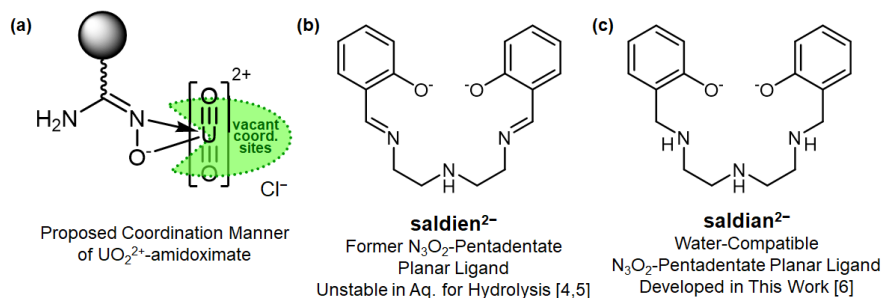


Fig. 1. Schematic structures of (a) proposed side-on type coordination of UO₂²⁺ bound to amidoximate anchored onto polymer resin and N₃O₂-type pentadentate planar ligands, (b) saldien²⁻ [4,5] and (c) saldian²⁻ [6].

A common approach to collect U from seawater is adsorption onto a chemically engineered resin. An amidoximate (Fig. 1(a)) is the most well-known functional group for this purpose, and widely employed as an adsorption site installed onto a polymer chain through chemical decoration or radiolytic grafting. Although the amidoximates actually exhibit affinity with UO₂²⁺ in an aqueous system, such complexation is not always strong enough especially under the seawater condition containing HCO₃⁻/CO₃²⁻ at pH ~8. The 1:1 complexation in the side-on manner (Fig. 1(a)) is supposed to occur during the adsorption process [3], where large vacancy still remains in the equatorial plane of UO₂²⁺. As a result, additional coordination should be present, although it would be difficult to control what actually happens there. An extra anion such as Cl⁻ is also required to be incorporated in this mechanism to compensate the remaining positive charge from UO₂²⁺ bound to the singly anionic amidoximate. It is also not very clear in a viewpoint of molecular design how amidoximates exhibit selectivity towards UO₂²⁺ superior to other concomitant elements present in seawater. We believe that there is still

much space for designing sophisticated U-capturing molecule, where its coordination chemistry will provide helpful hints. Herein, we propose a new pentadentate planar ligand structure designed for the U *harvesting* from seawater, and report its actual coordination behavior with UO_2^{2+} under simulated seawater conditions.

It is well known that UO_2^{2+} most typically accepts five-fold coordination in its equatorial plane. On this implication, we have designed N_3O_2 -pentadentate planar ligands to fully cover the equatorial coordination sites of UO_2^{2+} for anticipating the largest stabilization by chelating effect. Indeed, we have already succeeded in synthesis and characterization of UO_2^{2+} complexes with N_3O_2 -pentadentate Schiff base ligands, *saldien*²⁻ (Fig. 1(b)), having the basic structural motif proposed here [4, 5]. However, a series of the former *saldien*²⁻ ligands is no longer available for the U harvesting from seawater, because its azomethine groups ($-\text{CH}=\text{N}-$) tend to be readily hydrolyzed in an aqueous system. To overcome this issue, we converted these weak moieties to the corresponding amino groups ($-\text{CH}_2-\text{NH}-$) through reductive amination with borohydrides. This approach was rather successful to afford a water-compatible N_3O_2 -pentadentate planar ligand, *saldian*²⁻ (Fig. 1(c)) [6].

Under the simulated seawater condition (0.5 M NaCl + 2.30 mM $\text{HCO}_3^-/\text{CO}_3^{2-}$ at pH 8.00(3)), *H*₂*saldian* exhibits 5-step acid dissociation/association equilibria pronounced by $\text{pK}_{\text{a}1} = 4.15$, $\text{pK}_{\text{a}2} = 8.06$, $\text{pK}_{\text{a}3} = 9.51$, $\text{pK}_{\text{a}4} = 11.29$, and $\text{pK}_{\text{a}5} = 14.97$, corresponding to two phenolates and three amino groups of *saldian*²⁻ shown in Fig. 1(c). A reaction of *H*₂*saldian* with $\text{UO}_2(\text{NO}_3)_2 \cdot 6\text{H}_2\text{O}$ in ethanol immediately afforded orange powder of $\text{UO}_2(\text{saldian})$ (Fig. 2(a)), where all 5 donating atoms of *saldian*²⁻ fully saturate the equatorial plane of UO_2^{2+} as expected to make a stable chelate. A stability constant of $\text{UO}_2(\text{saldian})$ ($\log \beta_{11}$) under the simulated seawater condition was determined to be 28.05 ± 0.07 by UV-vis titration experiments. It is noteworthy that the stability of $\text{UO}_2(\text{saldian})$ is much higher than those of other ligands such as amidoximates and dicarboxylates reported so far in 10–15 order of magnitude. The characteristic absorption bands of $\text{UO}_2(\text{saldian})$ were well corroborated by the TDDFT calculations. Due to much greater stability compared with that of $\text{UO}_2(\text{CO}_3)_3^{4-}$ ($\log \beta_{13} = 21.84$), $\text{UO}_2(\text{saldian})$ is predominantly formed in the range from pH 4.3 to pH 12.7 including the seawater condition, pH ~8, as shown in the speciation diagram (Fig. 2(b)). Thanks to the unique pentadentate planar coordination, good selectivity for UO_2^{2+} from other metal ions (alkaline metals: Li^+ , Na^+ , K^+ ; alkaline earths: Mg^{2+} , Ca^{2+} , Sr^{2+} , Ba^{2+} ; divalent d-black metals: Ni^{2+} , Cu^{2+} , Zn^{2+} , Cd^{2+} ; and others relatively abundant: Al^{3+} , Zr^{4+} (surrogate of Ti^{4+}), VO_2^+ , MoO_4^{2-}) coexisting in seawater was also achieved as demonstrated by their separation factors at least greater than 10^3 . All the results obtained in this work indicate that *saldian*²⁻ is a promising ligand towards U harvesting from seawater.

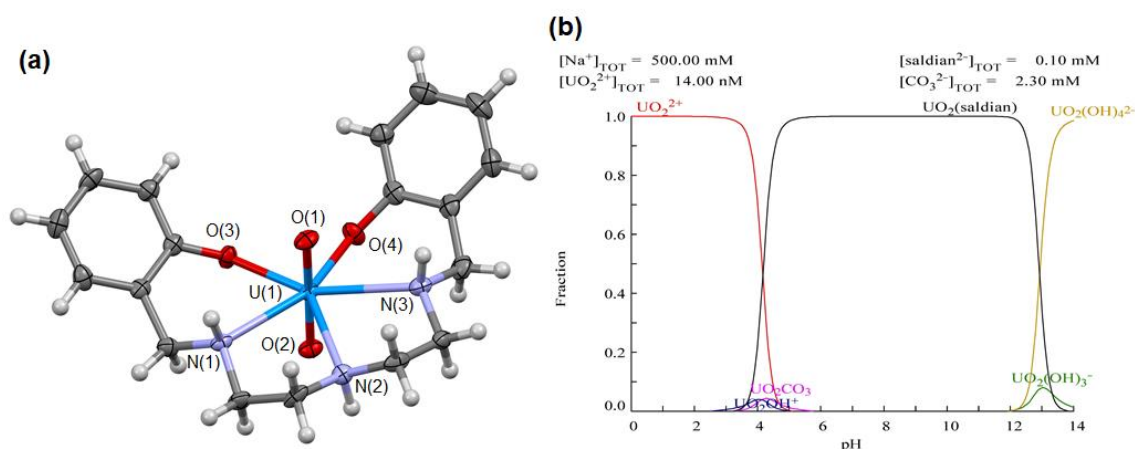


Fig. 2. Molecular structure of $\text{UO}_2(\text{saldian})$ complex (a) and speciation diagram of UO_2^{2+} (3.3 ppb = 14 nM) under simulated seawater condition (0.5 M NaCl + 2.3 mM $\text{HCO}_3^-/\text{CO}_3^{2-}$) at 298 K and different pH [6].

This work was supported in part by JAEA Nuclear Energy S&T and Human Resource Development Project through concentrating wisdom Grant Number JPJAI9P19209861, Grants-in-Aid for Scientific Research (20H02663, 21J11942), and World Research Hub (WRH) Program of International Research Frontiers Initiative (IRFI), Tokyo Institute of Technology.

Reference: [1] *Dalton Trans.* **2023**, 52, 9866–9881. [2] *Chem. Eur. J.* **2014**, 20, 14499–14506. [3] *Nat. Commun.* **2018**, 9, 1644. [4] *Inorg. Chem.* **2010**, 49, 2349–2359. [5] *Inorg. Chem.* **2021**, 60, 11435–11449. [6] *Inorg. Chem.* **2022**, 61, 6175–6181.

Complexation and Solvent Extraction Properties of the *N, N, N', N'*-tetraethyl-1,10-phenanthroline-2,9-Diamide Extractant with Ln(III) and An(III)

Emma M. Archer[†], Jocelyn M. Riley[†], Felipe A. Pereiro[‡], Elizabeth B. Flynn[†], Jacob P. Brannon[†], Stosh A. Kozimor[‡], Jessica A. Jackson[†], Jenifer C. Shafer[†], and Shane S. Galley[†]

Department of Chemistry, Colorado School of Mines, Golden, Colorado, USA[†]

Los Alamos National Laboratory, Los Alamos, New Mexico, USA[‡]

Characterization of the coordination chemistry of the trivalent actinides (An(III)) with extractants is vital to the remediation of nuclear fuel cycle waste. The chemistry of the An(III), beyond Am(III) and Cm(III), in solvent extraction is not widely understood in terms of extraction behavior, but is essential to understanding separation schemes. Phenanthroline diamide (DAPhen) ligands have been of recent interest in the *f*-element separation field due to having molar acid stability, no third phase formation, a rigid backbone structure for faster complexation kinetics, tunable amide arms, and binding through both nitrogen and oxygen ((N,O)-donor) atoms. Investigating trends across the trivalent lanthanide (Ln(III)) and An(III) series can provide insight into the bonding and extraction trends with DAPhen ligands. A series of studies have been completed with the *N, N, N', N'*-tetraethyl-1,10-phenanthroline-2,9-diamide (TetDAPhen) extractant to elucidate the bonding and extraction trends of the An(III) and Ln(III). Solvent extraction results have revealed higher affinity for An(III). The distribution ratios from Am(III)-Cf(III) have shown that Am(III) and Bk(III) have near identical extraction followed by Cf(III) and then Cm(III), resulting in an interesting trend. This decrease in Cm(III), Bk(III), and Cf(III) distribution ratios with respect to Am(III) has not been previously observed for the DAPhen systems. The figure below shows an example of a Ln(TetDAPhen)(NO₃)₃ complex. Interesting trends in bonding across the Ln(III) series from Pr(III)-Lu(III) have been observed, in addition to comparison to Am(III). This allows for investigation of any differences in bonding between the An(III) and Ln(III). These results will be presented.

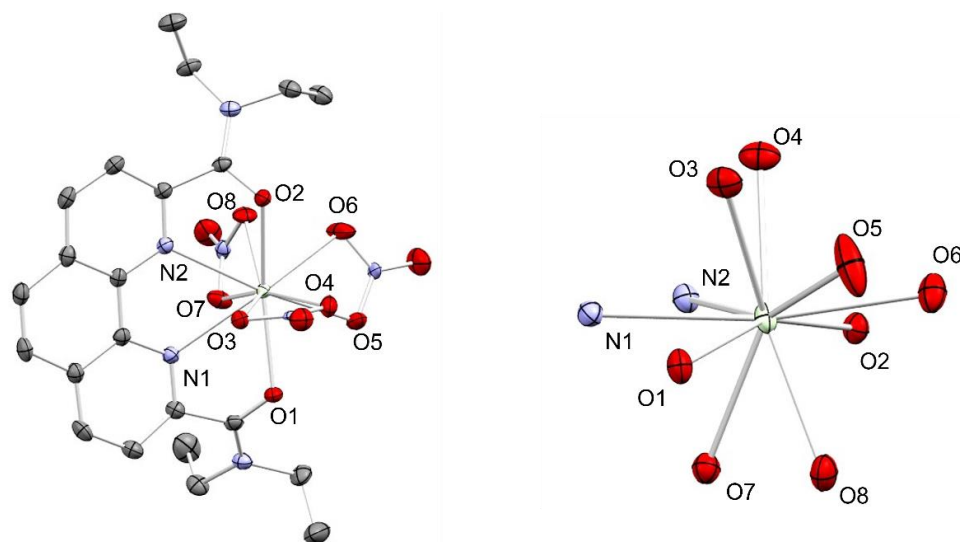


Figure. Example crystal structure of a Ln(TetDAPhen)(NO₃)₃ complex showing a 10-coordinate geometry and three bidentate nitrates coordinating to the metal center.

Speciation of Uranium(VI) with Amido-Phosphonate Ligands in Organic Phase and at the Solid/Liquid Interface Studied by Molecular Dynamics

Diego Moreno Martinez, Dominique Guillaumont, and Philippe Guilbaud
CEA, DES, ISEC, DMRC, Univ Montpellier, Marcoule, France

The amido-phosphonate extractants have recently been developed for the separation of uranium(VI) using liquid/liquid and solid/liquid extraction.^{1,2} The bifunctional structure of these molecules were conceived by coupling an acid organic function (phosphonate) and a solvating group (amide). Despite previous studies, a detailed characterization at the molecular and supramolecular scale is missing for those systems and the role of each functional groups is not fully understood. In this work, classical Molecular Dynamics was coupled to experimental data in order to describe the behavior of amido-phosphonate extractants and the speciation of uranium(VI) in liquid/liquid and solid/liquid extraction systems. Organic phases and solid/liquid interfaces were simulated based on experimental compositions with and without uranium. A fine description of the species and interactions within the aggregates could be given in the organic phase.³ Most of the aggregates are dimers and trimers interacting through phosphonate-phosphonate interactions. For the solid/liquid systems, where the extractants can be either grafted or impregnated on the solid support, two different supramolecular organization are observed. In the impregnated case, the extractants are interestingly predisposed to uranium complexation. Light is shed on the extraction mechanism, the uranium species are stabilized not only by complexation of extractants but also by weak interactions networks. Thanks to this, the extraction takes place without fully dehydrating the metallic center in all studied systems. These results underline the importance of considering weak interaction in the understanding of extraction processes and show how coupling molecular modelling with experiments leads to a fine exploration of the molecular interactions and supramolecular organization of such systems.

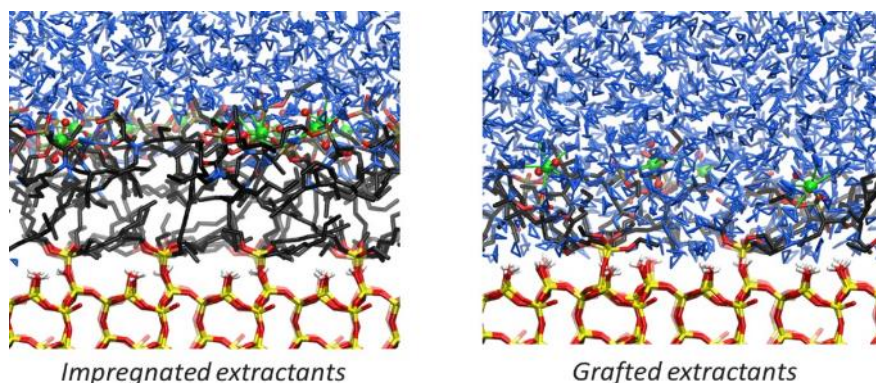


Figure 1. Molecular dynamics snapshots of the solid/liquid interface supramolecular organization depending on the incorporation mode of extractant molecules.

References

- [1] Pecheur, O. ; Guillaumont, D. ; Dourdain, S. ; Berthon L. ; Turgis R. ; Fillaux, C. ; Arrachart, G. ; Testard, F. ; *Solvent Extr. Ion Exc.*, **2016**, vol. 34, no 3, p. 260-273.
- [2] Le Nedelec, T. ; Charlot, A. ; Calard, F. ; Cueur, F. ; Leydier, A. ; & Grandjean, A. *New J. Chem.*, **2018**, vol. 42, no 17, p. 14300-14307.
- [3] Moreno Martinez, D. ; Acher, E. ; Vatin, M. ; Dourdain, S. ; Guillaumont, D. ; Guilbaud, P. *J. Phys. Chem. B.* **2021**, vol. 125, no 38, 10759-10771.

Probing the Metal Ion–Ligand Interaction in An(III) and Ln(III) Complexes: An Overview about Recent Advancements

Thomas Sittel¹, Patrik Weßling,^{1,2} Andreas Geist,¹ Petra J. Panak^{1,2}

¹Karlsruhe Institute of Technology (KIT), Institute for Nuclear Waste Disposal (INE), Karlsruhe Germany;

²Heidelberg University, Institute for Physical Chemistry, Heidelberg Germany

Tridentate N-donor and O-donor ligands form strong, ninefold coordinated complexes with trivalent actinide and lanthanide ions.^[1] Some selected ligands are under consideration for potential use as extracting agents in actinide recycling processes. Whereas O-donor ligands enable separation of trivalent lanthanides and actinides from nuclear fuels, N-donor ligands are suitable to selectively separate An(III) from Ln(III).^[2] Given these distinct extraction behaviors, conducting in-depth investigations into the coordination chemistry of An(III) and Ln(III) complexes with various N- and O-donor ligands is crucial. In this context, this overview aims to summarize recent advancements in this field, highlighting our utilization of a multi-method approach to strengthen the understanding of the coordination chemistry of An(III) and Ln(III).

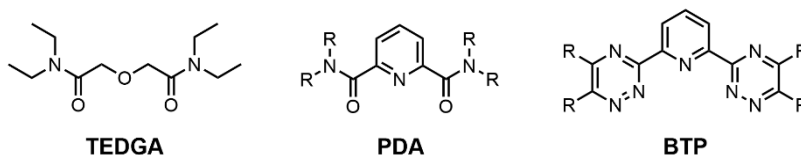


Figure 1: Representatives for O-donor, N,O-donor and N-donor ligands studied in recent years.

In close collaboration with the European actinides extraction community, our research involves solvent extraction studies aimed to determine the selectivity of an organic ligand. These investigations offer insight into the coordination chemistry of the An(III) and Ln(III) ions. Figure 1 showcases examples of ligand-types investigated in recent years. Solvent extraction distribution data indicate an increase in selectivity of An(III) over Ln(III) with an increasing number of coordinating nitrogen atoms: Selectivity for Am(III) over Eu(III) is in the range of $SF_{Am/Eu} > 100$ for BTP, $SF_{Am/Eu} \approx 10$ for PDA, and $SF_{Am/Eu} \approx 0.2$ for DGA.^[3,4,5] In fact, DGAs affinity for a given An(III) is similar to that of Ln(III) with similar ionic radius.

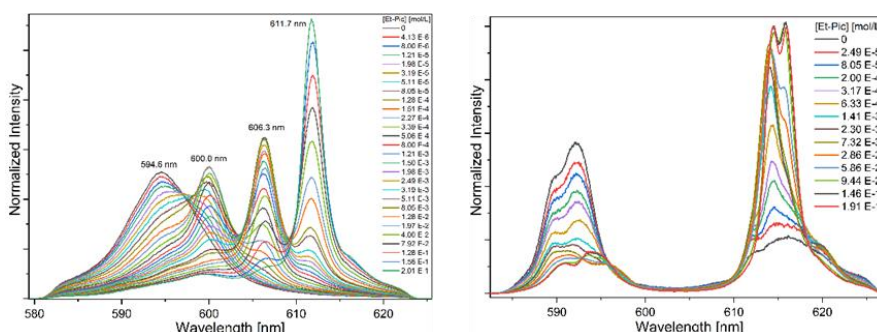


Figure 2: Emission spectra of Cm(III) (left) and Eu(III) (right) as a function of the Et-Pic concentration in acetonitrile.^[6]

The extraction studies are complemented by spectroscopic studies such as time-resolved laser fluorescence spectroscopy (TRLFS), a robust method for determining complex stoichiometry and stability constants. For instance, Figure 2 shows the evolution of the emission spectra for Cm(III) (left) and Eu(III) (right) as a function of the Et-PDA concentration. Spectral analysis confirms the presence of $[Cm(Et-PDA)_{1-3}]^{3+}$ and $[Eu(Et-PDA)_{1-3}]^{3+}$ complexes in solution. The complex stability constants for the individual 1:3 complexes are presented in Table 1 alongside the stability constants for the TODGA and nPr-BTP complexes. The table highlights significant distinctions in complex stability between Cm(III) and Eu(III)

complexes as the number of nitrogen atoms increases. This culminates in a difference by two orders of magnitude for $[\text{Cm}(\text{nPr-BTP})_3]^{3+}$ compared to the respective $\text{Eu}(\text{III})$ complex. This suggests different binding properties in the $\text{Ln}(\text{III})\text{-N}$ and $\text{An}(\text{III})\text{-N}$ bonds. Additionally, leveraging these stability constants enables the determination of selectivity in monophasic TRLFS experiments, aligning closely with separation factors determined through solvent extraction.

Table 1 Comparison of the stability constants and separation factors of the 1:3 $\text{Cm}(\text{III})$ and $\text{Eu}(\text{III})$ complexes with the O-donor ligand TODGA, the N-donor ligand nPr-BTP and the mixed N,O-donor ligand Et-PDA.

	$\log \beta_{3,\text{Cm}(\text{III})}$	$\log \beta_{3,\text{Eu}(\text{III})}$	$SF_{\text{Cm/Eu}}^{\text{TRLFS}}$	$SF_{\text{Cm/Eu}}^{\text{Extr.}}$
TODGA	14.9 ± 0.3	15.7 ± 0.2	0.16	0.19
Et-PDA	7.6 ± 0.4	6.3 ± 0.3	20	–
nPr-BTP	14.4 ± 0.1	11.9 ± 0.1	300	230

The differences in complex stability between $\text{Ln}(\text{III})$ and $\text{An}(\text{III})$ complexes with N-donor ligands are evident. Literature suggests a slightly more substantial covalent contribution to the $\text{An}(\text{III})\text{-N}$ interaction compared to $\text{Ln}(\text{III})\text{-N}$. However, literature lacks spectroscopic studies directly probing the metal ion–ligand interaction. To deepen our understanding of bonding properties in $\text{Ln}(\text{III})$ and $\text{An}(\text{III})$ complexes, we employ NMR spectroscopy. This method allows us to study the $\text{M}(\text{III})\text{-O}$ interaction – exploiting the delocalization of the lone pair of electrons of the amide nitrogen atom – and the $\text{M}(\text{III})\text{-N}$ interaction using ^{13}C and ^{15}N NMR techniques. Figure 3 shows the ^1H , ^{15}N correlation NMR spectra of $[\text{M}(\text{Et-PDA})_3]^{3+}$ and $[\text{M}(\text{nPr-BTP})_3]^{3+}$

($\text{M} = \text{Am}, \text{Sm}, \text{Lu}$). The results confirm the expected similarity of $\text{An}(\text{III})\text{-O}$ and $\text{Ln}(\text{III})\text{-O}$ bonds. However, substantial differences between the $\text{An}(\text{III})\text{-N}$ and $\text{Ln}(\text{III})\text{-N}$ interactions are evident from NMR shifts of the coordinated nitrogen atoms differing by nearly 300 ppm. This is widely accepted as evidence supporting a higher degree of covalent bonding in the $\text{An}(\text{III})\text{-N}$ interaction.

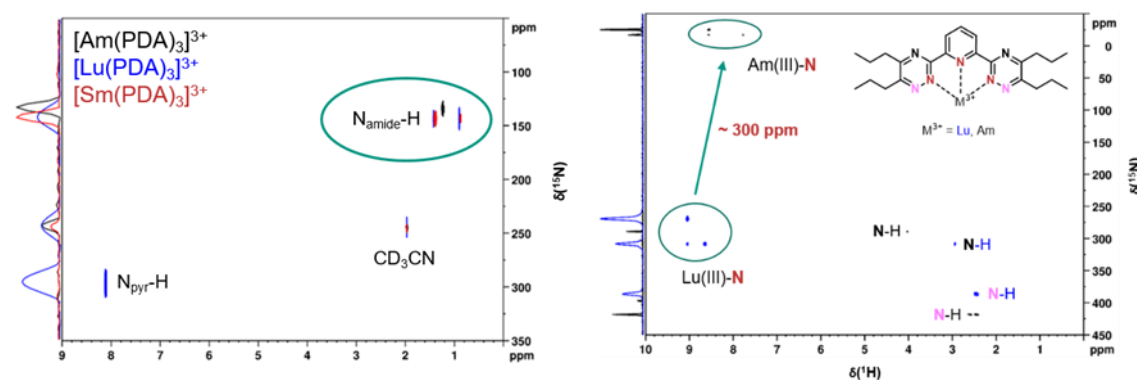


Figure 3: A comparison of the ^1H , ^{15}N HMQC NMR spectra between $\text{Am}(\text{III})$ and $\text{Ln}(\text{III})$ complexes with Et-PDA and nPr-BTP .^[6,7]

Financial support for this research was provided by the German Federal Ministry of Education and Research through the *f-Char* project under grant numbers 02NUK059A and 02NUK059C.

References

- [1] P. J. Panak, A. Geist *Chem. Rev.* **2013**, 113, 1199–1236.
- [2] A. Geist, P. J. Panak *Solv. Extr. Ion Exch.* **2021**, 39, 128–151.
- [3] A. Geist, U. Müllich et al. *Solv. Extr. Ion Exch.* **2012**, 30, 433–444.
- [4] A. Paulenova, M. Y. Alyapyshev et al. *Sep. Sci. Technol.* **2008**, 43, 2606–2618.
- [5] N. L. Banik, M. A. Denecke et al. *Inorg. Chem. Commun.* **2013**, 29, 172–174.
- [6] T. Sittel, P. Weßling et al. *Dalton Trans.* **2022**, 51, 8028–8035.
- [7] C. Adam, P. Kaden et al. *Dalton Trans.* **2013**, 42, 14068–14074.

Reactivity of Actinides Mono-Cations with NH₃ in Gas Phase: A Study Using ICP-MS and Quantum Chemistry

M. Goujet [1], A. Quémet [1] and D. Guillaumont [1]

[1] CEA, DES, ISEC, DMRC, Univ. Montpellier, Marcoule, France.

mathilde.goujet@cea.fr

Over the last decades, reactions between actinides mono-cations and small molecules in gas phase attracted a great interest. Gas phase reactivity is a simple approach (no matrix effect) to better interpret and understand the role of actinide's electronic structure and contribution of 5f electrons to their reactivity. Experimental studies using different mass spectrometry techniques revealed differences in actinide reactivity with several gaseous molecules (NH₃, O₂, CO₂, CH₄, C₂H₄ ...). An experimental correlation between actinides reactivity and their electronic promotion energies was established [1]. The electronic promotion energy is the energy required for the actinides to have 2 non-f electrons. The lower this energy is, the better the reactivity is.

To verify this correlation, an experimental study using reaction cell in Inductively Coupled Plasma Mass Spectrometry (ICP-MS) was achieved with NH₃. Th⁺, Pa⁺, U⁺, Np⁺ and Cm⁺, whose electronic promotion energies are below 0.5 eV, react completely to form AnNH⁺ unlike Pu⁺ and Am⁺, whose energies are above 1 eV. In addition, from an analytical point of view, these differences in reactivity helps to solve isobaric and polyatomic interferences that complicate the analysis of some isotopes in ICP-MS such as ²³⁸U/²³⁸Pu, ²³⁸U/²³⁹Pu or ²⁴²Pu/^{242m}Am/²⁴²Cm.

Quantum chemical computations were also performed to characterize reaction mechanisms between actinides mono-cations (Ac⁺, Th⁺, Pa⁺, U⁺, Np⁺, Pu⁺, Am⁺ and Cm⁺) and NH₃. The geometries of the transition states and the thermodynamic properties were determined using Density Functional Theory (DFT) and Coupled Cluster theory (CCSD(T)). In the case of Ac⁺, Th⁺, Pa⁺, U⁺, Np⁺ and Cm⁺, after formation of the An⁺--NH₃ complex, actinide mono-cation inserts itself in N-H bond until H₂ is eliminated via two transition states and intermediate species HANNH₂⁺. Figure 1 shows the reaction scheme for Cm⁺ with NH₃ (a similar mechanism is observed for Ac⁺, Th⁺, Pa⁺, U⁺ and Np⁺). For Pu⁺ and Am⁺, the limiting step is the formation of the first transition state (Figure 1). This step is only possible if the actinide has two non-f electrons: the electronic promotion energy of Pu⁺ and Am⁺ required to obtain this reactive configuration is too high.

Comparison of experimental and theoretical studies established a correlation between actinide reactivity and electronic structure. This prove the need for actinide mono-cations to have a reactive electronic configuration with two non-f electrons. The higher the electron promotion energy, the more difficult it is to achieve a reactive configuration to cross the first transition state.

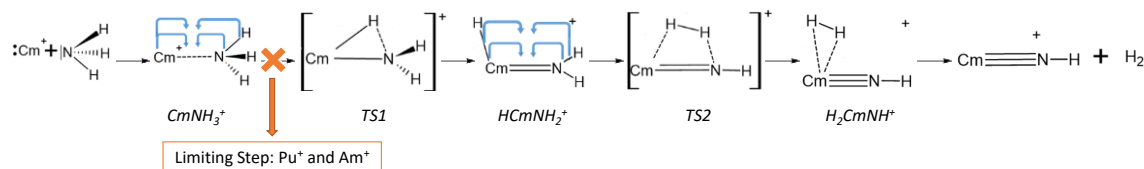


Figure 1 : Reaction scheme for Cm⁺ + NH₃ determined with DFT calculations

[1] J.K. Gibson, Gas-phase chemistry of actinide ions: probing the distinctive character of the 5f elements, Int. J. Mass Spectrom. 214 (2002) 1-21. [https://doi.org/10.1016/S1387-3806\(01\)00559-0](https://doi.org/10.1016/S1387-3806(01)00559-0)

Crystal Growth of New Uranium and Transuranic Phases via High Temperature Solution and Mild Hydrothermal Methods: Exploration of New Materials as Potential Nuclear Waste Forms

H.-C. zur Loye^{1,2,3,*}, T. K. Deason^{1,2,3}, A. T. Hines^{1,2}, H. Tisdale^{1,2}, T. M. Besmann^{1,2}, J. Amoroso^{1,3}, D. P. DiPrete^{1,3}

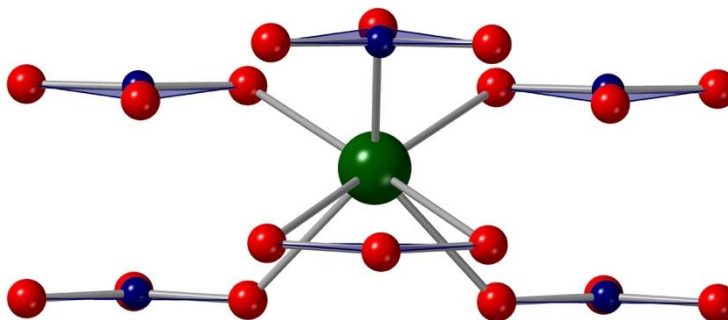
¹ Center for Hierarchical Waste Form Materials, Columbia, South Carolina 29208, United States

² University of South Carolina, Columbia SC, 29208, United States

³ Savannah River National Laboratory, Aiken, South Carolina 29808, United States

* The presenting author email: zurloye@mailbox.sc.edu

The crystal growth of uranium and transuranium containing phases has been accomplished via two different crystal growth routes, mild hydrothermal and high temperature solution flux growth. In both cases we are targeting the preparation of new compositions to evaluate their potential use as nuclear waste forms. The mild hydrothermal route works extremely well for crystallizing complex fluoride phases, such as $\text{Na}_3\text{GaU}^{\text{IV}}\text{F}_{30}$, $\text{Na}_3\text{AlNp}^{\text{IV}}\text{F}_{30}$, $\text{Na}_3\text{FePu}^{\text{IV}}\text{F}_{30}$, and $\text{Cs}_2\text{NiNp}^{\text{IV}}\text{F}_{16}$, [1,2] while the high temperature flux route works well for crystallizing oxide phases, such as $\text{Cs}_2\text{Pu}^{\text{IV}}\text{Si}_6\text{O}_{15}$, $\text{K}_3\text{Am}(\text{PO}_4)_2$, AmPO_4 , and $\text{Na}_2\text{Pu}^{\text{IV}}\text{O}_2(\text{BO}_3)$. [3,4] The synthesis and structures of these phases will be discussed, along with our approach of identifying potential compositions that we can pursue synthetically. [5] Surrogate containing analogs are further investigated for their resilience to radiation damage to help identify new nuclear waste forms. [6]



Local coordination environment of americium in AmPO_4 (Am – green, P – blue, O – red)

- [1] K.A. Pace, V.V. Klepov, T. K. Deason, M. D. Smith, D. P. DiPrete, J. Amoroso, H.-C. zur Loye, Chem. Eur. J., **26**, 12941-12944 (2020)
- [2] T. K. Deason, G. Morrison, A. Mofrad, H. Tisdale, J. Amoroso, D. P. DiPrete, G. Was, K. Sun, T. M. Besmann, H.-C. zur Loye, J. Am. Chem. Soc., **145**, 465-475 (2023)
- [3] K. A. Pace, V. V. Klepov, M. S. Christian, G. Morrison, T. K. Deason, T. M. Besmann, D. P. DiPrete, J. Amoroso, H.-C. zur Loye, Chem. Commun., **56**, 9501-9504 (2020)
- [4] Deason, T. K., Hines, A. T., Morrison, G., Smith, M. D., Besmann, T. M., Mofrad, A. M., Fondeur, F. F., Lehman-Andino, I., Amoroso, J. W., DiPrete, D. P., zur Loye, H.-C., "Flux Crystal Growth of the Extended Structure $\text{Pu}(\text{V})$ Borate $\text{Na}_2(\text{PuO}_2)(\text{BO}_3)$ ", J. Am. Chem. Soc., 2023, 145, 10007-10014.
- [5] M. Christian, K. A. Pace, V. V. Klepov, G. Morrison, H.-C. zur Loye, H.-C., T. M. Besmann Cryst. Growth Design, **21**, 5100-5107 (2021)
- [6] H. Tisdale, M. S. Christian, G. Morrison, T. M. Besmann, K. Sun, G. Was, H.-C. zur Loye, Chem. Mater., **34**, 3819-3830 (2022)

Molecular and Crystal Structures of Pu(IV)-Nitrate Complexes with Double-Headed 2-Pyrrolidone Derivatives in HNO₃(aq)

Ryoma Ono¹, Tomoyuki Takeyama¹, Robert Gericke², Juliana März², Tamara Duckworth², Satoru Tsushima^{2,3}, Koichiro Takao¹

¹ Laboratory for Zero-Carbon Energy, Institute of Innovative Research, Tokyo Institute of Technology, NI-32, 2-12-1, Ookayama, Meguro-ku, Tokyo 152-8550 Japan

² Institute of Resource Ecology, Helmholtz-Zentrum Dresden-Rossendorf (HZDR), Bautzner Landstraße 400, 01328 Dresden, Germany

³ International Research Frontiers Initiative (IRFI), Institute of Innovative Research, Tokyo Institute of Technology, O-okayama, Meguro-ku, 152-8550 Tokyo, Japan

1. Introduction

Tetravalent actinides (An(IV)) widely occurs in the nuclear fuel cycle. For example, Pu(IV) and Th(IV) are the main species of these elements there, while U(IV) is also employed to reduce extractable Pu(IV) to unextractable Pu(III) in the PUREX process [1]. Therefore, the An(IV) chemistry needs to be understood in depth.

Previously, we have reported that An(IV) (An = Th, U, Np) commonly form sparingly soluble compounds with double-headed 2-pyrrolidone derivatives (**L**), (HL)₂[An(NO₃)₆] (**L** = **14Cy** and **12Cy**, Fig. 1) in 3 M HNO₃(aq) [2-3]. Based on these results, we have proposed an advanced principle for nuclear fuel reprocessing, namely *NU*nuclear fuel *M*aterials selective *P*recipitation (NUMAP). In connection with this, we have preliminarily studied Ce(IV) as an inactive simulant of Pu(IV). However, Ce(IV) shows much different chemistry from that of An(IV), where [Ce₂(μ-O)(NO₃)₆(**14Cy**)₂]_n including a [Ce-O-Ce]⁶⁺ motif is formed despite high acidic system with 3 M HNO₃(aq) due to its strong hydrolysis tendency (Table 1) [4-5]. Up to now, Pu(IV) is known to exhibit both possibilities to form [Pu(NO₃)₆]²⁻ and [Pu-O-Pu]⁶⁺ in crystal structures [6-7]. Therefore, we wonder which (HL)₂[Pu(NO₃)₆] or [Pu₂(μ-O)(NO₃)₆(**L**)₂]_n is preferred to be taken by Pu(IV) under presence of **L** in 3 M HNO₃(aq). This makes critical difference in chemical stoichiometry of the Pu(IV) deposit for its recovery in the NUMAP reprocessing; the Pu:**L** mole ratio is 1:2 in (HL)₂[Pu(NO₃)₆], while 1:1 in [Pu₂(μ-O)(NO₃)₆(**L**)₂]_n. To answer this question, we have prepared Pu(IV)-nitrate complexes with **L** from HNO₃(aq), and determined molecular and crystal structures of them as well as those of M(IV) analogues (M = Ce, Th, U).

2. Experimental

Stock solutions of M(IV), HNO₃(aq), and **L** were layered in a glass tube (φ4 for Ce, Th, U or φ5 for Pu) from bottom to top to make [M(IV)]_{total} = 27.8 mM, [**L**]_{total} = 55.6 mM at different [HNO₃]. Deposited crystals of M(IV) compounds were characterized by SCXRD. The supernatants were also analyzed by ICP-AES for Ce, Th, U, or UV-vis spectrophotometry for Pu.

3. Result and Discussion

Pale green crystals of Pu(IV) with **14Cy** or **12Cy** deposited from 3 M HNO₃(aq). Figure 2 shows the molecular structures of these Pu(IV) compounds, where it is clearly presented that (HL)₂[Pu(NO₃)₆] (**L** = **14Cy**(a) and **12Cy**(b)) are given. In both phases, Pu(IV) is twelve-coordinated by 6 bidentate NO₃⁻ to form the hexanitrate complex, [Pu(NO₃)₆]²⁻, showing nearly T_h-

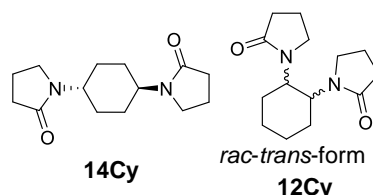


Fig. 1 Schematic structures of **14Cy** and **12Cy**.

Table 1. Ionic Radii and First Hydrolysis Constants (log β₁) of M⁴⁺ [5,8].

	Ionic Radius/Å*	log β ₁ **
Th	1.05	-2.50
U	1.00	-0.54
Np	0.98	0.55
Ce	0.97	3.20

symmetry. The mean bond length between Pu(IV) and O of NO_3^- (O_{NO_3}) is 2.49 Å. The value is consistent with that of common Pu(IV)-hexanitrate complexes (2.46–2.53 Å) reported so far [6]. Furthermore, the bond valence sum around Pu(IV) is 3.89–4.07 (**L** = **14Cy**) and 3.84–4.03 (**L** = **12Cy**), indicating that the tetravalence is maintained. The negative charge of $[\text{Pu}(\text{NO}_3)_6]^{2-}$ must be compensated in each crystal structure. This task is taken by anhydrous H^+ ($\text{H}(1)$) sandwiched by neighboring **L** to afford hydrogen bonded polymer, $(\text{HL})_2$. The crystal structures of $(\text{HL})_2[\text{Pu}(\text{NO}_3)_6]$ (**L** = **14Cy**, **12Cy**) are isomorphous with those of $(\text{HL})_2[\text{M}(\text{NO}_3)_6]$ (**M** = Th, U, Np) with respective **L**. In conclusion, Pu(IV) gives $(\text{HL})_2[\text{Pu}(\text{NO}_3)_6]$ under presence of **14Cy** and **12Cy** from 3 M $\text{HNO}_3(\text{aq})$ in a similar manner to other An(IV), but unlike Ce(IV) with **14Cy**. Such a gap between An(IV) and Ce(IV) most probably resulted from the difference in hydrolysis tendency shown in Table 1.

Figure 3 shows a relationship between M– O_{NO_3} length in $(\text{HL})_2[\text{M}(\text{NO}_3)_6]$ and ionic radii of M(IV) (r_i , CN = 12). Note that Ce(IV) also gives $(\text{H14Cy})_2[\text{Ce}(\text{NO}_3)_6]$ in 9 M $\text{HNO}_3(\text{aq})$ as we reported previously [4]. As a result, good correlation was observed, which seems to simply follow the actinide contraction.

In the NUMAP reprocessing, Pu(IV) will be recovered as $(\text{HL})_2[\text{Pu}(\text{NO}_3)_6]$ in a similar manner to other An(IV) we have found previously [2]. The yield of the $(\text{HL})_2[\text{Pu}(\text{NO}_3)_6]$ was 84% in use of **14Cy** and 99% with **12Cy**. The latter is better than the former as a Pu(IV) precipitant. Note that these **L** are also efficient for U(VI) recovery [3], indicating isolation of Pu is prohibited to resolve a security concern of nuclear fuel cycle.

Acknowledgement This work was supported by Grant-in-Aid for JSPS Fellows Grant Number JP22J23423 and JSPS Fostering Joint International Research(B) Grant Number JP20KK0119.

Reference: [1] IAEA-TECDOC-1587 2008. [2] (a) *Angew. Chem. Int. Ed.* **2019**, 58, 240. (b) *RSC Adv.* **2020**, 10, 6082. (c) *Chem. Lett.* **2020**, 49, 1201. [3] *Eur. J. Inorg. Chem.* **2020**, 3443. [4] *Inorg. Chem.* **2023**, 62, 454. [5] (a) NIST Critically Selected Stability Constants of Metal Complexes Database, ver. 8.0, **2004**. (b) *Second Update on the Chemical Thermodynamics of Uranium, Neptunium, Plutonium, Americium and Technetium*; OECD Nuclear Energy Agency Data Bank: Paris, France, **2020**. [6] (a) *Inorg. Chem.* **2022**, 61, 12337. (b) *Inorg. Chem.* **2012**, 51, 9165. (c) *Chem. Commun.*, **2018**, 54, 12014. (d) *Inorg. Chem.* **1996**, 35, 2841. (e) *Chem. Commun.*, **2018**, 54, 12582. (f) *J. Chem. Soc., Dalton Trans.*, **2002**, 2328. [7] *Chem. Eur. J.* **2020**, 26, 8115. [8] *Theor. Gen. Crystallogr.* **1976**, 32, 751.

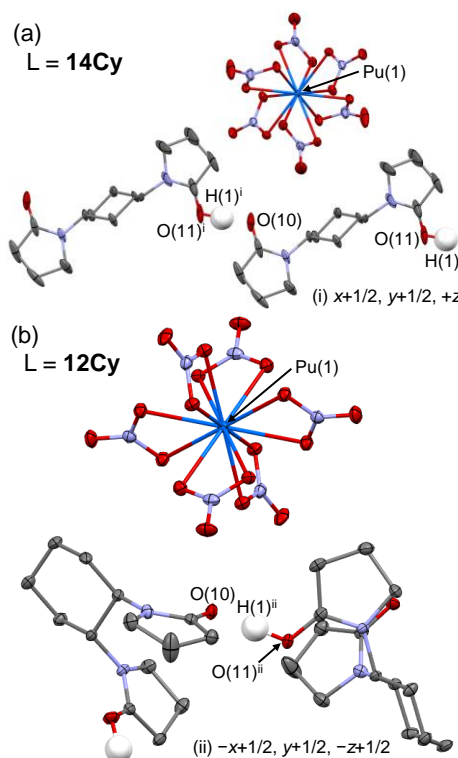


Fig. 2 Molecular structures of the $(\text{HL})_2[\text{Pu}(\text{NO}_3)_6]$ obtained from 3 M $\text{HNO}_3(\text{aq})$. **L** = **14Cy** (a) and **12Cy** (b). H atoms except H(1) were omitted for clarity. Thermal ellipsoids drawn at 50% probability.

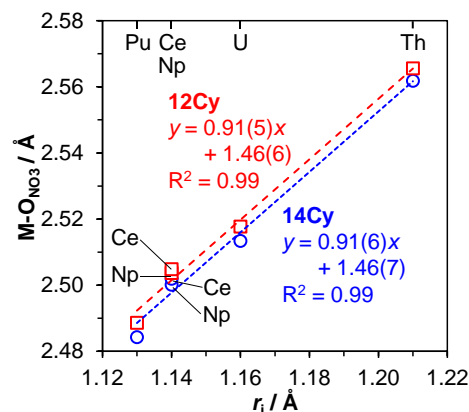


Fig. 3 Correlation between ionic radius (CN = 12) of M^{4+} and mean M– O_{NO_3} length in $(\text{HL})_2[\text{M}(\text{NO}_3)_6]$.

The Adsorption of Pu(IV) in the Presence of Cesium Phosphomolybdate, Barium–Strontium Nitrate, Zirconium Molybdate and Zirconium Hydrogen Phosphate

Joshua Turner^a, Christian White^a, Jessica Blenkinsop^a, Barbara Dunnett^a, Adam Bragg^a, Dan Whittaker^a, Richard Lynn^b

^aNational Nuclear Laboratory, Central Laboratory, Sellafield, Seascale, Cumbria, CA201PG, UK

^bSellafield Ltd., Sellafield, Seascale, Cumbria, CA20 1PG, UK

Understanding the behavior of Pu during both the recycling of nuclear fuel and any associated waste treatment is important to efficiently manage facilities in operation today as well as providing useful information for facilities that may support advanced fuel cycles. The chemistry of Pu is rich, both in terms of solution phase speciation and redox behavior. In addition, its fissile nature means that any chemical process that can potentially concentrate the Pu is important to understand. One such area is the interaction of Pu with solids that are formed during reprocessing and associated waste treatment of nuclear fuel.

The first stage of the PUREX process involves the separation of U and Pu from the rest of the dissolved fission products, creating a highly active raffinate stream. At major commercial reprocessing plants around the world this raffinate is concentrated in an evaporator to reduce the volume prior to interim storage and vitrification. The major solids that can form during concentration include cesium phosphomolybdate (CPM), zirconium hydrogen phosphate (ZHP) and nitrate crystallisation dominated by barium–strontium nitrate. During storage of the concentrated highly active liquor, CPM can convert to zirconium molybdate (ZM). Whilst the separation process extracts the majority of Pu, a small amount remains with the other fission products and ends up within the highly active liquor treatment facilities where it can interact with the solids.

The majority of discussion in the literature relates to the ion exchange behavior of Pu with Zr, specifically zirconium phosphates and ZM. However, there is little published information on experiments carried out under conditions representative of highly active liquor waste treatment and storage facilities. In addition, there are other solids present for which experimental data has remained unreported such as for barium nitrate and CPM. There are also uncertainties as to which mechanism of association is in operation, such as whether it occurs by a co-precipitation, ion-exchange or adsorption based process.

The talk will go over a summary of recent experimental work that has been carried out to improve the understanding of the adsorption processes. In these experiments, solutions of Pu(IV) nitrate in nitric acid were mixed in the presence of solids known to be present in highly active liquor waste (CPM, ZHP, ZM and barium–strontium nitrate). The study investigated change in variables such as acidity, fission product concentration and Pu concentration to identify conditions where Pu adsorption was most elevated. In addition, the reversibility of the adsorption was tested.

Performance and Design of HotXAS: the Future In-House XAS Apparatus at Atalante

S. Orlat^{1,2}, R. Bes², F. Tuomisto², **P. Martin**¹, P. Moisy¹

¹ CEA, DES, ISEC, DMRC, University of Montpellier, Marcoule, France.

² Department of Physics, University of Helsinki, P.O. Box 64, FI-00014 Helsinki, Finland.

Over the last 30 years, nuclear fuel studies have benefited from the specific developments of X-ray absorption spectroscopy (XAS) for radioactive materials. Thanks to its unique ability to probe the electronic and local structure of a given element in any type of sample, XAS has been applied to all the important topics in nuclear chemistry, in particular to the nuclear fuels from their fabrication [1-3] to their behavior under irradiation [4,5] and during storage [6].

Running XAS experiments on nuclear fuel remains quite challenging due to the radioactivity of the samples. Only a limited number of synchrotron beamlines worldwide can handle significant quantities of transuranic elements. Nevertheless, their activity limits usually require modification of the sample prior to transport, which can lead to a modification of the sample microstructure or, in the worst case, its chemical state through e.g. oxidation. The restricted accessibility of synchrotron beamtime also limits the number of possible experiments.

Thanks to recent developments in the fields of X-ray optics, sources and detectors, it is now possible to perform XAS experiments in the laboratory using tabletop setups [7]. Such developments have paved the way for in laboratory XAS studies of nuclear fuels, as demonstrated by recent experiments on uranium compounds [8, 9].

As part of a collaboration between CEA Marcoule and the University of Helsinki, a new compact laboratory XAS apparatus was developed with the aim of optimizing it for the acquisition of XAS spectra at energies relevant for actinide studies (16–22 keV). In the near future, this device will be used as a characterization tool in the ATALANTE facility dedicated to the studies on the reprocessing of spent nuclear fuel, including the manufacturing of mixed oxide fuels, and final nuclear waste management.

In this contribution, we will present the design and performances of the laboratory XAS device and demonstrate its potential for the evaluation of the speciation of actinides.

- [1] P. Martin et al., J. Alloys Compd. 444–445, 410 (2007).
- [2] R. Vauchy et al., Inorg. Chem. 55, 2123 (2016).
- [3] E. Epifano et al., Commun. Chem. 2, 59 (2019).
- [4] R. Bès et al., Appl. Phys. Lett. 106, 114102 (2015).
- [5] P. Martin et al., J. Nucl. Mater. 466, 379 (2015).
- [6] K. O. Kvashnina et al., Phys. Rev. Lett. 111, 253002 (2013).
- [7] P. Zimmermann et al., Coord. Chem. Rev. 423, 213466 (2020).
- [8] R. Bès et al., J. Nucl. Mater. 507, 50 (2018).
- [9] E. P. Jahrman et al., Rev. Sci. Instrum. 90, 024106 (2019).

Investigation of the Microcosmic Dynamics Behaviors of Hydrogen and Oxygen in Plutonium Oxide via Ab Initio Molecular Dynamics Simulations

Jun Tang

Science and Technology on Surface Physics and Chemistry Laboratory, Mianyang 621908, China

The hydrogenation and oxidation corrosion of metallic plutonium, intentional or unavoidable, is a crucial issue for its actual applications. However, due to the high chemical reactivity of plutonium, there is a complicated plutonium oxide overlayer grows over the metal surface inevitably, even under the very strict oxygen deficient conditions. Thus, the microcosmic dynamics behaviors of hydrogen and oxygen in plutonium oxides are quite important for a depth understanding of the hydrogenation and oxidation corrosion of plutonium. The current work performs systematic ab initio molecular dynamics (AIMD) calculations to reveal the microcosmic dynamics behaviors of hydrogen and oxygen in different plutonium oxides. Some dynamic parameters such as the diffusion coefficient and barrier of hydrogen and oxygen in plutonium oxides were obtained and the associated microscopic mechanisms on the atomic scale were revealed.

The results indicate that the hydrogen atoms are captured by the lattice oxygen atoms to form a hydroxyl in their migration process in plutonium dioxide, and they are hard to penetrate the plutonium dioxide layer to react with metal Pu in a realistic scenario. Thus, the plutonium dioxide works as the protective screen against plutonium hydriding. Whereas, in plutonium sesquioxide there is no hydroxyl formed but a favorable and stable capturing effect that comes from the oxygen vacancy (OV) was found. Moreover, due to the limited OV number in the plutonium sesquioxide matrix, the dynamical behavior of hydrogen in plutonium sesquioxide is greatly dependent on the concentration of hydrogen (n_H). At the low n_H cases ($n_H \leq \frac{8}{32}$) the OV is excessive for hydrogen atoms and all the hydrogen atoms could be captured by OV rapidly, thus the hydrogen atoms cannot penetrate this oxide layer to attack the metal plutonium matrix as well. When n_H is high enough ($n_H \geq \frac{24}{32}$), the OV is insufficient for capturing all the hydrogen atoms and the redundant hydrogen atoms keep migrating and finally penetrate this oxide layer.

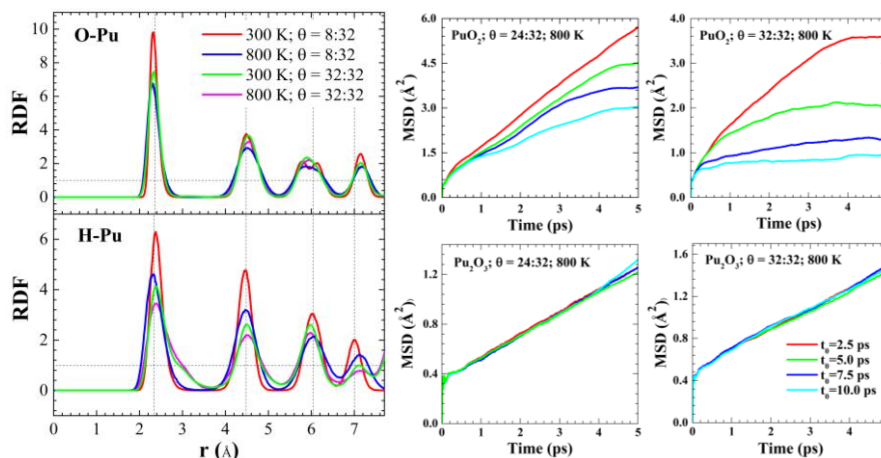


FIG. 1. The radial distribution function of O-Pu and H-Pu in plutonium sesquioxide (left) and the mean square displacements of hydrogen in plutonium dioxide and plutonium sesquioxide with high n_H (right).

As to the dynamics behaviors of oxygen in plutonium oxides, we discovered that the oxygen atoms are very difficult to migrate in plutonium dioxide due to its compact and oxygen-saturated spatial structure, but much easier to diffuse in the sparser plutonium sesquioxide lattice. In plutonium sesquioxide, the dynamical parameters of oxygen diffusion that

obtained by AIMD and climbing image nudged elastic band calculations are coincide with each other well, and the dominant mechanism is proved to be vacancy mediated with a path of first nearest-neighbor jumps. With regard to the diffusion at the interface accompanying oxidation and reduction, we identified three types of anisotropic oxygen diffusion processes prefer the [001] crystallographic diffusion pathway and proved that there may be a dynamic equilibrium of oxidation and reduction caused by oxygen diffusion near the interface. As our results accord with the experimental results of the ideal analogues of plutonium oxides (ceria oxides) [1] and provide a clear and reliable atomistic picture of the dynamic process of oxygen diffusion in different plutonium oxides and their interface for the first time, this work offers potential guidance for plutonium protection and long-term storage

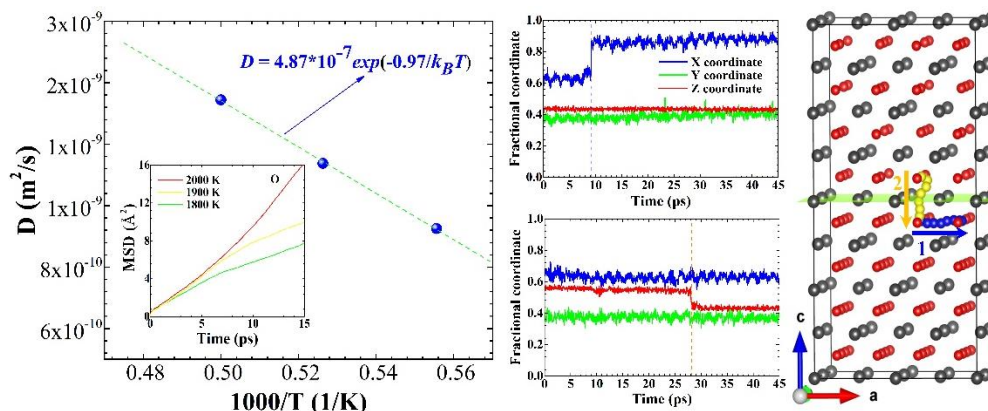


FIG. 2. The oxygen diffusion rate vs the reciprocal of temperatures in plutonium sesquioxide (left), the dashed lines are linear least-squares fits to guide the eye and their slope represents the diffusion barrier, the insert shows the mean square displacements of oxygen at different temperatures, and the fractional coordinate evolution of the jumping oxygen atoms and corresponding schematic diagrams of the diffusion during AIMD simulation(right), the jumping oxygen atom in the first and second steps is highlighted with blue and yellow, respectively.

References:

- [1] L. Zhu, X. Jin, Y. Zhang, *et al.*, Phys. Rev. Lett. 124 (2020) 056002.